Development of a modelling framework for integrated catchment flood risk management

Peter William Metcalfe

A thesis submitted in partial fulfilment of the requirements of the University of Lancaster for the degree of Doctor of Philosophy

November 2017

Authorship declaration

Contributions to each of the multi-author papers included in this thesis are indicated in the statements preceding each chapter. All other material is solely the author's own work.

Acknowledgments

This work was funded by the JBA Trust (project number W12-1866) and the European Regional Development Fund, with funding managed by the Centre for Global Eco-innovation (CGE), project number 132.

With thanks to my supervisors Professor Keith Beven, Dr Barry Hankin and Professor Rob Lamb, the members of the Brompton Flood Group, and all those involved in the Rivers Trust Life IP project (Dr Nick Chappell, Iain Craigen, David Johnson and Dr Trevor Page). Many thanks to the team at the CGE office, particularly the programme manager Dr Andy Pickard. Dr Mary K. Saunders helped devise the thesis plan and she contributed her professional GIS skills to Chapter 4.

Special thanks are due to the European Union, without which this work would have not been possible.

Dedicated to my father, Robert John Metcalfe 1938-1992.

Abstract

Flooding is one of the most significant issues facing the UK and Europe. New approaches are being sought to mitigate its impacts, and distributed, catchment-based techniques are becoming increasingly popular. These employ a range of measures, often working with the catchment's natural processes, in order to improve flood resilience. There remains a lack of conclusive evidence, however, for the impacts of these approaches on the storm runoff, leading to considerable uncertainty in their effectiveness in terms of mitigating flood risk.

A new modelling framework for design, assessment, and uncertainty estimation of such distributed, nature-based schemes is developed. An implementation of a semi-distributed runoff model demonstrates robustness to spatio-temporal discretisation. Alongside a new hydraulic routing scheme, the model is used to evaluate the impacts on flood risk of in-channel measures applied within an 29 km^2 agricultural catchment. Maximum additional channel storage of 70,000 m^3 and a corresponding reduction of 11% in peak flows is seen. This, however, would not have been insufficient to prevent flooding in the event considered.

Further modifications allow simulation of the impacts of wider measures employing natural processes. This is applied within an uncertainty estimation framework across the headwaters of three mixed-use catchments, ranging in size from 57 km^2 to 200km^2, across a series of extreme storm events. A novel surface routing algorithm allows simulation of large arrays distributed features that intercept and store fast runoff. The effect of the measures can be seen across even the most extreme events, with a reduction of up to 15% in the largest peak, albeit that this large impact was associated with a low confidence level.

The methodology can reflect the uncertainty in application of natural flood risk management with a poor or incomplete evidence base. The modelling results demonstrate the importance of antecedent conditions and of the timings and magnitudes of a series of storm events. The results shows the benefits of maximizing features' storage utilisation by allowing a degree of "leakiness" to enable drain-down between storms. An unanticipated result was that some configurations of measures could synchronise previously asynchronous subcatchment flood waves and have a detrimental effect on the flood risk.

The framework shows its utility in both modelling and evaluation of catchment-based flood risk management and in wider applications where computational efficiency and uncertainty estimation are important.

Contents

Figures

Glossary of terms

Actual Evapotranspiration	Abbreviated $E_{a..}$. Realised evapotranspiration given the soil water available. Always less than or equal to **potential evapotranspiration**.
Annual Exceedance Probability	The probability that a given event will occur within a given year. Reciprocal of **return period**.
Attenuation	Reduction in the size of a storm peak, typically by means of flood mitigation measures. Expressed as an absolute **discharge** or percentage.
AWS	Automatic weather station that collects metrological data such as rainfall.
Bankfull	The water level at which the top of a section of channel is overtopped.
Behavioural	A term applied in **GLUE** to identify model **realisations** whose outputs meet an acceptable level of fidelity with respect to the observed values.
Bund	A low earth or wooden dam designed to retain storm runoff.
Calibration	Fitting the parameters of a hydrological model to observed data, usually on the basis of a performance measure such as the **NSE**. Often undertaken using a **Monte Carlo approach.**
Canopy	Tree leaves and other vegetation that intercept precipitation.

CBFM	Catchment-Based Flood Management. An approach that aims to increase the overall flood resilience by measures upstream of affected areas. distributed across the catchment, rather that solely within those areas.
Celerity	The speed at which a wave of the disturbance of a conserved quantity such as specific storage moves through a fluid.
Continuity equation	The principle that the rate of change of a quantity within a system, or discrete element of that system, is equal to the difference between the entry rate and output rate. When applied to mass referred to as mass continuity (equation).
Contributing area	The area of the catchment contributing to the storm **hydrograph** at a particular time.
Critical flow	The point at which open channel flow switches between **subcritical** and **supercritical** states. Occurs in a **hydraulic jump.**
CRS	Coordinate Reference System. Any system that maps a given set of coordinates to a unique point on the Earth's surface.
DEM	Digital Elevation Model. Ground surface elevation, typically held as a **raster**, with surface objects such as trees and buildings removed.

Differential equation	A relationship expressed in terms of rates of change of one or more dependent and independent variables representing a system state.
Discretisation	(a) An approach applied in a numerical scheme to divide time and space steps equally. (b) The subdivision of a catchment into distinct **HRUs** sharing common characteristics.
Discharge	Rate of flow through a section of a river. Given in m^3/s (cumecs) or as a **specific** discharge in mm/hr.
Distributed (model)	A model that predicts at continuous spatial locations the states of a system.
DSM	Digital Surface Model. Ground surface elevation, typically held as a **raster**, that include surface objects such as trees and buildings.
Equifinality	The proposal that there are many cases numerous models of a systems that can produce **behavioural** outputs and different models can produce identical results.
Evapotranspiration	Abbreviated *Et,* ([L]/[T]; mm/hr). The combined evaporation and transpiration rate from the surface and vegetation or canopy See **potential evapotranspiration** and **actual evapotranspiration**.
Explicit	A solution scheme that uses only the previous states of a state variable in order to predict its current value.
FRM	Flood Risk Management. Any measure or strategy designed to reduce flood risk.

HRU	Hydrological Response Unit. See **discretisation.**
Hydrograph	A plot of discharge against time at a particular point on a river.
Hyteograph	Rainfall against time recorded for example by a **TBR** rain gauge.
Hydraulic jump	The region in which a flow changes from subcritical to supercritical, or vice versa. Will involve some energy loss or **head**.
Geographical reference system	A **CRS** where coordinates correspond directly to points on the Earth's surface, within the limitations of the system. Preserves direction but grid cells vary in size and shape.
Geo-referenced	Values that are located on a unique point or extent on the Earth's surface and include a **CRS**.
GLUE	Generalised Likelihood Uncertainty Estimation. A methodology for quantifying uncertainty by combining a variety of likelihood measures to score model outputs.. Multiple realisations of models configurations and parameters sample from prior distributions and scored according to one or likelihood functions.
GIS	Geographical Information System. A software tool for maintenance, analysis, manipulation and integration of spatial data.

Hydraulic conductivity	The rate of movement of water per unit area per unit head gradient through a medium such as soil. Dimensions are [L]/[T] and typical units m/hr.
Hydraulic head	The amount of energy per unit weight of a fluid. In hydrology and hydraulics expressed in units of length ([L]; m). In an open channel the head comprises potential (or elevation), velocity head from downstream movement and pressure head due atmospheric pressure.
Hysteresis	In the context of hydrology, a relationship between two state variable such as capillary pressure and soil moisture that develops distinctly under wetting and drying conditions.
Implicit	Describes a procedure for solving numerically an expression for state variables of a system at a particular point in space and time, where the solution scheme includes the current state.
Infiltration	The vertical movement from the surface into the soil.
Insolation	Intensity of solar radiation on a surface (kW/m^2)
LiDaR	Light Detection and Ranging. A remote sensing method using an airborne pulsed laser to measure distances to points on the Earth's surface and thus determine their elevations. Often used to produce a **DEM** or a **DSM**.

Macropores	Large soil **pores** created, for example, from tree root voids and macroinvertebrate activity, animal burrows, and desiccation, that can act as preferential pathways for infiltration and subsurface flow.
Monte Carlo (simulation)	Model simulation employing many runs taking parameters sampled from random distributions.
Morphology	The shape of a surface feature or river channel.
Network Width Routing	Time delay histogram derived from distances of the points on the channel network, or on the hillslopes, from the catchment outlet.
NSE	Nast-Sutcliffe Efficiency. A performance measure commonly used to determine the fidelity of a runoff simulation against observed flows. Frequently used as a likelihood measure in **GLUE**.
ODE	Ordinary Differential Equation. A **differential equation** formulated in terms just one independent variable such as time.
Open channel flow	Free surface flow at atmospheric pressure.
Orographic	Describing precipitation caused by uplift due to relief.
Overbank (flow)	Storm flow that takes place outside the usual river channel.

PDE	Partial Differential Equation. A differential equation formulated in terms of more than one independent variable such as time and distance. Examples include the **Shallow Water Equations** and the **Saint Venant Equations**.
Peds	Aggregation of soils into irregular blocks separated by **soil pores**.
Pore	Voids in the soil matrix between **peds**.
Potential evapotranspiration	Abbreviated E_p. Dimensions [L]/[T] and typical units mm/hr. The maximum theoretical rate of **evapotranspiration** given insolation and unlimited water supply to the root zone.
Projected coordinate reference system	A **CRS** where the values are projected from a plane onto the Earth's surface and thus directions are preserved.
Raster	Format for values covering a two dimensional field (usually a spatial plane) where the values are evenly spaced within a grid.
Rating	Development of a **rating curve** for or a channel section or engineered hydraulic structure such as a flume.
Rating curve	A relationship derived empirically between river stage and discharge.
Realisation	A model whose parameters and inputs have been fixed to particular values and can produce predictions.
Return period	The average length of time between events of a given magnitude.

Riparian (zone)	The area immediately around the river channel.
Saint Venant Equations	A series of **PDE**s analogous to the **Shallow Water Equations** in one spatial dimension describing **open channel flow**.
Saturated zone	The region in the subsurface where the soil is completely full and cannot contain any more water.
Semi-distributed	A model where the spatial complexity is minimised by aggregating areas into **Hydrological Response Units**.
SWE	Shallow Water Equations. A series of equations derived from the Navier-Stokes equations for fluid flow. They describe free surface movement of water across a plane, where the flow depth is much smaller than its extent and the assumption of a uniform velocity profile is acceptable. Combines mass continuity with energy conservation in order to produce three **PDE**s formulated in two spatial dimensions.
Spatio-temporal	Describing a state or quantity that varies in both state and time.
Specific	Describing a measurement given in terms of its value per unit area, also known as intensity.
Stage	Water level at a point in the river, typically at a gauge where it is measured with a stage meter and converted to a **discharge** using a **rating curve**.

Subcritical (flow)	In terms of open-channel hydraulics, describing flow where the majority of the **head** is composed of potential energy.
Supercritical (flow)	In terms of open-channel hydraulics, describing flow where the majority of the **head** is composed of kinetic energy due to the water's movement.
Tarlweg	Midline of a river channel
TBR	Tipping bucket recorder. A common type of rain gauge that consists of a small container on a see-saw type arrangement. Once the bucket is filled with rain water the bucket tips and empties the container. Each time this occurs it is recorded, thus the rainfall rate can be estimated.
Transmissivity	The rate of water transmitted per unit contour per unit head gradient. Dimensions are $[L]^2/[T]$ and typical units m^2/day or $\log(m^2/hr)$.
Unsaturated zone	The region in the subsurface where some of the soil pores have spare capacity.
Water table	See **saturated zone**.
Wet canopy evapotranspiration	Direct loss of precipitation from the canopy through evaporation

Chapter 1. Introduction

1.1. Overview

Flooding is the most damaging natural hazard, in terms of its economic impacts, facing the UK and the rest of Europe (EEA, 2011). The 2007 summer floods in the south of England caused damage of around £3.2 billion (EA, 2010) and the costs of 2013-2014 winter storms were at least £1.3 billion (EA, 2016). Those of the 2015-2016 floods are likely to exceed £1.5 billion (Marsh et al., 2016). Floods are the most common weather-related disasters worldwide, and in 2011 the worldwide cost of flooding stood at around $24 billion (IPCC, 2014)

Across Europe there were significant floods in 2002 (Danube and Elbe) and in 2005, affecting mainly Austria, Germany, Romania and Switzerland (Kundzewicz et al., 2013). In 2006 and 2009 the Danube and Elbe were again affected and in 2010 the Central European Floods caused further damage in Poland, the Czech Republic and Hungary (EEA, 2011; Kundzewicz et al., 2013). Associated economic losses are estimated at €52 billion (EEA, 2011).

In addition to its economic consequences, the loss of lives and social and environmental impacts of flooding are immense. Notwithstanding any increase in flood frequency, this effect has increased globally since the mid 20th century due to increased exposure of human habitation and activities in affected regions (IPCC, 2014). In the period 1998 to 2009 over 1000 lives were lost in EU nations due to flooding and 500,000 people were displaced from their homes. In Venezuela in 1999 30,000 died as a result of flooding, and almost 2000 were killed in Mozambique in 2000/2001 (Guha-Sapir et al., 2014). Floods in China in 2013 affected 130 million people (IPCC, 2014)

Flooding is likely to increase globally with predicted climate change (Delgado et al., 2010; Hirabayashi et al., 2013; IPCC, 2014). In Western Europe climate-change models indicate increased winter rainfall totals and lower but more intense summer rainfall, with much of the change projected to come within the 2020s (Ramsbottom et al., 2012; IPCC, 2014; Westra et al., 2014). Some studies suggest that in the UK the annual cost of flooding could rise from £1.2 billion at present to between £1.6 billion and £6.8 billion in 2050 (Ramsbottom et al., 2012).

Flooding can be defined as "the temporary covering by water of land not normally covered by water." (EU, 2007). There are a number of causes of flooding (Dadson et al, 2017). Pluvial flooding is the result of rainfall intensity exceeding the infiltration capacity of the subsurface, with the excess flowing overland. Fluvial flooding occurs when discharge within a river reach exceeds its conveyance and overtops its banks. Coastal flooding is a consequence of extreme tides, weather and erosion. Overloading of artificial drainage is also referred to as Combined Overflow Discharge (COD). Groundwater flooding occurs at points, particular hollows, where the water table rises to the surface after prolonged recharge.

The European Commission recognised the scale of the threat caused by flooding and the European Floods Directive became effective in 2007. This requires member states to categorise the flood risk of their rivers, other water courses and coasts, map probable flood extents and quantify risks to human life and property and to formulate effective measures to reduce flood risk. The UK has enacted the measures specified by the Floods Directive and in England and Wales the UK Environment Agency (EA) is tasked with its implementation. In Scotland the Scottish Environmental Protection Agency (SEPA) is responsible for the enactment of the . The Pitt Review (Pitt, 2008) was another comprehensive set of recommendations for improving flood resilience in

the U.K produced in response to the serious floods of 2007. The EA has incorporated many of the suggestion in the Review into its Flood Risk Management strategy (EA, 2012), in particular its recommendation to work with natural processes in order to reduce flood risk.

1.2. Traditional Flood Risk Management (FRM)

Conventional approaches to fluvial flooding often involve hard-engineered downstream defences that increase effective channel conveyance, These may be combined with artificial storage upstream to retain runoff and release it in a controlled fashion. Engineered defences can be designed to meet a rating specification expressed in terms of their ability to withstand and contain an event with a given annual exceedance probability (AEP), typically 1 in 100 years or 1%. The AEP is the nominal probability that such an event will occur in any given year.

Urbanisation is expanding the area under threat and other changes in land use are anticipated to increase the risk of flooding (Wheater & Evans, 2009). In December 2015 in Carlisle in Cumbria, defences upgraded to withstand a so-called "1 in 200 year" event were overwhelmed by a 1 in 1000 year event (Marsh et al., 2016).

A systems-based approach has been developed for the management and evaluation of flood defence assets (Hall et al., 2004). It is adopted by the EA in their Risk of Flooding from Rivers and Sea maps. In order to evaluate probabilistically the long-term risk of defence overtopping and performance failure the approach uses Monte-Carlo sampling of flood defence fragility curves (the probability of damage given an event's magnitude).

1.3. Catchment based approaches to FRM

Integrated, Catchment-Based Flood Management is increasingly being applied (CBFM, Dadson et al., 2017; Lane, 2017). This aims to increase resilience to floods through upstream widely-distributed interventions, possibly in conjunction with downstream defences. It includes techniques to decrease fast runoff, for example by changes in land management to increase infiltration or by disconnection of surface flow pathways from the channel. Other measures are the addition of runoff storage on hillslopes through the introduction of soft-engineered features such as bunds; or by providing space on the floodplain for overbanked storm flows. The overall aim is to retain storm runoff in the headwaters and release it more slowly than for the unmodified catchment and thus reduce peak flows in affected areas downstream.

One variety of CBFM is an approach known as Natural Flood Management (NFM) that meets its aims by enhancement of the natural processes within the catchment. Natural flood management "… involves techniques that aim to work with natural hydrological and morphological processes, features and characteristics to manage the sources and pathways of flood waters" (SEPA, 2016). Associated measures such as tree-planting can reduce water yield through increased evaporation. NFM can enhance ecosystem services across the catchment and help meet the chemical and ecological status requirements of the Water Framework Directive (Nisbet et al., 2011; Barber & Quinn, 2012; Iacob et al.; 2014; EEA, 2016).

Catchment managers will require effective tools to enable the design and rating of proposed CBFM and NFM interventions. Emplacement of measures such as tree-planting are time-intensive and their effects will take a number of years to become noticeable. Of particular concern is the possibility that inappropriately sited measures could in fact have a detrimental impact on the flood response. There is considerable

uncertainty in the hydrological impacts and hydraulic performance of soft-engineered measures. Realistic modelling approaches that incorporate uncertainty are essential for strategic placement of such measures to optimise their benefits in terms of flood risk mitigation, and to identify where their locations could slow flow inappropriately and potentially increase flood risk. The implementation of the European Floods and Water Framework Directives has further increased the importance of methodologies for development of the required river basin management plans.

The complexity of fully-distributed river and runoff models limit their application to larger catchment scales. Conversely, the crude spatial resolution of lumped or statistical catchment models significantly limits their use for assessment of detailed flood measures. There appears to be scope for an intermediate scale modelling approach that can incorporate sufficient detail to simulate both widely-distributed arrays of smaller features and larger scale measures but that is sufficiently simple that it can be used within a uncertainty estimation framework.

1.4. Project overview

1.4.1. Aims and objectives

The overall aim of the project is to develop a scalable and computationally efficient computerised modelling framework for the design and assessment of distributed, soft-engineered approaches to flood-risk management.

Research questions that will be addressed include:

1. What are efficient strategies for modelling flood mitigation interventions widely-distributed across hillslopes and channel networks of meso-scale (10-1000 km²) catchments?

2. What are the effects of antecedent conditions and timings and magnitude of sequences of storm events on the effectiveness of NFM schemes?
3. Do NFM measures have any mitigating effect through extreme events?
4. Do the synchronisation or desynchronisation of subcatchment flood waves have significant effects on the effectiveness of distributed FRM?
5. How best can uncertainty and "fuzzy" evidence be reflected in the application of natural flood mitigation measures?

Objectives to help answer these questions and meet the project aim are:

1. To develop a scalable, robust, computationally efficient runoff model
2. To develop a model which can simulate in-channel features and their combined effect on the storm flows within the channel network
3. To develop a scalable surface routing method that can represent the effects of measures to intercept overland storm runoff
4. To develop a framework for modelling the effects of widely-distributed hillslope interventions at a catchment scale
5. To apply the model developed in objective 4 within an uncertainty estimation framework.

1.4.2. Approach

The catchments used in the studies were chosen to demonstrate the validity of the models developed at increasing spatial scales and a variety of land-use types. In Chapter 3 the runoff model is tested against a 3.7 km², well-instrumented upland catchment, In Chapter 4 it is used within a 29 km² intensively-farmed catchment. In the research project described in 0 and Chapter 6 the model is applied to three

catchments ranging in size from just under 100 km² to over 220 km², displaying a combination of upland, marginal grazing and arable land with urban areas at their outlets.

The models described in the project were, in general, implemented in the R language and environment. This has been applied in a number hydrological applications (e.g. Buytaert, 2008; Mehrotra et al., 2015; Turner et al., 2016). It was also considered appropriate as:

- It is open source and has a wide user community
- There are many "packages", self-contained third-party modules delivered via the Comprehensive R Archive Network (CRAN). Packages are accepted on CRAN only after passing rigorous QA and cross-platform compliance. Extensive use were made of third party modules such as those listed below.
- It has fully-featured packages for analysis, manipulation and presentation of data, and time series, particularly useful for hydrological contexts, e.g. `xts` (Zeileis, Grothendieck, 2005) and `data.table` (Dowle et al., 2014).
- It has packages for spatial analysis and wrappers to spatial libraries such as GEOS and GDAL (`rgeos`, Bivand & Rundel, 2014; `rgdal`, Bivand et al., 2014) .

Compiled libraries implemented in C (e.g. `deSolve`, Soetaert et al., 2010; `LAPACK`, Anderson et al., 1999) were utilised for the solution of systems of Ordinary Differential Equations (see Chapter 3 and Chapter 4) and for geoprocessing with the RGDAL and RGEOS packages.

1.4.3. Scope

There are attempts to model flood risk globally using subgrid scale parametrisations of remotely-sensed elevation and hydrometric data (e.g. Yamazaki et al., 2011). Availability of hydrometric data for input to, and calibration of such models is in general restricted. The limited spatial resolution of data such as that of the Shuttle Radar Topography Mission (SRTM) means that it will be difficult to represent the small-scale flood mitigation interventions proposed for natural flood management.

In the UK high resolution topographic and hydrometric data are readily available from sources such as the Environment Agency. This study will, therefore, use catchments from the UK. The techniques developed, however, will be broadly applicable to temperate catchments worldwide, subject to suitable data being available. Pluvial and fluvial flooding only will be considered.

1.5. Document structure

The thesis is comprised of this introduction, a literature review of modelling of catchment processes and natural flood mitigation strategies (Chapter 2), and four multi-author papers, on three of which the thesis author is first author. A summary of the author's contributions to each of the included papers can be found in the supporting statement preceding each paper. Three appendices detail the mathematics behind the models developed.

The conclusion summarises the findings and details how the aim and objectives of the project have been met. It suggests wider-scale and more diverse applications of the framework that was developed.

1.5.1. Dynamic TOPMODEL: A new implementation in R and its sensitivity to time and space steps

This describes a new, open source, implementation of a semi-distributed model developed to simulate runoff and soil moisture deficits. The paper describes its underlying methodology, modular structure and an application to a simulated landscape and a small (3.65km²) catchment in Wales, UK. Various spatial and temporal discretisations are applied to a single calibration period. The implementation demonstrates robustness to the various schemes and convergence to a limiting output. Appendix 1 details the flux calculations and new surface routing method introduced in this implementation.

1.5.2. A modelling framework for evaluation of the hydrological impacts of nature-based approaches to flood risk management, with application to in-channel interventions across a 29 km² scale catchment in the United Kingdom

This study develops a depth-averaged 1D hydraulic routing model that can be applied to route in and out of bank channel flows in river networks of arbitrary scale and structure. It can take into account the effect of insertion of any configuration of structures designed to mitigate storm flows. It applies parameterised channel geometries and a simplified flood plain representation. The model is applied to an agricultural catchment where a NFM -type approach is suggested to reduce flood risk but where land use and regulatory constraints preclude the use of hillslope measures. The Dynamic TOPMODEL implementation developed in Chapter 3 is used to simulate the hillslope runoff for a storm period. The hydraulic model applied to investigate the effects of various configuration and geometries of in-channel barriers on the response.

Appendix 2 details the hydraulic routing scheme for channel routing. and Appendix 3 suggests formulations for the hydraulic characteristics of selected in-channel flood mitigation measures.

1.5.3. Strategies for testing the impact of natural flood risk management measures.

This chapter describes a four month long project undertaken for the Rivers Trust in liaison with Lancaster Environment Centre and JBA Consulting. The author acted as research associate and developed the computer model with which the detailed modelling was undertaken. The project aimed to investigate the potential for applying a nature-based approach for flood mitigation across the headwaters of three Cumbrian catchments badly affected by the extreme storm events of the winter of 2015-2016.

The runoff model described in Chapter 3 was further developed to allow simulation of the effect of the addition of various types of widely-distributed hillslope interventions for flood mitigation. These include peat restoration, soil structural improvements, tree-planting on hillslopes and riparian areas, and deepening of existing accumulation areas to provide detention storage area for surface runoff.

A catchment partner workshop was undertaken and opportunity mapping based on runs of the fully-distributed JFLOW surface runoff model applied to identify priority areas. The chapter describes the tiered methodology developed to incorporate the opportunity mapping with JFLOW, catchment partner input, and detailed modelling of runoff with and without intervention measures using an enhanced version of Dynamic TOPMODEL. It outlines the evidence and literature base for the parameter and input data changes applied to simulate these larger-scale interventions.

1.5.4. Simplified representation of runoff attenuation features within analysis of the hydrological performance of a natural flood management scheme

A measure simulated in the project described in Chapter 5 was the insertion of runoff attenuation features (RAFs) intended to intercept and store overland storm runoff. The new surface routing module developed in Section A.1.4 was modified to allow modelling of these features. This chapter describes the modelling using this approach, through the storm period from the previous study, of approximately 4500 of such features across the 228km² headwaters of the Eden, Cumbria, UK.

The study applies an uncertainty estimation framework to the simulated runoff for unmodified and intervention cases. Features with a number of different "leakiness" characteristics are applied. Some conclusions are drawn on the effects of different drain-down times across extreme events such as those studied. The chapter discusses whether the simplified representation is valid and suggests some experimental approaches to determining the behaviour of such features and their effects on the catchment response.

The issue of synchronisation or desynchronisation of subcatchment flood waves, and its impact on the effectiveness of NFM interventions, is considered. Experimental approaches, both computerised and field-based are suggested as a means of investigating, in further studies, this issue and the robustness of the modelling results

Chapter 2. Review of literature and modelling of catchment processes

2.1. Introduction

Models play an important role within catchment management (Jakeman & Letcher, 2001; Lerner et al., 2010). Beven (2012) provides a comprehensive review of catchment model development, from the formulation of a perceptual and conceptual structure to implementation, calibration and validation.

2.2. Modelling approaches

Beven (2012) categorises models as "lumped-conceptual" or "physical / process-based". In the first case, the catchment, its processes and internal states are treated as a whole and modelled statistically or probabilistically. In physical, or process-based, models the internal processes are modelled explicitly according to physical laws and applied to update internal state variables over time.

A simple example of a lumped-conceptual models is the Unit Hydrograph technique, which considers the response of the catchment to a single unit of effective rainfall as an additive property on which linear algebraic operations can be performed in order to derive its response to more complex hyetographs.

Another example is the Probability Distributed Moisture Model (PDM: Moore & Clarke, 1981; Moore, 2007). This simulates spatial heterogeneity through the application of-a distributed probability function (PDF) for storage capacity at all points within the catchment, but has no explicit spatial representation of its interior. Catchment storage is divided into slow and fast components, corresponding to surface and subsurface storage, and is treated a treated as a collection of simple linear stores (Figure 2.1). At each time step the runoff is determined by the contribution, as

determined by the PDF, of the excess over capacity of stores that have filled. The distribution is updated according to the incident precipitation, runoff and evapotranspiration of the likely transfer of storage between elements.

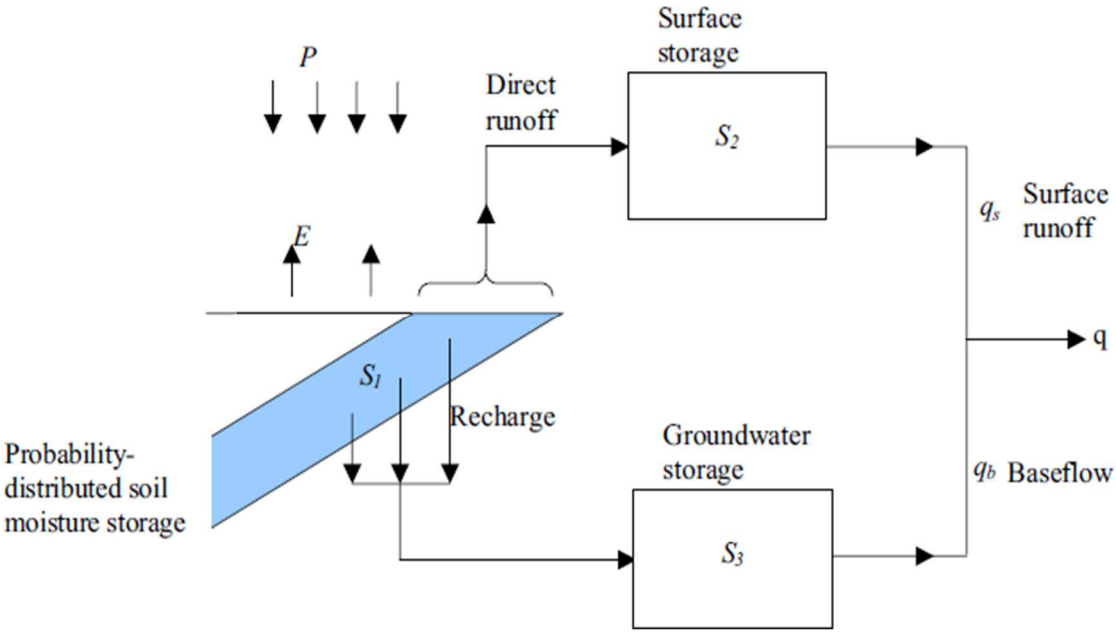

Figure 2.1. PDM structure (Moore, 2007)

The PDM approach is flexible and scalable and has been used as the hydrological model underlying other applications such as Grid-to-Grid (G2G; Bell & Moore, 1998; Bell et al., 2007).

Increased spatial resolution is introduced in semi-distributed models. These attempt to simplify the complexity of the problem domain by grouping together areas with similar properties. They may then be treated each as a conceptual store known as a hydrological response unit (HRUs) or hydrological similarity unit (HSU) whose constituents can be partially mapped back into space.

In models such as TOPMODEL (Beven & Kirkby, 1979) the response units are identified according to the local value of the topographic wetness index (TWI), defined as $ln(a/tan(\beta))$, where a is the upslope area and $tan(\beta)$ is the local slope. The Soil and Water Assessment Tool (SWAT, Arnold et al., 1998) and Dynamic

TOPMODEL (Beven and Freer, 2001a) allow for a more general grouping approach that can, for example, take into account hydrologically-significant heterogeneity within the catchment such as land cover or soil type.

INCA (Integrated Nitrogen model for multiple source assessment in Catchments; Whitehead et al., 1998) is a water quality model that incorporates a semi-distributed runoff component. Here landscape units are identified with the areas draining to individual reaches in the river network.

In spatially-explicit, fully-distributed models, state variables are maintained across the catchment at points that can be mapped directly into actual space. Such models are usually physically-based (Beven, 2012). Examples include the Système Hydrologique Européen (SHE, Abbott et al., 1986) and later variants including MIKE-SHE (Refsgaard & Storm, 1995). HydroGeoSphere (Therrien et al., 2010; Brunner & Simmons., 2012) is a recent example that makes use of modern parallel computation techniques to solve for three-dimensional fluxes in the unsaturated zone. HydroGeoSphere was developed from the FRAC3DVS subsurface transport model (Therrien & Sudicky, 1996) with the addition of a 2D component for overland flow routing.

A combination of spatially-explicit, lumped and semi-distributed approaches may be used. The G2G model uses a grid-based model for production of surface and subsurface runoff, lumped at the scale of the grid element, coupled with a spatially-explicit hillslope and channel routing procedure that employs the kinematic approximation to the Saint Venant equations (Figure 2.2).

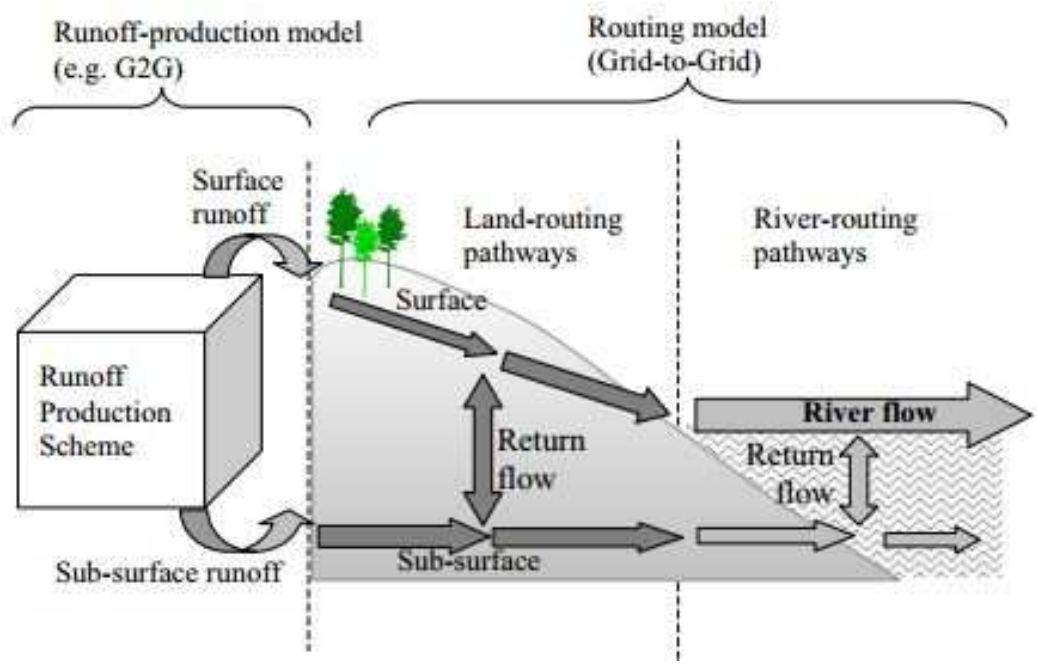

Figure 2.2. Grid-to-Grid modular structure (Bell et al., 2007)

Multi-scale models apply different treatment of space and time to distinct components of the system. A coarse spatio-temporal discretisation or static risk or opportunity mapping stage may be applied in order to identify areas that have a significant impact on the system response. An example of such a models is SCIMAP (Reaney et al., 2007). SCIMAP uses a network connectivity index calculated from flow distances of areas from the channel network (Lane et al., 2004) combined with the Topographic Wetness Index in order to identify critical source areas (CSA, Heathwaite et al., 2005) that are likely to both provide a source of pollution and are connected to the channel. A spatially-explicit model, Connectivity of Runoff Model (CRUM, Reaney et al., 2007) is then applied to those areas to estimate the dynamic solute mass flux from the critical areas to the channel network.

2.3. Uncertainty and equifinality

It is practically and theoretically infeasible to set up experiments or collect field data at a spatial and temporal resolution and extent to measure or to represent a

catchment's internal state (Beven, 1989, 1993, 2000). However, it is those states and their response to modification that will be of most interest to a catchment manager investigating potential flood mitigation interventions.

A typical approach is to apply model(s) that represent the catchment processes mathematically and to link their outputs to produce estimates of the quantities of interest. Any observational data available are used to determine the likely parameters of these models by reconstructing or calibrating against historical flows and states; these are then applied to predict the response of the system to future inputs. For example, a rainfall runoff model will take time series of rainfall and evapotranspiration in order to predict the discharge at the catchment outlet. Given a set of observed discharges, the parameters of this model will be adjusted or calibrated so that its outputs match the observations. Given residual errors in the model, this will help to predict the catchment response to different inputs, such as sets of spatially coherent designed extreme rainfall events and to assess the impact of interventions on the runoff.

In this approach the model is considered to be correct. Epistemic errors (lack of knowledge of the processes involved) introduce significant uncertainty(see e.g. Beven, 1989; 2009). In addition, observations of environmental data are more uncertain than for engineered systems (Jakeman & Hornberger, 2003), errors may vary non-linearly with state and be non-stationary over time (Beven, 2006). Given this inherent uncertainty, even if a perfect theoretical representation of the catchment were available, it is doubtful whether calibration could fix a "true" set of parameters (Beven, 2006; Jakeman & Hornberger, 2003).

Highly-defined process models can lead to over-parameterisation, with increasing complexity returning little improvement in accuracy, and introducing variables for

which calibration data are scarce or non-existent (Beven, 1989; Jakeman & Hornberger, 2003). Furthermore, Beven (1993, 2006) observes that different choices of model structure and parameter sets can give rise to similar, and acceptable, predictions of the observed outputs. Such "equifinality" means that in practical terms the components of a catchment system may have to be treated as "black boxes", with only input and output states known within the limitations imposed by observational error. In practice, the physical states within grid cells of fully-distributed models are not completely defined, and each could in fact be considered an individual lumped-conceptual model (Beven, 1989, 1993).

The Generalised Likelihood Uncertainty Estimation (GLUE) methodology (Beven & Binley, 1992 and 2014) accepts the equifinality of parameter sets and formalises this approach. It provides a framework in which behavioural parameter sets, in that they replicate adequately the response of the system to observed inputs, are identified within multiple (Monte Carlo) runs of the model. One or more likelihood measures may be used and combined to produce a single metric. A simple function is triangular across an interval defining the acceptable range of the observable: the midpoint value is unity and those outside the limits zero, and values are linearly interpolated between these points.

In the limits of acceptability approach (Beven & Freer, 2001b; Lui et al., 2009) all of the measures must be non-zero otherwise the realisation is rejected. An example of weightings calculated from three outputs (NSE, saturated contributing area A_c and maximum predicted discharge q_{max}) plotted against q_{max} is shown in Figure 2.3. See Section 6.3 for more detail of this calculation.

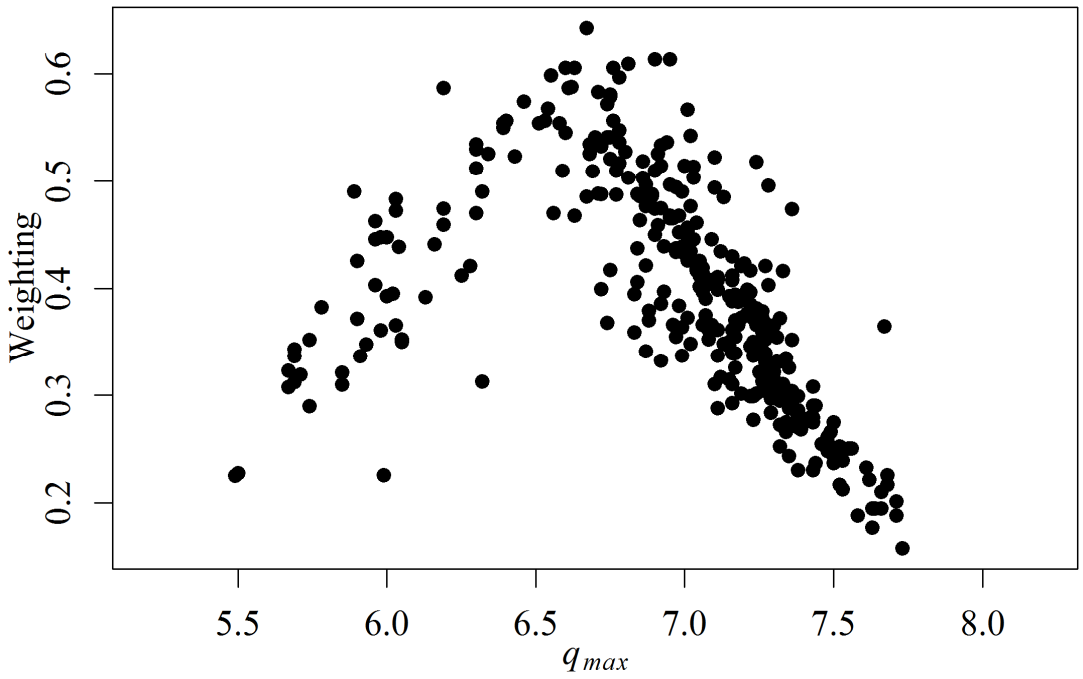

Figure 2.3. Example "dotty" plot showing the overall weighting of realisations against one observable from a flood simulation, the peak discharge q_{max}. This must lie within the given range determined from the observed values or the simulation is rejected.

Examples of applying GLUE to FRM modelling are found in 0 and 6.

2.4. Data for hydrological models

Depending on their formulation, hydrological models will require meteorological data (precipitation, evapotranspiration), catchment elevations and boundaries, and location and properties of river reaches. They may require other hydrometric data such as rated discharges for calibration. Physically-based, distributed models may be required much more detailed information such as surface effective roughness, soil water retention characteristics and hydrological conductivity. These may be difficult to measure, particularly at extensive spatial scales, and is open to question how well the measurement of a physical value at a single point can scale to the size of a grid element (Beven, 1989).

2.4.1. Topographic data

Many physical models use digital elevation data in order to infer the spatial variation of hydraulic gradient; a common assumption is that this is approximately parallel to the local surface. This is most appropriate for hillslopes with thin soils and impermeable bedrock. It should be noted, however, that the form of the bedrock can often have a greater impact on flow pathways than that of surface topography McDonnell et al. (1996).

Geo-referenced elevation data are widely available and generally provided as gridded rasters in GEOTiff or ASCII format, for example. Buildings and vegetation canopies are removed algorithmically from these data to produce a digital terrain models (DTM), the ground surface elevation. Elevation data that include buildings and vegetation yield a Digital Surface Model (DSM) and are more appropriate for mapping of surface water flooding in urban areas, for example. Datasets such as the ASTAR-GDEM (Advanced Spaceborne Thermal Emission and Reflection Radiometer Global DEM) and SRTM (Shuttle Radar Topography Mission), obtained through remote-sensing ,provide world-wide coverage at horizontal resolutions of between 30 and 50m. Data at 10m resolution are available for the entire UK via the OS Digimap datasets, accessible via the EDINA service. Intermap provide the NEXTMap commercially-licenced data that include UK-wide 2m DTMs / DSMs. As of 2015 the Environment Agency have made available for public use their LiDaR (Light Detection & Ranging) elevation data. Coverage in 2009 was 72% of the UK. Horizontal resolutions range from 2m to 25cm and elevation accuracies are up to 5cm (EA, 2009).

Worldwide catchment extents, flow directions, channel networks and other hydrological information are maintained in the HydroSHEDs database (Lerner et al.,

2008). The Integrated Hydrological Units (IHU, Kral et al., 2015) and Ordnance Survey OpenRivers archives provide catchment boundaries and rivers networks across the UK.

Indices of similarity calculated from gridded data are likely to be sensitive to the grid size (Saulnier et al., 1997). Gridded data with resolutions of over 100m are considered too coarse for use in hydrological models. (Beven, 2012).

2.4.2. Land use, land cover and soil types

Spatial data on land cover may be required by physically-based models with interception stores based on vegetation (and by inference, canopy type). Semi-distributed models such as SWAT allow for grouping of landscape units according to the land cover and vegetation type.

The Hydrology of Soil Types (HOST, Boorman et al., 1995) is a 1 km resolution raster dataset. It classifies the soils of the UK into 29 types according to hydrological characteristics that affect the catchment-scale response. These include SPRHOST, the Standard Percentage Runoff or proportion of incident rainfall that contributes to the fast response. Each grid cell in the raster indicates the predominant type within that area. The Flood Estimation Handbook (FEH; Institute of Hydrology, 1999) and Revitalised Flood Estimation Handbook (ReFH; Kjeldsen et al., 2005) employ catchment descriptors utilising values derived from predominant soil HOST classes.

SPRHOST values of greater than 50% are associated with soils such as Gleys displaying low hydraulic conductivity that are most likely to produce overland flow during storm conditions. These can be identified with areas in which measures to improve soil structure and effective conductivity, such as tree planting, would be most beneficial.

The Land Cover Map (LCM; Morton et al., 2007) comprises a vector and 25m raster dataset covering the UK. The vector data indicate the predominant land cover in terms of one of 23 broad habitat classifications, such as broadleaved woodland, and the subcategory of that classification. The raster data indicate the likely habitat category within each 25x25m cell. One application of the LCM relevant to flood modelling is to identify areas of improved grassland where soil structure can be improved and thus reduce fast runoff.

The European CORINE land cover (CLC) raster map is remotely-sensed at a resolution of 100m and comprises 44 land cover classifications. CLC was last updated in 2012. The dataset can, for example, be used to exclude areas from application of NFM measures according to their proximity to certain land use types.

2.5. Components of physically-based models

The Stanford Watershed Model (SWM, Crawford & Linsley, 1966) was the first computer software implementation of a hydrological model. Freeze & Harlan (1969) subsequently proposed a "blueprint" for physically-based models which has become the basis for the most subsequent approaches (Beven, 2012). The blueprint divides a hydrological model into discrete conceptual components with well-defined interfaces for transfer of water flux between them (Freeze & Harlan, 1969; Beven, 2012). The number of spatial degrees of freedom may vary between components, often according to the direction of the dominant directions of water flow.

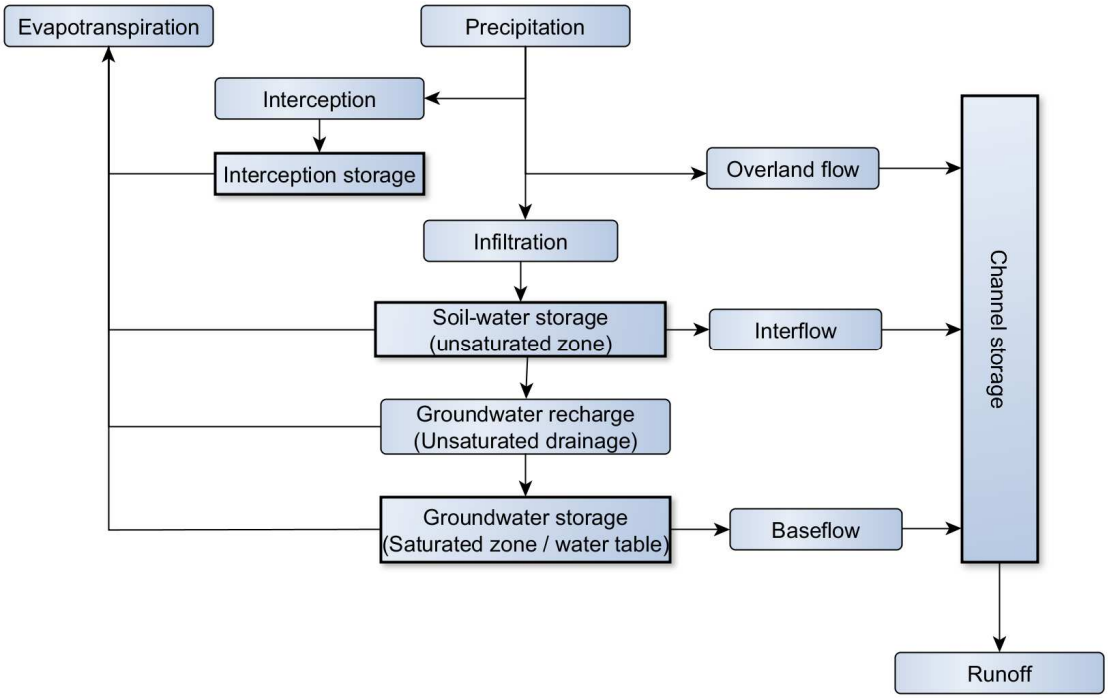

Figure 2.4. Common components of a hydrological runoff model (after Freeze and Harlan, 1969)

Singh (1995), Shaw et al. (2011), and Beven (2012) provide reviews of widely-used models and their implementations of the components of the Freeze-Harlan template. This section will review these and the corresponding literature.

2.5.1. Evapotranspiration and interception

Evapotranspiration is the removal of water from the surface or near-surface, through a combination of evaporation from the soil and plant transpiration. It accounts globally for 60% of the water lost from the land surface into the atmosphere (Yamazaki et al., 2011). In temperate climates it will make up 25 to 65% of the output from the catchment. In hot climates with seasonal rainfall it can make up the overwhelming majority of the water lost from the system (Shaw et al., 2011).

Potential evapotranspiration, E_p ([L]/[T]; mm/hr), typically expressed in mm/hr, is the maximum theoretical outward moisture flux due to these processes. E_p is always

greater than or equal to the actual evapotranspiration E_a (or E_t) and will depend on isolation, relative humidity, wind speed and soil moisture content.

The Penman-Monteith relationship (Montieth, 1965) can be used to calculate actual evapotranspiration from the interception and near-surface plant uptake stores (root zone) as

$$E_a = 3.6 * 10^6 * \frac{R_n\Delta + \frac{\rho c_p \delta_e}{r_a}}{\lambda\left(\Delta + \gamma\left(1 + \frac{r_c}{r_a}\right)\right)} \qquad \text{(Eqn. 2.1)}$$

with R_n= net radiation input (kW/m²); Δ = gradient of saturation vapour pressure against temperature (kPa/ºC), r_a and r_c the aerodynamic and canopy resistances respectively (s/m), ρ the density of air (kg/m³), λ latent heat of vaporisation for water (kJ/kg), δ_e the vapour pressure deficit (kPa), c_p the specific heat of air (kJ/kg) and γ the psychrometric constant (kPa/ºC).

The current version of SWAT allows the use, depending on the meteorological data available, of the Penman-Monteith, Priestley-Taylor (Priestley & Taylor, 1972) or the Hargreaves method (Hargreaves & Samani, 1982). The second two methods require only temperature and radiation input. In addition to the Penman-Monteith equation, MIKE-SHE and HydroGeosphere can use the Kristensen-Jensen scheme (Kristensen and Jensen, 1975) in order to estimate interception and evapotranspiration.

Plant canopies, particularly of trees, will intercept and retain precipitation and a significant proportion of input can be lost from this interception storage through evaporation. Beven (1979) showed that the rate removed as calculated by Eqn. 2.1 is extremely sensitive to the canopy resistance and aerodynamic drag parameters r_a and r_c, which are much larger for tree cover than for other vegetation types. Field studies show that between 10 to 40% of incident rainfall can be lost in forested areas (Zinke,

1967; Rutter et al., 1971). Rates for deciduous trees vary through the year depending on their leaf cover: a study from southern England found interception losses of 29% and 20% in the leafed and leafless periods, respectively (Herbst et al., 2008).

Models such as SHE and the Institute of Hydrology Distributed Model (IDHM: Beven et al., 1987; Calver and Wood, 1995) include an interception store from which evapotranspiration is removed and the remainder passed on to the surface by throughfall. A Rutter interception model (Rutter et al., 1971) is used. The canopy storage C ([L], mm) satisfies the relationship

$$\frac{\partial C}{\partial t} = Q - ke^{b(C-S)} \qquad \text{(Eqn. 2.2)}$$

where S is the canopy storage capacity (mm), b (mm^{-1}) and k (-) are drainage parameters, and Q (mm/hr) is the recharge rate due to rainfall less evapotranspiration, scaled by the proportion of ground obscured by vegetation.

TOPMODEL and Dynamic TOPMODEL implement a simple interception and "root zone" filled by incident rainfall and from which actual evapotranspiration in removed at a rate proportional to the potential as that time step divided by $S_{rz.max}$ ([L]; mm), its maximum capacity:

$$E_a = E_p . \frac{S_{rz}}{S_{rz,max}} \qquad \text{(Eqn. 2.3)}$$

where S_{rz} is the storage ([L], mm). This requires the specification of a time series of E_p. Calder et al. (1983) showed that the assumption of a sinusoidal variation in daily potential evapotranspiration through the year is a good approximation to more sophisticated methods. This model takes just one parameter, the annual mean daily potential evapotranspiration $\overline{E}_p$. For year day number d the total potential evapotranspiration is

$$E_{p,d} = \overline{E}_p \left(1 + sin\left(\pi \left(\frac{d}{365} - 0.5 \right) \right) \right) \qquad \text{(Eqn. 2.4)}$$

If the insolation is taken to also vary sinusoidally through daylight hours a time series of potential evapotranspiration at a time *t* after sunrise can be calculated from the day length at the catchment's latitude.

2.5.2. Precipitation

Rainfall data may be obtained at multi-instrumented AWS or at individual gauges of varying design. Radar provides good estimates for spatial extent of rainfall but is less accurate in determining its quantities. Many meteorological data are recorded at automatic weather stations (AWS) or manned stations. The Met Office Integrated Data Archive System (MIDAS, Met Office, 2012) contains many of these data collected across the UK from 1853 to the present. Temporal resolutions found in the MIDAS dataset range from 15 minutes to hourly, daily, weekly and months.

Rainfall is unlikely to be spatially homogeneous across a catchment, but a single hyetograph may be applied uniformly over the catchment, as for the Unit Hydrograph method. Models may allow for multiple spatially-distributed inputs corresponding, for example, to readings from gauges within or close to the catchment. The catchment could be divided according to the Thiessen polygons centred around each available gauge. Dynamic TOPMODEL allows the specification of a gauge ID for each HRU in order to associate rainfall input to areas in that grouping. Using this approach, Younger et al. (2008) demonstrated the use multiple rainfall data as input to Dynamic TOPMODEL applied to the Brue catchment in SW England. Other approaches attempt to interpolate the rainfall data between stations, or apply a weighting factor or factors according to altitude that take into account the effect of orographic (relief) rainfall.

Designed rainfall data can be useful for testing models and for rating flood defence schemes against events of known AEP. The SWRRB (Simulator for Water Resources in Rural Basins, Williams et al., 1985) applies a statistical approach to simulate daily rainfall input. The probability of rain given rain the previous day for the month and monthly averages are supplied for the basin and the series generated by a stochastic first-order Markov Chain model. Keef et al. (2013) provide a method to generate set of spatially-distributed rainfall events.

Snowmelt contributes some input to systems in higher latitudes and mountainous areas but in the UK is of less importance (Shaw et al., 2011). The accuracy of rainfall data in upland regions may be affected when collecting devices are covered by snow (e.g. Kirby et al., 1991). Calculation of snow melt equivalent to liquid precipitation is complex but a more straightforward approach is incorporated in SHE and variants . The amount of melt input M (mm/day) to the subsurface as $M = M_f(T_a - T_b)$, where T_a is the air temperature (Cº) and T_b a reference temperature with $T_a > T_b$ and M_f a factor appropriate to the aspect, region and season. When $T_b = 0$, M_f is known as the degree-day factor (Linsley, 1943).

SWAT incorporates an empirical snow melt component that provides input when the temperature of second soil layer rises above freezing, hence $M = T_a(1.52 + 0.54.T_s)$, with T_s the snow pack temperature in degrees celsius.

2.5.3. Infiltration

Infiltration is the movement of water from the surface into the subsurface. In physical models its rate is often calculated as a function of the soil moisture content and the surface water depth. The Richards Equation (Richards, 1931) for gravity drainage is derived from mass continuity combined with Darcy's Law

$$\frac{\partial \theta}{\partial t} = \frac{\partial}{\partial z}\left(D\frac{\partial \theta}{\partial z} + K\right) \qquad \text{(Eqn. 2.5)}$$

where θ is the specific soil moisture content, z the depth below the surface (m), K the hydraulic conductivity (m/hr) and the soil water diffusivity $D(\theta) = K\frac{\partial \psi}{\partial \theta}$ (m^2/hr). General solutions are not available and it must be solved by numerical means and applying the appropriate boundary conditions.

The Green-Ampt Equation (Green & Ampt, 1911) is particular solution of the Richards Equation allowed by assuming a sharp boundary at a depth z_f (mm) between an upper saturated region and soil at some initial wetness. The vertical (downwards) rate of infiltration f ([L]/[T], mm/hr) is:

$$f(t) = K_s\left(\frac{h_0(t) + \psi_f}{z_f} + 1\right) \qquad \text{(Eqn. 2.6)}$$

where t (hr) is time after the start of infiltration, h_0 (mm) the depth of ponded water on the surface, K_s ([L]/[T], mm/hr) the saturated hydraulic conductivity and ψ_f a parameter that relates to the capillary potential gradient across the wetting front. It can also be formulated in terms of the capillary drive $C_D = \psi_f(\tilde{\theta} - \theta_i)$ (mm) where $\tilde{\theta}$ is the field saturated soil moisture content (-) and $\theta_i$its initial state.

More straightforward infiltration formulas have been derived experimentally, such as the Horton Infiltration Equation (Horton, 1933) or by analytical solutions of simplifications of the Green Ampt equation. Examples of the latter include the Philip Equation (Philip, 1957) that makes use of the soil sorptivity s, ([T], hr) which must be found empirically:

$$f(t) = \frac{s}{2\sqrt{t}}K \qquad \text{(Eqn. 2.7)}$$

A storage-based formulation developed by Kirkby (Kirkby, 1975) is used in the CRUM model and the first version of TOPMODEL (Beven & Kirkby, 1979) and gives an explicit expression for the infiltration in terms of the current soil moisture

$$f(t) = a + \frac{b}{\theta} \qquad \text{(Eqn. 2.8)}$$

where a and b ([L]/[T], mm/hr) are empirically-determined parameters for the soil type.

In a later version of TOPMODEL the infiltration rate is simply taken to be the precipitation excess, the rainfall intensity minus any evapotranspiration, and water absorbed by spare capacity in the "root zone".

2.5.4. Unsaturated zone drainage (water table recharge)

The one-dimensional Richards Equation for gravity drainage can also be expressed in terms of the capillary (pressure) potential ψ ([M], Pa) and soil-water capacity ($[L]^{-1}$) $C = \frac{\partial \theta}{\partial \psi}$ and R ($[T]^{-1}$) a specific recharge / loss term due, for example to root zone uptake, evapotranspiration or direct input, with z again positive in the vertical downward direction:

$$C\frac{\partial \psi}{\partial t} = \frac{\partial K}{\partial z} + \frac{\partial}{\partial z}\left(K\frac{\partial \psi}{\partial z}\right) + R \qquad \text{(Eqn. 2.9)}$$

MIKE-SHE (Graham & Butts, 2005) models unsaturated drainage with an implicit numerical solution of the one-dimensional Richards Equation. The relationship between θ and ψ is specified via a retention curve that should be determined empirically for the specified soil type. MIKE-SHE considers only a single-valued function, although hysteresis is observed in the relationship. In HydroGeoSphere solution is formulated in three spatial dimensions in order to take into account variation of soil moisture across the hillslope:

$$\frac{\partial \theta}{\partial t} = \nabla.(\boldsymbol{K}\nabla\phi) + R \qquad \text{(Eqn. 2.10)}$$

TOPMODEL uses a simpler approach that estimates the unsaturated drainage rate u_z(mm/hr) at a particular time as $\frac{s_{uz}}{t_d S}$, the ratio of the overall moisture deficit in the unsaturated zone, s_{uz} (mm), to the total storage deficit *S* (mm) and a time delay constant t_d([T]/[L]; hr/mm). This is equivalent to a linear store with mean residence time of t_d hours.

The assumption of Darcy-Richards flow in the near surface for soils displaying macropores (large continuous voids) and preferential flows has been called in question by Beven & Germann (1982, 2013), amongst others. These macropores may allow direct recharge of the subsurface with little interaction with the soil matrix and spatial heterogeneity of flow pathways not well accounted in a framework that treats the soil as a continuous porous medium.

2.5.5. Saturated zone (water table)

As the movement of water downslope through the soil is slow, the Reynolds number will be less than unity. Most physically-based models therefore ignore changes in momentum when routing hillslope subsurface runoff.

The main axis of flow in the subsurface given by the direction of greatest hydraulic gradient. If the water table is taken to be approximately parallel to the local surface, this vector is perpendicular to the elevation contour lines.

Many models use an approximation for subsurface flows that assume a functional relationship between storage, or deficit, and specific flux per unit length of contour. Application of the mass continuity equation to subsurface flux *q* per unit contour width combined with Darcy's Law results in a kinematic formulation for hillslope runoff routing:

$$\frac{\partial q}{\partial t} + c\frac{\partial q}{\partial x} = S \qquad \text{(Eqn. 2.11)}$$

where x (m) is distance measured in the downslope direction, and S is the specific storage deficit (mm). The wave velocity, known as the celerity, is $c = \frac{\partial q}{\partial S}$ (L/T; m/hr), which may be much in excess of the flow velocity (Beven, 2010; Davies & Beven, 2012; McDonnell & Beven, 2014)

A kinematic approach is taken to routing flow between the gridded hillslope elements in G2G. Dynamic TOPMODEL also uses a kinematic routing procedure, except that this is now applied to route flow between the response units. The proportion of subsurface flow into downslope units, including themselves, is specified via a pre-calculated weighting matrix. This is determined from the topography, given an assumption of slope - hydraulic gradient equivalence. Contribution to channel flow is determined by the amount of hillslope flux redistributed by the matrix to a lumped "river" unit.

Transmissivity is the specific downslope subsurface flow per unit hydraulic head gradient. HydroGeoSphere and MIKE-SHE apply a three-dimensional scheme to deal with, for example, heterogeneity in the subsurface due to differential aquifer profiles. In the case where an aquifer's analytical transmissivity function can be defined, the formulation can be integrated over the depth of the water table to produce a two-dimensional scheme. TOPMODEL applies by default an exponential relationship for hydraulic conductivity versus and depth which results in an exponential transmissivity profile parametrised by a shaping factor m ([L]; m). The model applies a succession of quasi-steady state water table configurations where the rainfall input is considered to match the specific discharge. At each time step the entire catchment area is updated to

identify areas that have reached saturation according to the relationship for the storage deficit across a particular HRU (see Beven & Kirby, 1979; Beven, 2012)

$$D_i = \overline{D} + m\left(\gamma - ln\left(\frac{a}{tan\beta}\right)\right) \qquad \text{(Eqn. 2.12)}$$

with γ equal to the mean value of the TWI ([ln(L^2)]; ln(m^2)) and $\overline{D}$ ([L]; m), the mean deficit across the catchment. If $D_i <= 0$ then the corresponding area is taken to be contributing runoff that enters the channel.

Dynamic TOPMODEL, by contrast, determines saturated excess runoff which it then. Areas of saturation excess are determined from the soil moisture deficits maintained for each unit and updated at each time step by the difference between downslope output and input from upslope units and unsaturated drainage.

The lumped conceptual model PDM determines the runoff by determining the excess over capacity of areas that have filled over the time step. These are scaled by their sizes relative to the catchment area, as determined by a PDF, to obtain the runoff over the time step. Storages are then updated by that runoff and the rainfall and evapotranspiration and storage transfer between areas is estimated probabilistically.

2.6. Surface runoff

In most catchments the largest proportion of runoff reaches the channel via subsurface pathways. Even in humid catchments with high rainfall where the ground is close to saturation much of the time, 80% of the runoff is subsurface or near surface (Chappell et al., 1999, 2006).

Surface runoff is, however, a significant process. Its velocity will be much greater than in the subsurface. On natural surfaces velocities of up to 200 m/hr have been quoted (Barling, 1994), but through dense vegetation such as sphagnum moss

velocities are much lower, between 10 to 30 m/hr (Beven & Kirkby, 1979; Holden et al., 2008). Transport of sediment and erosion will largely take place during periods of surface runoff. In agricultural catchments overland flow is the primary means of transport of nutrients such as phosphorus (P) that cause ecological damage to water bodies (Heathwaite et al., 2005; Barber & Quinn, 2012; Thomas, et al. 2016). Efforts to mitigate nutrient over-enrichment will therefore identify areas with a propensity to produce this type of runoff (hydrologically sensitive areas or HSAs) that are hydrologically connected to the channel (critical source areas, CSAs) and seek to disconnect them through bund or other measures (Heathwaite et al., 2005; Thomas, et al. 2016; Roberts et al., 2017).

The significance of overland flow to flood risk is its contribution to fast response of catchment areas at or close to saturation. These areas are most likely to be close to the channel and will contribute to the rising limb of the hydrograph, bringing forward and intensifying the peak. FRM measures that reduce overland flow velocities will in theory slow this runoff so that it contributes to the falling limb instead.

2.6.1. Surface flow production

Surface runoff can arise through saturation excess, when the water table meets the surface and excess flows overland (Dunne & Black, 1970). Return flow occurs when unsaturated upslope drainage exceeds any remaining downslope soil moisture deficit (Cook, 1946). Infiltration excess, when incident rainfall intensity exceeds the maximum infiltration rate, can also produce surface runoff. Surface flow can be due also to fluvial flooding, such as when a section of channel overbanks and the excess propagates overland.

2.6.2. Modelling of surface runoff

Many hydrological models include a component to handle surface flow. There are also dedicated surface runoff models such as JFLOW (Lamb et al., 2009). A statistical approach is applied in the FEH and ReFH. In the former the Standard Percentage Runoff, SPRHOST, catchment descriptor determines the proportion of runoff taking surface pathways. Higher values of SPRHOST indicate that the soil class tends to produce more saturated overland flow as a consequence of lower hydraulic conductivities that inhibit drainage downslope. In the ReFH the Base Flow Index, BFIHOST, is used in conjunction with the PROPWET descriptor. PROPWET is the proportion of the catchment that is producing overland flow. 0 discusses the use of the SPRHOST descriptor in targeting areas suitable for flood mitigation measures designed to intercept or slow overland flow.

A topographically-based overland routing scheme is applied in TOPMODEL. Given a single overland flow velocity parameter v_{of}, ([L/T], m/hr) the time taken for overland flow generated at any point in the catchment to reach the outlet is

$$\sum_{i=1}^{N} \frac{x_i}{v_{of} tan(\beta_i)} \qquad \text{(Eqn. 2.13)}$$

where the x_i are the lengths of the segments of the flow pathways and the $\beta_i$their slopes. Flow pathways can be calculated from an elevation raster using a method such as the D8 algorithm, which follows the steepest slope between cell midpoints (Quinn et al., 1991). Multiple pathways are computed by the M8 algorithm, which calculates downslope flow proportion at each cell with by the weighted averages of the slopes to surrounding cells (Quinn et al., 1991). In both approaches travel times are then grouped into a time-delay histogram for each value of the surface runoff contributing

areas, and applied to route any overland flow generated by the model to future predictions of discharge at the outlet.

Hydraulic schemes for routing surface flows are generally based on versions of the Navier-Stokes equations for an incompressible fluid. Depth of flow is usually taken to be much less than the horizontal length scale of the channel or region of flow. The vertical component of velocity is presumed to be small and the pressure gradient due only to depth (i.e.is hydrostatic). Given these assumptions, the velocity can be integrated through the depth of flow to give the depth-averaged the Saint Venant or Shallow Water Equations (SWE, see Murilloa et al, 2008; Lamb et al., 2009, and many others).

The SWE are often expressed as single vector equation expressing conservation of both mass and momentum in an orthogonal spatial basis $\boldsymbol{x} = \begin{pmatrix} x \\ y \end{pmatrix}$ with velocities in these directions (Lamb et al., 2009):

$$\frac{\partial \boldsymbol{U}}{\partial t} + \frac{\partial \boldsymbol{F}(\boldsymbol{U})}{\partial x} + \frac{\partial \boldsymbol{G}(\boldsymbol{U})}{\partial y} = \boldsymbol{S}(\boldsymbol{x}, t) \qquad \text{(Eqn. 2.14)}$$

where

$$\boldsymbol{U} = \begin{pmatrix} h \\ hu \\ hv \end{pmatrix} \qquad \boldsymbol{F} = \begin{pmatrix} hu \\ u^2h + \frac{1}{2}gh^2 \\ huv \end{pmatrix} \qquad \boldsymbol{G} = \begin{pmatrix} hv \\ huv \\ v^2h + \frac{1}{2}gh^2 \end{pmatrix} \qquad \text{(Eqn. 2.15)}$$

The local water depth is h (m), u and v are the orthogonal velocity components (m/hr), and g is the gravitational acceleration constant = 9.81 m^2/s. If the source term $\boldsymbol{S}$ ($[L^3/T]$, m^3/hr) is non-trivial this is a non-conservative form of the SWE. The elements of $\boldsymbol{S}$ can comprise net mass recharge, r, from direct precipitation, evapotranspiration and infiltration, and momentum and energy change introduced, for example, through bed friction.

JFLOW solves the SWE for each cell in a gridded raster to obtain flood extents, water velocities and heights. An explicit numerical scheme is used that applies appropriate boundary conditions from neighbouring cells, edges of the raster, or wetting and drying fronts. Any friction source terms calculated from the Manning surface roughness. Parallel and grid computing techniques are applied that allow the model to be applied over large spatial extents at high resolution. The surface is modelled as though impermeable, but a proportion of the rainfall can be removed to emulate infiltration, artificial drainage or other losses. These can be estimated, for example, from the ReFH BFIHOST descriptor relevant to the catchment.

Making use of the commercially-licenced NEXTMap 5m DSMs, JFLOW produced the Updated Flood Map for Surface Water (uFMfSW, EA, 2013) that assists in predicting flood risk across England and Wales. This is used by Local Lead Flood Authorities (LLFA) in order to meet the requirements of the European Floods Directive. Local planning authorities, utilities and businesses also make use of the maps to make strategic decisions. Designed events of AEP of 1%, 0.3% and 0.001 & are applied.

Approximations to the Shallow Water Equations can be derived from neglecting some of its terms (Beven, 2012). Their applicability depends on the importance of the conserved terms, the magnitude of the time and space variations in the system and the relative contributions of the source terms. If the friction is neglected in the source term then the gravity wave approximation results. This is suited for deep water such as lakes and is not generally used in overland routing. If the flow velocity depth at a particular point is taken to be slowly varying in time $\frac{\partial u}{\partial t}$ and $\frac{\partial v}{\partial t}$ can be set to zero, resulting in the steady dynamic wave approximation which varies in space but not in time.

If the flow velocities are taken to vary slowly in space the spatial derivatives of u and v can be neglected. The assumption is known as the diffusion wave approximation to the SWE. Flow is driven by any imbalance between the bed friction (friction slope) and the gravity acting on the water surface (Bradbrook et al., 2004). An explicit expression for the velocity vector $\boldsymbol{v}$ at each point across time can then be shown to be (Bradbrook et al., 2004):

$$\boldsymbol{v} = -\frac{h^{2/3}\boldsymbol{\nabla} z}{n|\boldsymbol{\nabla} z|^{4/3}} \qquad \text{(Eqn. 2.16)}$$

where n is the Manning roughness coefficient (T/[L]$^{1/3}$; s/m$^{1/3}$) and z the surface elevation above a datum and h the water depth, both in m. The Manning roughness coefficient is frequently utilised in surface and channel routing models. Typical values are in the range 0.03 for short grass to 0.15 for dense willow growth. Chow (1959) supplies tables of n values for artificial surfaces, common ground cover types and other natural surfaces. Effective roughness can vary considerably from these values depending on the depth of flow and the nature of vegetation (e.g. Holden et al., 2008).

The kinematic wave approximation to the SWE arises by further equating the friction slope with the bed slope within the source term. The water surface is everywhere then assumed equal to the local slope, $\boldsymbol{\nabla} z = \boldsymbol{s_0}$. The velocity – depth ranges for which the kinematic wave formulation gives an acceptable approximation for surface flow routing is given by kinematic wave parameter (see Vieira, 1983).

2.6.3. Channel routing

In order to produce a time series of discharges flow entering the river channel components of a model must be routed to the catchment outlet. This may be undertaken hydrologically, i.e. via properties of the catchment taken as a whole, or hydraulically, whereby the channel state such as flow velocity and water depth are

modelled explicitly in space and time. Shaw et al. (2011) review a number of other methods for channel routing.

One hydrological approach, most suited for small catchments where hillslope runoff dominates over in-channel processes, is the Network Area or Channel width function method (Beven & Wood, 1993; Beven, 2012). Here the flow distance to the outlet for all areas in the catchment is calculated, and with a channel velocity applied across the network a time delay histogram produced. Earlier versions of TOPMODEL (such as that described by Beven & Kirkby, 1979) used the network area approach but at time *t* applied a non-linear wave speed determined from the current overall discharge *Q* (m^3/s) at time *t*:

$$c(t) = \alpha Q(t)^{\beta} \qquad \text{(Eqn. 2.17)}$$

where α (m^{-1}) and β (-) are parameters for the network. However, results from Beven (1979) suggest that a fixed wave speed could be more appropriate as well as being more stable and later versions (including Dynamic TOPMODEL) apply a single parameter v_{chan} (m/hr) across the entire simulation period.

Hydraulic routing approaches are found in many physically-based models. These are often one-dimensional approximations of the SWE with the *x* axis through the local midline and the velocity in the *y* direction, *v*, set to zero. Reasonably laminar flow is assumed Analogously to Eqn. 2.14 and Eqn. 2.15, the one-dimensional SWEs can be written

$$\frac{\partial \boldsymbol{U}}{\partial t} + \frac{\partial \boldsymbol{F}(\boldsymbol{U})}{\partial x} = \boldsymbol{R}(x,t) \qquad \text{(Eqn. 2.18)}$$

where $\boldsymbol{U} = \begin{pmatrix} h \\ hu \end{pmatrix}$ and $\boldsymbol{F} = \begin{pmatrix} hu \\ u^2h + \frac{1}{2}gh^2 \end{pmatrix}$.

The source term can take in account net mass change r arising from overland or subsurface flow, direct precipitation onto the channel or evapotranspiration loss, and frictional losses or gains from potential energy released due to flow down the sloping bed, e.g.:

$$\boldsymbol{R}(x,t) = \begin{pmatrix} r \\ -ghS_0 + gr^2/2 \end{pmatrix} \qquad \text{(Eqn. 2.19)}$$

For non-rectangular channels the source terms no longer scales linearly with the water depth and the equations are often written in terms of flow area A and the total discharge through this area, Q. It can be shown (e.g. Murilloa et al., 2008) that

$$\frac{\partial Q}{\partial t} + \frac{\partial}{\partial x}\left(\frac{Q^2}{A}\right) + gA\frac{\partial h}{\partial x} = gA\left(S_0 - S_f\right) + \frac{rQ}{A} \qquad \text{(Eqn. 2.20)}$$

where the friction slope $S_f = \frac{Q|Q|n^2}{A^2R^{4/3}}$ (-) and R (m) is the hydraulic radius, the ratio of the wetted perimeter P (m) to the flow area, A (m^2).

As for surface routing the kinematic or diffusion wave approximations can be used in channel routing. Another approach to hydraulic channel routing is to solves the Energy Equation for open-channel flow, a form of Bernoulli's Equation, for adjacent cross sections along the river length:

$$\frac{v_2^2}{2g} + h_2 = \frac{v_1^2}{2g} + h_1 - E \qquad (2.1)$$

where v_i and h_i are the flow velocity and midline water depth, respectively, at section i and E ([L]; m) is the head lost in the river segment between the two due to friction with the bed and structures impeding the flow. Head may also be lost due to contraction or expansion and changes in direction of the channel. The equation is solved by an iterative procedure called the Standard Step Method (Brunner, 2002).

For a given energy there are two solutions for mean water depth h and velocity v corresponding to critical and subcritical modes of flow. The value of the dimensionless Froude number $Fr = \sqrt{\frac{v^2}{gh}}$ indicates the flow mode. If > 1 the flow is supercritical, if < 1 subcritical, and Fr=1 indicates critical flow. The energy at which the flow is just critical is known as the critical energy and the equivalent water depth the critical depth.

The Energy Equation is not suitable across hydraulic jumps, where flow changes from critical to subcritical modes, or where significant momentum is added to the system. This can occur at a spillway, contraction or sudden change in bed height or at a river confluence. In these cases a momentum conservation equation must be used.

Mean velocity has been taken as $V = \frac{Q}{A}$, however channel flow is generally non-uniform through the cross section due, for example, to viscous and frictional forces interacting with the bed and banks. In the depth-averaged Saint Venant formulation a scaling factor β (-) can be introduced to take into account of the velocity distribution. In HEC RAS (Hydrologic Engineering Center River Analysis System; Brunner, 2002) the flow is partioned into channel, and L and R banks, allowing a different roughness and mean flow for each section.

TUFLOW (Two-dimensional Unsteady FLOW; Syme, 2001) and Flood Modeller Pro (formerly ISIS; Hill, 2015) are other commercial hydraulic channel routing models that employ full solutions of the Saint Venant Equations. As for HEC-RAS these are now linked to fully-distributed 2D components solving the SWE to route out-of-bank flow across the flood plain. JFLOW can also be used for this purpose. The Manning Roughness Coefficient is employed by all these models to express the roughness of the surface. Through altering its value in the corresponding grid cells, the models

therefore allow the investigation of effects on the storm response of increasing riparian roughness to slow and retain overbank flow.

2.7. Natural and catchment-based FRM

Upstream, distributed, nature-based approaches to FRM are reviewed by Quinn et al., (2013), EA (2014), SEPA (2016), Dadson (2017) and Lane (2017). The EA undertook a meta-study that collected 65 UK-wide case studies of flood risk management using WWNP (EA, 2017). JBA Trust (2016) have also provided an online resource that maps the known NFM implementations in the UK. This also now includes spatial mapping of opportunity areas for various types of flood risk interventions working with natural processes. These are identified as described in the user manual.

This section briefly reviews the measures applied in NFM. Dadson et al. (2017) and Beedell et al. (2011) categorise these measures in terms of their objectives. They are discussed in the following sections.

2.7.1. Hillslope runoff retention through improved infiltration

Hydrologically-sensitive areas (HSA; Thomas el al., 2016; Roberts et al., 2017) are regions of the hillslope that have a tendency to produce fast overland runoff. These may be regions with low infiltration rates, potentially with large upslope drainage areas relative to their slope.

Measures in this category aim to allow more runoff to enter the subsurface and thus mitigate the effects of flow via fast surface pathways and remove or avoid the creation of HSAs. This can be achieved through hillslope tree planting, which improves soil structure and increases permeability (Chandler & Chappell, 2008). Improved agricultural tillage and arable practices can avoid soil degradation and compromised infiltration. Here, and in urban areas, the use of more permeable ground cover, including different crop types, can be encouraged.

Afforestation can also increase evaporation losses significantly (Calder et al., 2003). This will affect the antecedent catchment wetness prior to an event, but will have more effect in summer events than in a sequence of winter events when potential evaporation rates are low.

2.7.2. Runoff retention through land-channel connectivity management and hillslope drainage

HSAs that are connected to the channel through fast overland flow pathways, or by other means such as artificial drainage, are referred to as Critical Source Areas (CSAs; Heathwaite et al., 2005). The measures in this section aim to disconnect fast pathways from the channel and thus disconnect CSAs, or to add additional hillslope runoff storage.

Well-sited tree shelterbelts (see Caroll et al., 2004) can intercept surface runoff and allow re-infiltration into faster-draining soils that may have spare moisture deficit. Small structures known as runoff attenuation features (RAFs) can also be placed in accumulation areas and across flow pathways (Wilkinson et al., 2010a, 2010b; Nicholson et al., 2012; Quinn et al., 2013) to intercept and store surface runoff. They are constructed from wood or earth and their capacity will be of the order of 20m³ to 1000 m³ (Deasy et al., 2010; Nicholson et al., 2012). The storage will leave through the permeable walls of the structure or a drainage pipe. Ground scrapes or ponds will also be able to retain some runoff and allow it to return to the subsurface by re-infiltration. Farm layouts can be redesigned, e.g. through careful siting of gates, to avoid poached areas that act as HSAs, connected to the channel by vehicle "tramlines".

Blockage of moorland "grips" , for example by infilling with peat turves or bale dams also reduces connectivity (Odoni & Lane, 2010; Holden et al., 2006, 2011). Buffer

strips between the agricultural land and arterial drainage channels will have a mitigating effect on fast runoff (Deasy et al., 2010).

2.7.3. Floodplain storage and river conveyance

This includes measures to better utilise floodplain storage and to manage the river and riparian area to slow channel and overbanked velocities. Additional roughness, for example through tree growth, will impede and retain overbank flow storage (Nisbet & Thomas, 2007; Nisbet & Thomas, 2008; Dixon et al., 2013).

Offline ponds can be partially connected to the channel to retain a portion of the overbank flow (Quinn et al., 2013). Wetland areas are also seen as a means of providing floodplain storage alongside ecosystem benefits (Acreman & Holden, 2013). Another initiative with these benefits is the reintroduction of beavers to a catchment, where their dams can introduce significant quantities of channel storage (Brazier et al., 2016; Puttock et al., 2017).

Large woody debris dams (LWD) and barriers within the watercourse will reduce flow velocities and increase channel storage through backwater effects (Odoni et al., 2011; Thomas & Nisbet, 2012). This could reconnect the channel with the floodplain, where measures to roughen this area will reduce effective flow velocities and increase utilisation of hillslope storage.

2.8. Summary

Table 2.1 summaries the models reviewed in this chapter. Table 2.2 presents a selection of representative NFM schemes and studies, indicating which measures discussed in Section 2.7 were applied, and which, if any, models were applied.

Table 2.1. Summary of models reviewed in Chapter 2

Model	Type	Primary purpose	Reference(s)
CRUM	Distributed	Hillslope runoff	Reaney et al. (2007)
Dynamic TOPMODEL	Semi-distributed	Hillslope runoff	Beven and Freer (2001a); Metcalfe et al. (2015)
FEH	Lumped conceptual	Flood forecasting	Institute of Hydrology (1999)
Flood Modeller Pro	Coupled hydraulic 1D / 2D	River and floodplain routing	Hill (2015)
Grid-to-Grid	Distributed	Hillslope runoff and river routing	Bell and Moore (1998); Bell et al. (2007)
HEC-RAS	Coupled hydraulic 1D / 2D	River and floodplain routing	Brunner (2002)
HydroGeoSphere	Distributed	Hillslope runoff	Therrien et al., 2010; Brunner and Simmons (2012)
INCA	Semi-distributed	Water quality modelling	Whitehead et al. (1998)
JFLOW	Distributed	Hillslope runoff / floodplain routing	Lamb et al. (2009)
MIKE-SHE	Distributed	Hillslope runoff	Refsgaard, and Storm, (1995)
PDM	Lumped conceptual	Hillslope runoff	Moore and Clarke (1981); Moore (2007)
ReFH	Lumped conceptual	Flood forecasting	Kjeldsen et al. (2005)
SCIMAP	Distributed (static)	Water quality modelling	Reaney et al. (2007)
SHE	Distributed	Hillslope runoff	Abbott et al. (1986)
SWAT	Semi-distributed	Water quality modelling	Arnold et al. (1999)
TOPMODEL	Semi-distributed	Hillslope runoff	Beven and Kirkby (1979)
TUFLOW	Coupled hydraulic 1D / 2D	River and floodplain routing	Syme (2001)

Table 2.2. Selected NFM studies and /or schemes across the UK

Study / catchment /region	Scale	Interventions considered	Model(s) applied	Reference(s)
Belford Burn, Northumberland	5.6 km^2	Hillslope - channel disconnection, bunds, leaky wooden dams; overflow storage areas; enhanced hillslope storage	FEH, ISIS, TOPMODEL	Wilkinson & Quinn (2010a, b); Wilkinson et al. (2010) Nicholson (2012); Quinn et al. (2013)
Pontbren, Powys (five subcatchments)	6 km^2	Hillslope shelter belts; reforestation; ditch blocking; land-use and management change		Jackson et al. (2008) , ;Wheater et al. (2008); Nisbet & Page (2016)
Holnicote, Aller and Horner Water, Somerset	22 km^2	Online leaky dams and sluices, land use change; tree planting, enhanced floodplain storage, upland ditch blocking; moorland restoration	JFLOW, ISIS, PDM, TUFLOW	Hester et al. (2016); National Trust (2015)
Brompton, N. Yorkshire	28 km^2	Online underflow barriers	Dynamic TOPMODEL	Metcalfe (2016); Metcalfe et al. (2017)
Pickering, N. Yorkshire	67 km^2	Enhanced floodplain roughness, riparian tree-planting; online leaky wooden dams, forest and moorland ditch blocking; bunds	OVERFLOW	Odoni et al. (2010); Lane et al. (2011); Nisbet et al. (2011)
Tarland Burn, Aberdeenshire	74 km^2	Hillslope runoff attenuation features, enhanced hillslope storage (ponds), riparian buffer strips	ISIS, TUFLOW, FEH	Ghmire (2013); Ghmire et al. (2014); Wilkinson and Jackson-Blake (2016)
Rivers Trust Life IP project, Cocker, Kent and upper Eden, Cumbria	226 km^2	Peat restoration, hillslope and riparian tree planting, enhanced hillslope storage	JFLOW, Dynamic TOPMODEL	Hankin et al. (2016, 2017)
Devon Beavers project, Otter and Tamar, Devon	250 km^2	Reintroduction of native species, woody debris and earth dams		Brazier et al. (2016); Puttock et al. (2017); Andison et al. (2017)

This chapter has discussed conceptual approaches to modelling rainfall-runoff processes. It has outlined the approaches taken by commonly applied physical models to implementing the Harlan-Freeze template. It has considered issues of uncertainty in the use of models and interpretation and presentation of their results. The processes that generate surface runoff and contribute to fast storm response have been described. and routing models for this runoff reviewed.

Catchment and nature based approaches to flood risk management have been discussed. Forthcoming chapters will describe these in more detail and develop new methodologies for modelling their impacts on storm runoff and their use in FRM.

Chapter 3. Dynamic TOPMODEL: a new implementation in R and its sensitivity to time and space steps

Reference

Metcalfe, P., Beven, K., & Freer, J. (2015). Dynamic TOPMODEL: A new implementation in R and its sensitivity to time and space steps. Environmental Modelling & Software, 72, 155-172.

Author contribution

- Primary authorship of text
- Collection and assimilation of data from third party sources
- Development of computer model code and generation of data
- Analysis and presentation of data
- Submission of initial version
- Preparation of all figures
- Responses to reviewers
- Revision of initial paper given reviewers' responses
- Submission of revised version
- Amending final proofs
- Preparation of figures for final publication

Abstract

In 2001, Beven and Freer introduced a "dynamic" variant of TOPMODEL that addressed some of the limitations of the original model whilst retaining its computational and parametric efficiency. The original assumption of a quasi-steady water table was replaced by time-dependent kinematic routing within hydrological similar areas. The new formulation allows a more flexible discretisation, variable upslope drainage areas and spatially variable physical properties.

There has, however, never been a freely distributable version of dynamic TOPMODEL. Here, a new, open source, version developed in the R environment is presented. It incorporates handling of geo-referenced spatial data that allows it to integrate with modern GIS. It makes use of data storage and vectorisation features of the language that will allow efficient scaling of the problem domain.

The implementation is evaluated with data from a 3.65 km^2 catchment. The formulation of the model in terms of a flow distribution matrix is described and its use illustrated for treatment of surface and subsurface flow routing. The model uses an improved implicit solution for updating the subsurface storages and fluxes. Discretisations of up to 12 units and time steps of between one hour and 5 minutes are considered. The model response stabilises around 8 to 10 units. The predictions applying successively smaller time steps approach those of the limiting case monotonically. The paper focuses on the robustness of the predicted output variables to these changes in the space and time discretisations.

Keywords: Dynamic TOPMODEL, R, Gwy, Plynlimon, distributed hydrological model

3.1. Introduction

Increased computing power, storage and availability of geo-referenced elevation and landscape data has made feasible, in theory at least, the implementation of fully spatial distributed hydrological models. However, in most catchments, the representation of complex fine scale process interactions in heterogeneous flow domains would still quickly overwhelm all but the most powerful hardware. Furthermore, the practical limits on the accuracy and spatio-temporal resolution of catchment data lays open to question whether it could ever contain sufficient information to justify such complex modelling schemes (Beven, 1993; Beven & Freer, 2001b; Jakeman & Hornberger, 2003; Beven et al., 2015)

Earlier generations of models were limited, by necessity, to a highly simplified representation of catchment processes. One example is TOPMODEL, a semi-distributed, hydrological model that has been applied in many studies (see Beven, 2012, and references cited therein). Subject to important simplifying assumptions it can simulate the response of a catchment to precipitation falling within the watershed and can also predict the spatial distribution of storage deficits and saturated areas and the initiation of saturation excess overland flow. The principles, assumptions and mathematics underlying TOPMODEL have been discussed in detail by many authors including Beven and Kirkby (1979), Barling et al. (1994), Beven (1997, 2012), Kirkby (1997), and Lane et al. (2004) and will not be explained in detail here. The fundamental principle is the aggregation of hydrologically similar areas of the catchment according to the value of a static topographic index. This, combined with a parametrically "parsimonious" approach and straightforward treatment of evapotranspiration and routing, simplifies the computational complexity and allows the model to be run extremely quickly. These properties have allowed the model to be

applied in studies of uncertainty estimation requiring many different model realisations and for long simulations for flood frequency estimations (e.g. Cameron et al., 2001; Freer et al., 1997; Blazkova & Beven, 2009).

The "dynamic" extension to TOPMODEL of Beven & Freer (2001a) attempted to address the issues arising from the simplified dynamics in the original model whilst retaining its computational and parametric efficiency. In particular, the assumption that the water table could be treated as a succession of steady state configurations consistent with the current subsurface drainage was discarded; instead a kinematic solution was applied to supply a time-dependent solution for the subsurface storage and downslope basal fluxes. The new flow routing and solution procedure for the storage deficits allowed relaxation of the assumption that downslope flows on hillslopes were always connected. It also freed discretisation strategies from the constraint of a single topographic index, and alternative schemes using any hydrologically significant, spatially distributed, characteristics could now be adopted. It also allows a wider spatial application, as the topographic index used by the original model begins to lose physical meaning at resolutions approaching that of global DEMs such as the SRTM (Shuttle Radar Topography Mission) and ASTAR GDEM data sets.

Applications of Dynamic TOPMODEL have included defining the parameter distributions needed to predict spatial water table responses (Freer et al., 2004); understanding sub-period seasonally different catchment behaviours (Freer et al. 2003); incorporating stream chemistry to understand flux behaviour (Page et al., 2007); the incorporation of different landscape response units to improve spatial conceptualisations (Peters et al., 2003); uncertainty estimation (Liu et al., 2009) and

quantifying the effect of spatial rainfall errors on model simulation behaviour (Younger et al., 2009).

The introduction of just one new parameter sd_{max} ([L], m), allows the model to simulate a variable upslope contributing area due, for example to the breakdown of downslope connectivity (Barling et al., 1994; Jencso et al., 2009; McGuire & McDonnell, 2010). The transmissivity profile is truncated at sd_{max} and when the overall storage deficit for a response unit reaches that level it ceases contributing to downslope flow. This may help to avoid the apparent overestimation of saturated transmissivity to compensate for an overestimation of effective upslope areas in the static topographic index noted by Beven et al. (1995) and Beven (1997, 2012).

3.1.1. Catchment discretisation

Dynamic TOPMODEL implements a formal treatment of the catchment as a "meta-hillslope". Topography, upslope drainage areas and flow distances are important properties of hillslope elements that fix their position and connectivity within this meta-representation (Beven & Freer, 2001a). It is still assumed within Dynamic TOPMODEL that areas with similar properties can be grouped together for computational purposes. This reduces run times, always an advantage of the original model, but now allows much more flexibility in defining these Hydrological Response Units (HRUs). In the limiting case where each HRU is identified with an individual raster grid cell this would be equivalent to a fully-spatially kinematic distributed solution at the corresponding grid resolution similar to the DHSVM model formulation (e.g. Wigmosta & Lettenmair, 1999). Carefully selected hydrologically significant GIS overlays can be introduced to provide a more detailed discretisation. A hydrological soils classification can be used to inform suitable values for spatially heterogeneous parameters such as porosity and surface conductivity. Geology,

vegetation cover and land use could also have a significant impact on hydrological response and spatially-referenced data for these are now widely available, albeit that this is not usually associated with estimates of effective values of the required hydrological parameters. Other spatially derived input data can also be attributed to each HRU allowing for spatial rainfall fields (e.g. Younger et al., 2009) as well as other variables of interest. Therefore, the model provides a flexible and powerful modelling framework which allows the user to embed different conceptualisations of hydrological responses within the landscape, thereby maintaining their spatial pattern, and exploring what amount of spatial disaggregation of parameters and structures are needed for individual applications.

Assuming the TOPMODEL kinematic slope-hydraulic gradient approximation, the downslope connectivity can now be inferred from a high –resolution digital elevation model (DEM). This procedure is not constrained to use rectangular gridded data and any method for calculating upslope contributing areas on a digital terrain model could be used (e.g. Tarboton, 1997). Here the M8 multiple flow directional algorithm of Quinn et al. (1991) has been used. This uses elevation data in a regular grid and distributes fluxes to all downslope cells, weighted by the slope in each direction. The result is a "flux-distribution" matrix characteristic to a catchment and discretisation that describes the likelihood of flux transfer from elements in one response unit to another. Much of the flux will be redistributed to the same HRU, which is to be expected, as it reflects the downslope transfer of flux through the unit until reaching its boundary with another HRU. This "recycling" proportion will reflect the spatial extent and contiguity of the unit in terms of the probabilities of exchanges between units. These probabilities form the flux distribution matrix within which non-zero elements reflect the positions of the HRU elements in the meta-hillslope.

This matrix, termed $\boldsymbol{W}$ (for weightings), is an important part of the discretisation and programme operation: it maintains information on the connectivity of landscape units in a compact, scale independent structure and is used in the implicit numerical scheme to route subsurface flow between response units. In the new implementation it is also invoked for the routing of surface flow and for model state initialisation. The matrix is constructed by aggregating all the proportions of subsurface flow within each unit, as identified by the M8 algorithm, which flow into other units or reaches of the river network. For *n* such response units, $\boldsymbol{W}$ is defined as:

$$\boldsymbol{W} = \begin{pmatrix} p_{11} & \cdots & p_{1n} \\ \vdots & \ddots & \vdots \\ & \cdots & \end{pmatrix} \qquad \sum_{i=1}^{n} p_{ij} = 1$$

Element $p_{i,j}$ represents the proportion of flow out of areas in unit *i* into those of unit *j*. Given a $n \times 1$ vector $\boldsymbol{s}$ representing the storage in each HRU at a given time step, $\boldsymbol{W}^T \boldsymbol{s}.dt$ will be a vector whose elements give the total mass flux from all units transferred across the small time interval *dt* into the corresponding groups.

3.1.2. Root and unsaturated zone moisture accounting

The representation of unsaturated zone fluxes and evapotranspiration in Dynamic TOPMODEL is straightforward and similar to the original version of TOPMODEL. More complex representations could be included, but Bashford et al. (2002) demonstrated that it was difficult to justify more complex representations of actual evapotranspiration even when "observations" were available at some grid scale above a heterogeneous terrain.

Actual evapotranspiration from each HRU is calculated from the supplied potential evapotranspiration and root zone storage. During dry periods actual evapotranspiration out of unsaturated areas, E_a ([L]/[T]; mm/hr), is calculated using a common formulation that minimises parametric demands (Beven, 2012), and is outlined in

Appendix 1. Evaporation is removed at the full potential rate from saturated areas and river channels. Rainfall input is added directly to the root zone, and then actual evapotranspiration calculated and removed. If the root zone is filled at this stage any excess rainfall input remaining is added to the unsaturated zone storage. Total drainage into the unsaturated zone across a time step is capped at the amount of remaining storage: overfill is added to the storage excess store and routed overland.

Recharge from the unsaturated zone to the water is at a rate proportional to the ratio of unsaturated zone storage to storage deficit and the gravity drainage time delay parameter, T_d ([T]/[L], hr/m). This is equivalent to a time-variable linear store with a residence time per unit of deficit given by T_d (Beven & Wood, 1993; Beven, 2012).

The canopy and root zone are implemented as a lumped store for each HRU. Moisture is added to the root zone store by rainfall input and removed only by evapotranspiration; interaction with the unsaturated zone, for example by capillary uptake, is not considered in this formulation (but see, for example Quinn et al., 1995). Rainfall input is added to each root zone store until "field capacity", the maximum specific storage available, $S_{rz,max}$ ([L]; m), is reached, when it becomes rainfall excess. If storage remains in the unsaturated zone then this is routed to the subsurface, otherwise it contributes to saturated excess flow and routed overland. Fast runoff is generated when the storage deficit in any unit is replenished. This will include both saturation excess runoff and return flows to the surface in areas of convergent topography.

3.1.3. Subsurface, surface and channel routing

The model assumes that in moderately steep catchments movement in the unsaturated zone is primarily due to gravity drainage to the water table as lateral velocities will be much lower than those in the vertical direction except in steep areas close to

saturation. In the 2001 implementation an implicit four-point time stepping scheme (based on that in Li et al., 1975) was implemented to solve the kinematic approximation for the subsurface fluxes. This has been modified in the current implementation to allow for the case where the HRUs are not strictly ordered downslope, as reflected in the general case of $\boldsymbol{W}$ with arbitrary diagonal and off-diagonal elements.

One or more elements of the flux distribution matrix will represent channel reaches and their values represent the proportions of subsurface drainage from each land unit that is transferred to the corresponding river reach. The convention used is for the river units to be held in the initial elements in an order reflecting their downstream positions. The first element of $\boldsymbol{W}$ will therefore generally maintain information for the catchment outlet reach.

A linear network width function routing algorithm, derived from the topography, is used to route channel flow to the outlet (e.g. Kirkby, 1975; Beven, 1979). A fixed channel wave velocity, parameter v_{chan} ([L]/[T]) is assumed with typical values in the range 1000-5000 m/hr. Beven (1979) has shown, based on field evidence, that this is a good approximation for the wave celerity in smaller catchments, even when flow velocities change nonlinearly with discharge. Beven and Wood (1983) demonstrated that hillslope runoff would dominate the hydrograph shape in small catchments, but channel routing would become more significant as the channel travel times start to exceed the model time step. At larger scales, therefore, an improved model could implement a more flexible channel routing procedure that included consideration of network connectivity, bed gradients and other forms of flow depth–discharge relationships.

3.2. The new implementation

Beven and Freer (2001) implemented the Dynamic TOPMODEL in FORTRAN-77. The code has not previously been released, but collaborations were welcome, and a number of derivatives developed (e.g. Page et al., 2007). In consequence, the model has not been exposed to the range of applications and alternative formulations of the original TOPMODEL. With this goal in mind, advantage has been taken of technological, data availability and storage improvements since the original release in order to make available a new, open source version.

Advances since the Dynamic Topmodel was first implemented include:

- software tools for processing of large scale spatial data: in raster and vector formats, for example the Geographic Digital Abstraction Library (GDAL and OGR, www.gdal.org),
- widespread availability of desktop GIS software;
- increased availability of geo-referenced data and improvements in bandwidth to allow their electronic delivery;
- availability of storage that allows large quantities of high-resolution digital landscape data to be maintained and computing power for their analysis.

Commercial and open-source GIS now provide extensive scripting capabilities that can be leveraged to provide a programme utilising GIS geo-processing facilities. It was felt, however, that a loosely coupled implementation that utilised data formats compatible with these environments, but that was not dependent on their use, would make the implementation available to the widest audience. This allows users to source and manipulate data in the tool of their choice before supplying it to the model.

3.2.1. Development environment

The R language and environment (R Core Team, 2013) was used to develop this new version. R was originally intended as a statistical analysis programming language, but many open-source third party "packages" have extended its capabilities to include time series handling (`zoo`, Zeileis & Grothendieck, 2005; `xts`, Ryan & Ulrich, 2008), spatial analysis (`sp`, Pebesma & Bivand, 2005; `raster`, Hijmans, 2014) and interoperability with GIS and geo-processing libraries (e.g. `spgrass6`, Bivand, 2014; `rgdal`, Bivand et al., 2014). In addition, the environment's origin in statistics and data mining means that it is optimised for integration, analysis and visualisation of large heterogeneous data sets such as those commonly encountered in hydrological analysis (see Andrews et al., 2011). The Python language and MATLAB environments were also considered as potential implementation platforms, but currently possess relatively basic spatial functionality except through integration with third party GIS software.

The new version of Dynamic TOPMODEL has been implemented as an R package `dynatopmodel` available via the Comprehensive R Archive Network (CRAN) at http://cran.r-project.org/web/packages/dynatopmodel/index.html. The R environment's package system provides a flexible and robust system for delivery and installation of third-party code. Packages are maintained by CRAN are subjected to rigorous, largely automated, quality-control before being accepted. This may go some way towards providing scientific users with the confidence to incorporate external code into their work flow. In addition, under the terms of the CRAN submission policy, documentation, working code examples and source code must be made available. This allows users to both validate the functionality and underlying algorithms of third-party modules and to understand their usage and concepts of the

codes.

The R environment is free, open source and multi-platform and provides a useful program development environment for the hydrological researcher. It is intended that other researchers should be able improve, modify and integrate this model with their own work thus the code has thus been structured with readability taking precedence over strict efficiency. As an interpreted language R can have some run time speed issues, such as when many Monte Carlo model runs are required, for example, but the environment can also call executable versions of core programs, as in the R implementation of the original TOPMODEL (see Buytaert et al., 2008).

3.2.2. Landscape pre-processing

A number of R packages for spatial data handling and analysis have been used extensively in the landscape pre-processing routines supplied in the `dynatopmodel` package. R may also integrate with GIS tools such as GRASS through API wrappers, but this would run counter to the "loosely-coupled" approach adopted. Cross-platform file formats such as tiff tagged raster (GeoTIFF) and vector (e.g. ESRI Shapefile) are used, with any non-spatial data maintained as ASCII text.

The `sp` package implements an extremely comprehensive class library for spatial data compatible with the R data structures such as `data.frame` and vector attribute tables maintained in Shape files. Other packages such as `rgeos` (Bivand & Rundel, 2014) and `rgdal` utilise the class hierarchy implemented in `sp` and provide most of the spatial operations found in GIS via interfaces to the GDAL and GEOS geo-processing libraries. The `raster` package inherits from `sp` and, in particular, enables disk-paging of large multi-band rasters such as those used in digital elevation models (DEM). These are commonly used to maintain gridded catchment elevation data sharing a common extent, resolution and coordinate reference system (CRS). The use of

spatially-qualified data significantly improves the geographical and functional range of applicability of the model, allowing landscape layers of different resolutions, extents and CRS to be consistently and quickly integrated and analysed.

Catchment data for a model run comprise a DEM in GeoTiff format and any relevant landscape layers used, and the location of the channel network supplied as a vector Shapefile, with individual reaches and their average widths specified in the `id` and `chan.width` columns of the attribute table. An overall width may be supplied if, as is the default, the river network is treated as a single channel. The procedure and output are illustrated diagrammatically in Figure 3.1.

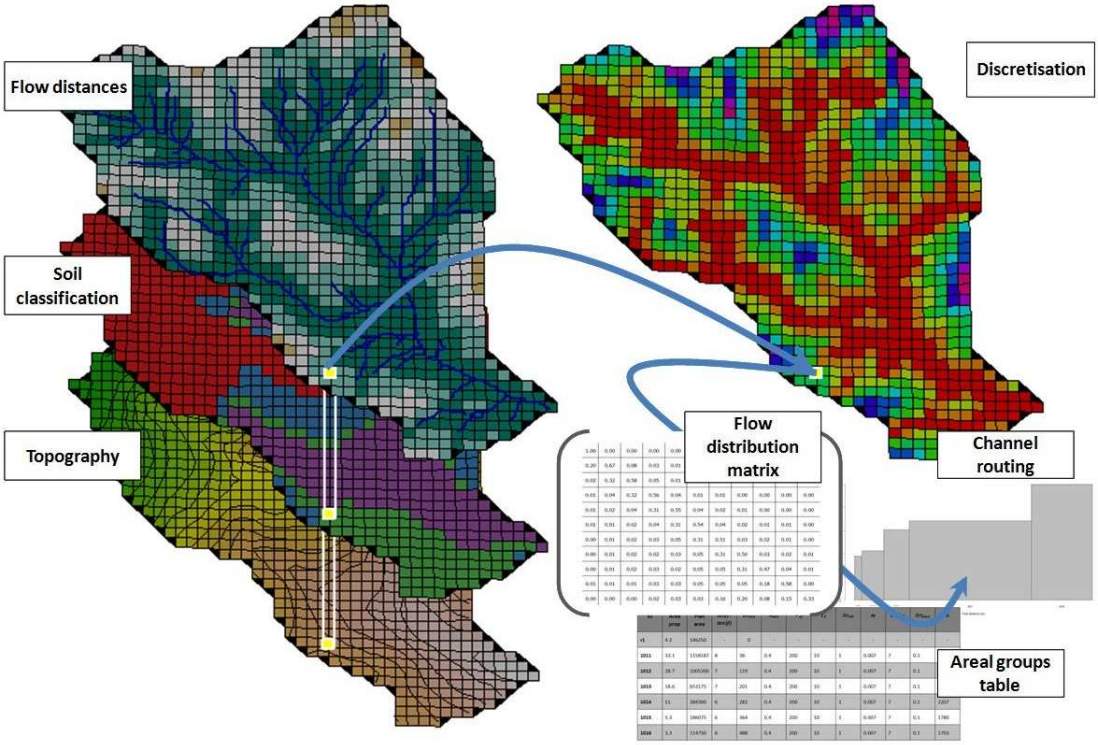

Figure 3.1. Aggregation of landscape layers into a catchment discretisation and its associated data structures

A discretisation strategy is specified by the order and number of breaks to apply to any of the raster layers provided and the chosen definition of the channel network. The routine `disc.catch` provided by `dynatopmodel` generates the files to run a simulation against observation data. This now allows a fast and flexible approach to

testing different discretisation strategies and hypotheses regarding the aggregated representations of catchments and landscape layers. Furthermore, it allows the user to test the results of adding features of an arbitrarily spatial scale that are expected to have a significant impact on the catchment's response. Examples would include impermeable areas that display very fast runoff such as areas of thin soils over granite bedrock found in the Panola catchment study (Peters et al., 2003). Discretisation output comprises:

- A multi-band raster composed of the spatial distribution of the response units followed by the catchment data that were combined to produce the distribution.
- The flow distribution matrix ***W***. Entries in other rows describe, for the HRU represented by that row, the fractional flux out of that unit either to this or another unit or to one of the river reaches.
- Tabulated HRU attributes (see Table 3.2).
- A channel routing table. This comprises a matrix whose rows represent outlet flow distance distributions, one for each HRU. The columns hold the proportion of the unit's flux that enters the channel at the corresponding distance from the outlet.

Any number of discretisations may be applied to a catchment using `disc.catch` and associated with a single "project" created with `create.proj` (see below). This allows their respective behaviour and performance to be compared and hypotheses regarding the nature and contribution of spatial heterogeneity to be evaluated.

3.2.3. Data pre-processing and management

Hydrological and meteorological data for runoff models are often of different time ranges and resolution. In addition, spatial data as are required by a semi-distributed

model may also vary in extent and resolution and in their coordinate reference systems. Managing these data can become problematic and many software tools have implemented solutions. Some GIS, for instance, have the concept of a geodatabase that can maintain spatial data for a single project.

The `dynatopmodel` package implements a simple project data structure to maintain the heterogeneous data required for analysis of a single catchment. Any number of discretisations applied to a catchment may be associated with a single "project", and, along with rainfall and observed flows, allows their respective behaviour and efficiencies to be easily compared. These facilities are described in more detail in the package documentation for `create.proj`, `add.disc` and related routines, found at `http://cran.r-project.org/web/packages/dynatopmodel/dynatopmodel.pdf` .A suggested workflow for incorporating existing catchment data and discretisations

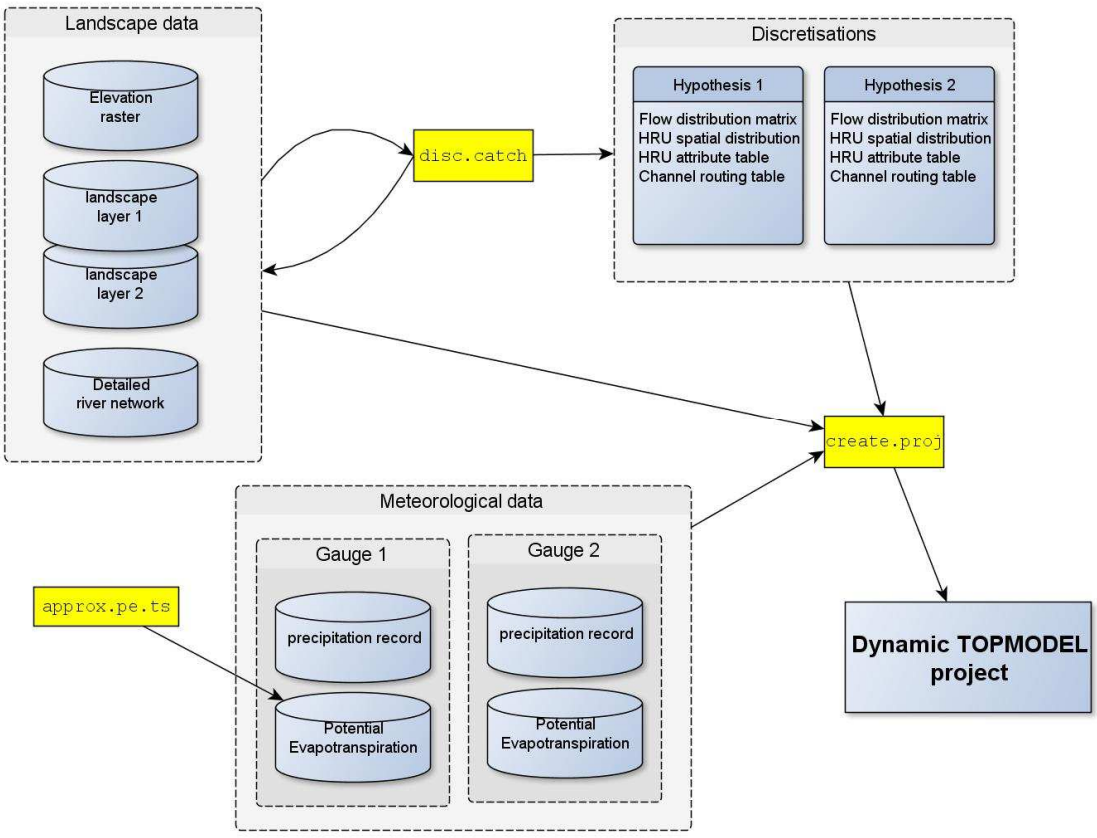

Figure 3:2. Dynamic TOPMODEL pre-processing workflow

into a Dynamic TOPMODEL project is given in Figure 3.2. Time series input data comprise rainfall, evapotranspiration and any observed discharges. If few meteorological data are available to calculate potential evapotranspiration directly, an additional module `approx.evap.ts` supplied in the can generate a representative time series given a daily maximum and minimum potential evapotranspiration (E_p) supplied by the user. This assumes a simple sinusoidal form for daily total insolation across the year and a linear relationship between insolation and E_p. Daily insolation is also assumed to vary sinsuoidally between sunrise and sunset and to integrate to the daily totals.

The routine `run.proj` handles the aggregation and checking of input data maintained in a "project" file created with `create.proj`. Time series are aggregated and averaged to the specified time step and their extents checked for consistency before being supplied to the main simulation routine `dtm.main`.

3.2.4. Initialisation

The model's behaviour is sensitive to the initial storage and fluxes. The programme allows specification of an initial discharge q_0 ([L]/[T]), assumed to be solely due to subsurface drainage into the river. Determination of the associated storage and unsaturated zone fluxes is then required to prevent a discontinuity in the initial discharges. One approach to achieve this would be to run the model for a "bed-in" period to allow its internal states to stabilise. For the original TOPMODEL this could take up to 2 weeks of simulation time (Beven et al., 1995). It is non-trivial to determine a generally-applicable initialisation period that would ensure that subsurface flows, storages and the river discharge have entirely stabilised by the start of the simulation run. In larger, slower draining and gentle sloped catchments this

could be considerable and running for a suitable bedding-in period would affect the run-time performance.

The new implementation instead applies an analytic steady state solution for the specific subsurface flows out of each HRU group, derived by mass balance considerations, and subsurface storages consistent with these discharges calculated by a method outlined in Beven (2012). The procedure is described in more detail in the appendix. The initial state of the catchment is taken to be a steady configuration where rainfall recharge and unsaturated zone drainage are everywhere equal to the initial specific discharge q_0. Assuming that this results only from subsurface flow, it can be shown that the discharge is related to the average initial storage deficit $\overline{D}$ within each group, which leads to an expression for $\overline{D}$ in terms of q_0. Gravity drainage flux is then initialised to the desired recharge rate q_0, and the corresponding unsaturated storage calculated.

3.2.5. Subsurface routing

In the earlier version of the model an implicit four point numerical scheme was used to solve for the subsurface fluxes out of each response unit over time. The new implementation employs a similar approach, but equates the inputs q_{in} into the response units q_{in} with the distribution of base flows q_b by the flux distribution matrix $\boldsymbol{W}$ and unsaturated drainage recharge obtained by the method described in 3.1.2. This reduces the relationship to a series of differential equations in q_b. The simplified scheme is then solved numerically by the `lsoda` algorithm (Livermore Solver for Ordinary Differential Equations, Petzold & Hindmarsh, 1983) accessed via the `deSolve` package (Seibert et al., 2010). This automatically selects the approach most suitable for the situation encountered: for "non-stiff" systems it employs an explicit predictor-corrector solution, whereas for "stiff" systems an implicit Backwards

Differentiation Formula (BDF) is used. Both approaches may be employed during the course of a simulation run. The explicit solution is tried first, and the implicit version introduced if the system is found to be substantially non-linear at that simulation time. This approach combines the speed of an explicit approach for periods where flow is fairly stable with the accuracy and stability of an implicit solution when flow is changing rapidly.

3.2.6. Surface and channel routing

The programme models and reports on overland flow generated by saturation excess, where rain falls on areas that have reached saturation as a result of volume filling from above and from return flow when lateral flux from upper areas exceeds the throughput capacity of downslope areas. Infiltration excess overland flow can also occur when rainfall intensity exceeds the soil's infiltration capacity, but as for the 2001 version, is neglected in the current version in order to avoid introducing additional parameters.

Maximum subsurface flows in each HRU are calculated from the transmissivity profile parameters and limiting transmissivity and local wetness index at each point within the HRU. Flow exceeding this is routed as saturation excess runoff. HRUs are assumed to behave homogenously within their plan area, so that when saturation excess runoff begins anywhere in the HRU it does so across its entire area. This can give markedly different results if the same parameters are applied to groupings of differing resolution (and thus contributing area) or based on different landscape criteria. Sensitivity to the discretisation is tested below.

In the original TOPMODEL, the distribution of the topographic index and model outputs indicate that saturation excess overland flow can often be generated in flatter areas on the hilltops, even though effective contributing areas will be small (Barling, 1994). This will not always be the case. Areas close to the divide with better drainage

or larger storage capacities due, say, to thicker soils may remain unsaturated. It is also the case that some or all of the surface flow from upslope might be absorbed, or re-infiltrated, into the "spare" storage capacity of downslope HRUs before reaching the channel. The new version of Dynamic TOPMODEL can handle these types of situation. At each time step, after subsurface fluxes and storages have been updated, surface flow generated in each HRU is added to an excess store for that unit. These are then distributed to downslope areas using the flow distribution matrix and a fixed overland flow velocity for that unit. Depending on the effective surface roughness, overland velocities can range from up to 100 – 200 m/hr (Barling, 1994) to as low as 10 – 30 m/hr (Beven & Kirkby, 1979) through grass and bog vegetation such as sphagnum moss. It is not therefore guaranteed that all surface flow will reach the channel within one time step. The surface excess storages are calculated to the end of the current time interval for all units simultaneously using an implicit scheme. The procedure, described in Appendix 1, solves a coupled set of differential equations resulting from consideration of the mass balance between input due to redistribution from upslope areas and output through overland flow downslope out of each unit. Overland excess distributed to the channel is routed to the outlet along with subsurface base flow, and updated surface storages in other areas are allocated as rainfall input of the relevant units at the next time step. The excess store is then emptied.

Channel routing is via a fixed wave velocity linear algorithm, as for the original implementation and TOPMODEL. Beven (1979) provides an empirical justification for this approach. Flux transferred to river elements is aggregated across the inner time steps, and on return to the main loop is routed to the outlet through a time-delay table calculated from the routing table input and the channel wave velocity. An

implicit time stepping scheme was implemented using a kinematic wave model but found to have little effect on the results. The modular nature of the code means that swapping out the channel routing logic for a more sophisticated approach based on the Saint-Venant equations, for example, could be used. However, in the test basins considered in Section 3.3.1 the linear routing was found to perform well.

3.2.7. Run time model structure

Input data, such as rainfall, evapotranspiration and those specific to a catchment discretisation, are supplied to the main routine via its arguments shown in Table 3.1. The entries in Table 3.1 are supplied as named parameters to the routine `dtm.main` shown at the start of the programme flowchart in Figure 3.4. A conceptual model of a Hydrological Response Unit within the new implementation, along with linkages with other units and model components is shown in Figure 3.3. The storages associated with HRU entities are defined in Table 3.3 and flows (shown by arrows linking entities in Figure 3.3) in Table 3.4.

Table 3.1: Main routine input parameter list

Internal name	Description	Symbol	Units	Default
`groups`	Response unit info		-	
`dt`	Main time step	Δt	hr	1
`w`	Flux distribution matrix	$\boldsymbol{W}$		
`rain`	Precipitation times series		m	
`pe`	Potential evapotranspiration		m	
`qobs`	Observed discharges		m/hr	
`v.chan`	Channel routing wave velocity	v_{chan}	m/hr	3000
`ntt`	Number of inner time steps		-	2
`disp.par`	Display parameters.		-	
`routing`	Routing table		-	
`run.par`	List of run parameters.		-	

Areal grouping properties, storages and fluxes associated with each HRU are maintained in R data frames, similar to the tables from relational databases. Each row corresponds to a single HRU and each column to the (possibly time-varying) quantities or fixed properties for that area. The vectors corresponding to each column can be referred to by name and operations between them quickly performed element-by-element.

Table 3.2: `groups` input table structure

Int. name	Description	Symbol	Units	Default
`id`	HRU ID	**-**	-	
`gauge_id`	Rain input gauge ID	**-**	-	1
`area_pc`	Catchment areal contribution of unit		%	-
`area`	Total plan (map) area of unit		m²	-
`atb_bar`	Average value of $ln(a)/tan(\beta)$index		m²/m	-
`sd_max`	Max deficit before subsurface flow	sd_{max}	m	0.3
`v_of`	Overland flow velocity within area	v_{of}	m/hr	100
`td`	Unsaturated zone drainage delay	t_d	hr/m	10
`srz0`	Root zone storage initially occupied	srz_0	%	100
`m`	Recession parameter	m	m	0.01
`ln_t0`	Saturated transmissivity	$ln(T_0)$	m²/hr	5
`srz_max`	Maximum root zone storage	srz_{max}	m	0.1

On initialisation external rainfall input is distributed between the groups. The model assumes spatially homogeneous rainfall but allows for spatially distributed input by associating each HRU with a particular rainfall record via the column index of the rain given by the value of `gauge_id` in the `groups` table.

The properties and state of each HRU are maintained in `groups` and `stores` data frames, and the internal and external fluxes that link them to other units and the exterior of the catchment by `flows`. The `groups` frame is supplied externally from the results of catchment discretisation, and `stores and flows` at each step in the simulation period are calculated and returned by the programme.

Table 3.3: `stores` internal table structure

Internal name	Description	Symbol	Units
`id`	HRU ID		
`suz`	Unsaturated zone storage	s_{uz}	m
`srz`	Root zone storage	s_{rz}	m
`ex`	Saturation excess storage	s_{sat}	m
`sd`	Saturated storage deficit	s_d	m

Table 3.4: `Flows` internal table structure

Internal name	Description	Symbol	Units
`id`	HRU ID		-
`pex`	Precipitation excess draining root zone	$p_{ex}p$	*m/hr*
`uz`	Gravity drainage from unsaturated zone	q_{uz}	*m/hr*
`qb`	Specific subsurface downslope flow	q_b	*m/hr*
`qin`	Upslope total input flow	q_{in}	m^3/hr
`qex`	Saturated excess flow	q_{ex}	*m/hr*

Flows and stores map to components of the conceptual response unit shown in Figure 3.2.

The module `init.input` validates the input, establishes the required data structures and initialises subsurface fluxes and storages using the approach outlined above. The programme then steps through the simulation period using the specified time interval `dt`, with the moisture accounting and subsurface routing undertaken in an inner loop. The modular programme structure is illustrated in Figure 3.3.

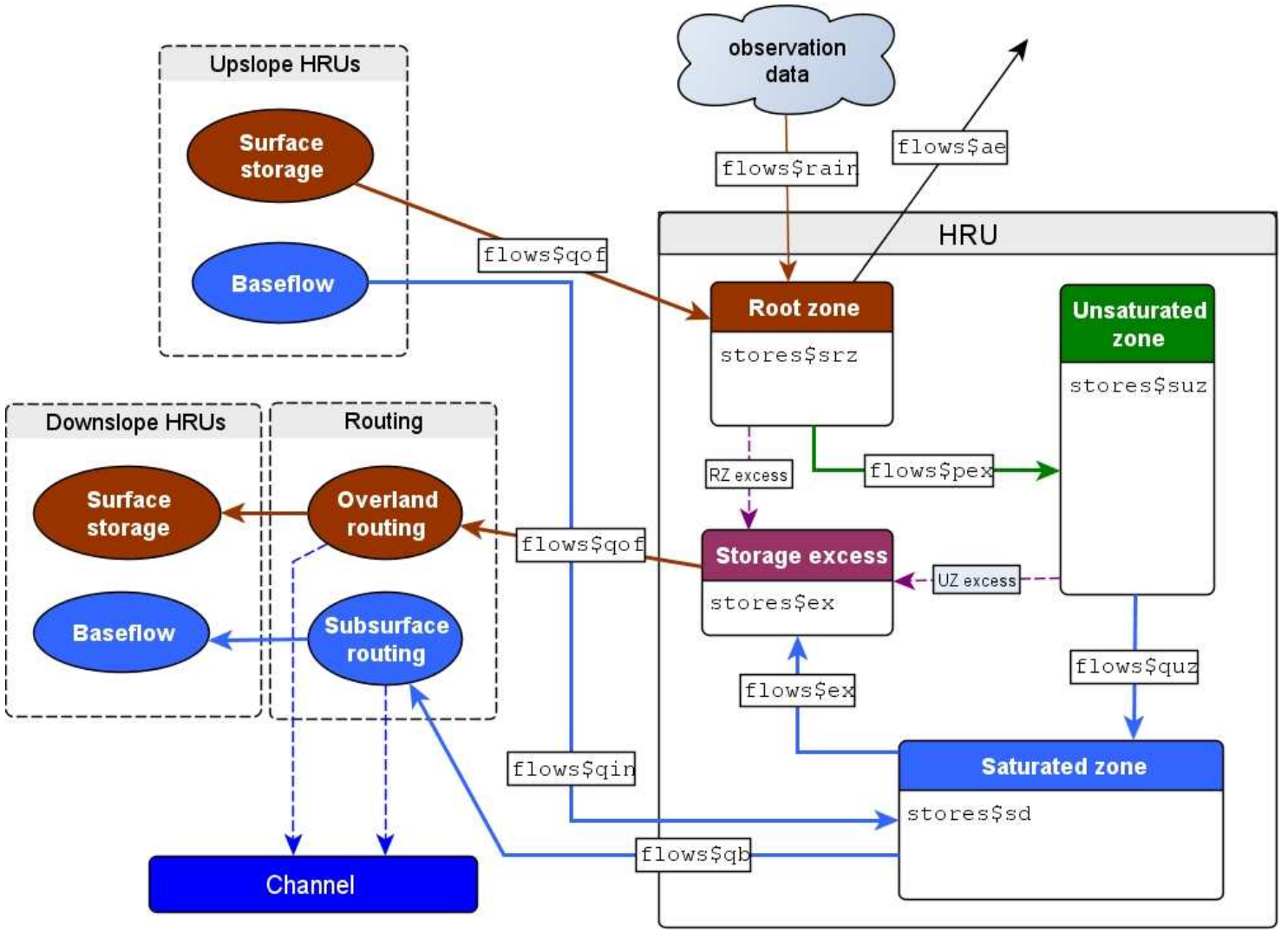

Figure 3.2. Conceptual structure and interfaces of hydrological response groups.

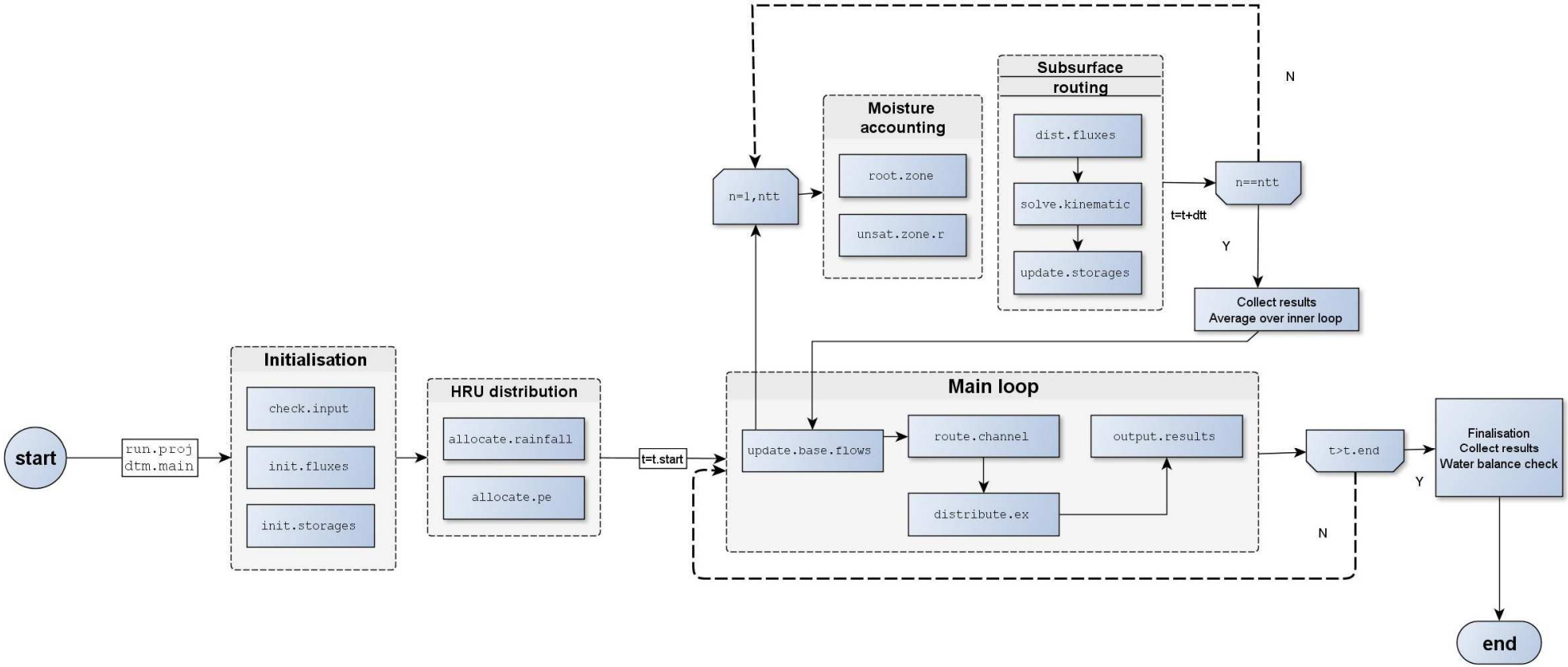

Figure 3.3. Dynamic TOPMODEL modular programme structure

3.3. Test data

3.3.1. Artificial landscapes

The basic operation of the model code and the sensitivity of the results to changing space and time discretisations were tested with a simple ”artificial” catchment divided into increasing numbers of downslope classes. The catchment takes the form of a V-shaped valley, with a convergent source area and convexo-concave hillslopes (Figure 3.4).

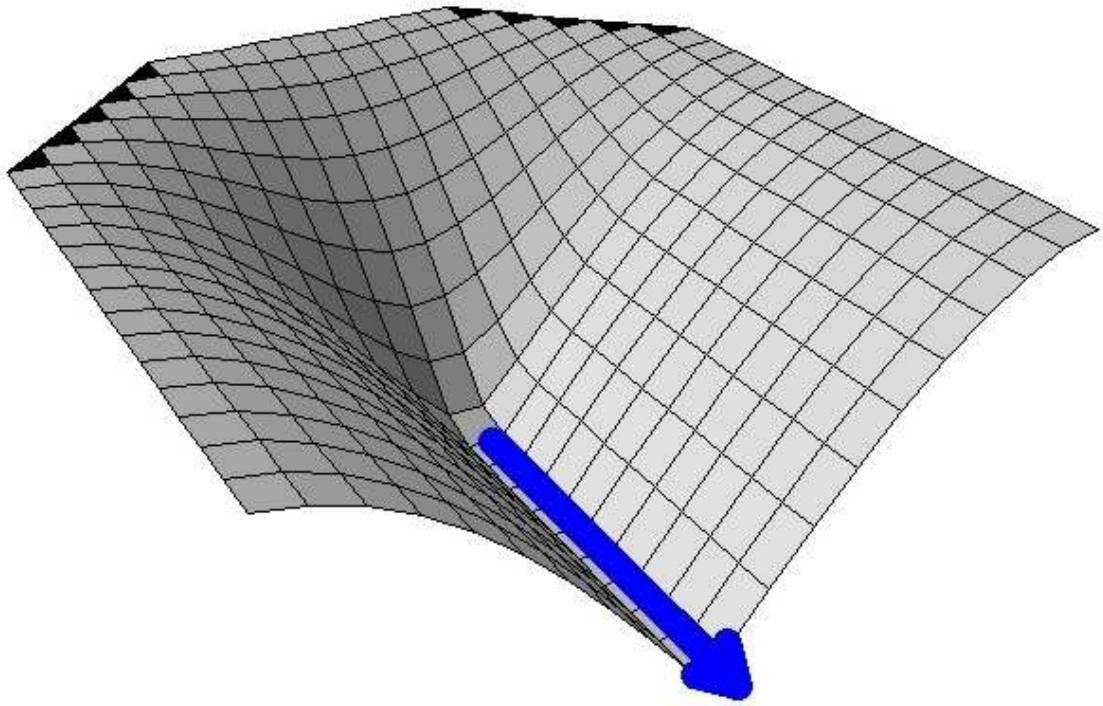

Figure 3.4. Simulated upland basin with a simple straight channel used in initial spatial and temporal sensitivity tests.

Rainfall data used were from a representative period from the Gwy catchment that will be described below, but the response to “artificial” rainfall events such as a short, intense impulse event was also examined.

3.3.2. Gwy test catchment

Data for a well-instrumented upland catchment were used to test the model for its

performance against observed discharge data and response to spatial and temporal schemes applied to actual topographic data. The Gwy forms the headwaters of the River Wye in Powys, Wales, draining the highest part of the Plynlimon massif, and has an average elevation of 586m. It is contained within the Plynlimon research catchments established in the late 1960s by the then Institute of Hydrology (now the Centre for Ecology and Hydrology, CEH) in order to investigate the differential uptake of water by forestry and open grassland. It has an area of 3.65 km² divided between a main basin and a southern tributary, the Nant Gerig. Soils are blanket peat on the flat summit areas, peaty pozdols on the hillslopes and gleys in the valley bottoms (Kirby et al., 1991; Newson, 1976b). The highest areas are heath, grassland predominates on the better-drained hillslopes and mires occupy the valley floors. Underlying bedrock is Ordovician massive gritstone whilst higher elevation areas are slates and Silurian mudstones (Newson, 1976b). Precipitation is high, averaging around 2600mm pa, dominated by synoptic rainfall that occurs throughout the year. Peat on south to south-westerly aspects is subject to desiccation which when on slopes steep enough (>0.2) to impart sufficient hydraulic gradient has lead to the formation of intricate networks of near surface "soil pipes" (Newson & Gilman, 1980; Jones, 2010). The catchment has been instrumented since the early 1970s and flows at 15 minute intervals collected at a gauging station established in 1999, just upstream of its confluence with the Nant Iago. The flume is a rectangular, side contracted critical depth design accurate across a range of discharges and easy to clear of solids deposited by the heavy sediment loads.

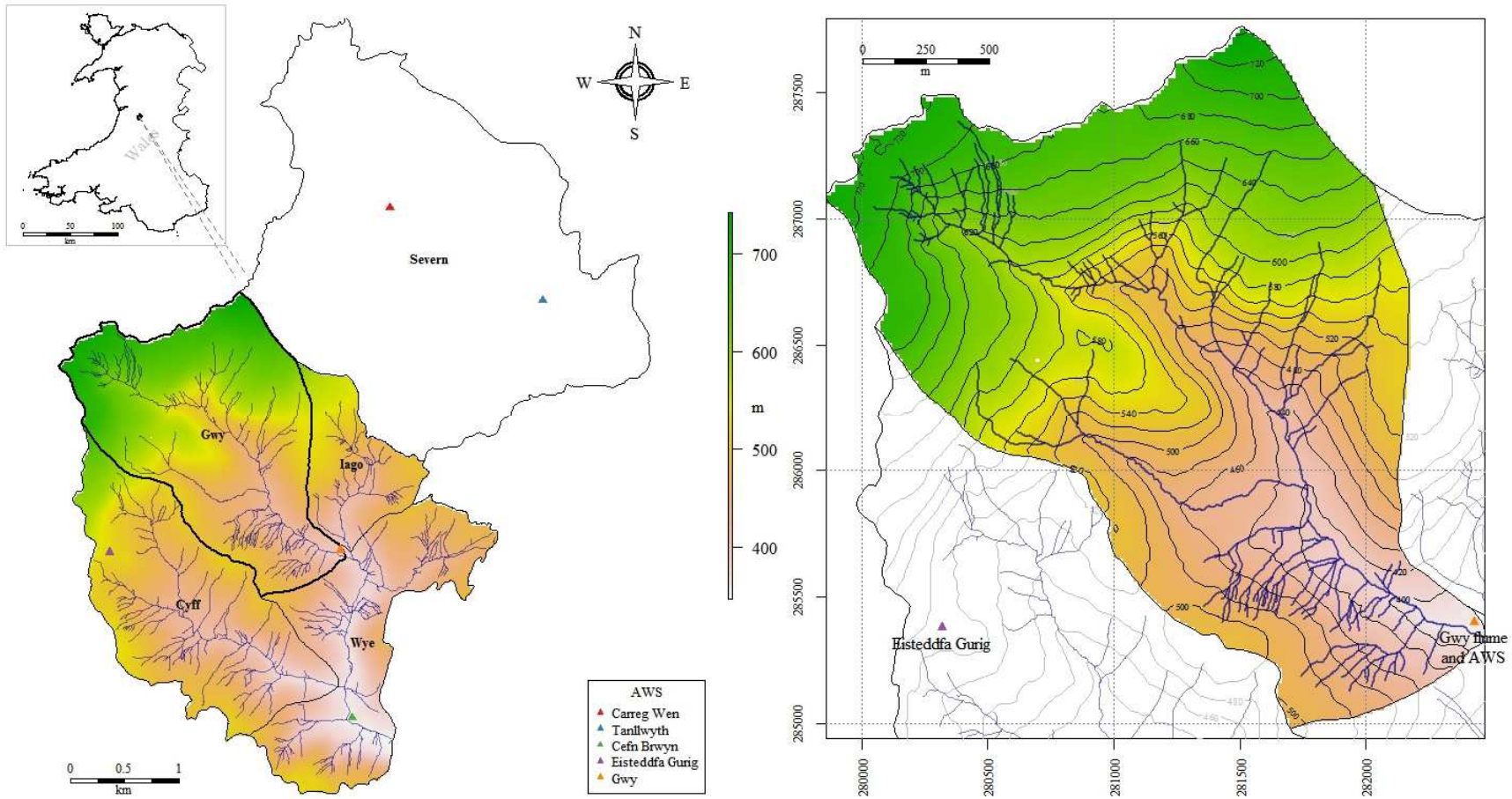

Figure 3.5. Overview of Gwy test basin, showing its location within the Plynlimon research catchments in mid Wales. The channel network for Wye and weather station locations are also shown. Digital elevation data ©Ordnance Survey (GB), 2012. Catchment boundaries and digital river network, CEH (2012)

Hourly rainfall and a variety of other chemistry and meteorological data have been collected since 1976 from Automatic Weather Stations at Carreg Wen and Eisteddfa Gurig, located at about 500m in the upper parts of the Hafren and Cyff subcatchments bounding the Gwy to the north and south, respectively, and at Cefn Brwyn near the catchment outlet. Newson (1976a) noted significant variations across small spatial scales in these catchments, which she attributed mainly to orographic effects. Data for 2008 for the two upper gauges obtained from CEH and displayed good agreement, with a correlation of 0.88, and for this study the rainfall input for Carreg Wen was applied homogeneously across the catchment.

A test period of around 4 months from early 2008 was chosen (Figure 3.6). Discharge and rain records are continuous across the period and other AWS data show that snow fall was negligible. The period contained both a series of intense rainfall events that took place in the week of the 14th to 21st January when storm flows of up to 7.33 mm/hr were recorded, and an extended recession period in mid-February which saw over a week of discharges < 0.05 mm/hr. The storm events allowed us to test the model's capacity to simulate high flows where saturation excess overland flow becomes significant. Simulation of low flows and the response in wetting-up periods can also be considered during the dry period in February and the subsequent prolonged rainfall. Average time from peak rainfall to discharge in the order of just 1 to 2 hours; in the first storm the discharge is seen to rise within 9 hours from a minimum at the end of a recession period of 2.6 mm/hr to a maximum of 6.9 mm/hr.

Long term studies of the water balance of the area (e.g. Marc and Robinson, 2007) have concluded that the catchments are relatively impermeable with little loss of water through the bedrock. Thus the 250 mm excess of rainfall over discharge observed in 2008 was taken to be solely due to evapotranspiration. This is considerably lower than

figures of between 435 mm and 491 mm for the entire Wye catchment (see Marc & Robinson, 2007, and references cited therein). It is, however, consistent with average E_a they quote of 255 mm/pa for the Gwy in the years 1972-2004. McNeil (1997) gives an estimate for 1992 of 0.91 for the E_a/E_p ratio in the upper areas of the Wye. If this is assumed to be entirely evapotranspiration, the total E_p estimated for the year would be 288 mm. An hourly time series consistent with this total was generated using the `approx.pe.ts` routine provided in the `dynatopmod` package, specifying a maximum daily total potential evapotranspiration of 1.5 mm and minimum of zero.

Discretisations based around the local slope, upslope contributing area and flow distance to the nearest channel (both obtained through the D8 algorithm) were tried. These were considered as well-correlated with the spatial distribution of the hillslopes and so allow the effect of increasing the numbers of downslope groups to be more easily observed. The upslope area was selected as it is quickest to calculate from within the programme environment and so could be used to investigate the response to spatial discretisation.

The channel network used was derived from aerial survey commissioned for the Plynlimon project. Due to the small size of the catchment and relatively high bed gradients most flow entering the channel is likely to pass through the outlet within an hour time step. Although the programme allows for multiple reaches with varying widths, the channel was therefore represented as a single reach of nominal width of 1m throughout; the resulting channel approximation occupied 1.7 % of the catchment area.

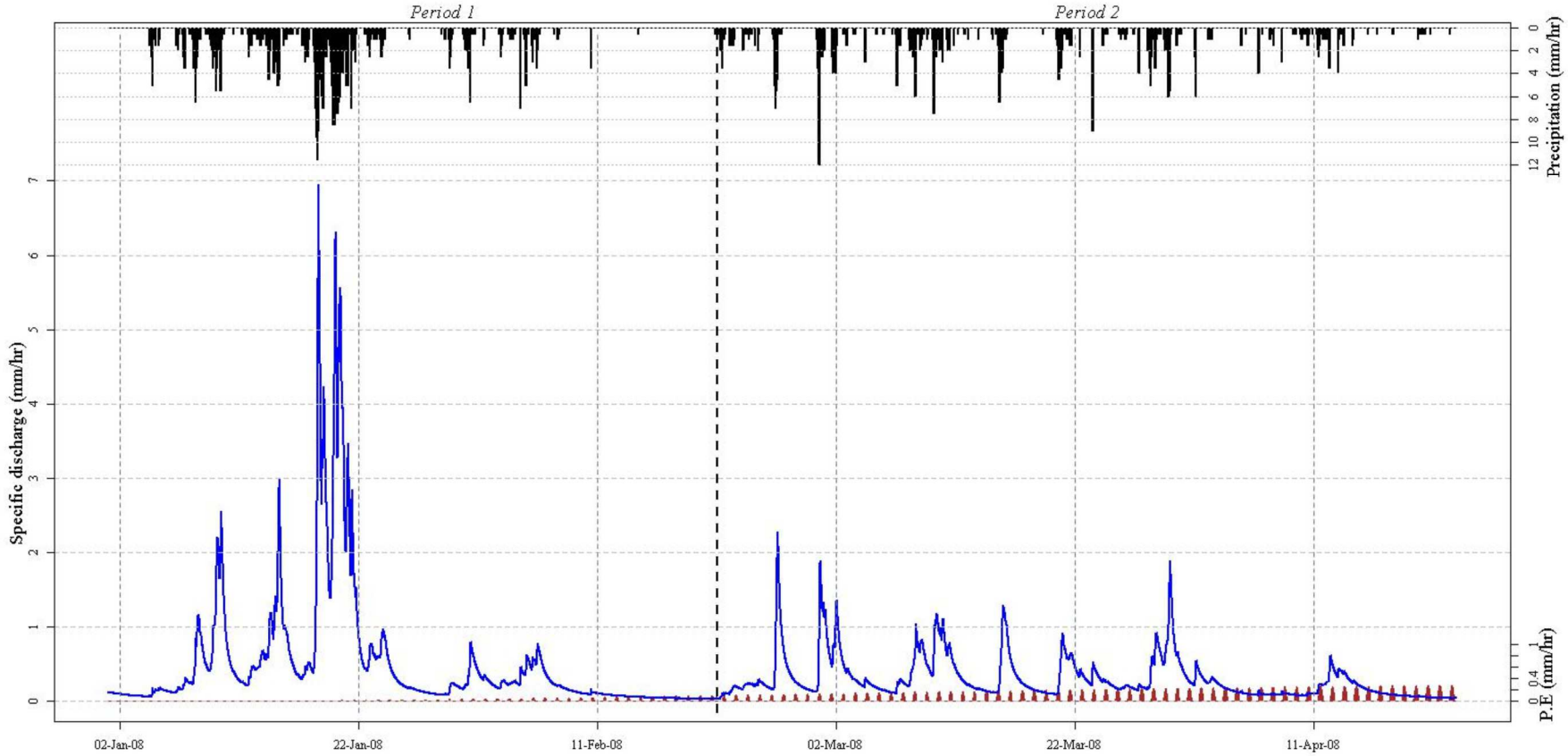

Figure 3.6. Test period showing rainfall, estimated potential evapotranspiration (in brown, simulated) and observed discharges at the Gwy flume. Storms occupy the first month of the simulation, separated by a week of dry weather from a period of less intense, but persistent, rainfall lasting from late February through to April.

3.4. Results

3.4.1. Parameter estimation

The emphasis of this paper is on the numerical performance of the model, but for this to be carried out a behavioural parameter set is required. A likely range for the recession parameter *m* can be estimated from the falling limbs of the hydrograph using the semi-automated technique of Lamb and Beven (1997). The onset of saturated excess overland flow is largely controlled by the limiting transmissivity $\ln(T_0)$; *t*he initial rapid response and storm-level discharges appeared to require the initiation of these flows. For example, the peak on the 15th January could best be simulated by allowing two to three hours of overland flow to occur; while in the later storms additional return flow was required to match the peak flows. Manual adjustment of the parameter values and examination of its effect on the flow peak thus allowed a probable range for $\ln(T_0)$ to be estimated. Approximately 5000 parameter sets were sampled from the ranges given in Table 3.5 and a simulation run for each, using a 7.5 minute time interval, across the first series of storm events in the test period. This showed the performance to be most sensitive to the values of $\ln(T_0)$ and *m* but, inside a broad range of values, relatively insensitive to unsaturated drainage delay t_d and initial and maximum root zone storage, srz_{max}; their effect was greatest at the start of the simulation and the onset of flow after a recession period. As these occupy a small proportion of the simulation time their effect on any quantitative measure of model fit is unlikely to reflect the effect on the qualitative fit. These latter parameters were therefore fixed at representative values well inside these stable regions. Given that the test period contained no extended dry spells with high evapotranspiration the maximum deficit sd_{max} was not found to be relevant.

Table 3.5: Parameter ranges and values used in response tests.

Parameter	Description	Units	Lower	Upper	Applied
v_{of}	Overland flow velocity	m/hr	10	150	100
m	Form of exponential decline in conductivity	m	0.0011	0.033	0.0068
srz_{max}	Max root zone storage	m	0.01	0.2	0.1
srz_0	Initial root zone storage		0.5	1	0.98
v_{chan}	Channel routing velocity	m/hr	500	5000	3000
$ln(T_0)$	Lateral saturated transmissivity	m²/hr	3	16	15.2
sd_{max}	Max effective deficit of saturated zone	m	0.2	0.8	0.5
$1/t_d$	Reciprocal of unsaturated zone time delay (delay in brackets)	m/hr	0.01 (100)	100 (0.01)	2 (0.5)

The code limits unsaturated zone drainage across a time step to the contents of the zone, meaning that very small values of t_d effectively drain the entire zone within one time step. Corresponding values for time delay are shown in brackets. The parameters identified were then used in the following responses tests.

3.4.2. Sensitivity of model outputs to temporal discretisation

The kinematic approximation for the subsurface storage, although solved with an implicit solution scheme, is sensitive to non-linearity in the storage-discharge relationship. This leads to a potential loss of accuracy in periods where the response is most non-linear. Numerical inaccuracies that arise due to inappropriately applied time-stepping schemes can even outweigh structural errors within a model (see Clark & Kavetski, 2010). Dynamic TOPMODEL implements a scheme to solve for the subsurface fluxes across time and allows this to be run within an inner loop with an arbitrary number of time steps. The number of steps is set in the parameter `ntt`, defaulting to two. This should reduce numerical dispersion and the potential for non-convergence where non-linearity has greatest impact. Root and unsaturated zones are updated explicitly and here the choice of time step will have greater impact, and these

routines are also run within the inner loop. The inner loop enables discharges to be simulated at the same outer time step as observed flows, for example, whilst running internally at a much finer time interval. Surface routing makes use of an implicit approach and channel routing a time delay algorithm, and both are run in the outer loop. A further advantage of using an inner loop is, therefore, that the same channel routing table may be used for a range of inner time steps.

3.4.3. Temporal response - test landscapes

To test the effect of the inner time interval a simulation using five response units was run repeatedly, at each stage increasing the numbers of steps. A representative parameter set was used with values taken from the last column of Table 3.5. Channel routing velocity was 3000 m/hr, which ensured that all flow left the basin within one time step. An outer time interval of 1 hour was used and 1, 2, 4, 8 and 12 inner steps applied, corresponding to intervals of 60, 30, 15, 7.5 and 5 minutes respectively. Responses are summarised in Figure 3.7and Table 3.6.

Table 3.6: Temporal sensitivity response: $q_{\Delta t_i}$ is the simulated discharge when using the time interval Δt_i .

Δt	**Water bal. %**	**$\sum q_{\Delta t_i}$ (m)**	**$\overline{\left\|(q_{\Delta t_i} - q_{\Delta t_{i-1}})\right\|}$**	**$\overline{\left\|(q_{\Delta t_i} - q_{\Delta t=5})\right\|}$**
60	1.2	0.62		3.2
30	1.2	0.62	1.7	1.5
15	1.2	0.62	0.88	0.6
7.5	1.2	0.62	0.45	0.15
5	1.2	0.62	0.15	0

Mean absolute difference of observations between successive trials is given by $\overline{\left|(q_{\Delta t_i} - q_{\Delta t_{i-1}})\right|}$. The mean difference of observations between each trial and the trial with the smallest time step is given in the column headed $\overline{\left|(q_{\Delta t_i} - q_{\Delta t=5})\right|}$ in Table 3.6.

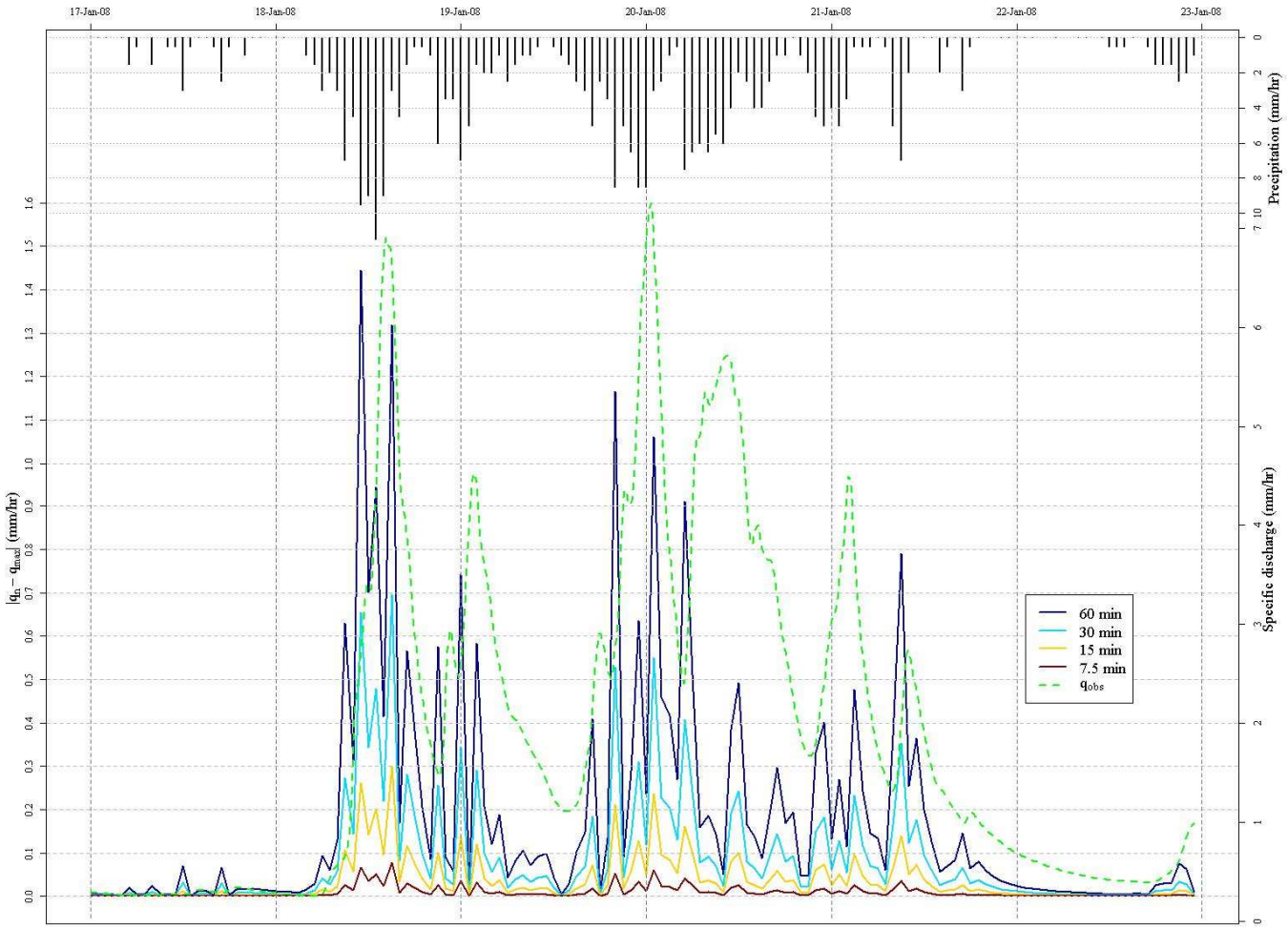

Figure 3.7. Response of hypothetical catchment to changes in time interval. Shown are the absolute difference of the predicted discharges within each trial from those predicted using a time step of 5 minutes. Central part of storm event within test period show; evapotranspiration output suppressed.

A rapid convergence between successive trials and approach towards the final response is seen. As the time interval decreases flood peaks become more pronounced and model response more rapid. Water balances and flow totals are consistent, demonstrating the soundness of the internal operation of the model and its moisture accounting logic. The excess is due to channel and root zone storage that has not been accounted for between the start and end of the runs.

3.4.4. Temporal response - Gwy

Sensitivity tests to time and space intervals were undertaken as for the simulated catchments. A discretisation comprising eight response units was used with the parameters shown in the final column of Table 3.5 were applied to all units. The mean percentage difference between observations from consecutive trials is given by $\overline{\left|\left(q_{\Delta t_i} - q_{\Delta t_{i-1}}\right)\right|}$. The mean percentage difference of observations between each trial and the final run, using a 5 minute time interval, is given as $\overline{\left|\left(q_{\Delta t_i} - q_{\Delta t=1}\right)\right|}$ in Table 3.7. The total discharge through surface saturation flow, $\sum q_{ovf}$, is also recorded.

Table 3.7: Temporal response for Gwy catchment. Figures to 2 s.f.

Δt (min)	**Water bal %**	$\sum q_{\Delta t_i}$ **(mm)**	$\sum q_{ovf}$ **(mm)**	$\overline{\left\|\left(q_{\Delta t_i} - q_{\Delta t_{i-1}}\right)\right\|}$ **%**	$\overline{\left\|\left(q_{\Delta t_i} - q_{\Delta t_5}\right)\right\|}$ **%**
60	0.18	0.62	0.23		2.2
30	0.18	0.62	0.16	1.2	1
15	0.19	0.62	0.12	0.6	0.41
10	0.19	0.62	0.1	0.2	0.2
5	0.19	0.62	0.063	0.2	0

Successive trials steadily approach the results of the final run and the differences between successive runs also decrease in a predictable manner. Overland flow totals decrease with time interval. This may be due to saturation excess flows of duration shorter than the time step, where the entire interval might be identified with the saturated flow leading to an apparent overestimation. Total discharges over the

simulation period are constant, however, showing that flow not routed overland is being routed by fast subsurface flow.

3.4.5. Sensitivity of model outputs to spatial discretisation

The model allows the catchment to be discretised to any level of detail until the limiting case where a single grid cell is identified with a single HRU. Experience with the original TOPMODEL shows, however, that there is likely to be a number above which any improvements in the model's performance is outweighed by performance overheads and the limitations in the observed input and output data (e.g. Beven and Smith, 2014). To test this effect in the new model, a parameter set and time step were fixed and successively finer discretisation based on upslope specific drainage areas applied.

Onset of saturated flow is largely controlled by limiting transmissivity and the overall wetness index. As the latter increases exponentially with distance downslope, very fine discretisations can lead to areas close to the channel apparently providing overland flow in response to any rainfall. This effect was overcome in the catchment pre-processing by applying a minimum areal contribution of 1% for an area to appear in the discretisation; smaller areas are amalgamated with those adjacent until the threshold is reached.

3.4.6. Spatial response - test landscapes

As for the temporal response analysis, the mean difference of observations between successive trials is given in Table 3.8 in the column labelled $\overline{|(q_i - q_{i-1})|}$. The mean difference of observations between each trial and the trial with the finest spatial discretisation is again given in the final column. The outer time step was 1 hour with 2 inner steps applied and the parameters as for the temporal response tests.

Table 3.8: Sensitivity to change in spatial discretisation: 1 to 12 downslope elements (figures to 2 s.f.).

No. groups	Water bal %	$\sum q_i$ (m)	$\overline{\lvert(q_i - q_{i-1})\rvert}$ %	$\overline{\lvert(q_i - q_n)\rvert}$ %
1	1.2	0.61		0.011
2	-1.3	0.62	2.5	2.6
5	0.14	0.62	1.5	1.1
8	0.65	0.61	0.51	0.56
12	1.2	0.61	0.56	0

The responses are plotted in Figure 3.8. The response stabilises above 2 units, with flood peaks becoming progressively more pronounced as the number of units passes 8. The highest peak does appear to decrease after this point, however, and there is also slight increase in the difference between the successive trials.

3.4.7. Spatial response - Gwy

Real landscapes are more spatially heterogeneous than the artificial catchment considered and likely to show sensitivity to discretisation. A spatial response analysis was therefore also undertaken for the Gwy. As before, the parameter set from Table 3.5 was used, a 15 minute outer time step and two inner steps applied. The results are presented in Table 3.10; with the final column giving the mean difference of observations between each trial and that employing the finest spatial discretisation.

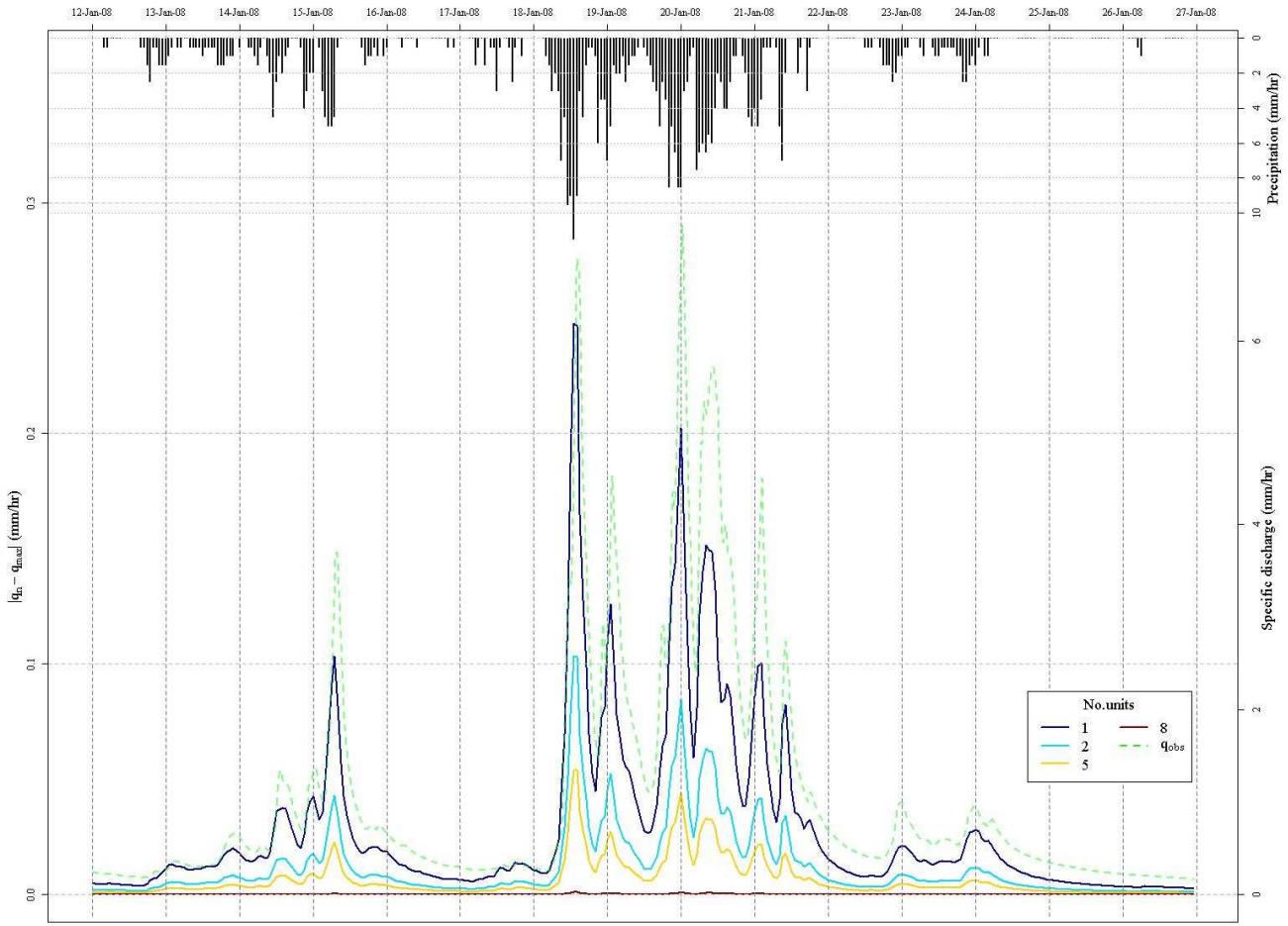

Figure 3.8. Response of hypothetical catchment to changes in spatial discretisation. Shown are the absolute difference of the predicted discharges within each trial from those predicted using a time step of 5 minutes. Central part of storm event within test period shown and evapotranspiration output suppressed. Observed discharges are shown using the RH axis for scale

Table 3.9: Sensitivity to changes in spatial discretisation within Gwy catchment, n_{max}=12 units. Figures to 2sf

n	Water bal %	$\sum q_n$ (m)	$\overline{\lvert(q_n - q_{n-1})\rvert}$ %	$\overline{\lvert(q_n - q_{n_{max}})\rvert}$ %
1	0.2	0.63		0.85
3	0.14	0.63	1	0.32
6	0.098	0.63	0.18	0.14
9	0.071	0.63	0.11	0.029
10	-0.084	0.63	0.62	0.6
12	0.064	0.63	0.6	0

The model seems responsive to spatial discretisation only up to a few groupings and it quickly converges towards the final results, although there seem to be some fluctuations in differences between successive trials.

3.4.8. Testing the Gwy catchment model

The aim of this paper is to present the new implementation of Dynamic TOPMODEL and investigate its numerical consistency. However, to illustrate the model performance for the Gwy catchment, Figure 3.9 shows discharge predictions for the four-month test period described. using a five minute inner-time interval. At 0.94, the Nash-Sutcliffe Efficiency (NSE) of this simulation is excellent. It can, however, be seen from a scatter plot of simulated and observed daily maxima (Figure 3.10) that the model consistently over-predicts low flows and under-predicts storm flows. Another simulation across the whole of 2008 using the same parameters yielded an NSE of 0.88.

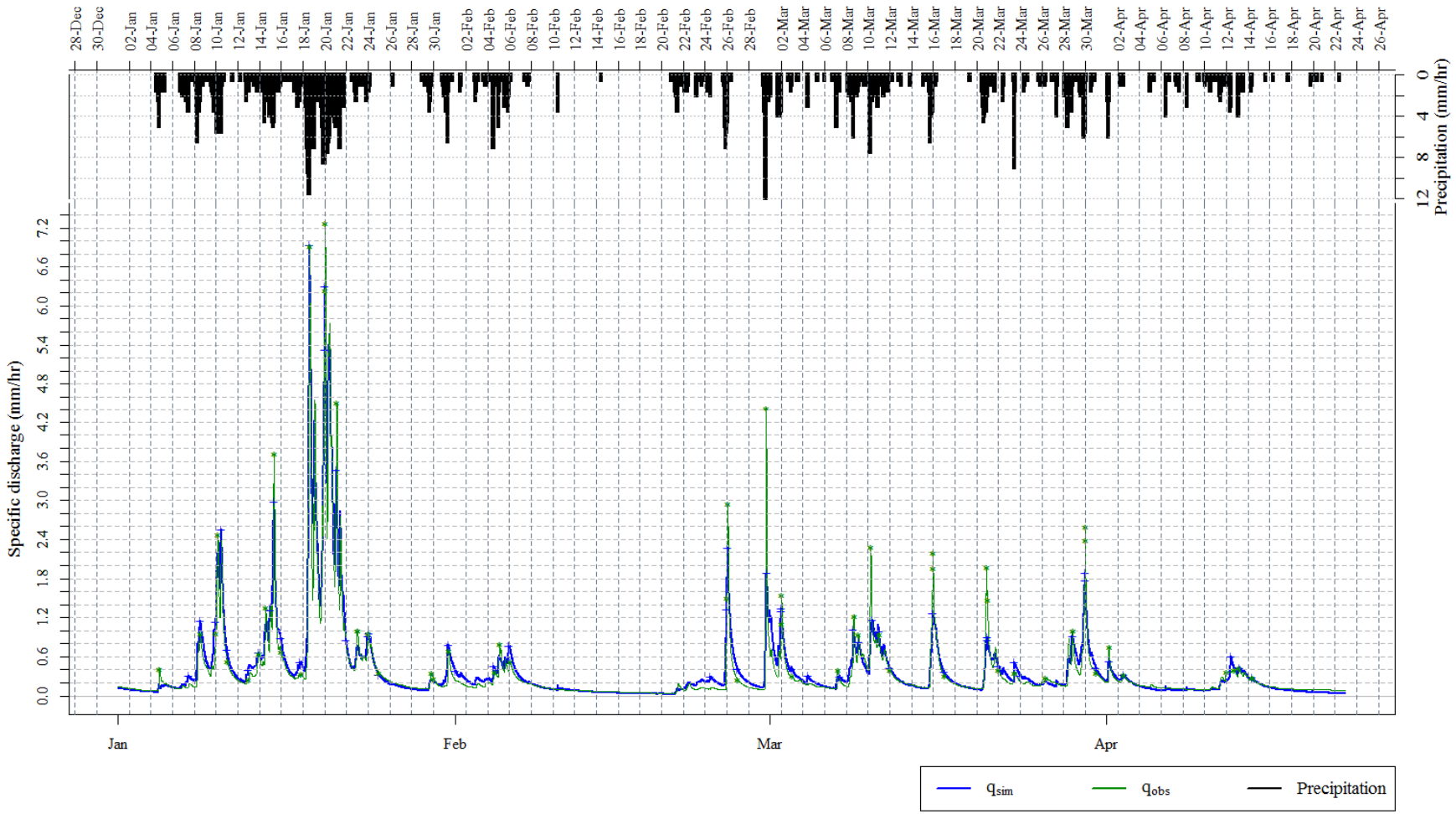

Figure 3.9. Four month validation period showing observed discharges (green) and simulated (blue) values calculated with a 15 minute time interval and 3 inner steps. Observed and simulated daily maxima within 75th percentile are shown as crosses and asterisks, respectively. Calculated actual evapotranspiration in brown using the scale on the RH axis.

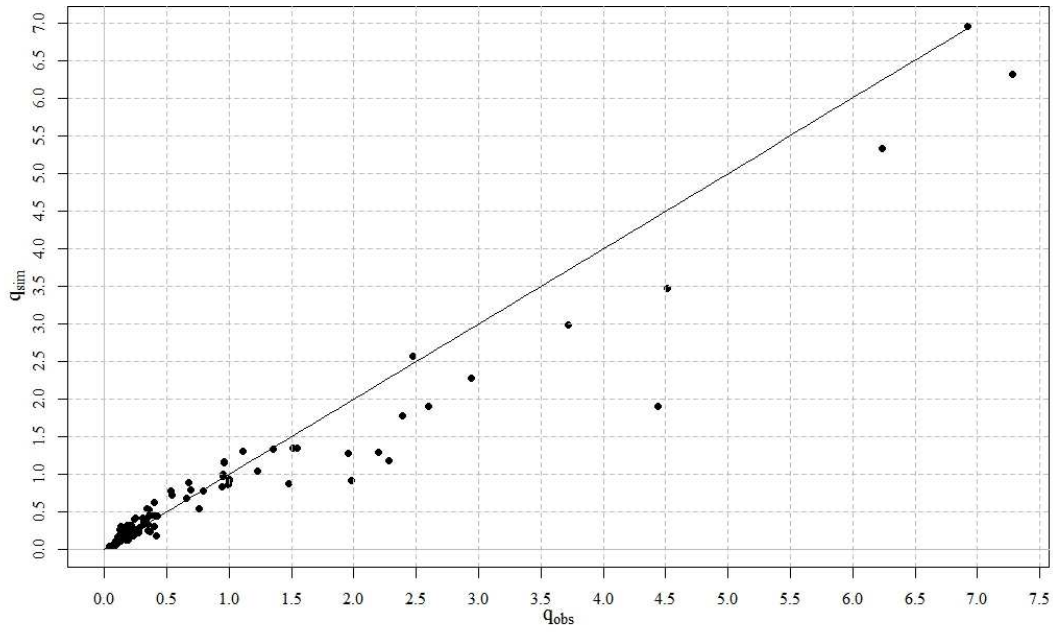

Figure 3.10. Daily maxima of simulated versus observed discharges, showing consistent over-prediction of low flows and under-prediction of flood peaks

3.5. Discussion

Modelling can be seen as a means of mapping a complex physical system to a simplified representation tractable to simulation and hypothesis testing (e.g. Beven 2002; Clark et al., 2011; Beven et al., 2012). The discretisation process employed by Dynamic TOPMODEL allows aggregation but at various scales within the same structure, in the same way that spatial data in vector format allows features of any scale to be represented with minimal storage requirements. Recent years have seen increasing interest in multi-scale and ensemble environment models, and these frameworks recognise that the optimal aggregation of a physical system is dependent on the dominant processes at the scale being considered (see e.g. McDonnell et al., 2007). Given sufficiently detailed elevation and river network data, the Dynamic TOPMODEL approach achieves such a simplification up to catchment scale whilst retaining information on hydrological connectivity between hydrological response units and the associated channel network (via the flow distribution matrix). The

important aspect of TOPMODEL, that the results from a relatively simplified model structure can still be mapped back into space is retained, and provides additional information for testing whether a model is acceptable in its representation of runoff processes and deciding whether additional spatial complexity of parameters is justified.

This study has concentrated on the numerical characteristics of the model. This revealed that while the original implementation of Dynamic TOPMODEL made use of an implicit time stepping scheme for each HRU derived from a kinematic wave analogy, the implementation of this method was not fully implicit because the flows from "upslope" were only estimated at the start of the iteration. This works correctly if the HRUs are arranged in downslope order, but not when there is potential for interaction between the different grouped HRU elements through the flow distribution matrix. The solution was therefore redesigned, such that the flow distribution matrix incorporated directly into the solution. Explicit schemes for root and unsaturated zone moisture accounting remain and may be improved in the future. Thus the tests in this paper show that the predicted discharges are sensitive to both the time and space discretisations, but converge as the internal time step is reduced and the number of downslope HRUs increase. This concurs with Clark and Kavetskis' (2010) conclusion that the use of coarse time resolutions and spatial discretisations will have an impact on the parameter values required for the model to give an acceptable fit to observations.

Further work will also be required to develop a version with run times fast enough to be used effectively within hypothesis testing approaches. It is also currently inadequate for calibration and uncertainty estimation, or for evaluation over longer time periods. The ability to run the kinematic solution within in an inner time stepping

loop may, however, allow an adaptive scheme that could improve the model's performance. The inner time period would be decreased in period of high subsurface flow and low deficit when the model sometimes appears to require a shorter interval to fully capture the dynamics of storm flows. An improved treatment of the unsaturated zone, as suggested by Beven and Freer (2001a), may further improve performance. Explicit schemes for root and unsaturated zone moisture accounting make these more sensitive to the time interval: in the response tests a stable response appeared as the time interval was decreased; below this no further change in the response could be seen. In the test catchment the critical time interval appears to be around 5 minutes, but is likely to be catchment-specific and longer for less responsive areas.

The more CPU intensive routines could be delivered as compiled modules written in C++ or FORTRAN, as was done by Buytaert (2011) in his implementation of TOPMODEL, although this might reduce the flexibility and portability of the implementation. The R byte code compiler (R Core Team, 2013) may also be able to reduce run-times. Use too could be made of pre-compiled libraries for efficient manipulation of data structures.

The size and resolution of the discretisation used seemed to have little impact on run times, and beyond about five to eight units a surprisingly small impact on the model response. In larger catchments more numerous HRUs may be required to adequately represent spatial heterogeneity, and repeated multiplication by the flow distribution matrix $\boldsymbol{W}$ is likely to have performance effects. Operations on sparse matrices such as $\boldsymbol{W}$ would be handled much more efficiently by making use of the `spam` package (Furrer & Sain, 2011).

3.6. Conclusions and further developments

This paper has described the new implementation of Dynamic TOPMODEL and demonstrated its stable response to a range of spatial and temporal resolutions in simple catchments. The enhancements described provide much improved usability and interoperability with external data in portable formats. Distribution through the CRAN package mechanism will encourage the wider use of the model. The CRAN package includes all the information required to run an application to an agricultural catchment in the UK of around 10km² in size. This displays much more variability in land use and vegetation cover than the Gwy catchment, but the model performed satisfactorily against observed data with only minimal calibration.

Further developments will investigate applications of the model to more complex and heterogeneous basins in order to test the model's ability to simplify the system representation whilst retaining the key aspects of its dynamics and spatial variability. Testing of the channel routing algorithm for larger catchments, and improvements to the simple representation of the unsaturated zone while not increasing the number of parameters, would be valuable. The run-time performance of the model in its current implementation for the multiple realisations required for model calibration and uncertainty estimation is still an issue, but could be improved at the cost of losing some flexibility.

The simpler TOPMODEL code has been used in many different countries of the world, including applications where the basic assumptions are clearly violated. Dynamic TOMODEL relaxes some of those assumptions whilst retaining many of the advantages of the original model. It is hoped that the guidance given in this paper about the sensitivities of the outputs to time and space discretisations will provide a useful guide to future applications.

Chapter 4. A modelling framework for evaluation of the hydrological impacts of nature-based approaches to flood risk management, with application to in-channel interventions across a 29 km² scale catchment in the United Kingdom

---

Reference

Metcalfe, P., Beven, K., Hankin, B. & Lamb, R., (2017). A modelling framework for evaluation of the hydrological impacts of nature-based approaches to flood risk management, with application to in-channel interventions across a 29 km² scale catchment in the United Kingdom. *Hydrological Processes*. https://doi.org/10.1002/hyp.11140

Author contribution

- Primary authorship of text
- Collection and assimilation of data
- Development of computer models and generation of results
- Fieldwork in study catchment
- Analysis and presentation of data
- Submission of initial and revised versions
- Preparation of all figures, apart from Figure 4
- Responses to reviewers
- Revision of initial paper given reviewers' responses
- Submission of revised version
- Amending final proofs
- Preparation of figures for publication

Abstract

Nature-based approaches to flood risk management are increasing in popularity. Evidence for the effectiveness at the catchment scale of such spatially-distributed, upstream measures is inconclusive, however. It also remains an open question whether, under certain conditions, the individual impacts of a collection of flood mitigation interventions could combine to produce a detrimental effect on runoff response.

A modelling framework is presented for evaluation of the impacts of hillslope and in-channel natural flood management interventions. It couples an existing semi-distributed hydrological model with a new, spatially-explicit, hydraulic channel network routing model.

The model is applied to assess a potential flood mitigation scheme in an agricultural catchment in North Yorkshire, UK, comprising various configurations of a single variety of in-channel feature. The hydrological model is used to generate subsurface and surface fluxes for a flood event in 2012. The network routing model is then applied to evaluate the response to the addition of up to 59 features. Additional channel and floodplain storage of approximately 70,000m³ is seen with a reduction of around 11% in peak discharge. While this might be sufficient to reduce flooding in moderate events, it is inadequate to prevent flooding in the double peaked storm of the magnitude that caused damage within the catchment in 2012. Some strategies using features specific to this catchment are suggested in order to improve the attenuation that could be achieved by applying a nature-based approach.

Keywords: Natural Flood Risk Management, flood hydraulics, semi-distributed hydrological models, nature-based solutions

4.1. Introduction

Since the Second World War more intensive agricultural practices, improved field drainage and changes to land management in the UK have led to a significant decrease in many catchments' capacity to retain storm runoff (Wheater et al., 2008; Wheater & Evans, 2009). It has been suggested that this has contributed to the occurrence and severity of flooding downstream of such catchments (O'Connell et al., 2007).

In the period 1980 to 2010 there were 563 recorded individual flood events across 37 European countries, and between 1998 and 2013 flooding caused damage estimated at €54 billion (EEA, 2016). The European Floods Directive (EU 2007), was implemented in November 2007 and requires member states to evaluate the extent and risk of flooding and to take action to mitigate those risks. Amongst other recommendations it emphasises the need for "natural water retention" for flood risk mitigation.

The Pitt Review (Pitt, 2008) that followed extensive floods in England in 2007 contained a recommendation to "work with natural processes" to mitigate flood risk. The UK Environment Agency and other bodies with interests in flood management responded positively to the Review's recommendations (Environment Agency, 2012), and the approach was included in the Flood and Water Management Act (2010).

In the years since these pieces of legislation were enacted flood mitigation approaches known variously as Natural Flood (Risk) Management (NFM/NFRM), Natural Water Retention Measures (NWRMs, see http://www.nwrm.eu), Nature-based Solutions (NBS), or Working With Natural Processes (WWNP) have gained popularity across Europe. They aim to increase interception and infiltration, slow overland and channel flows and add catchment storage by introducing changes to land use and surface roughness and networks of "soft" engineered features constructed mainly from natural

and immediately sourced materials (SEPA, 2012; Quinn et al., 2013). The principle is to restore and improve the catchment's natural ability to retain storm runoff and to release it slowly, leading to attenuation of downstream flood peaks, whilst retaining or enhancing its ecosystem services such as water quality (Holden et al., 2006; Barber & Quinn, 2012; Maclean et al., 2013; Thomas et al., 2016) and biodiversity in wetland environments (Acreman & Holden, 2013).

The Floods Directive is envisaged to be implemented in coordination with the Water Framework Directive (WFD; EU 2000), which requires member states to implement river basin management plans that ensure their good ecological and chemical status. It is recognised that nature-based approaches to river basin flood-risk management may also target the objectives of the WFD (Wharton & Gilvear, 2007; EEA, 2016) by improving the chemical status of the catchment.

Conventional flood protection schemes employ engineered structures and measures, often in combination as a whole system, with two main objectives. Some measures such as raised walls or flood banks (levées) and dredging either increase channel conveyance to reduce water levels locally or simply hold water back from spilling onto the floodplain. Others, such as dams and overflow basins aim to attenuate the input signal of an upstream flood wave. The hydrology of flood mitigation schemes utilising artificial reservoir storage is well understood and the discharge characteristics are largely controllable. Reservoirs are regulated in the UK by the Reservoirs Act (1975), amended by the Flood and Water Management Act (2010), which now applies to features with storage capacity greater than 10,000m³.

Nature-based approaches, in contrast, include such techniques as afforestation of hill slopes to increase permeability and downslope transmissivity and so reduce saturated surface runoff and shelterbelts to intercept such flows (Wheater et al., 2008). Tree

cover also reduces effective precipitation input through increased canopy interception and evaporation losses. Bosch and Hewlett (1982) reviewed 94 international studies and concluded that, on average, water yield reduced by between 10 and 40mm for every 10% of catchment reforested, evergreens providing the most effect.

Introduction to the channel of wooden screens or barriers, engineered log-jams (ELJs) or large woody debris (LWD) adds friction and reduces flow velocities (Thomas & Nisbet, 2012; Quinn et al., 2013; Dixon et al., 2016). One significant impact of such in-channel interventions is to create a backwater effect (Quinn et al., 2013). This may lead to reconnection of the flood plain with the channel at storm flows, and the effect can be substantially enhanced if combined with riparian tree-planting to increase flood plain roughness (Thomas & Nisbet, 2007; Nisbet & Thomas, 2008).

Careful positioning of features such as low earth bunds can disconnect fast overland flow pathways from the channel (Quinn et al., 2013). Offline storage areas can also be used to retain flood water diverted from the channel (Nicholson et al., 2012). Typical capacities are in the range of 200m³ to 1000m³ (Quinn et al., 2013), which means they are unlikely to become subject to the Flood and Water Management Act.

Across Europe many NWRM schemes have piloted, for example in areas affected by the Central European floods of 2010 (Skublics & Rutschmann, 2015). In the UK there are now over 150 schemes in place (see the online map at http://naturalprocesses.jbahosting.com, JBA Trust, 2016). One of the earliest was in the Belford Burn catchment in Northumberland (see Wilkinson et al., 2010a, Nicholson et al., 2012). Significant flooding of the Burn affected the town of Belford, most recently in 2007. A traditional "hard" engineered approach to flood mitigation was rejected due to cost and the relatively few properties benefiting (Wilkinson et al., 2010b). Instead, a nature-based approach was proposed that made use of distributed,

unsupervised, on-and off-line features. A feasibility study using a simulated pond network with an aggregate capacity of approximately 20000 m³ showed a 15-30% reduction in peak flows. The storage equates to a total runoff of 3.5mm, or around 1mm/hr over the duration of the smallest storm that caused flooding (Nicholson et al., 2012). Initially 35 of these features were installed, adding approximately 9000-10000 m³ of static storage. The effective storage would, however, be greater due to backwater effects of in-channel features (Quinn et al., 2013). Construction costs were estimated at between £70,000 and £100,000 (Quinn et al., 2013). A further 20 features were subsequently added by the UK Environment Agency.

As a bottom-up approach, NFRM presents many opportunities for stakeholder engagement, and an essential element is the participation of local stakeholders from an early stage. This was the case of the Ryedale scheme upstream of Pickering in North Yorkshire (Lane et al., 2011; Nisbet et al., 2011). Here a partnership including residents, local authorities and Forest Research were able to install a total of 167 woody debris dams within the channels and 187 bale dams blocking gullies in the upper moorland areas (Nisbet et al., 2011). This was estimated to provide capacity sufficient to protect the affected areas from a 1 in 25 year event. Significant funding subsequently became available and the original approach evolved into a hybrid design with the addition of a £2m, 120,000m³, engineered flood detention basin.

Since the Belford scheme was established Nicholson et al. (2012) report a reduction in the magnitude of storm flows. Evidence for the effectiveness of NFRM applied at larger scales is inconclusive (Blanc et al., 2012) and a generalised model to assess its impacts has, up to now, been considered impractical. Individual features can be shown to provide benefits on a local scale. Ghimire et al. (2014) applied hydrodynamic modelling to a single storage feature and demonstrated a reduction of 9% in peak

flows immediately downstream of the feature, achieved by diverting flood discharge into a pond with a capacity of 27,000 m³. Thomas and Nisbet (2012) estimated a reduction in flow velocities of up 2.1 m/s achieved through the restoration of five woody debris dams in a 0.5 km reach and a 15 minute retardation in the downstream flood peak. Thomas and Nisbet (2007) simulated flood flows thorough new riparian woodland along a 2.2km reach and demonstrated a best case 50% reduction in velocity and delay of 140 minutes in the time to peak.

Despite these localised studies, there remains a need for a modelling approach that can assess the impacts of NFM on realistic catchment scales and the interactions between individual interventions and subcatchments. The effectiveness of riparian measures for flood risk mitigation is considered to be due primarily to desynchronisation of subcatchment flood peaks (Thomas & Nisbet, 2007; Nisbet & Thomas, 2008; Dixon et al., 2016). Dixon et al. (2016) estimated a 19% potential reduction in peak flows, mainly due to this effect, downstream of a catchment in which 20-40% of the area had been reforested. There remains uncertainty whether the effects of interventions within individual subcatchments could in fact combine to synchronise previously asynchronous peaks (Blanc et al., 2012). The effects of overflow, or even cascading failure, of in-channel structures could also have a detrimental effect on the response (Nicholson et al., 2012).

A coupled hydrological hillslope runoff and hydraulic channel model is developed to evaluate the impact on storm runoff of a variety of interventions at scales up to that of a small catchment (<100km²). It is able to take into account the effects of antecedent conditions, noted to have a significant impact on a scheme's performance (Blanc et al., 2012). It allows examination of the water level and discharge throughout the channel network which allows the local impacts of in-channel interventions to be

estimated. In order to reduce data demands the model utilises by default simplified, but realistic, channel geometries but allows the use of empirical geometries determined from ground surveys.

The study applies the model to evaluate the impact on storm runoff response of a small, intensively cultivated catchment to emplacement of various configurations of in-channel features. A single variety of such feature will be investigated in this paper. but potentially the framework model could be used to evaluate the impacts of other types of feature and hillslope interventions. These include enhanced flood plain roughness and hydrological alterations introduced by land use change such as afforestation.

4.1.1. Modelling approach

A fully-distributed representation of a realistic catchment and of the processes affected by NFM measures would be both practically and computationally infeasible. In our approach the spatial complexity of the problem is significantly reduced by first applying a semi-distributed hydrological model to simulate hillslope runoff into the channel network. This aggregates similar areas together and treats these as single units within the simulation. Broad-scale measures such as tree-planting and more localised, but greater than grid-scale, features such as runoff detention areas can be included as discrete units in the aggregation. Modifications to those units' parameters and structure to reflect changes introduced when the measures are applied will allow examination of their effects on the response, both at the scale of the unit or on the catchment as a whole.

Lacking a spatially-explicit channel network representation, the hydrological model alone is unable to model the local effects of sub-grid scale, in-channel, features such as debris dams. Network routing is therefore handled by a 1D hydraulic scheme

employing a spatially-explicit channel representation, which receives as input the surface and subsurface runoff predicted by the hillslope component. The presence of runoff attenuation features can be simulated in the hydraulic model by altering the stage-discharge relationship applied to route discharge through successive sub-reaches of the reaches comprising the network.

Thus the hybrid model can not only handle wider interventions whose effects become noticeable only when applied on the regional scale, but can include sufficient spatial detail to capture features that have greatest local impact.

The modelling approach is shown in Figure 4.1.

4.1.2. Hillslope Runoff component

Hillslope runoff into the channel network is estimated using the semi-distributed hydrological model Dynamic TOPMODEL. Details of the principles and use of Dynamic TOPMODEL are given in Beven and Freer (2001a) and Metcalfe et al. (2015). The implementation used in this study is that by Metcalfe et al. (2016), which employs the open-source R language and environment and is freely available from the Comprehensive R Archive Network (CRAN) archive (https://cran.r-project.org/).

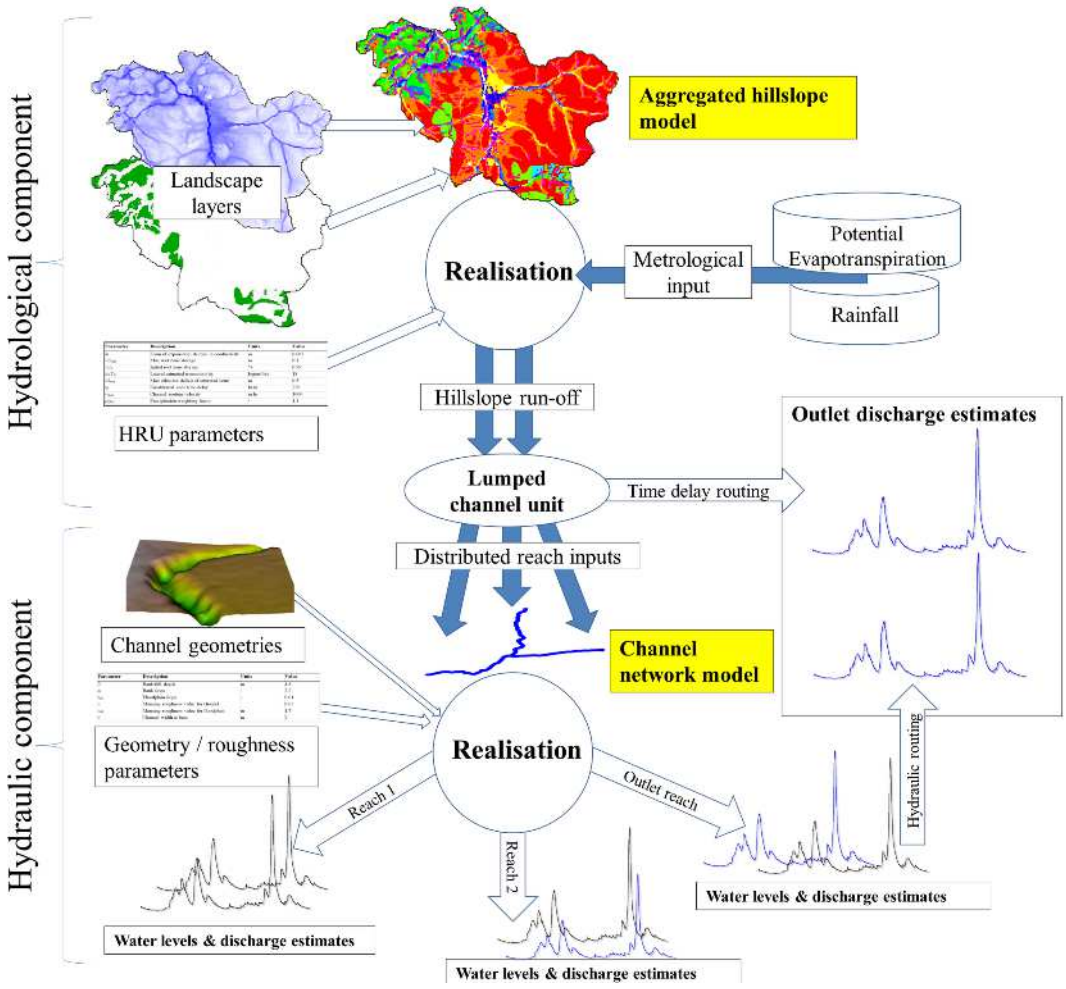

Figure 4.1. Overview of the coupled hydrological hillslope- hydraulic network routing modelling framework employed in the study. The hydrological component combines landscape layers to provide an simplified hillslope representation as Hydrological Response Units (HRUs). A realisation applies HRU parameters and meteorological inputs to generate input to the channel network of the hydraulic routing component. This module combines the reach inputs with channel geometries into a realisation and outputs water levels and discharges across the network which allows, for example, examination of the effects of in-channel interventions. The two components generate complementary estimates for the catchment outlet discharge

The model groups the catchment into hydrological response units (HRUs) according to landscape characteristics such as topography, land cover or soil type. These units are not necessarily spatially contiguous but they and their time-varying states, averaged over their areas, may be mapped back into space. Each unit is treated as a

separate store, the downslope discharge out of which is determined by a suitable storage-discharge relationship. Subsurface flows between the units are distributed according to a flow distribution matrix $\boldsymbol{W}$ estimated from surface slopes used as proxies for the direction of maximum hydraulic gradient. This, along with the units' storage-discharge relationships, leads to a kinematic wave formulation for downslope flow out of each unit, with a fixed wave speed characteristic to it and its parameters. The hydrological component has relatively few parameters (see Table 4.1), making the simple to configure and run and allows rapid identification of behavioural model realisations against observed discharges. Each unit may, however, take a distinct set of parameters. It allows the response to spatially-distributed landscape intervention that may alter hydrological characteristics to be investigated.

Table 4.1. Dynamic TOPMODEL parameters Values are those calibrated against November 2012 storm event, or defaults if not included in calibration.

Parameter	Description	Units	Value
m	Form of exponential decline in conductivity	m	0.002
srz_{max}	Max root zone storage	m	0.1
srz_0	Initial root zone storage	%	0.99
$ln(T_0)$	Lateral saturated transmissivity	log(m²/hr)	18
sd_{max}	Max effective deficit of saturated zone	m	0.5
t_d	Unsaturated zone time delay	hr/m	230
v_{chan}	Channel routing velocity	m/hr	1000
v_{of}	Overland flow routing velocity	m/hr	50
pr_{fact}	Precipitation weighting factor	-	1.1

Saturated excess overland flow is routed to the channel downslope through the HRUs using a surface flow distribution matrix $\boldsymbol{W_{of}}$ similar to that applied to the subsurface, and the mean overland flow wave velocity parameter v_{of} ([L]/[T]) whose value can be specified separately for each unit. The effects of introducing surface roughness to slow saturated overland flow, for example through afforestation, can be approximated

by changing the value of v_{of} in the appropriate unit. To the simulate behaviour of features to intercept overland flow the appropriate elements of $\boldsymbol{W_{of}}$ can be changed to restrict the downslope drainage out of areas associated with those features.

The flow distribution matrices are also applied to route hillslope subsurface and surface runoff to the channel, represented as a single lumped unit. An estimate for discharge at the catchment outlet is obtained at each time step by routing the channel input in that interval using a time delay histogram derived from the network flow distances. A fixed channel wave velocity v_{chan} ([L]/[T]; m/hr) is applied throughout the network.

4.1.3. Channel routing

The simple treatment of channel routing in the hydrological model does not allow access to water levels and flow velocities throughout the river network. These will be required in order to assess the local effects of in-channel interventions, in particular their effect in reconnecting the channel with the flood plain. A spatially-explicit, 1D hydraulic channel routing scheme has therefore been implemented.

There exist numerous hydraulic models that allow detailed routing of channel discharge. The model employed by Thomas and Nisbet (2007), for example, is HEC-RAS (Brunner, 2002). This solves the steady state Energy Equation or Saint Venant unsteady flow equations through successive channels sections. It models the effect of a structure impinging the channel such a bridge as a head loss component additional to friction and contraction / expansion losses.

Addition of features and specifications of channel profiles and reaches with these detailed modelling packages is, however, a complex task, and not amenable to automation or rapid modification and calibration. The structures that can be evaluated

are generally limited to those implemented by the software, and may not correspond to those evaluated as part of an NFM scheme.

Our simpler routing model allows rapid specification of a channel network using spatial vector data and parametric channel and overbank geometries. It enables programmatic definition of in-channel features and their insertion at arbitrary locations across the network. Given suitable constraints on the degrees of freedom allowed in their definition, it can be used to calibrate channel and overbank geometries and roughness. The use of simplified, but realistic, channel geometries allows our model to be run quickly and cheaply where detailed morphological data are not available.

The model employs a composite channel section, similar to that used by HEC-RAS, where flow is portioned between overbank and in-channel components and combined to produce the total cross-sectional discharge. This approach has limitations in non-prismatic channels with high sinuosity and where there are significant interactions between the floodplain and channel flow. It is however generally adequate for flood routing problems where only predictions of discharges and water levels are required (Knight, 2005).

A separate roughness coefficient may be applied to channel and overbank areas. The effect of introducing roughness to the floodplain to slow overbanked flow can therefore be investigated by altering the coefficient applied to the overbank component, albeit there may be variations in the effective roughness due to hydrodynamic effects of flow around obstacles such as fallen trees (Thomas & Nisbet, 2007).

In the solution scheme each river reach is divided into approximately equally-sized sub-reaches. At each time step a system of differential equations for sub-reach storages through every reach in the channel network is solved using an iterative, upwinded implicit numerical scheme (described in the Appendix). Boundary conditions at the upstream inlet to each reach are determined from a channel distribution matrix calculated from the detailed river network. Total discharge between successive sub-reaches Q is then calculated according to the common Manning Equation for open channel flow (see Appendix 2).

$$Q = \frac{AR^{\frac{2}{3}}\sqrt{S_0}}{n} \qquad \text{(Eqn .4.1)}$$

where S_0 is the local bed slope, n the Manning roughness, R the hydraulic radius and A the flow area perpendicular to the principal downstream flow. Although not used here a correction coefficient could be applied to take into account a non-uniform velocity profile through the channel section. Combined with the mass conservation equation (4.1) results in a Diffusive Wave approximation to the Saint Venant equations for open channel discharge.

With a known channel cross sectional geometry A and R can be determined in terms of water depth. For parametric morphologies such as a trapezoid these will be analytic expressions, for those obtained from empirical data they will be in the form of a look-up table. This yields stage-discharge relationships for subcritical flow through the unobstructed sub-reaches.

Åkesson et al. (2015) demonstrated that for flood discharge prediction, routing and hydraulic model performance may be more important than channel morphology. Thus by default a simple channel geometry is used in the network routing model. This is a trapezoidal channel section with gently sloped straight floodplain areas extending indefinitely on either side. Such geometries can be parametrised by the channel base width w, the bank slopes s_b, floodplain gradient s_{ob} and bank-full level, D (see Figure 4.2). Here $s_b = D/x_b$ and $s_{ob} = z_{ob}/x_{ob}$.

The input supplied by the hillslope runoff component to its lumped channel unit is distributed between the reaches according to their length and relative upslope areas. This provides a lateral recharge term for each reach, applied uniformly along its length. The solution scheme outputs, for each time step in a simulation, water levels, flow areas and total discharges through those areas at the mid-point of every sub-reach in the network.

4.1.4. Representation of in-channel features

The addition of runoff attenuation features to the channel network will alter the stage-

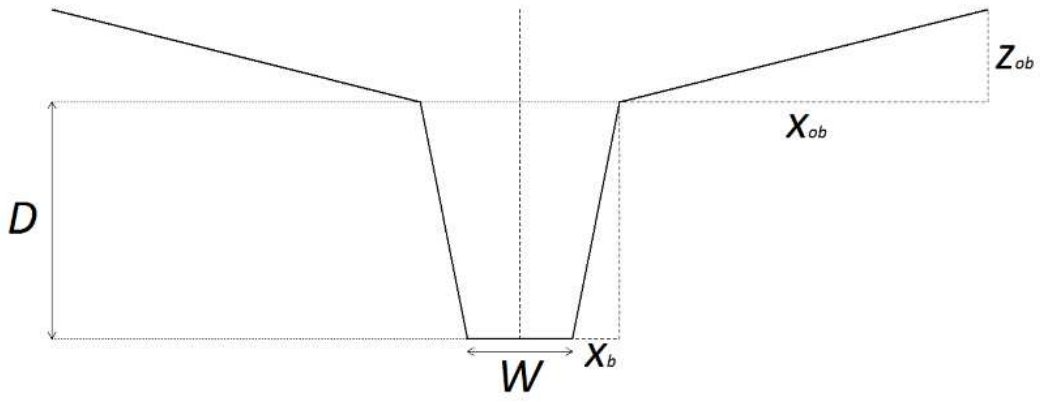

Figure 4.2. Definition sketch for composite trapezoidal channel profile employed by the routing model. See text for definitions.

discharge relationship for the sub-reaches in which they are placed. By replacing the default relationship with those appropriate to the types of features inserted, the local and aggregated effect of an NFM intervention comprising a configuration of in-channel features can be evaluated.

A feature such as weir or barrier may be used that introduces a hydraulic jump. In this case associated energy loss must be taken into account in the relationship. The feature, jump and return to subcritical flow should also be completely contained within a sub-reach. A suitable discharge function, such as a Weir-type equation, can be defined to deal with situations where the feature is overtopped.

Suggested stage-discharge and overflow relationships for some channel features are presented in Appendix 3 Although the geometries considered are highly simplified, Hailemariam et al. (2014) demonstrated that similar idealisations performed adequately against observed data within a simulation of a flood event in a low-lying agricultural catchment in the Netherlands.

4.2. Study area

The Brompton catchment (Figure 4.3) lies in the Swale, Ure Nidd and Upper Ouse WFD management catchment, North Yorkshire, UK, part of the Humber River Basin District. The 29.3 km² area upstream of the village of Water End (-1.416976W, 54.36302N) is predominately well-drained, undulating arable land with a mean elevation of 68m AMSL. Brompton Beck becomes North Beck downstream of the village before joining the Wiske in Northallerton. Throughout the catchment superficial deposits of sandy clay glacial till with gravel and boulders are overlain on a mudstone bedrock. Rainfall averaged 624 mm p.a. in the period 2008-2014. Convective storms are seen in the summer and synoptic rainfall dominates in the

autumn and winter. Water End suffered severe flooding in 2000, with further flooding in September and November 2012. The earlier event had estimated Annual Exceedance Probability (AEP) of 1% and those in 2012 an AEP of 1.3%.

A scheme similar to that implemented in Belford has been suggested for Brompton, but there are significant differences between the catchments. Brompton is intensively farmed, with 95% of its area classed as arable or improved grassland. In Belford only the lower half is in this classification, with rough pasture and upland grazing making up the higher reaches (Nicholson et al., 2012). There are few areas of woodland in Brompton, which largely precludes the use of low-cost, locally-sourced woody debris dams employed in the wooded riparian area at Belford (Wilkinson et al., 2010; Nicholson et al., 2012).

The Belford scheme was determined to require at least 20,000 m^3 of detention storage within the 5.7 km^2 catchment area (Nicholson et al., 2012). Brompton is approximately 5 times the plan area of Belford and the storage requirements of an effective scheme will be commensurately greater. Quinn et al. (2013) consider that an areal contribution of 1 to 10% would be required to add sufficient storage to significantly attenuate the storm hydrograph. Given arable land prices of up to £18000/ha (RICS, 2016) dedicated artificial storage area could be prohibitively expensive. To avoid this, Quinn et al. (2013) suggest placing features within the channel or in areas of marginal land in steep-sided banking around it. Storage areas will come into operation comparatively rarely and a complementary approach would be to compensate landowners for damage due to periods of inundation. Guidance is available on appropriate rates for various grades of agricultural land subject to different drainage conditions. For example, a week-long flood is estimated to cause damage of £650/ha to extensive arable under good drainage (Penning-Rowsell, 2013).

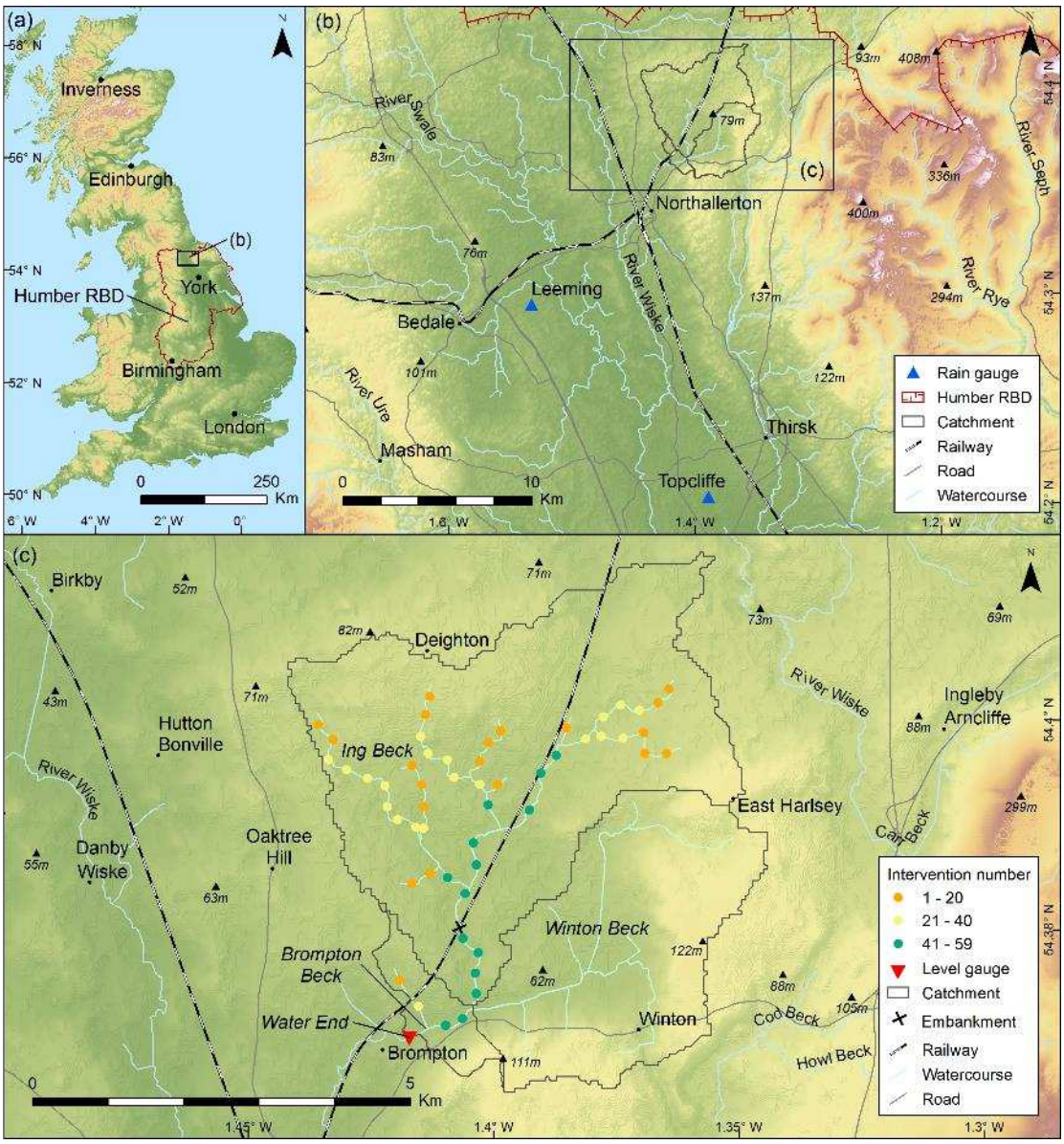

Figure 4.3. Overview of the Brompton study catchment and its two subcatchments, North Yorkshire, United Kingdom, showing regional (b) and national (a) context within the Humber River Basin District (RBD). Shown are the positions of the hypothetical in-channel features whose influence on the storm response are the main subject of the study, along with an indication of the batch in which they were applied. The position of the rail embankment crossing the main channel of Ing Beck, discussed in the text is shown. Locations of the outlet gauge in Water End and the two nearby rain gauges at Leeming and Topcliffe also provided.

In contrast to the largely natural channels within Belford, the Brompton network is heavily modified. There are many enlarged and artificial ditches increasing land-channel connectivity; density is 1203m per km² and there is evidence of extensive and well-maintained subsurface field drainage that connects directly to this ditch network.

4.3. Available data

A Digital Terrain Model (DTM) of the catchment was built from ground-scraped elevation data at 2 metre spatial resolution sourced from the UK Environment Agency. Catchment boundaries above the level gauge at Water End were determined using SAGA GIS. The Detailed River Network (DRN) obtained from the EDINA DigiMap service was "burnt" into the DTM to a maximum depth of 2m, with a small graduated buffer to impose a consistent hydraulic gradient and flow direction within the channels. Thirty-five river reaches were identified with a median length of 674m.

Hourly rainfall data for nearby weather stations were obtained from the BADC MIDAS repository (Met Office, 2006). The nearest station is at Leeming, about 10km to the SW and at a similar elevation; there is also a gauge at Topcliffe, 17km south of the catchment (see Figure 4.3b). Using the evapotranspiration module provided with the Dynamic TOPMODEL package, a time series of potential evapotranspiration was generated to give a total actual roughly equivalent to a typical yearly water balance of 230mm.

There is a single gauge at the catchment outlet in Water End, recording stage data at 15-minute intervals. Data for the period 2002-2013 were obtained from the UK Environment Agency.

In 2005 a feasibility study for a flood mitigation scheme upstream of Northallerton was undertaken by JBA Consulting. As part of this a HEC-RAS project was set up for

North Beck which connects Brompton with the Wiske. Detailed channel profiles and rating curves are supplied for every reach, including one in which the gauge is found. The first data point was at 1.1m, a level that was exceeded in less than 10% of the September– December 2012 period studied in the subsequent analysis. The rating was extrapolated from this first level to zero by back-solving for a roughness coefficient *n* in the Manning Equation (4.1) used to estimate discharge in the routing scheme. The local bed slope from the HEC-RAS data was applied and flow area and hydraulic radius for the 1.1m stage were estimated from the channel profile provided. The corresponding discharge was substituted and a value $n = 0.03$ obtained. The resulting rating curve allowed a time series of reconstructed discharges to be obtained for the entire study period.

Given the uncertainty introduced by the simplified DRN vector data in determining accurate elevations for channel cells, it was felt that the simplicity of applying an overall bed slope for the entire network would more than compensate for the possible improvements in model accuracy from using a slope calculated for each reach. A value was therefore estimated from the elevation range of DTM cells containing the main channel of Ing and Brompton Becks divided by its total length.

4.3.1. Field drainage

Subsurface field drainage discharging directly into the channels is apparent in many areas of the catchment. They are mostly less than a metre below the surface, constructed from clay, metal or terracotta and up to 30cm in diameter. According to local farmers some date from the late 19th Century and others were installed as a result of subsidies for field drainage in the 1980s; recent work in the NW of the catchment has used plastic piping of a smaller diameter.

Dynamic TOPMODEL by default utilises an exponential transmissivity profile. This is parameterised by T_0 ([L]²/[T]), the limiting (saturated) transmissivity and m ([L]) a parameter controlling the decline of conductivity with depth. Such a form is not required and any suitable profile can be used. A discontinuous transmissivity profile was tried to take into account the effect of the additional capacity introduced at the depth where the drains were found. This, however, gave only marginally closer results to observed hydrographs and introduced extra parameters requiring calibration. The effects of the field drainage appeared to be adequately simulated by favouring parameter sets with high T_0 to reflect higher downslope throughput rates introduced by artificial drainage and small absolute values of m to reflect conductivity that declines rapidly beneath the level of the drains.

4.3.2. Taking account of tunnels beneath the railway line

At (-1.4082W, 54.37606N) Ing Beck is crossed by the Northallerton–Middleborough railway, which is carried by an embankment around 30m wide (marked as a cross in Figure 4.3c). The beck flows through an arched concrete-reinforced tunnel within a brick viaduct, with soffit approximately 4m above the channel bed. Guidelines suggest these features to be considered bridges rather than culverts (Ackers et al., 2015).

It was noted that the area immediately upstream of the crossing provides one of the largest areas of marginal riparian land in the catchment. This is probably due to relatively frequent inundation at storm flows resulting from backwater effects introduced by the tunnel. One of the hypothetical measures considered in the following analysis was to close off the tunnel under the railway line with an engineered sluice gate such as those utilised in flood storage basins. An empirical storage-depth relationship was deduced from the elevation data for the riparian area for the reach approaching the tunnel and applied to the representation of that reach in

the flow routing scheme. The results of the simulated intervention are presented in Section 4.7.

4.4. Storm events, September and November 2012

A wet summer in 2012 led to the soil moisture content and water table in early autumn being higher than normal. In the early hours of the 25th of September intense rain led to a rapid rise in flow rate and flooding within the village later that day. Reconstructed peak flow through the level gauge was 19.2 m³/s at 3:15pm. Two months later another series of storms caused further flooding (see Figure 4.4).

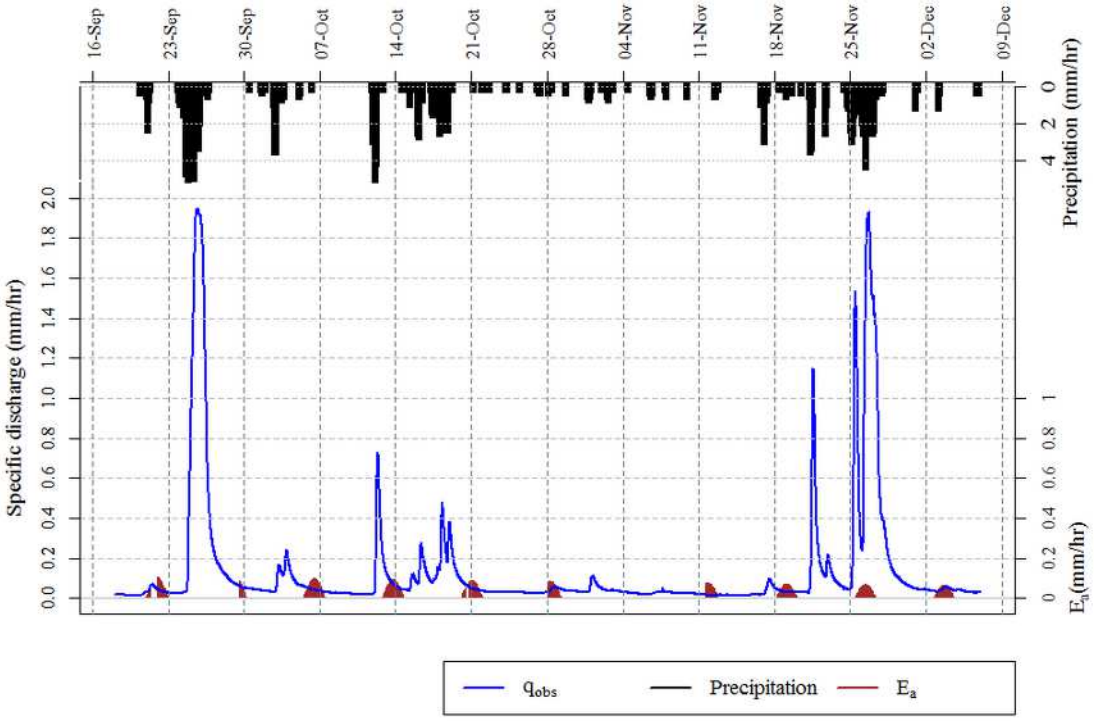

Figure 4.4. Reconstructed specific discharges for the series of storms described in the text in the period September-November 2012.

A minor storm on the 22nd with maximum intensity of 3mm/hr apparently saturated the soil but did not flood the village. After a more prolonged rainstorm of the same maximum intensity a larger peak discharge of 11.2 m³/s is seen in the hydrograph on Sunday 25th, but local residents reported water levels just below that which would cause flooding. There was an overnight recession followed by another storm that

began in the early hours of the following day, with rainfall intensity peaking at 4.4mm/hr around 10am. Rated flow through the gauge peaked at 14.0 m³/s around 5pm. A number of houses were flooded on this occasion. This suggests that for a scheme to prevent flooding in an event of this magnitude it would have to reduce peak flows by the difference in the two maxima, i.e. by approximately 2.8 m³/s, equivalent to a specific runoff of 0.38mm/hr or around 20% of the peak.

4.4.1. Calibration of hydrological and hydraulic models

Dynamic TOPMODEL was run using a time step of 15 minutes for the double-peaked storm event of 25th – 27th November 2012. Rainfall data from the Leeming AWS (see Figure 4.3b) were used and applied evenly across the catchment area. Data from Topcliffe showed similar timings and quantities, indicating that this event was a synoptic event typical of winter rainfalls in this area. A small scaling factor was applied to reconcile the water balance between input rainfall and observed discharges across the event. Dynamic TOPMODEL does allow for individual rainfall inputs and / or scaling factors for individual HRUs within the catchment model. Given the small extent of the catchment, around 6.5 km^2, and the nature of the event it was considered that a uniform rainfall input was adequate for the study.

The model parameters shown in Table 4.1 were calibrated by running through approximately 5000 realisations with parameters selected at random from the ranges given in the table and applying a performance metric (the Nash Sutcliffe Efficiency, NSE) to the simulated and reconstructed flows at the outlet with a weighting that took into account the amount of saturated overland flow predicted. Simulations with lower amounts of overland flow were favoured with this weighting in order to reflect the subsurface drainage in evidence. Predicted surface and subsurface hillslope runoff a

well-fitting simulation were distributed between the reaches of the channel network and applied to the hydraulic channel routing model.

The default symmetrical, trapezoidal cross-sectional geometries were applied throughout the channel network as they agreed qualitatively with morphologies observed from catchment walkovers. Although noting the potential for differences across the network, in order reduce the degrees of freedom an identical parametrisation was used throughout. The response to variations in the channel geometry parameters and Manning roughness values was then used to calibrate the routing model. The timings of both flood peaks were matched to within 15 minutes of those observed. Around 1500 realisations were analysed, and the parameters selected are presented in Table 4.2.

Table 4.2. Hydraulic model parameters calibrated for November 2012 storm event

Parameter	Description	Units	Value
D	Bank-full depth	m	1.8
s_b	Bank slope	-	2.2
s_{ob}	Floodplain slope	-	0.01
n	Manning roughness for channel		0.03
n_{ob}	Manning roughness for floodplain	m	1.7
w	Channel width at base	m	2

4.5. Selection and sensitivity analysis of flood mitigation interventions

The intensively-farmed nature of the study catchment means there are few options for widespread tree planting and little marginal land in which to site off-line-storage features. In-channel features such as rubble and debris barriers that operate at lower flow stages were also not thought suitable interventions. The Swale and Ure Internal

Drain Board (IDB) manages much of the catchment and installation of such features would run counter to the Board's remit of keeping the channels clear of debris.

Overland flow barriers or bunds are used to disconnect fast surface flow pathways from the channel and retain the runoff for the duration of an event. Catchment walkovers suggest that much of the main channel is already partially disconnected from the floodplain by low levées formed from dredging during channel maintenance undertaken by the IDB. In addition, most behavioural model simulations weighted to favour higher transmissivities to reflect subsurface field drainage suggested little overland flow. Most of this was generated in areas immediately beside the channel which are likely to have been inundated across much of the event. Overland flow interception barriers were therefore not considered an effective or practical intervention for this catchment.

Barriers or screens with an opening beneath allow unobstructed flow at normal levels but impinge on storm flows that exceed the underside clearance. They slow these higher flows and introduce channel storage through their backwater effect. These structures are similar to the underflow sluice described in Chow (1959) and their hydraulic characteristics are outlined in Appendix 3. Impermeable, rather than "leaky", barriers would be most effective in attenuating open channel discharge, although potentially subjected to high hydraulic stresses. The height of the opening could be configured to meet the levels expected for events of a given return period. In practice the geometry of such features is likely to be constrained by compliance with IDB regulations and environmental legislation such as that to allow fish passage (see for example Baudoin et al., 2014).

The storm peak during the simulated November 2012 event arrived about 30 minutes earlier at the outlet of the Winton Beck subcatchment than at the outlet of Ing Beck.

Assuming that the rainfall was not a localised convective event, this suggests that measures to slow the combined catchment response should concentrate on Ing Beck as delaying Winton Beck's response could result in the two peak flows coinciding. There are in addition access issues preventing measures being deployed around Winton Beck.

A sensitivity analysis was undertaken to determine the effect of adding increasing numbers of the in-channel features on the catchment response to the flood event. 59 potential sites for underflow ditch barriers were identified along the 4.7 km length of Brompton and Ing Becks and their unnamed tributaries (see Figure 4.3c). Features were added in batches of 10, each separated from the nearest upstream barrier by at least 300m, from the highest reaches downstream until the available network was filled. Initially a configuration where all barriers shared the same clearance of 30 cm above the channel bed was considered. An approach aimed at maximising storage utilisation was then tried, where the barriers' clearances were decreased on tributaries and increased on the main channel.

Features were sized according to the bank-depth of 1.8m with a small upper clearance to allow overflow to drain downstream over the feature rather than into neighbouring fields, as stipulated by the IDB. The barrier tops were set to 1.6m above the base of the channel. As features were added to the network, the functional relationship for the underflow barrier was applied to reaches discharging through a feature, and the routing algorithm run using the modified relationship applied for the corresponding element of the input discharge vector. In addition to discharge, water level and any overflow were recorded for each feature.

4.6. Results

4.6.1. Storm simulation

Figure 4.5 shows the discharge simulated for the storm event of 25th – 27th November using the parameters for the hydrological and hydraulic models given in Table 4.1 and Table 4.2, respectively.

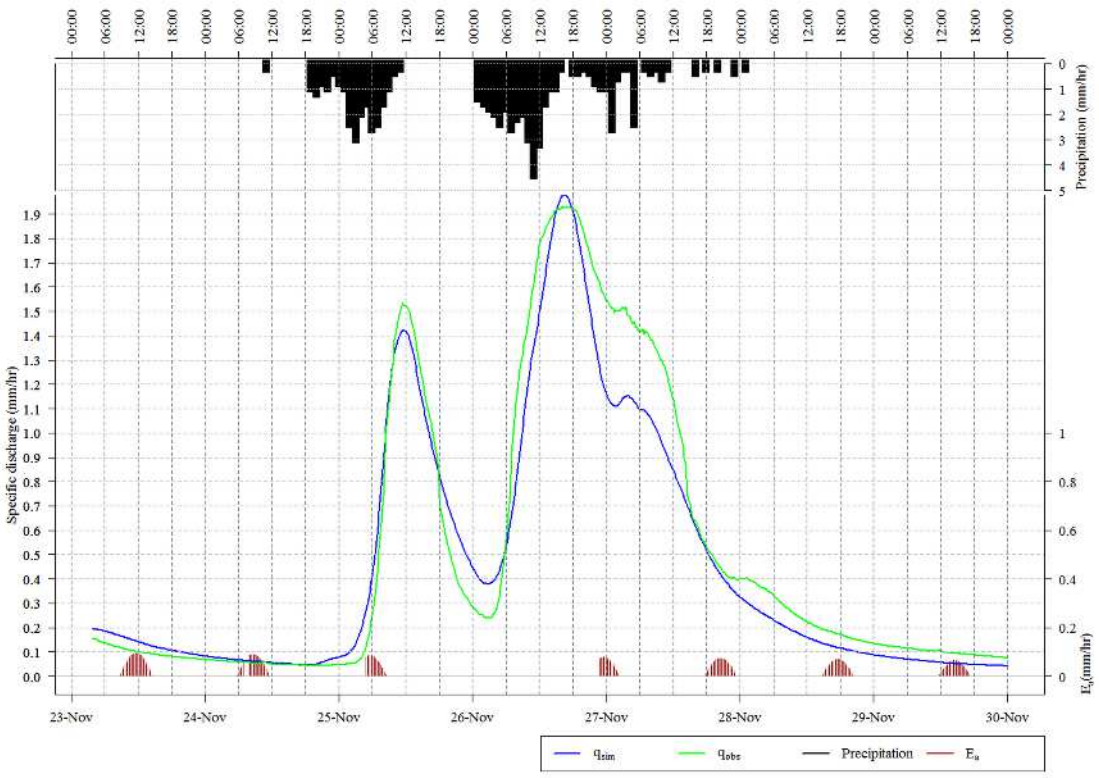

Figure 4.5. Simulated hydrograph for a storm event that occurred in November 2012 within the Brompton catchment. Discharges reconstructed from observed water levels shown in green, simulated values in blue. Uncertainty bounds of ±5% could be applied to the reconstructed flows.

Reconstructed flows from the observed water levels are also shown. While noting that the observed discharges may be rather uncertain in the way they have been reconstructed (see earlier) the calculated NSE of the simulated discharges was 0.95. The time of the first peak observed at the stage gauge was 11.30am on Sunday 25th November and the corresponding simulated peak was at 11:45am. Time at peak for simulated flows was 16:30 and for the reconstructed flows 17:00 on Monday 26th

November. The variation in observed discharges around the storm's peak during the hours of 4pm and 6pm was less than 0.25% of the total. This timing discrepancy was therefore considered to be within the range that could be accounted for by measurement uncertainty.

4.6.2. Response tests

Results for the batches 40, 50 and 59 barriers in the locations shown in Figure 4.3, using an opening h_b=0.3m and maximum height of 1.6m, are summarised in Table 4.3 and displayed graphically in Figure 4.6. This shows the times of peak discharge, difference between the maximum storage in catchment with and without the barriers, and an overall utilisation factor for the scheme *util*. At any one time the utilisation factor for an individual barrier is the proportion of the potential flow area above the barrier opening that is being intercepting. When the flow is unobstructed the factor is zero, when the water level is above the barrier opening but below its top it is 100%; when the feature starts overflowing the factor starts to falls as the total flow area exceeds the barrier area:

$$util(h) = \begin{cases} 0 & h < h_b \\ 1 & h_b \leq h \leq h_{max} \\ \dfrac{(A - A_o)}{A_b} & h > h_{max} \end{cases}$$

where A_0 is the opening area beneath the barrier, A_b is the barrier area above the opening, A the total channel flow area, h the water level, h_b is the barrier opening height and h_{max} its maximum height above the channel bed.

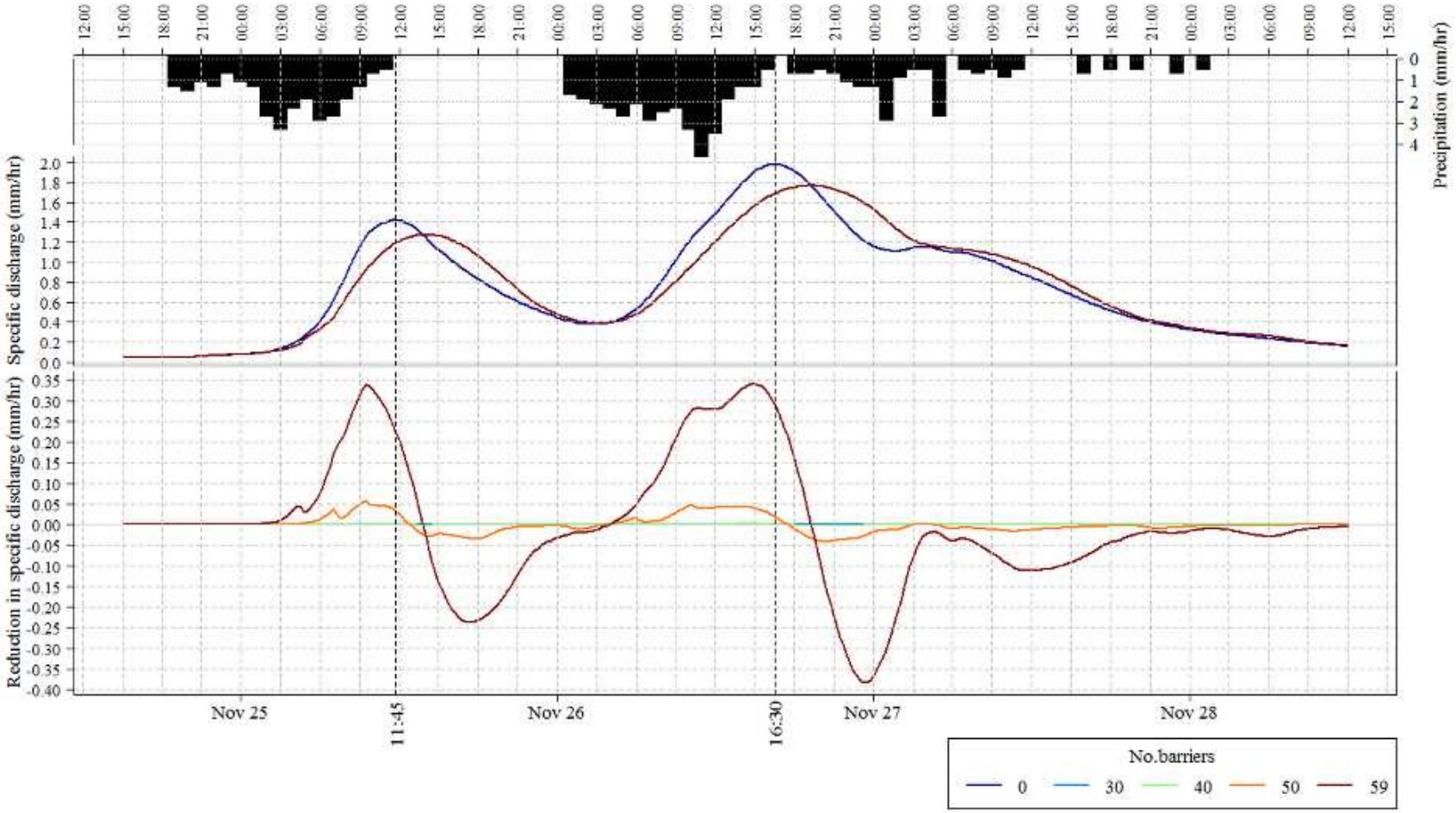

Figure 4.6. Absolute (top) and relative discharges for the various configurations employing a barrier clearance of 30cm for all barriers. Maximum attenuation of 0.35 mm/hr is seen within the rising limb of the main storm although largest attenuation of the peak is 0.21mm. Times at peak for the unaltered network are shown by the dotted lines. The maximal configuration delays the main storm peak by 2 hours 45 minutes.

Table 4.3. Summary of catchment response to adding up to 59 barriers, each with a clearance of 30cm, distributed at 300m intervals along the length of Ing Beck and its tributaries.

No. barriers	Time at peak 26th Nov	Delay to peak (hours)	Peak discharge (mm/hr)	Reduction in peak discharge (mm/hr)	% reduction of peak	Peak channel storage (m^3)	Max additional channel storage (m^3)	Max utilisation (%)
0	16:30		1.98			74846		
40	16:30	0	1.98	0.00066	0.03	75891	1045	2.5
50	16:45	0.25	1.96	0.018	0.93	90418	15572	21
59	19:15	2.75	1.77	0.21	10.64	170458	95612	27.4

There was virtually no effect on the response until the 40 barrier case and so results for fewer barriers are omitted. Examination of water levels for the 59 feature case shows that at the height of the storm just 20 barriers, mostly located on the main channel, were in operation; utilisation peaked at around 27%. Of the operational barriers 19 were actually overflowing at this point. The greatest attenuation in the peak discharge, seen with 59 barriers, is approximately 0.21 mm/hr or 10.7%. At about 0.35 mm/hr, the largest attenuation in discharge is, however, observed in the rising limbs of both storm peaks. This suggests that the storage capacity of the scheme is filled before both storm peaks. The maximal case delays the arrival of the main storm peak by 2 hours 45 minutes.

The impact increases rapidly as the final 9 barriers are added to the downstream reaches of Brompton Beck, suggesting that most of the effect is due to lower barriers. The disproportionate effect of these features appears to be due to their effect in diverting flow onto the floodplain, where the much higher roughness reduces flow velocities by a factor of 50. The lowest barrier, for example, diverts overland 45% of the flow from the sub-reach it drains, compared to just 0.3% for the corresponding sub-reach in the unobstructed channel.

The scheme seemed to be operating sub-optimally due to under-utilisation of the higher barriers and those downstream reaching capacity and overflowing. In an attempt to improve the impact a second configuration was applied that lowered the clearance of barriers on tributary reaches to just 10cm and raised barriers on the main channel to 80cm. The intention was to improve the utilisation of higher barriers whilst preventing those lower downstream from running out of capacity. The results are shown in Table 4.4.

Table 4.4. Summary of catchment response to adding up to 59 barriers with clearances of 80cm for those on main channel and of 10cm on its tributaries.

No. barriers	Time at peak 26th Nov	Delay to peak (hours)	Peak discharge (mm/hr)	Reduction in peak discharge (mm/hr)	% reduction of peak	Peak storage (m^3)	Max additional storage (m^3)	Max utilisation (%)
0	16:30		1.98			74846		
30	16:30	0	1.97	0.0065	0.33	77585	2739	83.1
40	16:30	0	1.94	0.036	1.84	82528	7682	87
50	16:45	0.25	1.91	0.063	3.2	94442	19596	77.1
59	18:30	2	1.79	0.19	9.39	144459	69613	70.3

The 30 barrier case now has some effect and, due to many more of the barriers coming into operation at peaks flows, utilisation improves considerably; up to 50 are used at some point. With 40 barriers in place, utilisation reaches a maximum of 87%. In contrast to the first configuration the utilisation then actually starts to decrease as further barriers are added (see Figure 4.7). This is a consequence of the lower barriers operating for shorter periods of time due to their much increased clearance. All of the barriers on the main channel still overflow at some point, however.

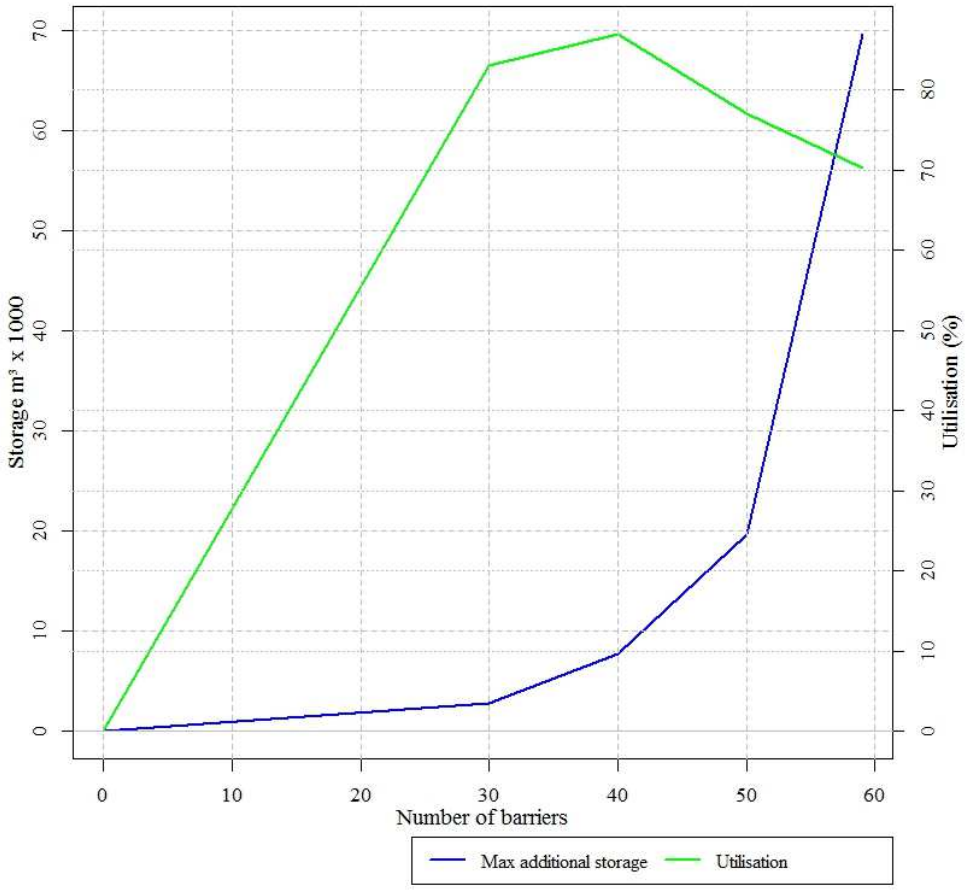

Figure 4.7. Additional channel storage introduced and utilisation for the 80cm barrier case. There is a clear exponential increase in storage as barriers are added to lower reaches, and the floodplain storage begins to be reconnected to the channel at peak flows. Maximal utilisation is seen in the 40 barrier configuration.

Despite the higher utilisation, at 9.4% the peak attenuation in the 10cm - 80cm clearance case is actually lower than for the 30cm clearance case and the delay in the main storm peak is reduced to 2 hours. It appears that some of the features are still draining after the first storm and that the remaining capacity is exhausted more quickly when the next storm arrives. Storage retained from earlier in the storm will contribute to the later storm flows. These barriers "run out" of capacity sooner on the rising limb of the second storm peak than the first, leading to a lower impact at the peak. Brim-full reaches will respond almost as quickly as open channels, leading to a smaller delay in the arrival of the peaks.

4.7. Discussion

Although the first configuration reduced peak flows by almost 11%, it would have not been sufficient to prevent flooding. The overall utilisation for the second configuration was larger but it could not provide any greater capacity to absorb the storm peak. It may be that a further approach with slightly higher upstream and lowered downstream clearances would have avoided this effect, and the simplicity of the routing model allows rapid set up and analysis of this and any other configuration. However, any conclusions drawn are likely to be predicated on the type of event considered. A single-peaked event, such as that commonly used in the assessment of flood scheme performance, might have produced markedly different conclusions. The scheme's performance would in this case be constrained only by its absolute storage capacity, rather than its ability to recover between events.

There are other options that would provide significant storage potential sufficient to retain the runoff of the entire event. For example, the railway embankment could be utilised as an "almost" NFM intervention by installing an engineered sluice across the tunnel conveying Ing Beck beneath the line. This could be lowered to reduce the maximum flow rate at storm flows and allow significant quantities of storage to build up behind the embankment during a storm event. The effect of this single intervention was modelled as for the underflow barriers used in the previous analysis but the maximum height h_{max} was set at 5m. Any overbank flow generated behind the embankment was intercepted and contributed to the build-up of storage. The response to applying sluice clearances of 1m and 0.5 m is shown in Figure 4.7 and summarised in Table 4.5.

Table 4.5. Summary of catchment response to installation of an underflow sluice across the tunnel conveying Ing Beck under the railway line.

Sluice clearance (m)	Time at peak 26/11/12	Delay to peak (hours)	Peak discharge (mm/hr)	Reduction in peak discharge (mm/hr)	% reduction of peak	Peak storage (m^3)	Max additional storage (m^3)
	16:30		1.98			74846	
0.5	15:30	-1	1.42	0.56	28.24	241710	166864
1	16:45	0.25	1.67	0.3	15.4	115400	40554

Applying a 0.5m diameter reduces the second peak by 25% to below the level that would have caused flooding. Peak storage is 168,000m, equivalent over the approximately 72 hour duration of the event to 0.3mm/hr falling across the 8 km^2 area draining through the viaduct. Maximum water depth of 3m immediately behind the gate was seen some hours before the flood peak and an area of approximately 20 ha flooded to an average depth of about 1m. The area is completely drained by the evening of the 28th, 36 hours after the storm peak. The smallest clearance brings the storm peak forward by one hour. This is simply due to its much smaller magnitude coinciding with a point midway up the rising limb of the unattenuated case.

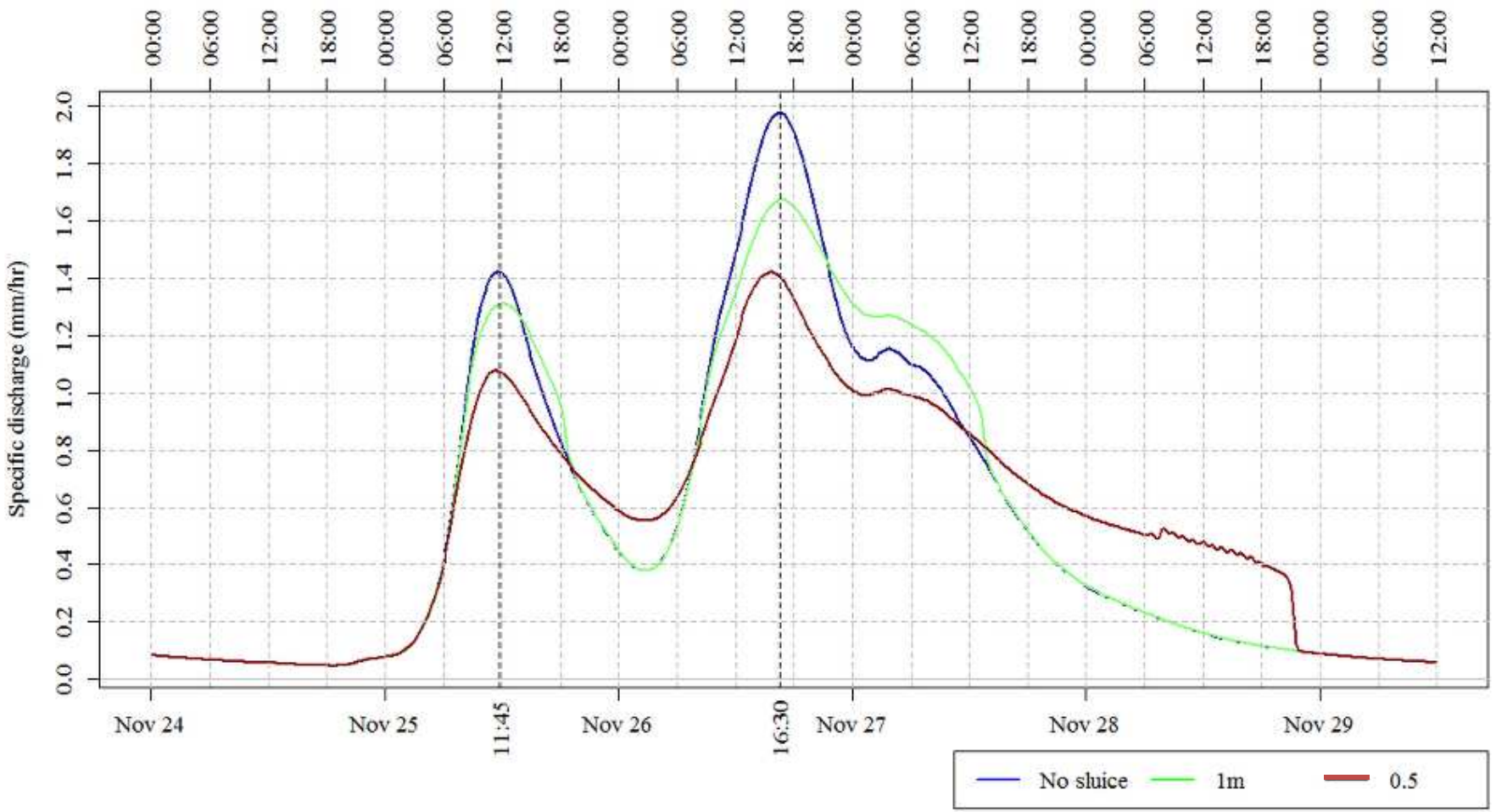

Figure 4.8. Theoretical attenuation of storm hydrograph achieved by installing a sluice across the railway viaduct tunnel and lowering its clearance to 1m and 0.5m. The smallest clearance attenuates the peak to under the discharge that would give rise to flooding at Water End. In this case storage retained behind the viaduct peaks at 168000m³ and is completely drained by the evening of 28th November, approximately 50 hours after the main storm peak.

It is important to recognise that the scenario involving flow restriction through the tunnel has been included solely as an illustration of the potential to gain significant additional storage capacity through a combination of topography and existing infrastructure. Such opportunities might be available in other catchments. In practice, there are many other considerations relating to the safety and operation of infrastructure, and it is highly unlikely that the owners would allow their asset to be subjected to hydraulic loading in this manner. The additional storage capacity introduced could also lead the intervention to become subject to the Reservoirs Act, requiring a detailed geotechnical survey, much higher design specifications and significantly greater capital cost.

Similarly, the constraints imposed by the IDB on the channel features, such as the requirement that they did extend into riparian areas or cause flooding here, clearly limited their effectiveness. Even so, in the modelled scheme downstream barriers appeared to be diverting large quantities of water onto the floodplain: the lowest retained up to 5000m³ in the channel and floodplain immediately upstream, compared to 1500m³ for the same sub-reach for the unobstructed case. This suggests that more relaxed design constraints could allow for a distributed solution that introduced the required storage whilst avoiding the regulatory and cost implications of a large single storage area. If combined with enhancement of riparian roughness to reduce overbank velocities and retain storage on the flood plain, such as was the case in the Ryedale scheme (Nisbet et al., 2011), this could provide significant impacts on storm flows.

The static linkage of the runoff model and channel routing component limited the ability to explore riparian rewetting, whereby floodplain storage is reinfiltrated and can potentially contribute to subsurface flow in further storms. This could be developed in further work.

Clearly, channel features extending into the flood plain to promote overbank flow would undergo significant hydraulic stress in the course of an event and would have to be constructed to high standards to prevent failure. Well-fixed sturdy impermeable wooden screens might be able to withstand the hydrodynamic stresses, but the channel bed and banking around them would be subject to scour. A regular maintenance regime would have to be established to ensure that the features' performance did not degrade across events and that their structural integrity remained intact.

4.8. Conclusions and further developments

This study has demonstrated that, with care, a distributed Natural Flood Risk Management scheme could be implemented in the study catchment to reduce peak flows, but that in-channel features alone would not provide sufficient attenuation to prevent recent flood events, at least given realistic constraints in their number and dimensions. It has shown that even an extensive scheme could be substantially underutilised and provide little or no attenuation to the storm hydrograph. Barriers furthest downstream contribute relatively more attenuation with the attendant risk of failure due to large hydraulic stresses.

A scheme utilising a reduction in the capacity of the railway tunnel feature specific to the catchment could, however, deliver the required response. However this might not be considered an acceptable solution for other reasons, such as the potential for damage at storm flows. In addition, the volumes involved mean that if a structure of equivalent storage capacity were built it would become subject to regulation by the UK Reservoirs Act.

It has been shown that that there can be a marked contrast between the potential attenuation provided by a network of features and the actual capacity utilised.

Designing such schemes to maximise the utilisation is likely to be difficult, and there is always the potential that an optimal configuration for one type of event may in fact prove to be less effective in others. It appears that a double-peaked storm event of the type considered, although not uncommon, can cause problems in distributed schemes. Their aggregated storage is theoretically able to retain much of the storm runoff but during the course of a storm much of this storage is either unused or overloaded. The available storage capacity may become saturated in intermediate events and not recover sufficiently quickly in order to provide capacity for later storms.

Much of the attenuation is due to the lower barriers, mainly through their effect of reconnecting the floodplain with the channel and diverting large quantities of overbanked flow through the rougher riparian area. It is suggested that schemes should concentrate on encouraging this effect using fewer, larger barriers further downstream in preference to many smaller barriers in the upper reaches. This approach, however, would also introduce much greater hydraulic stresses and correspondingly greater rating specifications and maintenance requirements, albeit that this would be reduced due to the fewer structures. The potential of cascading failures should be considered, not least due to the potential for blockage of downstream structures such as tunnels.

A coupled hillslope runoff – channel network routing model was developed to evaluate the scheme proposed for the catchment. Although applied here to features located entirely within the channel network, it provides a flexible framework within which many types of NFM intervention, including those across hillslopes, can be evaluated. Further studies could develop and extend this framework to apply it to measures such as those described in the introduction. It could be applied to larger catchments with more heterogeneous land-use, and with a wider variety of storm

events. This will provide a more robust evidence base on which to assess the applicability, design and effectiveness of flood management schemes across a range of catchments and scenarios. Given the significant uncertainties inherent in modelling systems of this nature, and lack of evidence on how best to simulate changes in the processes affected by NFM measures, uncertainty estimation should be an integral part of such an expanded modelling framework.

The (hypothetical) measures that provided the greatest effect were the throttling of the flow through the railway tunnels and emplacement of barriers downstream to divert water onto the flood plain, both of which would involve the inundation of significant areas of productive agricultural land. This introduces much potential for conflict with land owners and regulatory bodies such as the IDB, whose priorities in terms of channel and runoff management are likely to diverge from those of NFM practitioners. Experience from the Belford scheme where a pilot site was established before the main scheme was begun (Wilkinson et al., 2010a), and the stakeholder collaborative approach adopted in Ryedale (Lane et al., 2011) suggest ways that resistance to the adoption of such new approaches to flood risk management may be overcome.

Chapter 5. Strategies for testing the impact of natural flood risk management measures.

Reference

Hankin, B., Metcalfe, P., Johnson, D., Chappell, N., Page, T., Craigen, I., Lamb, R., Beven, K. (2017). "Strategies for Testing the Impact of Natural Flood Risk Management Measures" in Flood Risk Management. Hromadka, T. & Rao, P. (Eds.). InTech, Czech Republic. ISBN 978-953-51-5526-3.

Statement of author contribution

- Development of computer model for simulation of runoff and effects of interventions . Generation of simulations and organisation and analysis of results
- Editing and contributions to text
- Production of Figure 5:17, Figure 5:13, Figure 5:9 & Figure 5:12
- Analysis for and production of Table 5:5

Abstract

Natural Flood Management (NFM) is an approach that seeks to work with natural processes to enhance the flood regulating capacity of a catchment, whilst delivering a wide range of ecosystem services, from pollution assimilation to habitat creation and carbon storage. This chapter describes a tiered approach to NFM, commencing with strategic modelling to identify a range of NFM opportunities (tree-planting, distributed runoff attenuation features and soil structure improvements), and their potential benefits, before engagement with catchment partners, and prioritisation of areas for more detailed hydrological modelling and uncertainty analysis.

NFM measures pose some fundamental challenges in modelling their contribution to flood risk management because they are often highly distributed, can influence multiple catchment processes, and evidence for their effectiveness at the large scale is uncertain. This demands modelling of 'upstream' in more detail in order to assess the effectiveness of many small-scale changes at the large-scale. Demonstrated is an approach to address these challenges employing the fast, high resolution, fully-distributed inundation model JFLOW, and visualisation of potential benefits in map form. These are used to engage catchment managers who can prioritise areas for potential deployment of NFM measures, where more detailed modelling may be targeted. A framework applying the semi-distributed Dynamic TOPMODEL, in which uncertainty plays an integral role in the decision making process, is demonstrated.

Keywords: Natural Flood Risk Management, Uncertainty

5.1. Introduction

Natural Flood Management (NFM), often referred to in the UK as Working with Natural Processes (WWNP), has been defined as taking action to manage flood risk by protecting, restoring and emulating the natural regulating function of catchments, rivers, floodplains and coasts (Pitt, 2008). NFM can integrate improvements to the local landscape and ecology, thereby contributing to meeting environmental goals (such as European Water Framework Directive objectives). Compared to hard-engineered Flood Risk Management (FRM), NFM is becoming attractive to policy makers and catchment managers due to lower upfront costs, the potential to create multiple ecosystem benefits (e.g. carbon storage, diffuse pollution and sediment risk regulation), and for its flexible scale of deployment, which may also help to stimulate or encourage community involvement. The mechanisms to achieve such aims include runoff storage, increasing soil infiltration, slowing surface water movement and reducing flow connectivity.

Across a catchment there can be many different opportunities for NFM, including moorland restoration, revised and modified land management and land use, woodland creation, sediment management, built water storage, river restoration and development of Runoff Attenuation Features (RAFs) to intercept overland flow. These are typically small-scale and highly distributed, and potentially alter a wide range of catchment processes. As a consequence of their scale and local impact, they are mostly likely to be effective in reducing downstream flooding when implemented widely in the headwaters of catchments to reduce streamflow reaching downstream floodplains.

Catchment models routinely applied by regulatory agencies and water authorities for flood risk assessments, forecasting, water resources planning or water quality management, tend to represent upstream areas as discrete sub catchments with

uniform inputs. This can be very effective for simulating flows in the river further downstream near urban settlements, but averages over the effects of small scale interventions and thus loses information into their impacts on the various hydrological processes of interest. For highly distributed, smaller scale measures and interventions it will be vital to consider new approaches that not only scale their impact up more accurately but consider the uncertainty in the representation of how catchment processes might change. There are still large evidence gaps and a need to test the effectiveness of these distributed measures against observational data. This will require detailed monitoring of catchment processes. A recent survey (JBA Trust, 2016), however, showed that as few as 6% of schemes in the UK have intensive hydrological monitoring.

The approaches demonstrated here aim to address the scaling-up problem in a way that reflects the uncertainty in the representation of small-scale hydrological processes and flood mitigation methods. In doing the challenge is met put to environmental modellers (Beven, 2009) to give decision makers:

"…a realistic evaluation of uncertainty since this might actually change the decision that is made"

By means of an example, here a tiered approach is taken to planning NFM strategies within the headwaters of the Eden, Kent and Derwent catchments in Cumbria, UK (Figure 5.1). This aimed to prioritise where different measures are likely to be most effective. This was followed with an analysis of uncertainty in the environmental model parameters and of the fuzziness in the evidence behind the changes applied to these models to represent effects of NFM measures.

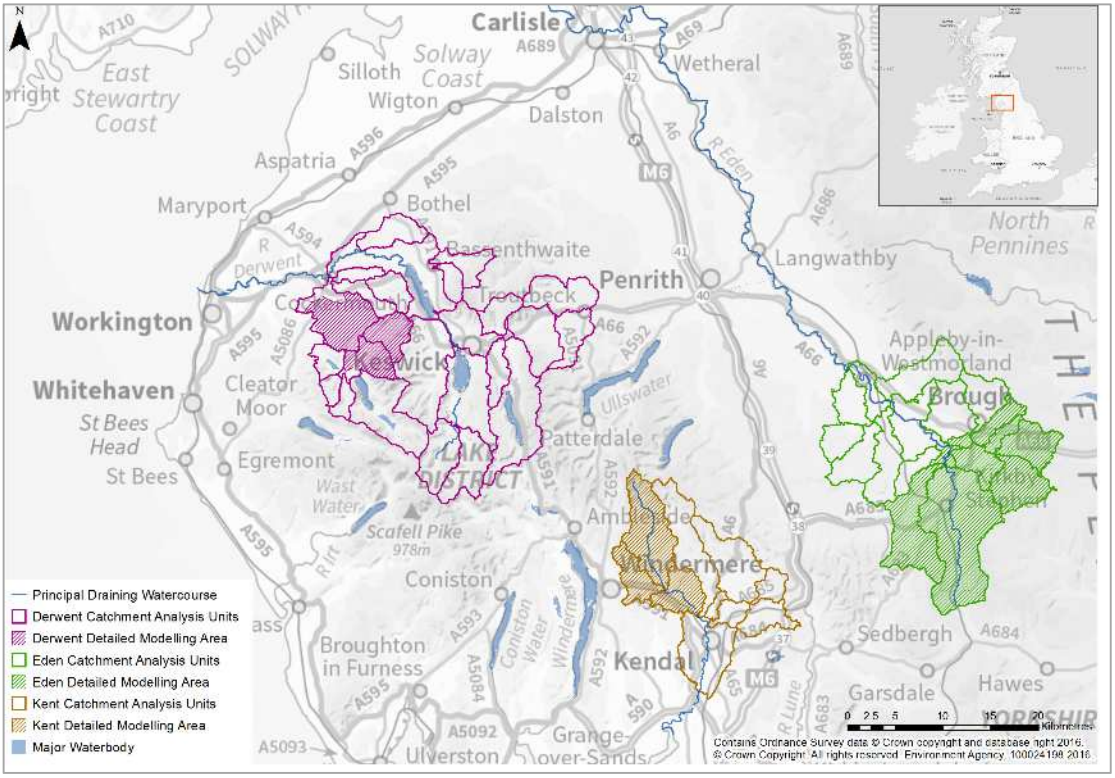

Figure 5.1. Overview of study area (after Hankin et al., 2017)

It is shown here effectiveness of very distributed NFM measures such as tree planting and enhanced storage in the headwater catchments can be appraised in a framework similar to established FRM. Advances in high resolution modelling (here an explicit modelling of runoff on a 2x2m resolution grid within a 100-million-cell model), have unlocked the potential to model 'upstream' at high resolution, and enable us to test the aggregated impacts of very small scale measures at the larger scale. This delivers a deeper understanding of the effectiveness of potential NFM plans in reducing peak runoff, but requires new strategies to consider 'synchronisation' issues (Metcalfe et al., 2017), whereby flooding can be made worse by slowing the time of arrival of a flood peak in one tributary such that it interferes constructively with that of the receiving watercourse. It also opens up ability to undertake continuous modelling through sequences of events, such that the antecedent wetness is taken into account.

Since NFM measures could be deployed in very many spatial configurations, it follows that synchronisation effects should be investigated against a wide range of plausible extreme loading conditions. The authors demonstrated such an approach in a recent UK government Flood Modelling Competition, where the winning entry (Hankin et al., 2017), combined high resolution modelling of NFM with advancements in spatial joint probability analysis of extremes (Lamb et al., 2010; Keef et al., 2013), whereby multiple extreme rainfall scenarios were simulated, with realistic spatial patterns based on the long term records at rainfall gauges around the catchment. The "average" effectiveness of NFM across the upper part of the 2,300km^2 Eden catchment was then tested against 30 simulated extreme rainfall events selected to span a range of spatial patterns.

5.2. A Risk Management Framework for NFM

Figure 5.2 highlights a pathway through the risk management cycle that attempts to integrate core elements needed for modern flood risk management, adapted for NFM with its distinguishing features of highly distributed interventions and uncertain impacts. This framework was developed and applied in the course of the Cumbrian project for identification of the types of NFM opportunities introduced earlier, with whole catchment modelling being applied to map potential risk reduction benefits.

This first step was undertaken for the Cumbrian project using rapid overland flow modelling approach using a 2m resolution 2D JFLOW model (Lamb et al., 2009) to identify where modification of features in the landscape to slow and store surface water flows might make the most difference. These included the use of RAFs at locations of high flow accumulation, tree-planting, and soil structure improvements. The speed of set-up, very high resolution and rapid run times of JFLOW allowed rapid

assessment of the effectiveness of these very distributed NFM measures, before they were shared with catchment partners.

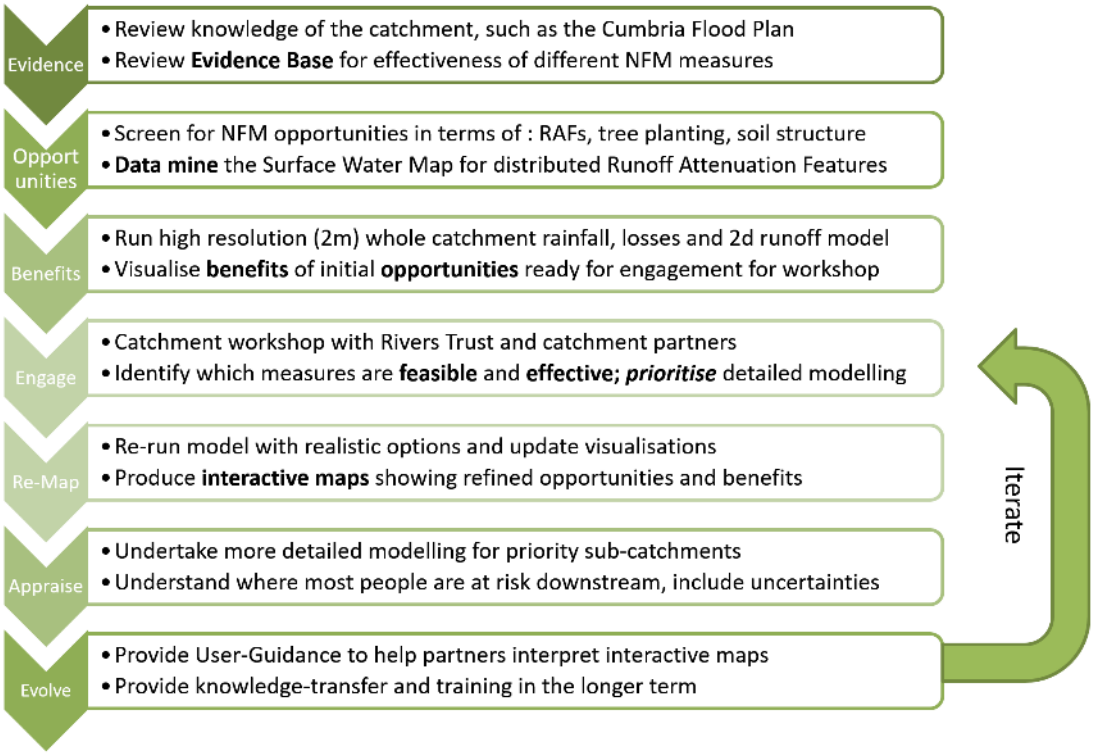

Figure 5.2. The risk management cycle for NFM (after Hankin et al., 2017)

Our work in Cumbria has involved a wide range of catchment partners including land owners, flood management agencies, voluntary groups and farming groups, who used the whole-catchment mapping to refine potential opportunities for NFM deployments, and also prioritise areas for more detailed modelling. The subcatchments containing the most promising opportunities based on the JFLOW modelling were prioritised for more detailed uncertainty investigation using Dynamic TOPMODEL (Beven & Freer, 2001a; Metcalfe et al., 2015) to compute the projected benefits of NFM.

Dynamic TOPMODEL provides a tool to help understand the effects of NFM on the total hydrograph, including contributions from overland flow and subsurface flow. The detailed models were calibrated against observed data collected during the period Nov - Dec 2015 in order to capture the flows arising from a sequence of prolonged

and intense rainfall events associated with Storms Abigail and Barney prior to the most severe storm, Desmond (4-6 December 2015), which led to extreme rainfall and flooding in Cumbria (PERC, 2015; Marsh et al., 2016).

An uncertainty framework was used to represent the uncertainties in the parameters used in the model, but also the gaps in the scientific evidence on how different NFM measures influence catchment processes (Figure 5.3). A large number of simulations were undertaken for each catchment, and a set of model parameterisations showing 'acceptable' performance on the basis of the evidence, were identified based on a range of measures including the ability of the models to reproduce the observed peak flow

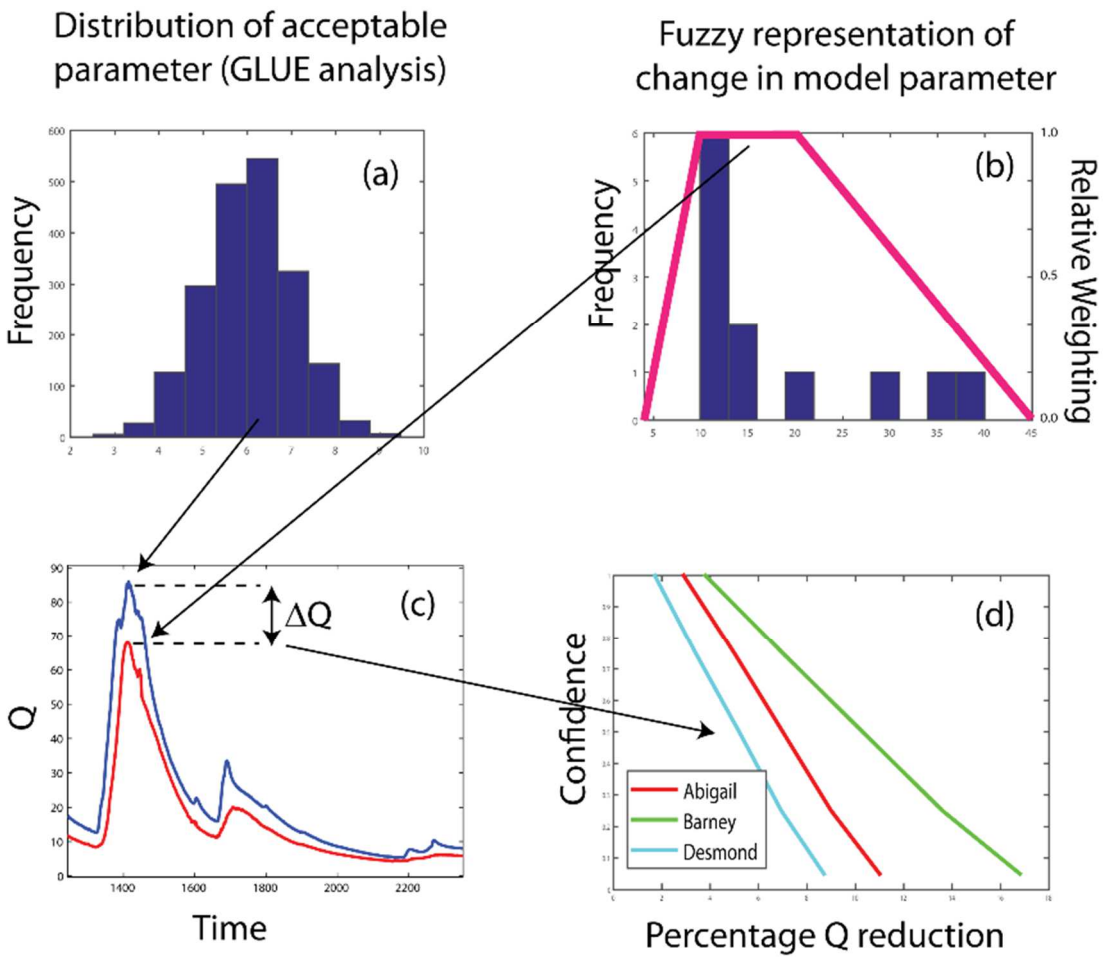

Figure 5.3. Stratified sampling of parameter uncertainty and fuzziness in evidence parameter changes to reflect NFM interventions (after Hankin et al., 2017)

for Storm Desmond. The next sections cover the broad steps in this flow chart.

5.3. Evidence for effectiveness of NFM

This section reviews evidence of the effects of NFM on catchment processes, and how this evidence was mapped on to the effective parameters that are used in the different modelling strategies adopted in the Cumbrian opportunity mapping project. This section gives an overview of how evidence of changes to physical processes in the UK was gathered, and how these were to mapped already uncertainly modelled processes.

For the JFLOW overland flow modelling, the physical influences considered were:

- Increasing roughness through land cover changes: grasses and mosses to shrubs and trees
- Increasing localised depression storage through construction of RAFs
- Increasing infiltration through improvements in soil structure

For Dynamic TOPMODEL the above processes are considered and also those influencing sub-surface flow. These include:

- Reducing surface overland flow velocities through woodland planting
- Increasing surface storage associated with RAFs using modified surface routing and a maximum storage parameter
- Increasing soil transmissivity through woodland planting
- Increasing wet canopy evaporation through woodland planting

The evidence for the above changes linked to tree-planting was considered with respect to deciduous woodland, which brings the most habitat and biodiversity

benefits in this environment, and is in line with current activity within NFM schemes across the UK.

5.3.1. Surface roughness

Considering the roughness of the ground covered by improved pasture, heathland or deciduous woodland, many different elements combine to produce an effective roughness for a whole hillslope. Within a deciduous woodland, roughness contributions come from: (1) roughness of the litter layer, (2) roots at the ground surface running across the slope, (3) obstructions to flow caused by tree stems/understory, (4) paths and tracks, (5) fence lines or walls, and (6) sub-grid topographic irregularities in slope. All components need to be characterised to provide an accurate measurement of the effective roughness of a whole hillslope.

Direct measurements of the roughness components across a range of surface vegetation conditions at floodplain sites in Florida (USA) (Medeiros, 2012) produced Manning's *n* (see Chow et al., 1988) values that ranged from 0.030 to 0.061 for forest areas against a range of 0.013 to 0.050 for other surfaces including barren land and grasslands. Chow (1959) states that floodplains covered by pasture should be ascribed a roughness value of 0.035, while those covered by light brush and weeds 0.050, dense brush 0.070 and dense forest 0.1-0.2. Thus in direct comparison with the direct measurements of roughness undertaken in Medeiros (2012), the differences between woody vegetation and pasture-cum-barren land are considerably less. Given: (1) the limited number of studies directly measuring hillslope roughness, (2) the discrepancies between the field-measured and tabulated (or estimated) values, combined with (3) the large variability in roughness values measured even within the same vegetation types, a large uncertainty should be placed on the range of possible roughness values used in models.

In this study, a comparison is made between with and without woodland, that amounts to a maximum increase of 50% in Manning's roughness, over the broad-scale 'upland' roughness value of 0.1 used to provide national flood maps in the UK. Thus a maximum of 0.15 was used compatible with the engineering tables of Chow (1959), but which requires more research to resolve the underlying physical processes contributing to frictional losses.

5.3.2. Peatland management

Similar issues arise when estimating the effects of peatland management on the effective roughness of hillslopes as with the comparisons between the effects of forest versus pasturelands. For example, peatland restoration may involve replacing patches of bare peat with Sphagnum spp. moss, changing micro-scale roughness, but also adding small obstructions within the artificial drains. Holden et al. (2008) used 256 bounded overland flow plots (0.5 m x 6 m) in the Upper Wharfe catchment (UK) and found that the roughness was greater when Sphagnum spp. moss rather than bare ground was present, resulting in a reduction of overland flow speeds by a factor of 3.3. This equates to an increased roughness of ~ 0.3, which was used in the JFLOW modelling and the reduced wave speed in Dynamic TOPMLODEL, albeit starting from the relatively high generic roughness factor used in the national mapping, of 0.1 and increasing it to 0.13.

This study only considered an increase in roughness, however, ditch-blocking is another peat-land restoration intervention that can reduce flood risk (Holden et., 2011). The effect of blockage has been studied by Holden et al. (2011), and where applied in NFM schemes such as Pickering (Nisbet et al., 2011) and Pontbren (Wheater et al., 2008).

5.3.3. Runoff Attenuation Features (RAFs)

Small ponds to capture and temporarily store overland flow on its way to stream channels have been described as 'overland flow interception RAFs' or 'overland flow disconnection ponds', where RAFs are 'runoff attenuation features'. Temporary storage of the overland flow on slopes could delay this component of the flow so that it reaches streams after the peak of the hydrograph has passed. However, if overland flow on a particular slope is generated on the rising stage of a stream hydrograph (Chappell et al., 2006), delaying it could have the unwanted effect of adding the overland flow contribution to the channel at the time of the peak in the streamflow. Clearly, understanding precisely when overland flow is being added to stream channels, and doing so within a spatial frame of reference, is critical for understanding how it should be managed. Only a few direct measurements of overland flow using plot studies are available in the UK (e.g. Wheater et al., 2008) to help quantify the timing of this process. The Belford Catchment Solutions Project in Northumberland has demonstrated how such features are able to retain and hence attenuate the initial phase of overland flow generation. Overland flow interception RAFs have been constructed at many locations in the UK and individually range from 20 to 1,000 m^3 in capacity (Deasy et al., 2010; Nicholson et al., 2012). RAFs added into the simulations for this study are 100-5,000 m^3 in volume and so are broadly similar in capacity.

5.3.4. Wet-canopy evaporation

Deciduous woodlands in the early winter (i.e., November-December) in Western Europe, when the overstory is leafless, exhibit only very small rates of transpiration (Vincke et al., 2005). Potentially, these rates may be marginally higher than those for improved grasslands, if the woodland is open and accompanied by a leafed understory vegetation of shrubs and/or longer grasses (Rychnovská, 1976; Black & Kelliher,

1989; Roberts & Rosier, 1994; Verón et al., 2011). This effect is, however, likely to be insignificant when compared with the contrasts in wet-canopy evaporation (also called 'interception loss' or Ewc).

Reynolds and Henderson (1967) noted '…although sometimes there is measurable reduction of interception losses in winter due to leaf fall, the effect is commonly surprisingly small…' Combined Ewc and transpiration losses from grasslands in the early winter are likely to be small, for example 5.6% of gross rainfall (16.3/289.5 mm) for months of December 1975-1985 (Kirby et al., 1991). However, in some contrast, the wet-canopy evaporation rate for deciduous woodland when the overstory is leafless in winter is likely to be within the range 10-20% of the gross rainfall for the conditions prevailing in the UK or for similar situations in continental Europe (Table 5.1). The first column was used directly to define the fuzzy set of wet canopy evaporation rates used in the Dynamic TOPMODEL.

Table 5.1. A wet-canopy evaporation range (over 1-3 months) that also encompasses most of the extremes in observed behaviour of leafless vegetation canopies would be 5-50% of gross rainfall

% P (by rank)	Dominant species	Reference	UK/Europe
40-50%	hawthorn (hedge)	Herbst et al (2006)	UK
36%	oak/birch	Noirfalise (1959)	Continental Europe
29%	hornbeam	Leyton et al (1967)	UK
22.5%	oak	Vinke et al (2005)	Continental Europe
19.8%	oak/birch	Herbst et al (2008)	UK
15.1%	beech/hornbeam	Aussenac (1968)	Continental Europe
14%	beech	Reynolds & Henderson (1967)	UK
12.1%	mixed	White and Carlisle (1967)	UK (Cumbria)
12%	oak coppice	Thompson (1972)	UK
11%	oak	Dolman (1987)	Continental Europe
10.5%	hornbeam/oak	Schnock (1969)	Continental Europe
10%	oak/beech	Staelens et al (2008)	Continental Europe
9.9%	oak	Carlisle et al (1965)	UK
7%	beech	Gerrits (2010)	Continental Europe

5.3.5. Antecedent moisture status

The higher rate of wet-canopy evaporation during winter leafless periods, combined with the higher combined rates of wet-canopy evaporation and transpiration from leafed deciduous trees in the proceeding summer and autumn in comparison to grassland (Brown et al., 2005), means that UK woodland soils are likely to be drier during the winter. A drier subsurface condition will reduce the proportion of rainfall delivering fast streamflow responses thereby reducing peak flood flows (Chappell et al., 2006, 2017). Finch (2000) observed drier soil moisture profiles (by 250 mm) beneath sweet chestnut and larch woodland and grasslands in Pang basin (Berkshire, UK) through December in 1997. Indeed, the profile did not reach its maximum saturation until April 1998. Similarly, Calder et al. (2003) show soil moisture deficits through December 2000 that are drier by 30 mm in the soil (0-0.90 m) beneath oak (Quercus robur L.) of Clipstone Forest (Nottinghamshire, UK) than beneath adjacent grassland. A scenario of 80 mm of additional soil moisture deficit beneath deciduous woodland compared to grassland in the early winter is within the 30-250 mm range of the two UK studies noted, but is clearly associated with a highly uncertain range.

NFM might feasibly give wetter antecedent conditions in a sequence of winter events, if the increased infiltration effects of tree planting on soil moisture are larger than those of enhanced wet-canopy evaporation ('infiltration trade-off hypothesis'). Here an attempted is made to account for this through detailed modelling of several consecutive storms, and although the drier antecedent soil moisture was taken into account, the deficit was reduced considerably after the first storm in the series.

5.3.6. Woodland on slowly permeable, gleyed UK soils

Overland flow on hillslopes may be caused by rainfall intensities (mm/hr) exceeding the saturated hydraulic conductivity (K_S; mm/hr) of a topsoil or other surface horizon

(equivalent to the 'infiltration capacity' or 'coefficient of permeability of the topsoil'). This rapid pathway of rainfall towards stream channels is called 'infiltration-excess overland flow' (Horton, 1933). If rainfall is reaching the ground at a rate less than saturated hydraulic conductivity of the topsoil, but cannot infiltrate because the topsoil is already saturated as a result of drainage from upslope areas, then the rainfall onto these saturated areas will move as overland flow across the surface. This pathway is called "saturation (excess) overland flow by direct precipitation" or SOF by direct precipitation (Dunne & Black, 1970). If the downslope subsurface flows exceed the ability of the downstream soils to discharge them directly into a stream channel, then subsurface water may emerge from the topsoil onto the ground surface as 'return flow' (Cook, 1946). This return flow may then travel overland towards a stream as so called "saturation (excess) overland flow by return flow" (SOF by return flow).

Soil types that typically have a lower saturated hydraulic conductivity have a greater likelihood of generating 'infiltration-excess overland flow', and where present in downslope areas, also a greater likelihood of generating surface flows by 'saturation excess overland flow by direct precipitation' and 'saturation excess overland flow by return flow'. The soil type called a Gleysol using the international soil classification system (FAO-UNESCO, 1990) or gley within the Soil Survey of England and Wales (SSEW) soil classification system (Jarvis et al., 1984) typically exhibits lower saturated hydraulic conductivity values throughout UK soil profiles. Table 5.2 shows an example K_S profile for a gley in the Lune Valley, Northwest England (UK). These measurements were undertaken in the field with a ring permeameter (see Chappell & Ternan, 1997) a technique demonstrated to give accurate values, even for disturbance-sensitive gley soils (Chappell & Lancaster, 2007).

Table 5.2. Horizon-specific saturated hydraulic conductivities (cm/hr) of a Humic Gleysol near Farleton, Lancashire (UK) after (Chappell and Lancaster, 2008, and Chandler and Chappell, 2007).

Depth (m)	Mean K_S (cm/hr)	Range (n = 56)
0.10	9.1	1.31–30.7
0.10-0.20	21.8	8.98–57.0
0.20-0.50	0.11	0.021–3.02
0.50-1.00	0.002	0.0007–0.21

Soils in England and Wales that are classified as gley cover a range of soil associations based on the SSEW (Soil Survey of England and Wales, 1983). As a result of their greater likelihood for generating overland flow, these gley soils are classified as having an SPRHOST (Standard Percentage Runoff based on Hydrology of Soils Types) value in excess of 50% (Boorman et al., 1995). Enhancing the permeability of such soils could have the greatest impact on reducing overland flow across catchments and thereby have the greatest potential to reduce flood peaks in rivers (Nisbet et al., 2011). As a result, tree planting to increase soil permeability includes areas with such gley soils.

Consequently, for NFM modelling a key need is to represent the permeability effects of planting deciduous trees on gley soils. Very few UK studies are available that quantify the difference in soil Ks of gley soils beneath deciduous trees relative to that beneath adjacent grasslands (Chandler & Chappell, 2008).

These limited studies are summarised in Table 5.3, and give a range of 1.5 to 3.5 factor increase in permeability for deciduous tree planting on gley soils. These K_s factors were then used to provide the fuzzy set of parameter changes in the Dynamic TOPMODEL scenarios.

Table 5.3 Ratio of K_S measured for deciduous trees to that grassland growing on gley soils in the UK

F/G1	Tree age (years)	Soil type	Location	Reference
1.81	2	713e-Brickfield-1	Tebay Gill, Cumbria	Mawdsley, Chappell & Swallow (2018)
2.43	10	721d-Wilcocks-2	Pontbren, mid-Wales	Marshall et al. (2009)
3.40	107	713f-Brickfield-2	Lancaster, Lancashire	Chandler & Chappell (2008)

This observed increase in permeability for gley is smaller than the factor of 5 difference between predominantly deciduous woodland and improved pasture recently observed on well drained Eutric Cambisol (SSEW Brown Earth) soils in Scotland by Archer et al. (2012, 2013). The observed effect on gley is also smaller than the effects observed on other soil types across the globe, the majority of which are between 2 and 20, with some outliers much greater than this, which is likely to be due to macropores along root channels. In any event, if the roughness of these high runoff areas can be increased through roughening up, then it may be possible to attenuate quick-flow from these soils.

Critically, it should be remembered that most of the stream hydrograph during floods comprises water that has primarily travelled to the stream via subsurface pathways. Even within very flashy, but undisturbed tropical streams, only small proportions of flow within the basin have been directly measured as overland flow (e.g., < 10% streamflow, Chappell et al., 1999). Therefore, while the overland flow pathways are important given their speed and sediment transport aspects, simulated flow pathways are likely to be dominated by subsurface pathways either close to the surface in soils or deeper within the surficial or solid geology (Ockenden & Chappell, 2011; Jones et al., 2014). These can also be fast – subsurface celerities in wet soils can even exceed overland flow velocities (McDonnell & Beven, 2014).

5.4. Opportunity Mapping of NFM

Opportunity maps can be developed from local knowledge, land cover maps, flood modelling outputs, or a combination of all three, as described here. In this chapter, opportunities for three core types of NFM (tree-planting, RAFs and soil structure improvements) were developed from different national strategic maps, and then through consultation at an engagement event. Ideally engagement would be a continuous process of refinement where more knowledge of the land scape and opportunities are built in through time, and evidence is co-produced (Lane et al., 2011). The following sections explain how these opportunities were identified and refined.

5.4.1. Runoff Attenuation Features

Research on RAFs (e.g. Odoni & Lane, 2010; Wilkinson et al., 2010b; Quinn et al., 2013) such as storage ponds, bunds, in-stream storage through woody debris dams and disconnecting drain flow pathways has shown that these features have the potential to reduce flood peaks and increase the time to peak for overland flows and stream flows. Applying RAFs within the headwaters of a catchment therefore has the potential to attenuate sudden short duration storm events and reduce the subsequent flood risk to more urbanised areas of the catchment downstream.

Opportunities to deploy RAFs can be identified from areas of high flow accumulation in surface water flood maps, and comprise small areas such as natural depressions within the landscape, or small in-channel storage as shown in Figure 4. The JRAFF model identifies the orange areas of isolated flow accumulation, such as ponds and small channels, which may be appropriate to excavate or bund, or disconnect from flow pathways through gully or ditch blocking. An additional storage of 1 m in depth

at these locations is represented through burning the Digital Terrain Model (DTM) deeper by 1m in the RAF model scenario.

The JRAFF tool places a set of constraints on the size and location of these accumulations:

- Area threshold between 100 m^2 and 5,000 m^2
    - This was considered suitable for local land management alterations, and well below the threshold on capacity that would fall under the UK Reservoirs Act (10,000 m^3).
- CORINE land cover 2012 dataset and a 2m buffer of OS OpenData buildings and roads deemed unsuitable to runoff attenuation features.
    - A 2 m buffer of roads results in a 4 m wide exclusion zone. This threshold has been derived based on typical road widths and ensures that opportunity features within any potential adjacent ditches are retained.

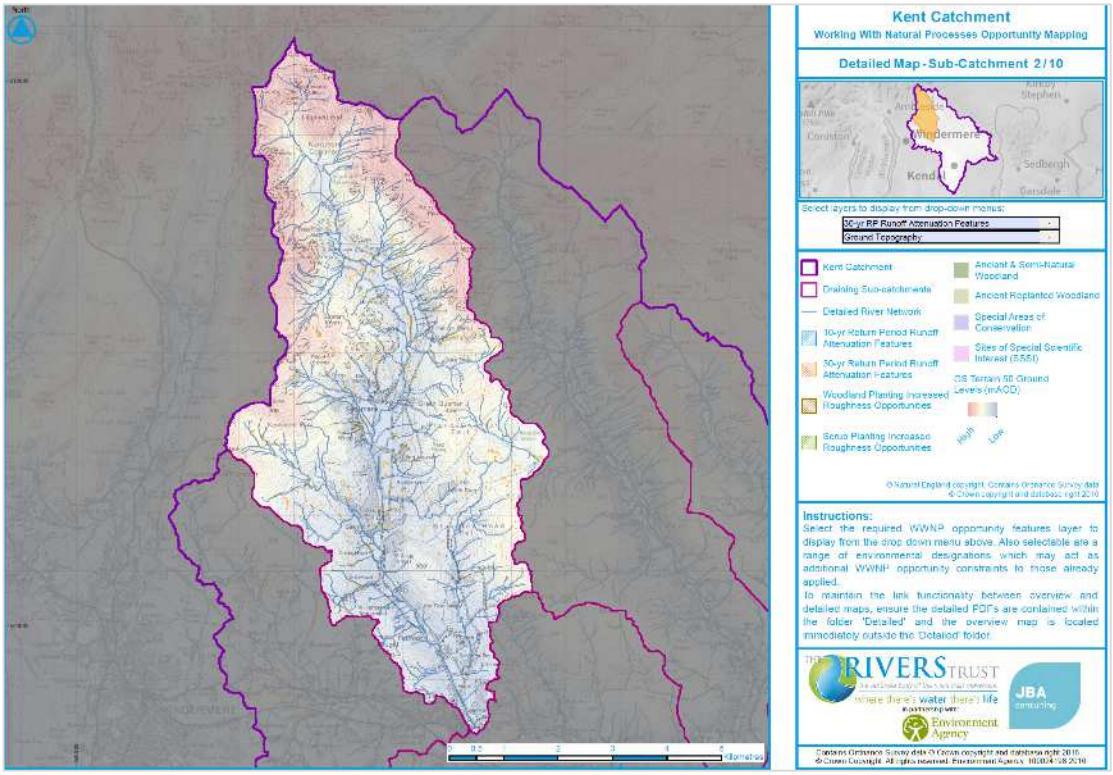

Figure 5.4. Runoff Attenuation Features (RAFs) and shrub and approximate woodland planting opportunities in the upper Kent (after Hankin et al., 2017)

In the application to Cumbrian catchments, the JRAFF model was used to calculate the additional storage volume if such areas were to be deepened (equally representing a bund around an existing flow accumulation area) by a further 1 m before summarising these volumes within priority subcatchments defined earlier. Within the Kent catchment only, any RAFs identified within peat soils were excluded where hillslopes were greater than six degrees. This constraint is based on current peat restoration practices (Moors for the Future Partnership, 2005). This process identifies a very large number of opportunities which can be incorporated into a model. These opportunities represent large scale, long term NFM delivery and provide the evidence required to take a strategic approach to optimising the benefits of providing additional distributes storage within the catchment.

5.4.2. Identification of tree-planting opportunities

Restoring the riparian zone and planting woodland within the floodplain has been simulated to provide the potential for significant flood attenuation (Thomas & Nisbet, 2007; Nisbet & Thomas, 2008). A combination of improvements in wet-canopy evaporation and transpiration, enhanced soil drying and soil infiltration together with increases in hydraulic roughness which arise from woodland creation can lead to reductions in flood peaks together with delaying and spreading of tributary hydrographs.

The Woodlands for Water (WfW) opportunity EA dataset was supplied by the Environment Agency for this project (Broadmeadow et al., 2011) and it was modified with local knowledge and through inspecting soil-series maps to give potential tree-planting opportunities (Figure 5.4). The dataset typically comprises a set of woodland planting opportunity areas such as riparian zones and floodplain areas together with a number of constraints such as urban areas, existing woodland and inland water. Whilst the source dataset infers opportunities to plant and enhance woodland areas, this scenario rather reflects a more general improvement in planting density between scrubland and mature forest as it is understood that conversion to mature woodland would not be appropriate across all land covers.

The modified WfW opportunity maps represent large, long term NFM delivery within each catchment. The incorporation of this opportunity into the model provides the evidence required to take a strategic approach to optimising the benefits of providing additional 'natural roughness' within the catchment.

5.4.3. Identification of opportunities for soil structure improvement

This scenario pertains to the fact that many soils have been compacted through more intensive farming practices over a long period of time, and if de-compacted, improved

soil structure has potential to take in and store considerably more of the incident rainfall (Packman et al., 2004; Marshall, 2014), when this can help reduce overland flow and reduce downstream flood risk, although could potentially have limited benefits in wet winters.

For the third type of opportunity, soil structure improvement, the JFLOW modelling targeted a particular land cover (improved grassland) which was identified as one of the most common land covers within each catchment based on the Land Cover Map 2007. For these areas, the catchment descriptor BFIHOST (Boorman et al., 1995), which influences amount of runoff routed over the landscape in the modelling (see below), was increased by 10% resulting in an approximately equivalent increase in maximum soil moisture storage and reduction in initial soil moisture storage capacity for these land cover areas across the catchment. Users can then assess the improvement relative to that for this type of land cover by scaling up by relative area compared to improved grassland (see Bilota et al., 2007).

This more targeted approach to improving soil permeability avoids overestimating the impact of soil improvement by applying an unrealistic blanket improvement across the catchment. Soils can only be improved if they are damaged. In a survey in the SW of England Palmer & Smith (2013) estimated that approximately 40% of soils were structurally damaged, the percentage being higher under arable and lower under pasture.

5.4.4. Strategic Modelling and Estimating benefits

The strategic modelling was undertaken using a fast 2D hydrodynamic modelling software JFLOW, which has been benchmarked against other 2D inundation models against a wide range of test-cases (Hunter et al., 2008). The approach, illustrated in Figure 5.5, builds on the blanket rainfall approach (e.g. Hankin et al., 2016), which

was developed further to include the ReFH losses model (Kjeldsen, 2005), and used to develop a national SW flood map RoFSW (EA, 2013).

The model integrates spatially varying rainfall, with representation of both rural infiltration using the ReFH rainfall to overland flow calculated losses (i.e., infiltration) model and urban sewer loss rates (a national average of 12mm/hour was used). Rural ReFH losses are controlled by the maximum soil moisture storage capacity (CMAX) which is estimated using the catchment descriptors BFIHOST and PROPWET whilst urban losses are based on estimated sewer capacity losses and percentage overland flow.

The floodplain is represented using a 2m Digital Terrain Model (DTM) based on a combination of filtered LiDAR, filled in with coarser scale photogrammetry or SAR data. Sinks and dams are removed in order to maximise hydrological flow pathway continuity. Spatially varying hydraulic roughness coefficients were adopted throughout, based on land cover and the same roughness coefficients adopted in national maps. The baseline scenarios were for the 10-year and 30-year return periods with a 6-hour storm duration.

Consideration is given to the placement of virtual monitoring locations around the catchment to monitor the hydrographs for different subcatchments and their modelled response to NFM interventions (Figure 5.6). For urban areas, culverts and 'cut-throughs' can be added to allow the passage of water downstream more realistically.

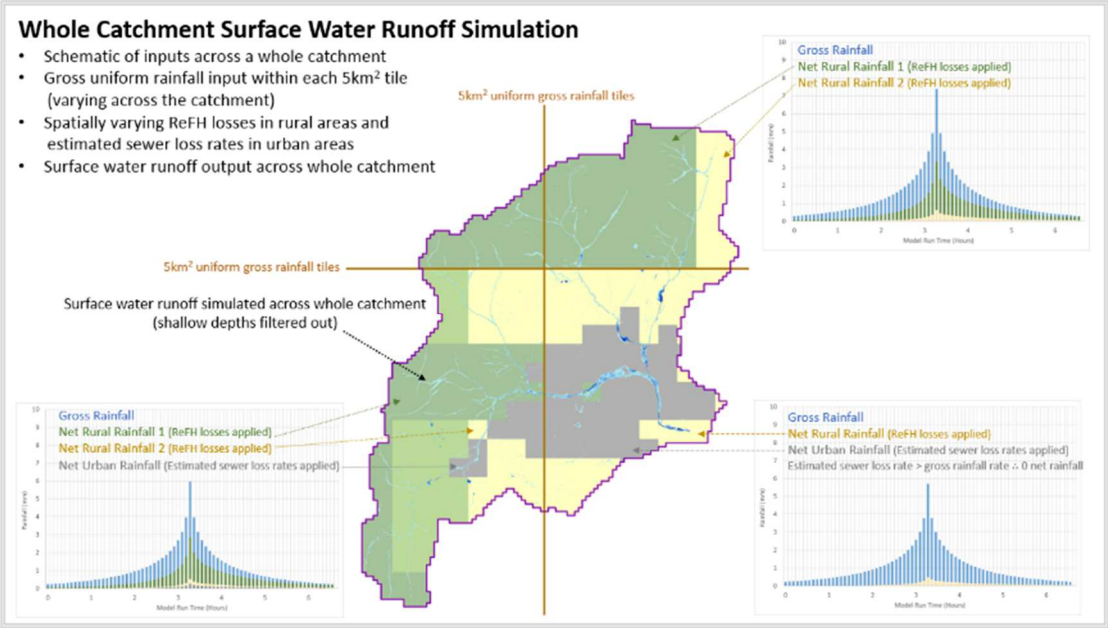

Figure 5.5. The rainfall and losses approach to whole catchment modelling (after Hankin et al., 2017)

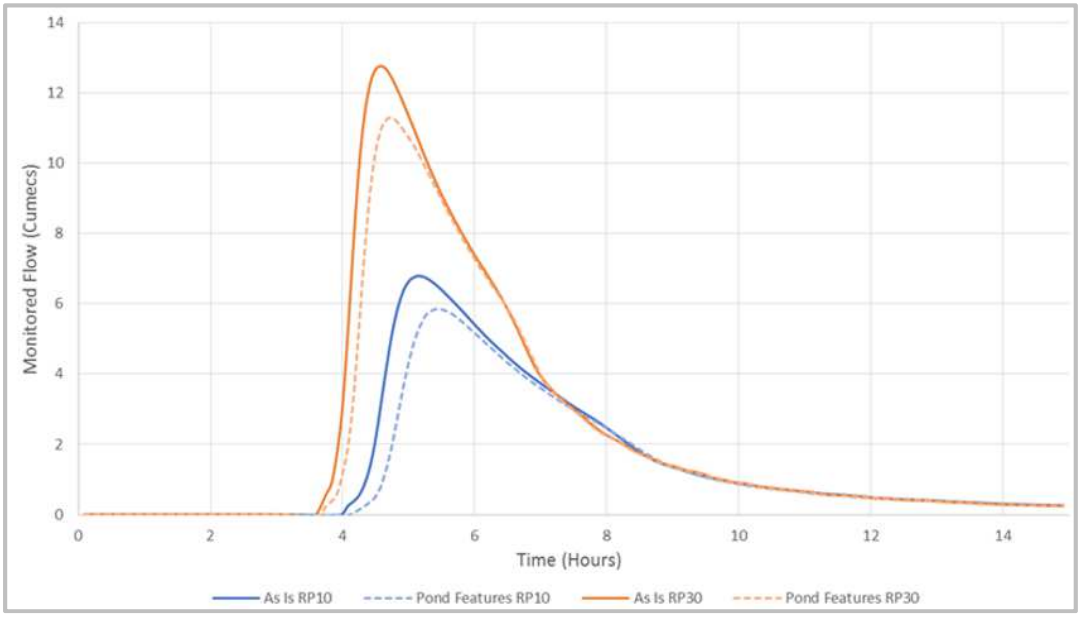

Figure 5.6 Example peak fast-flow reduction based on modelling NFM (after Hankin et al., 2017)

The percentage change in the peak runoff response for each sub-catchment was then visualised in a second set of 'benefit maps' (Figure 5.7), for use at the engagement workshops. These were colour themed in different ways, with the perimeters shaded to reflect the magnitude of the modelled peak runoff reduction and the fill based on the extent of the opportunity. Benefits are cumulative, in that every opportunity must be implemented within upstream subcatchments in order to obtain the visualised benefits.

These maps represent the potential benefits of large scale, long term NFM delivery across a catchment. They are most appropriately used in relative mode, allowing the user to identify particular subcatchments which provide greater benefit than other subcatchments and the different interventions that should be targeted to provide these benefits.

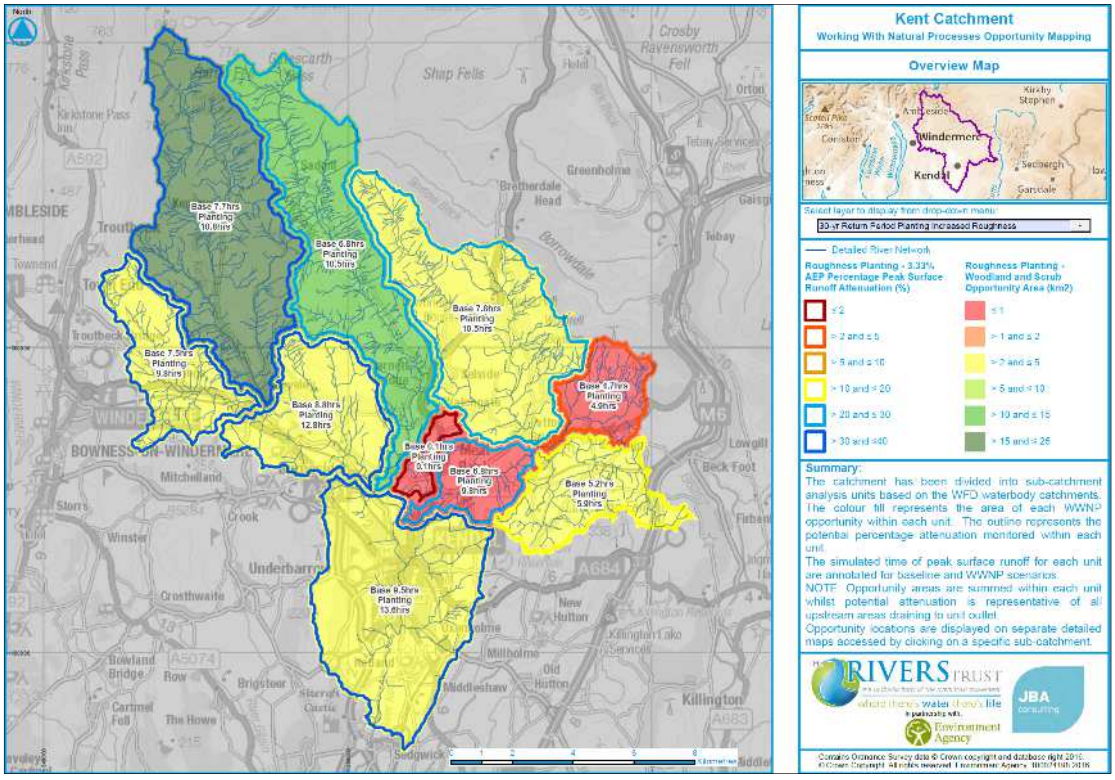

Figure 5.7. Visualisation of potential runoff reduction if all NFM opportunities taken up (after Hankin et al., 2017)

Other approaches to showing benefits or damages avoided have been developed, whereby the average property damages (Penning – Rowsell et al., 2005) per 1 km tile

are shown with and without NFM, and this helps put appraisal of NFM on a footing with more established methods.

5.5. Engagement and refinement

Visualisations such as Figure 5.4, 5.7 and Figure 5.8 have been found useful at engagement events, whereby catchment partners can mark the maps and alter the opportunities based on their local knowledge, then see the potential benefits based on the broad-scale modelling. Many of the identified opportunities will not be feasible due to land-ownership and access issues. There may already be interventions planned which can also be added to the maps. Following engagement, the models were re-run and the maps and interactive PDFs regenerated for the whole catchment.

One key benefit of the engagement approach is the development of a shared understanding of flood generation, routing and accumulation within a catchment. The opportunity for planners, water company engineers, land managers, FCRM, water quality and bio-diversity specialists to elicit hydrological understanding from modellers including issues of synchronisation is of enormous value. The engagement process also enables the modelling team to appreciate and incorporate a more credible set of opportunities and parameters back into the model. This two-way process builds confidence in the model outputs, allowing delivery organisations to make appropriate use of the modelling, based on improved understanding, as part of the weight of evidence required to develop a more strategic approach to NFM delivery.

In addition to the refinement of the opportunities, and through re-modelling the benefits, the catchment partners were asked to prioritise subcatchments for more detailed modelling to build confidence and implement NFM. A matrix was developed, based on the following criteria:

- Land ownership and access - are opportunities feasible?
- Observations based on local knowledge
- Observations from strategic maps
- Scale of downstream risk
- Existence and location of monitoring
- Catchment size
- Preferences counted in the workshop

The upper and mid-Kent and Gowan were prioritised, and it can be seen in Figure 5.8 that there are different centres of risk and strong reason to supplement any established FRM measures with NFM if possible. The catchments were also identified in the Cumbria Flood Plan for NFM-type interventions, largely for peat or bog restoration in the upper Kent.

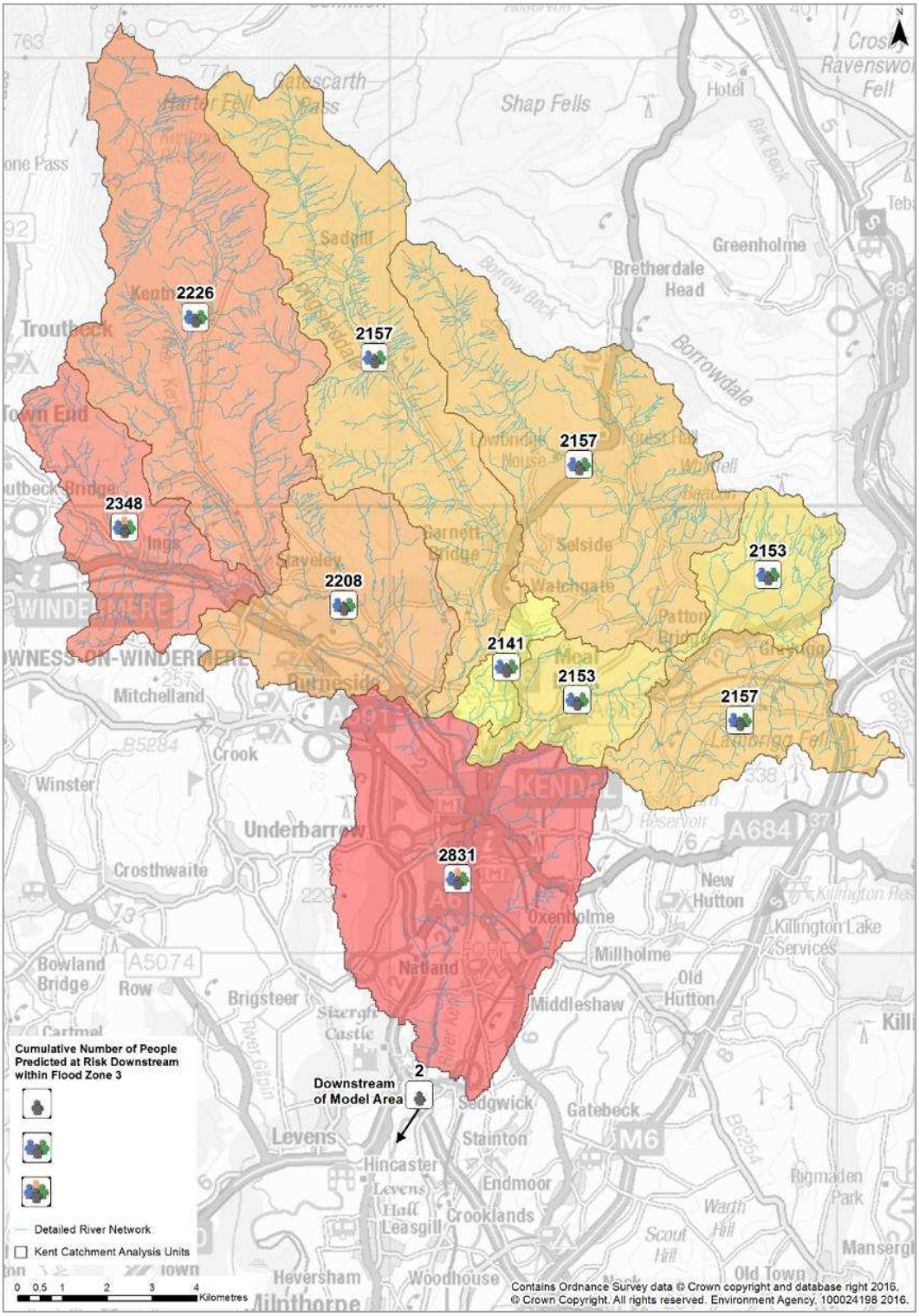

Figure 5.8. Downstream risk visualised for the Kent (after Hankin et al., 2017)

5.6. Modelling of NFM with Dynamic TOPMODEL

Given limited observational evidence effectiveness of NFM at scales > 10 km^2, the prioritisation of areas to model in more detail and through using Monte-Carlo simulations was considered essential to understand more about uncertainty and build on the screening-level modelling with JFLOW (despite its high resolution). The detailed modelling was therefore calibrated against an observed series of extreme events, Nov-Dec 2015, within three severely-impacted catchments up to 223 km^2 in area within Cumbria, UK . The results from one of these catchments, the upper Kent (90 km^2) are used in the following sections to illustrate the approach that was taken for all three catchments.

Lancaster University have recently developed an extended and flexible implementation of the Dynamic TOPMODEL model (Metcalfe et al., 2015; 2016), first implemented in FORTRAN by Beven & Freer (2001). It is an extension of the popular TOPMODEL (Beven & Kirkby, 1979) that has been applied in many studies. Dynamic TOPMODEL employs the efficient parameterisation scheme of TOPMODEL, but allows a more general approach to grouping of points in a catchment for calculation purposes, based on overlays of characteristics rather than simply the map of topographic index. All the model parameters needed to run the model are shown in Table 5.4, along with typical ranges of values applied in this project. Figure 5.9 provides a perceptual overview of Dynamic TOPMODEL.

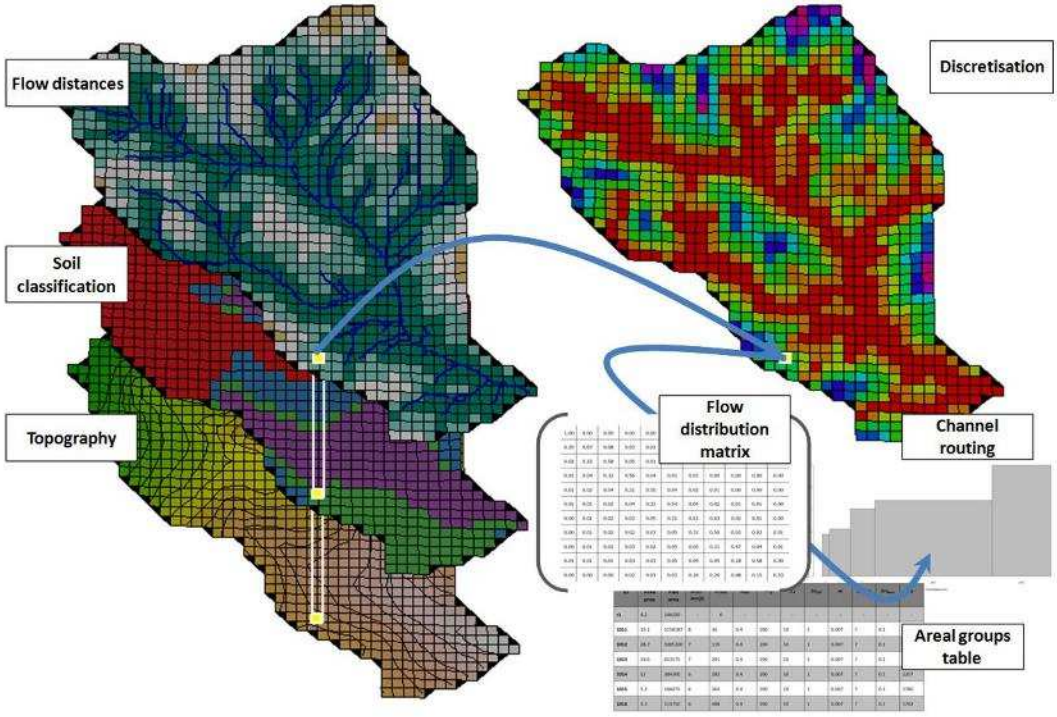

Figure 5.9. Schematic of Dynamic TOPMODEL (after Metcalfe et al., 2015)

Table 5.4. Parameter ranges / typical values within Dynamic TOMODEL (after Metcalfe et al., 2015)

Parameter	Description	Units	Lower	Upper
v_{of}	Overland flow velocity	m/hr	1	150
m	Form of exponential decline in	m	0.0011	0.033
SRZ_{max}	Max root zone storage	m	0.1	0.3
SRZ_0	Initial root zone storage	%	20	100
v_{chan}	Channel routing velocity	m/hr	500	5000
$ln(T_0)$	Lateral saturated transmissivity	m²/hr	3	12
$SDmax$	Max effective deficit of saturated zone	m	0.5	0.5
T_d	Unsaturated zone time delay	m/hr	1	10

It is a semi-distributed hydrological model that utilises areas of similar hydrological behaviour called HRUs (Hydrological Response Units). These units may be in the evaluation of NFM divided to represent distributed interventions within the landscape. It has sufficient complexity to represent the key catchment processes, notably subsurface and overland flow pathways, and there is some evidence to link NFM

measures to alteration of the parameters (e.g. transmissivity distribution) representing these processes. Its simple structure allows efficient operation, allowing thousands of model runs to be simulated to investigate uncertainties and sensitivities.

Overland flow velocity is fixed throughout each unit, and can be changed to reflect changes in surface roughness introduced by, for example, peat restoration or riparian tree-planting. The maximum transmissivity at complete saturation T_0 $[L]^2/[T]$ is a measure of the local maximum saturated downslope transmissivity per unit hydraulic gradient (where transmissivity is the integral of the permeability to the saturated depth). This is a key parameter in identifying the onset of saturation excess overland flow (SOF). When downslope flows into lower slopes filling remaining storage capacity, return flow is produced. SOF is also generated when rain falls onto these areas of already saturated ground.

An exponential transmissivity profile is assumed. The use of such a form is supported by experimental evidence (Davies et al., 2013), and reproduces the typically higher values of permeability found near the ground surface. The recession parameter m [L] controls the rate of decline of transmissivity T as water table reduces. Small values of m lead to very rapid declines in transmissivity, suggesting shallower, faster responding streamflow generation systems. Deeper active hydrological systems are represented by a slower decline in transmissivity.

Dynamic TOPMODEL routes subsurface flow downslope between HRUs using a routing matrix derived from the local topography. It is assumed that the local slope is a reasonable approximation for the hydraulic gradient.

The root zone storage SRZ_{max} must be filled before any water table recharge begins through incident rainfall. Transpiration (and soil evaporation) is removed from this

zone at a rate proportional to the actual storage. Direct observations of soil moisture content are unavailable for the catchments in the periods simulated, so a reasonable initial value was applied (SRZ_0 = 95%).

Dynamic TOPMODEL represents an intermediate level of complexity that incorporates the key hydrological processes, but without imposing too many assumptions resulting in a large number of parameters (related to say soil properties), for which direct measurements are not available. The model was also selected because it:

- Makes use of standard data formats for catchment topography (elevations, channel network) and relevant spatial data such as land cover.
- Presents results back to the landscape as well as formats such as streamflow hydrographs that are easily understandable by partners
- Uses real, spatially distributed rainfall data and can be rapidly calibrated against real event data (allowing for data quality).
- Incorporates spatial data overlays provided by the Rivers Trust (RT) and catchment partners of NFM interventions, for example tree-planting, soil restoration and addition of offline storage area (RAFs) and simulate the effect of these changes on streamflow response.
- Simulates a wide range of catchment scales (up to 223 km^2 in this study) and hydrological regimes such as the extreme flood event arising from Storm Desmond in December 2015;
- Allows for relatively quick application to future RT study catchments and different configurations of subcatchments within an existing project.

- Uses a framework that allows assimilation of meteorological and streamflow data supplied in standard formats, such as those collected by the Environment Agency.
- Allows for free-distribution of source or compiled code and, with suitable guidance and training, be operated by RT staff and catchment partners.

In conjunction with a hydraulic-routing scheme, also developed at Lancaster University, Dynamic TOPMODEL has been applied to the 29km^2 Brompton, North Yorkshire, catchment in order to simulate the impact of up to 60 in-channel NFM interventions (Metcalfe et al., 2017). The model is written in the open source R language, distributed under the GNU Lesser Public Licence (GNU LGPL v2.1) and can be run on most common operating systems. The R implementation has been released as a package on the CRAN archive (Metcalfe et al., 2016), passing the rigorous quality assurance and testing required by the submission process.

5.7. Representing NFM opportunities within HRUs for Dynamic TOPMODEL

A set of HRUs were developed based on local hydrological characteristics, the most important of which is the topographic wetness index (TWI). These were then split further so that individual NFM measures could be represented in the landscape. For example, the HRU representing the saturated area adjacent to the watercourse in the upper catchment becomes split into two, one where there is no change to the landscape, and another where there is tree planting.

- HRU1 – high SPR areas – Mimicking tree planting effects.

Modification of T_0 (1.5 to 2.5 multiplicative factor of the un-logged value)

- Decreased SOF velocity (reduced by: 0.5 and 0.75 – equivalent to change in roughness implemented for JFLOW).
- Wet-canopy evaporation increases implemented as a loss to the gross rainfall input (using a similar strategy to Buytaert & Beven, 2009).
- Modification of the initial root zone storage to mimic drier antecedent soil moisture conditions as a result of additional soil drying by enhanced wet-copy evaporation (and enhanced transpiration in previous months).

- HRU2 – RAF features
  - Increased storage by introduction of RAFs is based upon modified JFLOW RAF opportunity maps
  - Implemented by a modification to the root zone storage to 1m, making use of the existing store represented in the model

RAFs are "leaky", draining at a rate q_{drain} [L]/[T] proportional to their specific storage S [L]: $q_{drain} = S/T$, where the constant of proportionality T [T] is the residence time

- Assume all RAFs drain with the same time constant and discharge directly to water course via a "pipe".
- Implemented as a sensitivity of 3 "pipe" sizes to see differences in 'effective' pipe size in terms of peak reduction.

- HRU3 – Peat
  - Decreased SOF velocity (reduced by between 0.65 and 0.8 – equivalent to change in roughness implemented for JFLOW).

5.8. Uncertainty Framework

The scale of the flooding caused by Storm Desmond is in part dependant on the catchment wetting from the storm events that occurred over the preceding weeks. In consequence a 6-week period of rainfall and streamflow was selected in Nov-Dec 2015 (Figure 5.4) for the modelling, that included Storms Abigail (12th-13th November), Barney (17th-18th November), Clodagh (29th November) and Desmond (5th-6th December). The first and last of these events had the highest impact on the streamflow. Clodagh was primarily a "wind" storm and in Cumbria did not produce significant streamflow (Marsh et al., 2016). In November a south-westerly airflow described as an 'atmospheric river' became established bringing persistent warm moisture-laden air from subtropical regions resulting in persistent heavy rainfall. A three-day total of 138mm was recorded at the Shap automatic weather station in mid-November (Marsh et al., 2016), compared to the total of 145-180mm recorded at raingauges around the Kent catchment in September and October. Two gauges lying within the Derwent catchment recorded new UK record rainfall totals: at Honister Pass 341mm fell within 24 hours and 405mm within 48 hours at Thirlmere (Marsh et al., 2016). Dynamic TOPMODEL requires as input a time series of potential (or actual) evapotranspiration. The Calder approach (Calder et al., 2003) was used to produce and approximation of a diurnal sinusoidal variation in potential evapotranspiration.

5000 Monte-Carlo simulations were undertaken before applying an acceptability criterion which sorts behavioural simulations, from those that are not. Within the Generalised Linearized Uncertainty Estimation framework (GLUE: Beven & Binley, 1992; Beven, 2006; Beven & Binley, 2014), the degree of acceptance of any simulation is weighted (or scored) quantitatively and is associated with the simulation

during the entire analysis. Any simulations which are deemed physically unacceptable play no further part in the analysis and do not form part of the results.

The acceptance criteria were based on an overall performance measure over the whole modelled period (the Nash-Sutcliffe Efficiency statistic, NSE), the accuracy of the model prediction for the peak flow Q_{max} during Storm Desmond, and the maximum percentage of the catchment areas generating overland flow (by any of the processes described), SOF_{amax}. Figure 5.10 illustrates the spread in model uncertainties through the calibration time series based on the resulting 'acceptable' parameter combinations.

Given the range of acceptable model predictions for each storm the problem arises of comparing the NFM interventions for all acceptable models. To compare the respective hydrographs contemporaneously is likely to be misleading, since each series' maxima may occur at different absolute times due, for example, to the retardation of the flood peak by the NFM measures. The distribution of flows for a window of time-steps around the peak has therefore been generated so that the shift in the distribution can be compared. This is illustrated in Figure 5.11.

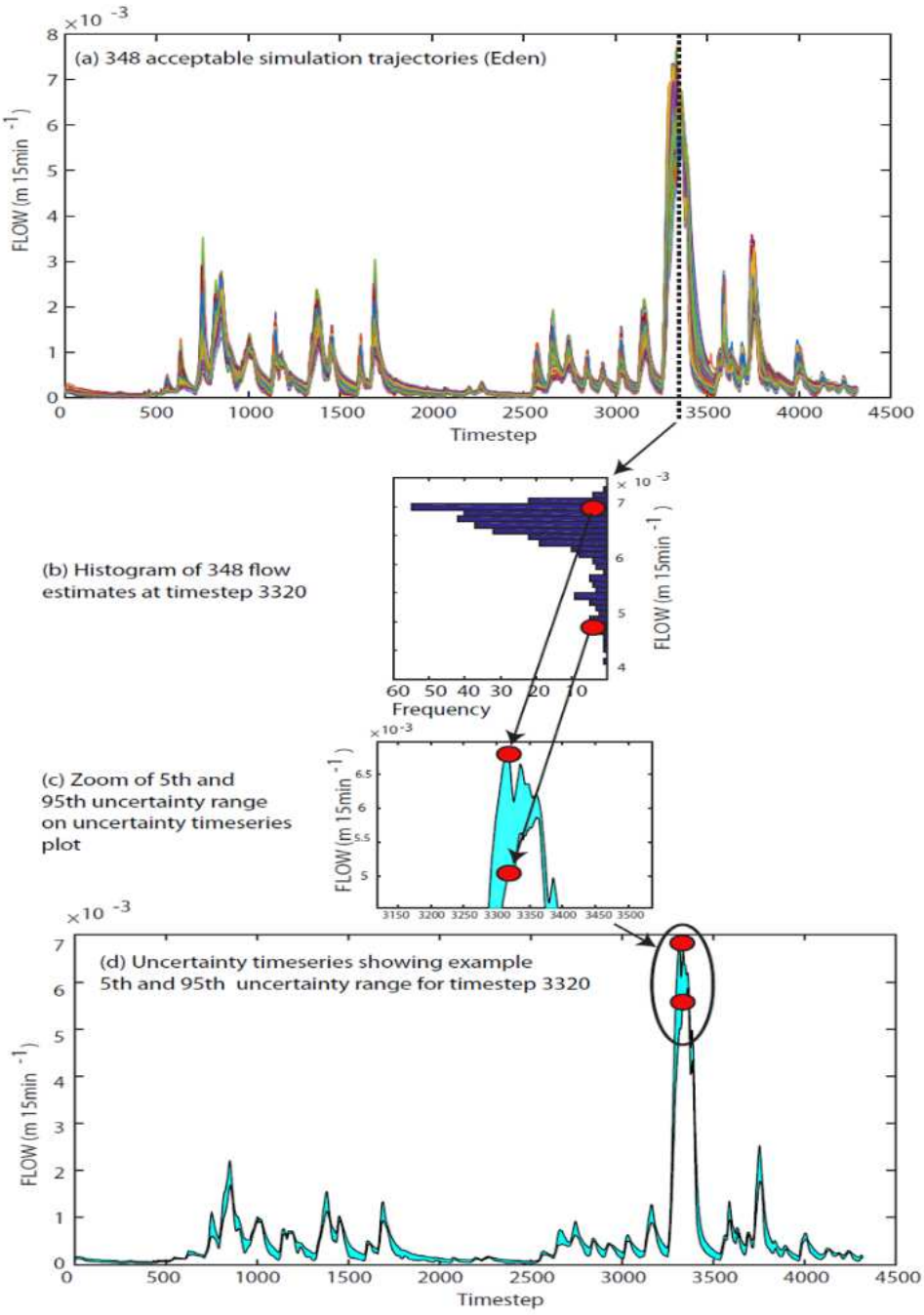

Figure 5.10. Translating uncertainty to model predictions (GLUE) (after Hankin et al., 2017)

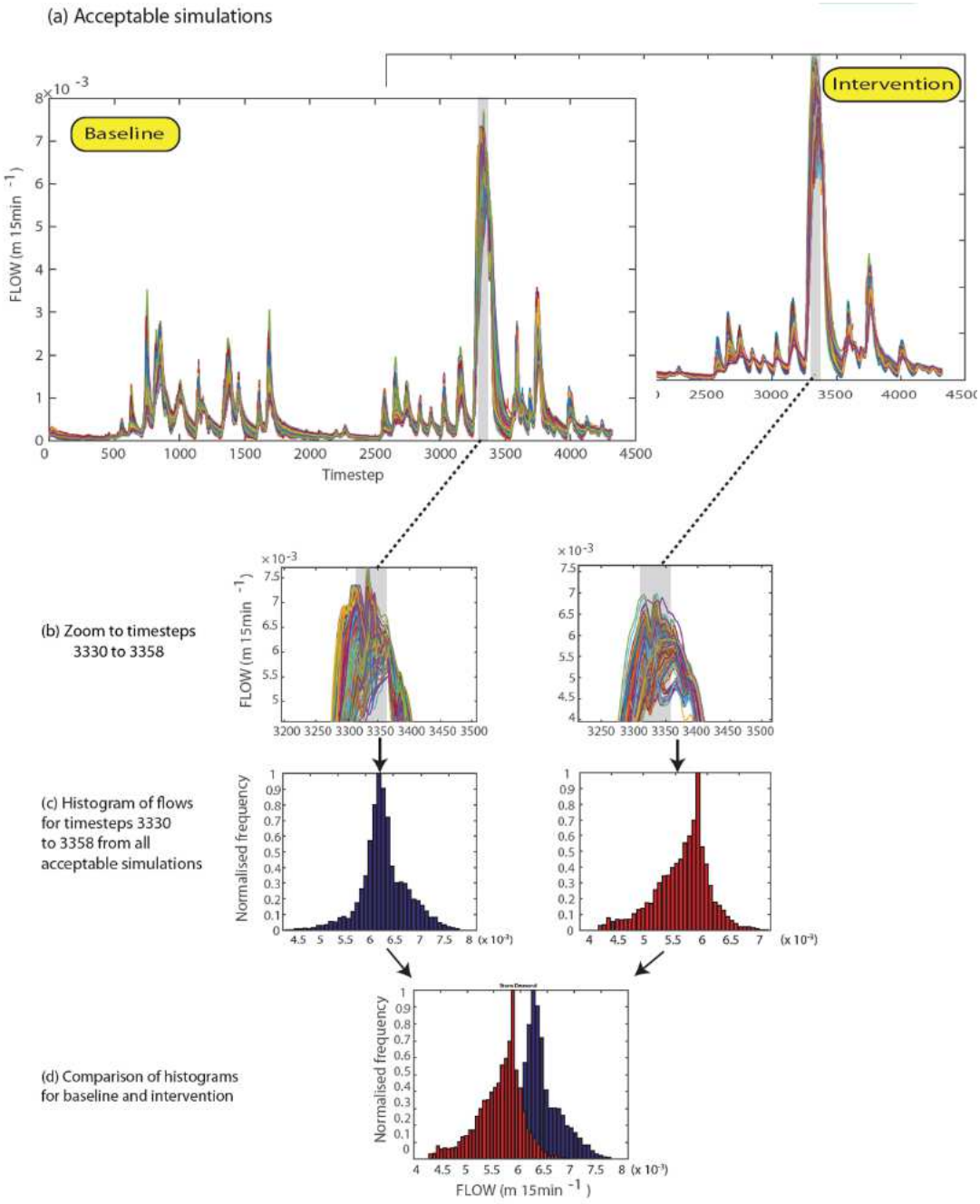

Figure 5.11 The change to predicted flow frequency distributions (after Hankin et al., 2017)

5.9. Results and Discussion: Comparison of models

In the main he results for the Kent catchment are presented, where the acceptance criteria discussed above were: NSE> 0.85; 6.9 < Q_{max} < 10.2; 0.1< SOF_{amax} <0.95, where Q_{max} is the peak flow per unit area for storm Desmond and SOF_{amax} was the very fuzzy range of acceptable fractional catchment areas producing SOF. This leads to 348 'acceptable' parameterisations, giving a range of predictions shown in Figure 5.12, for the RAF measures, designed to have a 1, 10 and 100 hour retention time.

Figure 5.13 shows the range of potential changes to the storm profile when three different levels of confidence are applied in the evidence for the effect that tree-planting has on the different catchment processes. It is easier to consider the range of predicted peak flow reductions for each storm as a function of the confidence placed in the evidence (Figure 5.15) than by plotting the five different levels of confidence.

Use can also be made use of the generic approach described and plot the matrix of changes to the predicted peak flow distributions for a window around each named storm as a function of confidence (rows) in Figure 5.14, with statistical significance of the changes highlighted in Table 5.5.

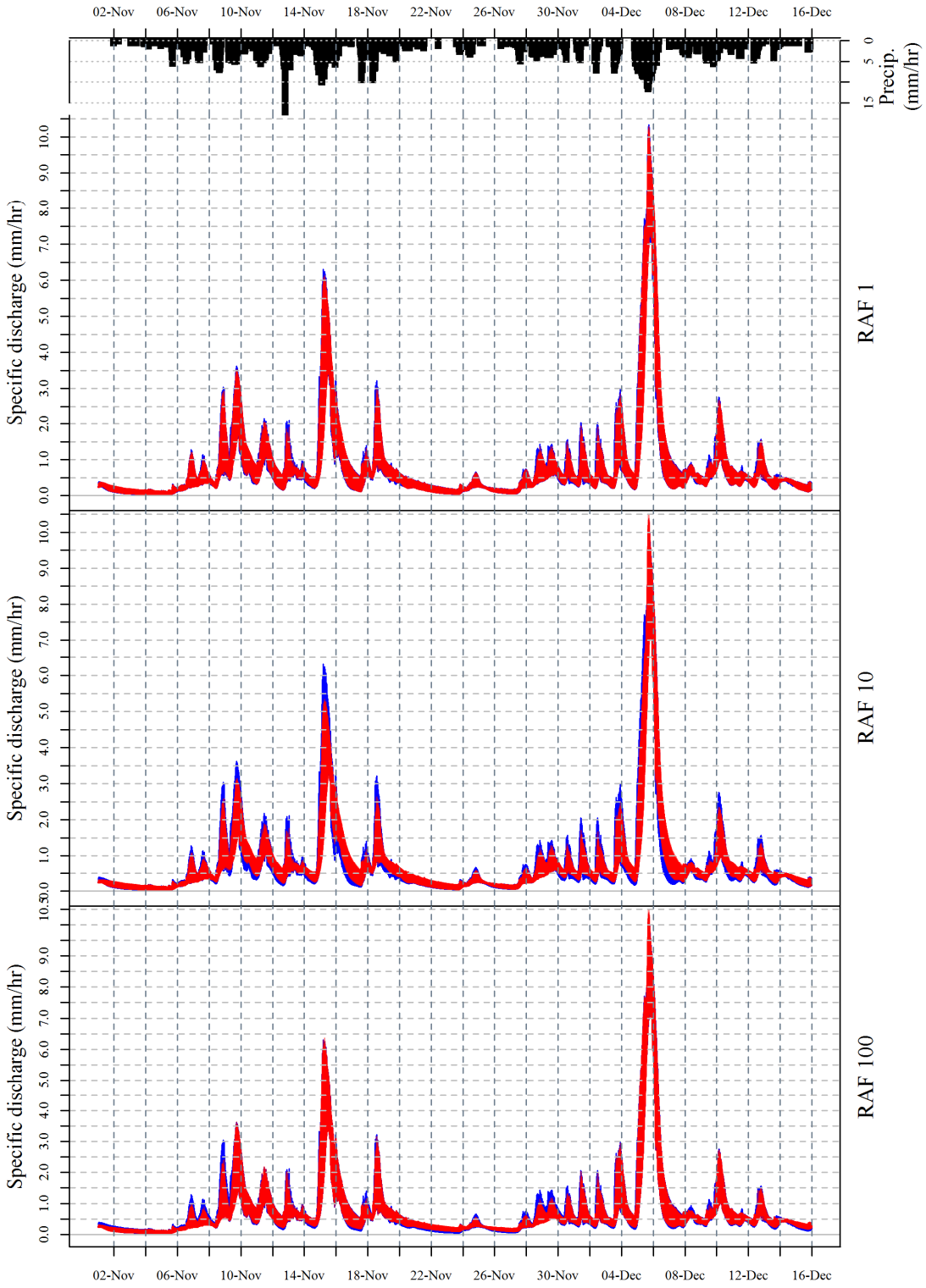

Figure 5.12. Range of predictions using acceptable combinations plus RAFs with a 1, 10 and 100 hour retention time

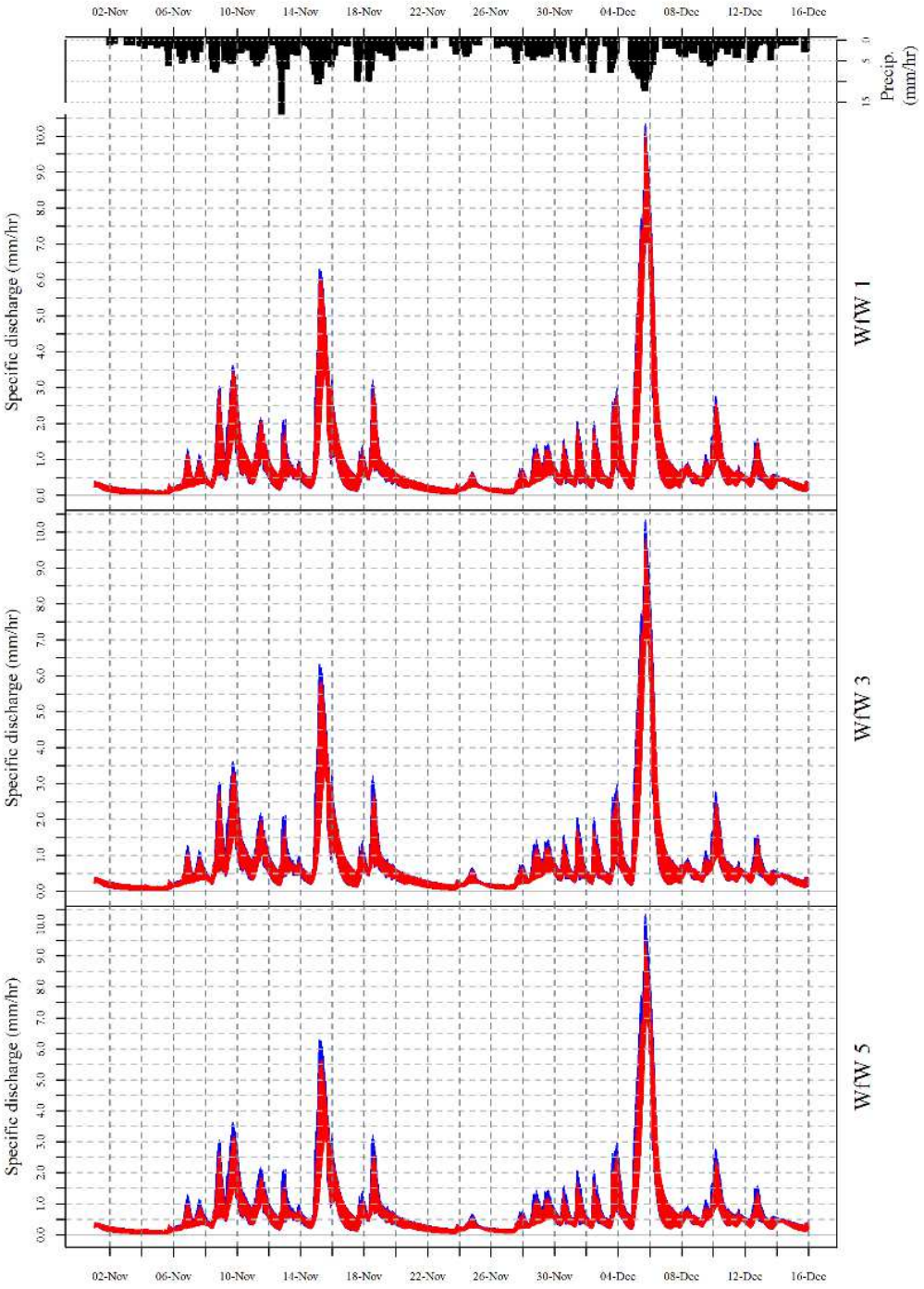

Figure 5.13. Effect of tree-planting opportunities with different levels of confidence in parameter changes

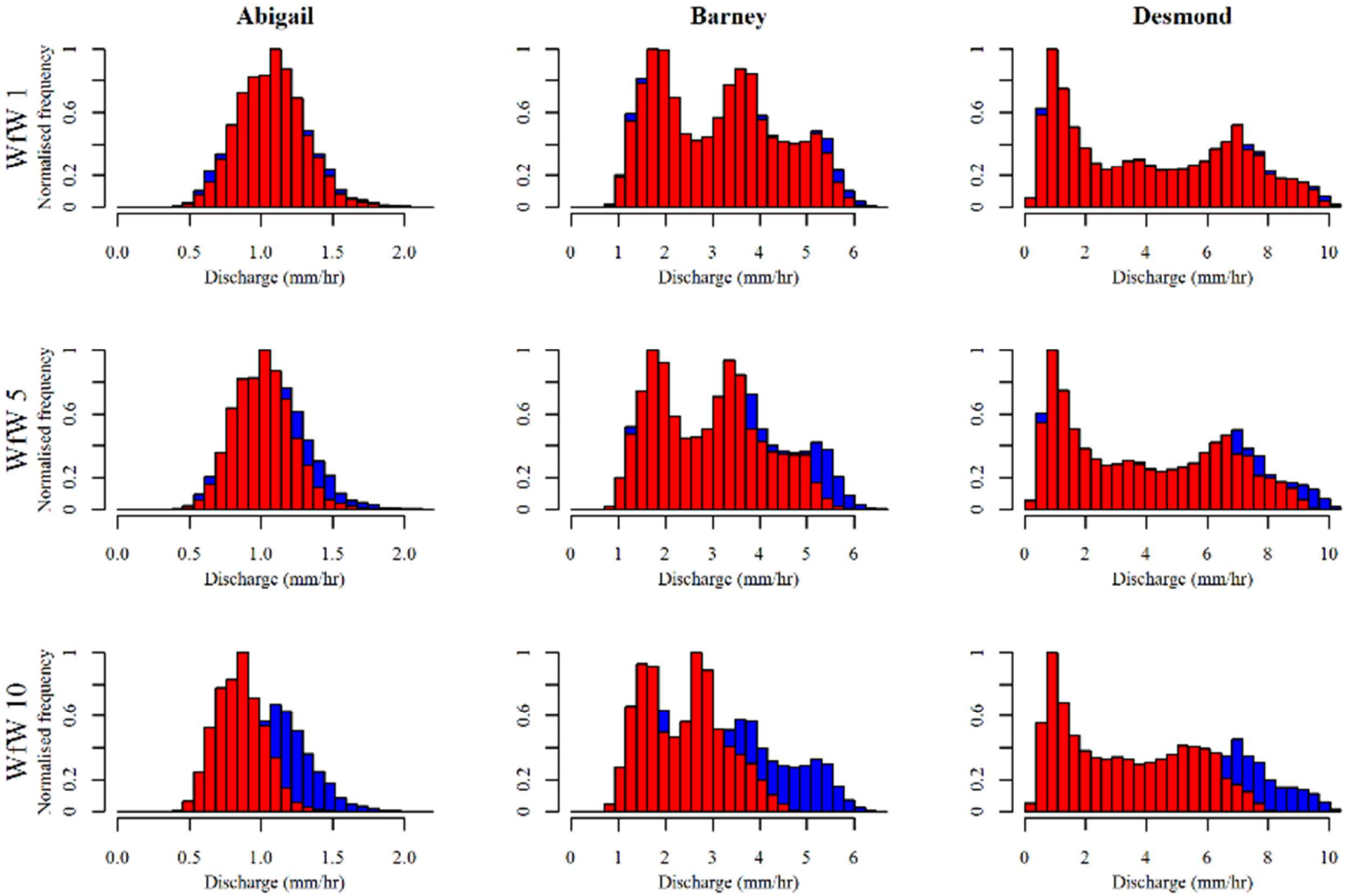

Figure 5.14. Matrix of shifts to distribution of flows predicted around peaks for 3 storms (columns) for three confidence levels (rows)

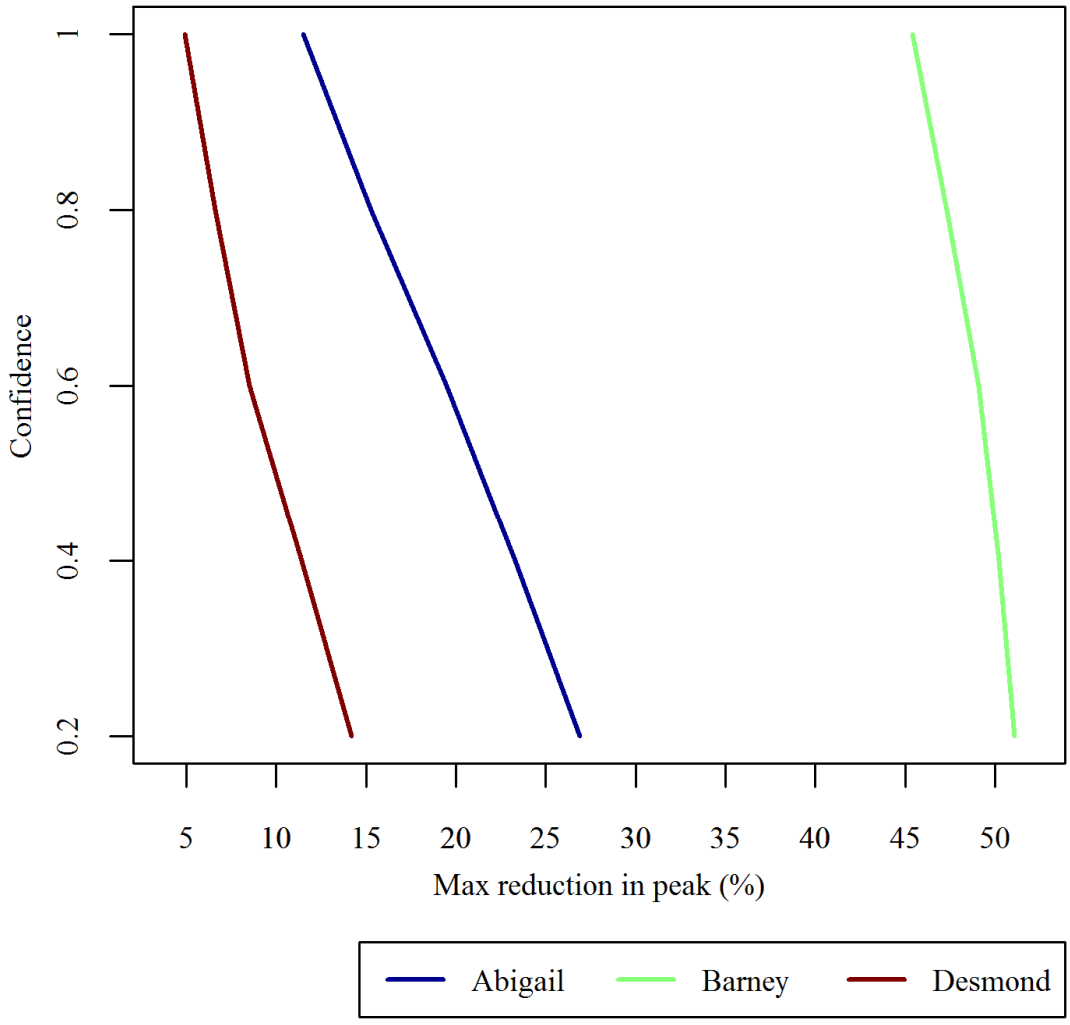

Figure 5.15. Confidence as a function of the percentage reduction for three of the named storms for tree-planting and roughening up.

Table 5.5. Statistics for WfW and RAF interventions for each of the named storms in the simulation period: Δqmax = maximum relative reduction in peak (%); $\overline{\Delta q}$ = mean relative reduction in peak (%); K-S = Kolmogorov-Smirnov Statistic

	Abigail			Barney			Desmond		
	Δq_{max}	$\overline{\Delta q}$	K-S	Δq_{max}	$\overline{\Delta q}$	K.S.	Δq_{max}	$\overline{\Delta q}$	K.S.
WfW1	20.5	3.1	0.027	11.5	3.3	0.025	4.9	1.7	0.019
WfW3	30.9	9.6	0.139	26.9	12.9	0.124	14.2	7.9	0.076
WfW5	40.7	23.1	0.423	45.1	31.5	0.328	36.3	24.2	0.22
RAF1	25.3	2.3	0.006	15.3	2.1	0.01	5.8	1.2	0.005
RAF10	28.6	7	0.067	22.5	13.7	0.118	4.5	0.1	0.055
RAF100	22.9	0.9	0.014	14.1	0.4	0.006	4.5	0.1	0.005

Using Dynamic TOPMODEL, drain-down of RAFs has been successfully modelling with different time constants. It has been shown that for the Kent, RAFs designed with an intermediate residence time of around 10 hours would be more effective for a series of flood events such as those in the period November through December 2015. The percentage reductions in peak flows are similar to the 2-5% peak runoff reduction predicted by JFLOW (30 year event) for the upper Kent for most of the period of modelling, apart from storm Desmond where Figure 5.12 shows less reduction, potentially because the RAFs have not emptied.

It is less straightforward to compare the results for tree-planting between the modelling approaches, but for the Upper Kent, JFLOW predicts very significant peak runoff reductions of between 30-40%, based on Figure 5.12, are at the lowest end of the confidence associated with the modelled change. However, these changes stem from very different physical processes, and further modelling showed that the perturbations to the wet canopy evaporation is the predominant effect in Dynamic TOPMODEL, although the modelled effect was greatest when combined with reduced velocities and transmissivity.

The potential impact of large scale NFM delivery on peak flow during extreme events such as storm Desmond is an important result. The evaluation of uncertainty enables us to use this finding appropriately and with greater confidence. The modelling allows us to see both the long term potential of NFM and, critically, the model parameters and processes to which this prediction is most sensitive. These findings not only improve our understanding of the benefits of NFM but also guide future monitoring strategies that will be required to refine the modelling and adaptively mange NFM, and therefore flood risk, within a catchment. A consistent theme within the engagement was that it would be unlikely that advantage could be taken of every

single potential opportunity, and so the results can seem overly optimistic, but could be used in a relative sense.

5.10. Testing resilience

These types of analyses provide us with more confidence in the predicted response of the upper Kent to large scale interventions of tree-planting and RAFs, but they have not fully tested the long term robustness nor the resilience in the face of different weather extremes. It would, in fact, be useful to test for a number of performance issues in order to gain greater confidence in the approach. These issues include:

- Synchronisation
- Effect of sequences of events on antecedent conditions
- Backwater effects
- Sedimentation
- Culvert or bridge blockage due to increased debris from tree-planting

These can be examined and tested through modelling of extreme events with different spatial rainfall fields (especially for larger catchments) as performed for the Defra competition (Hankin et al., 2017), for the Eden as shown in Figure 5.16.

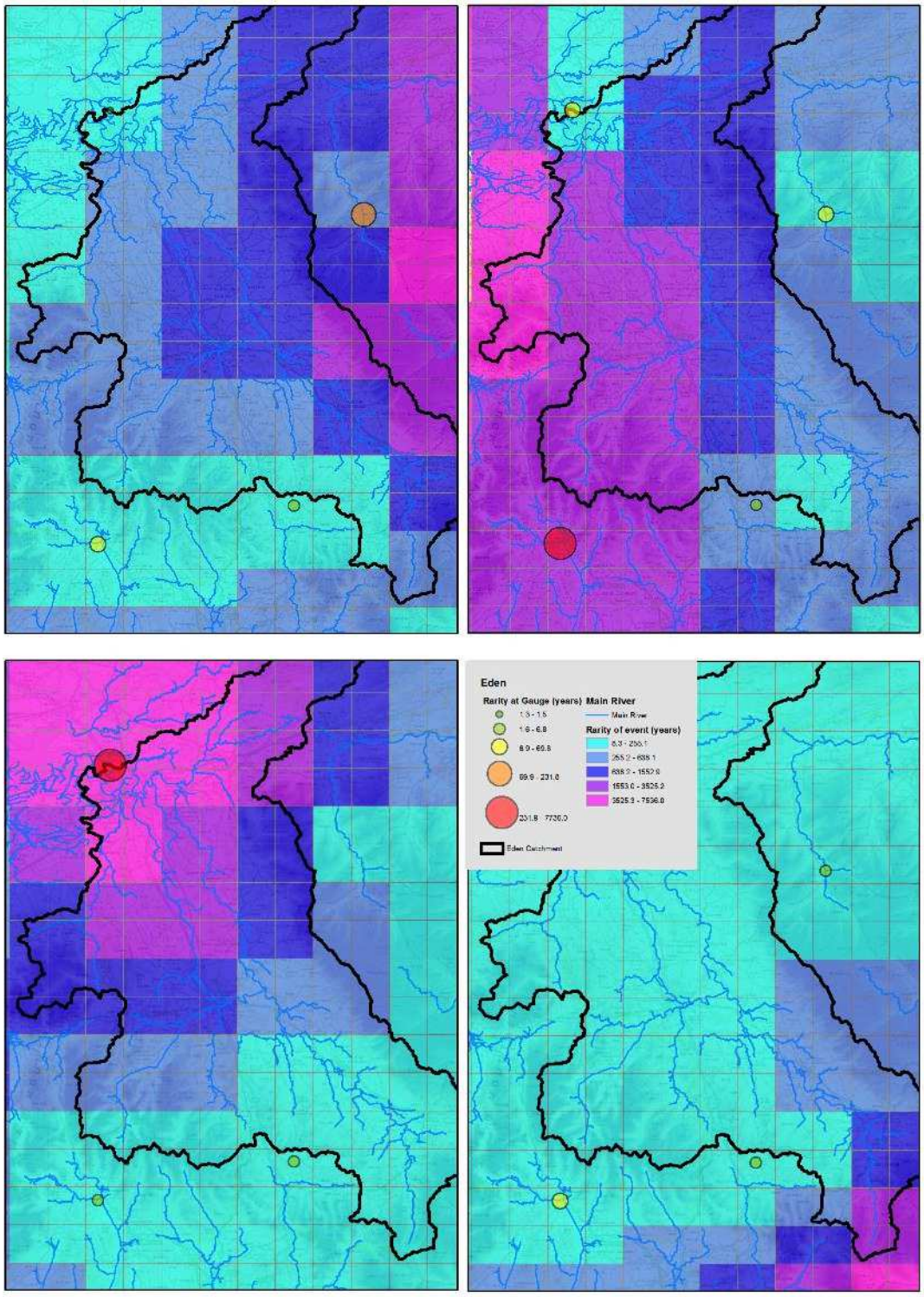

Figure 5.16 Spatial Rainfall Fields for plausible events (after Hankin et al., 2017)

Here the average beneficial effect of NFM across 30 extreme, but plausible, rainfall events was generated in order to test for robustness in using such distributed events in the larger Eden catchment in Cumbria.

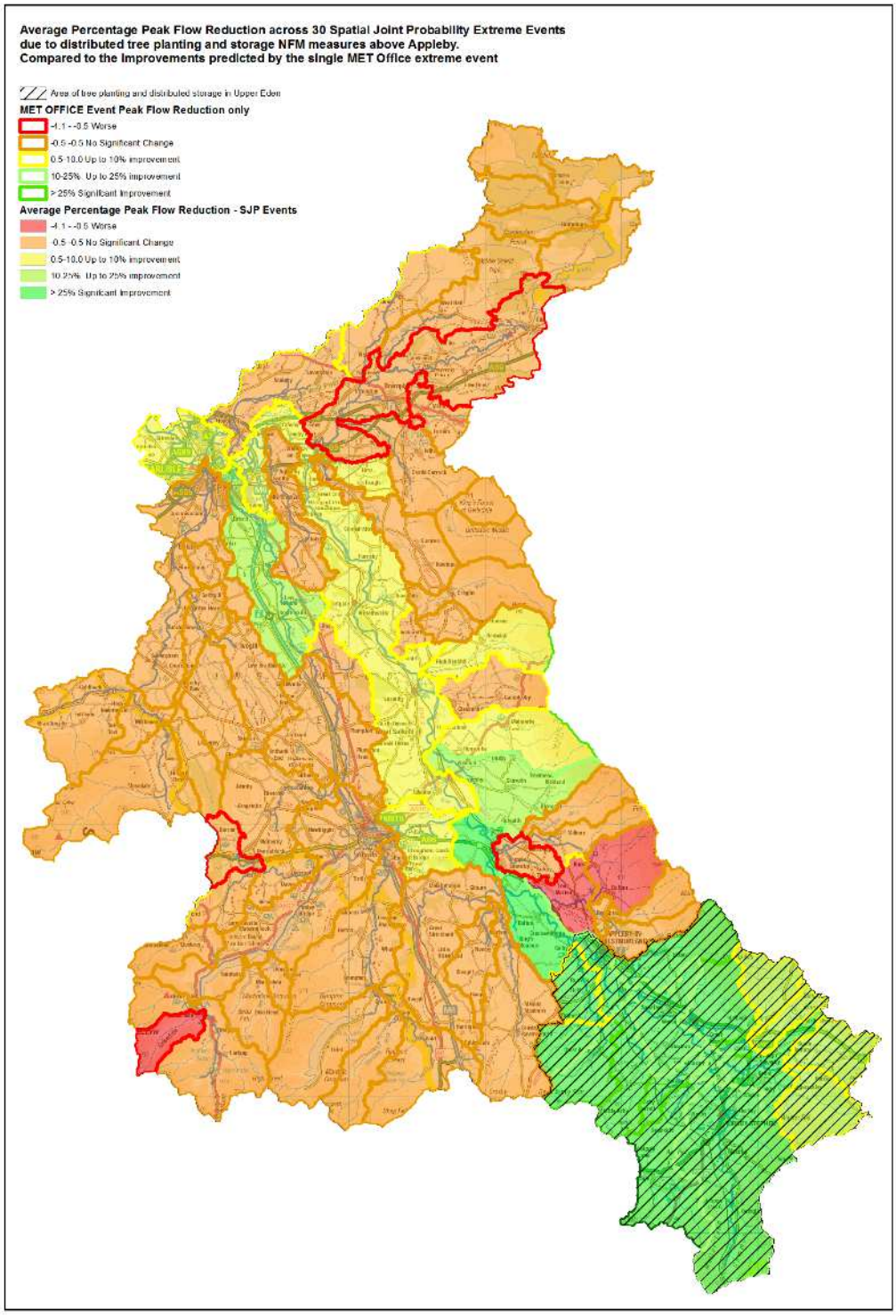

Figure 5.17 Average behaviour across 30 events with and without NFM (after Hankin et al., 2017)

Ideally the additional modes of failure of NFM should also be tested for through probabilistic modelling, as currently undertaken for established FRM in the UK. A systems based approach could be applied (Hall et al., 2003) as discussed in relation to wider processes from synchronisation of flood peaks, backwater effects, sedimentation effects whereby RAFs fill in through time, and blockage of downstream features such as culverts near urban areas due to an increase in woody material in the longer term (Hankin et al., 2016).

5.11. Conclusions

Demonstrated here is a generic flood risk management framework that caters for the distinct differences between NFM and established approaches such as engineered downstream flood defences. NFM measures are characteristically small-scale and may need to be widely distributed to be effective at larger scales, and can influence a range of catchment processes. This combination means that modelling their effectiveness will be inherently uncertain, but here it has been demonstrated a framework that is tolerant of this uncertainty and the fuzziness in the evidence for how model 'effective' parameters can be plausibly changed to reflect their effect.

The tiered approach involves strategic modelling, mapping of opportunities and benefits, consultation and then prioritisation of areas for more detailed modelling and eventual implementation. The engagement phase is essential and ideally should be more of a continuous process through time with details of the model landscapes (topography, distributed roughness, storage, tree-cover, land-use), being revisited regularly. This is not new, but this chapter has hopefully shown how it can be achieved practically in the reasonable timescale of just 6 months.

However, differences in the model predictions from the different modelling approaches require careful interpretation, and are only part of the picture set in the context of uncertainties on long-term ownership, maintenance and liabilities for NFM measures. The strategic overland flow process modelling is bound to lead to some different catchment responses than for the more complete hydrological model, yet both shed light on different risk management issues. For example, the surface water modelling approach is useful for identifying key flow pathways and accumulations where partial blockage or storage can make a greater difference, but Dynamic TOPMODEL tells us more about the whole hydrograph, and can integrate over more of the processes that tree planting is thought to influence. The two modelling strategies have helped to increase our knowledge of how and where in each catchment NFM measures can be more effective to reduce flood risk at large catchment scales. The models help shed more light on the complexities of parameterising change in model parameters, particularly at large catchment scales and for a range of flood events.

The potential for large scale NFM delivery to provide significant flood risk benefits, even in extreme events, is based on a translation of the limited available evidence on the impacts of NFM between the 'real world' and the 'modelled world', using an uncertainty framework. If it believed that the model is a reasonable physical simulator of the whole catchment, then the potential benefits of following the risk management framework demonstrated are to help express model outputs in a language which highlights uncertainties and makes them more central to decision making.

The models have helped to quantify by how much working with natural processes can improve flood regulation, depending on a fuzzy evidence base. The associated benefits can then be appraised alongside others, including carbon storage or reductions

in diffuse pollution, sediment transport and improved community resilience through working together.

Acknowledgements

With thanks to the Rivers Trust for their guidance and engagement, all the attendees of the workshop held on the 7th Oct, 2016, and to the Environment Agency for the large quantities of data supplied.

Chapter 6. Simplified representation of runoff attenuation features within analysis of the hydrological performance of a natural flood management scheme

Reference

Metcalfe, P., Beven, K., Hankin, B., & Lamb, R. (2017). Simplified representation of runoff attenuation features within analysis of the hydrological performance of a natural flood management scheme, Hydrol. Earth Syst. Sci. Discuss., https://doi.org/10.5194/hess-2017-398, in review, 2017.

Statement of author contribution

- Primary authorship of text, with contributions, comments and corrections from co-authors
- Collection and assimilation of data
- Development of computer models and generation of results
- Analysis and presentation of data
- Submission of initial version for publication
- Responses to reviewers' comments
- Preparation of all figures

Abstract

Hillslope Runoff Attenuation Features (RAFs) are soft-engineered overland flow interception structures utilised in natural flood management, designed to reduce connectivity between fast overland flow pathways and the channel. The performance of distributed networks of these features is poorly understood. Extensive schemes can potentially retain large quantities of runoff storage but there are suggestions that much of their effectiveness can be attributed to desynchronisation of subcatchment flood waves, and that inappropriately-sited measures may increase rather than mitigate flood risk. Fully-distributed hydrodynamic models have been applied in limited studies but introduce computational complexity. The longer run-times of such models also restricts their use for uncertainty estimation or evaluation of the many potential configurations and storm sequences that may influence the timing and magnitude of flood waves.

A simplified overland flow routing module and representation of RAFs is applied to the headwaters of a large rural catchment in Cumbria, UK, where the use of an extensive network of such features is proposed as a flood mitigation strategy. The model was run in a Monte Carlo framework over a two-month period of extreme flood events which occurred in late 2015 that caused significant damage in areas downstream. Using the GLUE uncertainty estimation framework, acceptable realisations were scored, and these weighted behavioural realisations were rerun with one of three drain-down time or residence time parameters applied across the network of RAFs.

The study demonstrates that the impacts of schemes comprising widely-distributed ensembles of RAFs can be modelled effectively within such a reduced complexity framework. It shows the importance of effective residence times on antecedent

conditions in a sequence of events. Uncertainties and limitations introduced by the simplified representation of the overland flow routing and RAF representation are discussed. Means by which features could be grouped more strategically are discussed.

Keywords: flood risk management; uncertainty; NFM; catchment-based approaches

6.1. Introduction

A catchment-based flood risk management (CBFRM) approach is becoming widely adopted (Werritty, 2006; Pitt, 2008; Dadson et al., 2017). Its principle is that storm runoff can be managed most effectively with a combination of catchment scale measures and downstream flood defences (Lane, 2017). A variety of CBFRM, often referred to as Natural Flood Management (NFM), or Working with Natural Processes (WwNP: EA, 2014), is an approach that utilises soft-engineered structures and interventions that both utilise and enhance the natural processes within the catchment (Calder and Alywood, 2006; SEPA, 2016; Lane, 2017). It is argued that NFM is a low-cost, scalable, approach that, in addition to improved flood resilience, can yield considerable benefits in terms of improved ecosystem services and stakeholder engagement (Lane et al., 2011).

This study arises from a project that was undertaken for the UK Rivers Trust intended to provide better understanding of how NFM could be applied strategically to the headwaters of three catchments in Cumbria, UK (Hankin et al., 2016). Measures included large-scale tree-planting to increase evaporation losses and to improve soil structure, and restoration of peat and heath to increase surface roughness. It included consideration of the installation on the hillslopes of a widely distributed network of

runoff attenuation features (RAFs) to intercept fast overland flow Each intervention was modelled separately, allowing the effects of each to be examined.

The work builds on the approach piloted by Hankin et al. (2017) in the Eden, a rural catchment in Cumbria, UK with an area of 2248 km² upstream of Carlisle. There was significant flooding in settlements around the middle and lower reaches in 2005, 2009, and during Storm Desmond during 5th – 6th December, 2015. A high resolution, 2D inundation model based on solution of the Shallow Water Equations, (JFLOW, Lamb et al., 2009, Environment Agency, 2013) was applied to assess potential sites for distributed measures and understand relative impacts on the hydrograph, in terms of downstream benefits or damages avoided. This model was driven by multiple rainfall event sets incorporating spatial joint probabilities observed in the extremes from time series of observed rainfalls around the catchment (Lamb et al., 2010; Keef et al., 2013). It showed the potential for a widely-distributed NFM approach, but did not undertake detailed modelling of the proposed interventions, or test the model against real rainfall and discharge data. The responses of headwater catchments have been identified as having a disproportionate influence on the overall downstream flood risk (Pattinson et al., 2014), and were selected for further examination in this study. The strategic screening stage combined the JFLOW analysis with a catchment partner workshop order to identify areas with the greatest opportunities for NFM.

6.1.1. Aims and objectives

There is considerable uncertainty in both predictions of runoff response (Beven, 2006) and the effect of application of distributed flood mitigation measures, particularly in terms of their effects on effective hydrological parameters (Dadson, 2017; Hankin et al., 2017; Lane, 2017). Additional uncertainty will be introduced by the lack of knowledge of the effects of RAFs on the effective hydrological parameters, their

response over series of storm events and hydraulic characteristics whilst filling and draining. The response may be complicated by spatial variation in rainfall, and the effect of the sequencing of storm events on antecedent conditions and runoff generation.

The effectiveness of natural and distributed flood management schemes has been attributed, in part, to the desynchronisation of subcatchment flood waves (Thomas and Nisbet, 2007; Blanc et al., 2012). This suggests the possibility that inappropriately-sited interventions could have a detrimental impact on the storm response by synchronising previously asynchronous waves, an impact that will be dependent on the configuration of subcatchments at different catchment scales. Given this, and the large combination of potential configurations and varieties of storm events, a pragmatic approach to evaluating the impacts of NFM would be "experimental" modelling such as proposed by Hankin et al. (2017), whereby many possible realisations of the catchment model and event sets are generated. The primary goal of the project was to deliver a computationally efficient runoff model and representation of RAFs that would allow such an approach to be undertaken in reasonable timescales. This would necessarily would involve some simplifications of the RAF responses, as a fully hydrodynamic treatment will introduce considerable complexity and much increased run-times to any modelling exercise A semi-distributed hillslope runoff model simplified the simulation of storm runoff and allowed multiple runs over large scales with reasonable run times. An efficient representation of features was sought that would allow modelling of their introduction without incurring significant computational cost. The approach is applied within the semi-distributed Dynamic TOPMODEL framework (Beven and Freer, 2001a; Metcalfe et al., 2015, 2016),

which aggregates hydrologically similar areas together whilst maintaining hydrological connectivity, provides a means to achieve this.

One objective of the project was to develop a representation for RAFs that incorporates sufficient information to adequately reflect the relevant aspects hydraulic response of the features as they fill and drain, including consideration of overflow characteristics. A new, storage-based overland flow routing algorithm was utilised that could be modified to take into account interception of runoff by RAFs. It maintains a record of water levels in RAF which can be used to examine the drain down, filling and possible overflow of these features during the course of storm events.

Chapter 4 investigated the impact of the installation of barriers with varying underside clearance within the channel network. It was observed that applying small clearances led to the filling of storage capacity in the course of a double-peaked storm events. Features with larger clearances, although able to recover capacity more quickly between events, had less of an impact in intermediate storms. The project aimed to determine whether for hillslope interventions there is a similar trade-off between fast-draining features that retain the intense rainfall but operate less effectively over events of longer duration, and less permeable designs that retain more of the runoff but can become overwhelmed in larger storms. This effect was investigated by application of different levels of "leakiness" through the walls.

The expectation is currently that NFM will have an impact on small to moderate scale events. However, to be a practical strategy, it will be required to operate effectively across extreme events, but there is as yet little evidence of what is required to have an effective impact in these conditions. The application therefore assimilated actual rainfall data from multiple gauges for a period containing a sequence of flood events,

including Storm Desmond, one of the largest events recorded in the UK, to modelling of the RAF intervention.

6.1.2. Runoff Attenuation Features as a Natural Flood Management technique

A wide range of measures are employed in catchment-based approaches to flood mitigation. These are intended to reduce hillslope – channel connectivity, slow surface and channel velocities and thus to mitigate the effects of fast runoff Techniques employed in NFM are reviewed by Quinn et al. (2013), EA (2014), SEPA (2016), Dadson et al., (2017) and Lane (2017) and will not be discussed in detail here. Structures commonly found in NFM schemes include wooden barriers or debris dams in ephemeral channels, earth bunds, and ground scrapes or ponds. These are designed to intercept and store overland or overbank flow and can be effective in disconnecting fast surface flow pathways from the channel and so increase hillslope storage. The walls of these structures are commonly constructed to be permeable or "leaky", reducing hydraulic stresses and allowing the stored runoff to drain out slowly. Another strategy is to have more impermeable walls but to allow the storage to drain to the channel via a pipe. Other strategies, such as tree planting in critical locations, are aimed at encouraging runoff to infiltrate and follow slower subsurface pathways downslope. Their aim is to delay the arrival of runoff at the channel until after the main flood wave has passed, such that the downstream storm peak is attenuated.

Ghmire et al. (2014) simulated a single hillslope pond of capacity 27000m³ in a 74 km² catchment and showed that it could reduce peak flows by 9% in a 1 in 2 year event. The capacity of RAF features is generally much smaller than this, and in the UK constrained by legislation that limits their size to 10000 m³ above which significant legal responsibilities are imposed (Wilkinson et al., 2010b). The storage

required for a significant mitigating effect on storm flows is large, however. The analysis in Chapter 4 showed that within a 29km² catchment 168,000m³ of hydrodynamic storage would be required to attenuate peak flow in order prevent flooding in a 1 in 75 year event. A scheme of a realistic scale could therefore involve installation of many hundreds of RAFs, although the number required might be reduced by applying other measures.

Pattinson et al. (2014) examined the interacting effects of the Eden subcatchment flood waves using data for a large flood event in Carlisle in 2005 and concluded that their timing and magnitude predicted the majority of the variance in modelled downstream flood peaks. It will therefore be necessary to design such installations with some care. Slowing runoff that would have contributed to the hydrograph *before* the peak could have the effect of increasing the peak magnitude. This is called the synchronicity problem. Peak timings vary, however, with the pattern and timing of rainfalls and antecedent wetness in the catchment and the way in which the hydrographs from different subcatchments interact. Thus, it will be necessary to test the sensitivity of a design before implementation using an appropriate model of runoff generation and mitigation measures. This might, in itself, require many model runs that reflect different event characteristics and patterns, storage and drainage characteristics of RAFs.

6.2. Modelling strategies to evaluate the effect of RAFs

6.2.1. Runoff modelling

To assess the effects on the storm runoff of emplacement of RAFs it is necessary to predict the hillslope runoff contributions to the stream channel and the routing of the flood hydrograph in the channel network. Before the implementation of any RAFs the predicted catchment outlet discharges will allow calibration of model parameters

against observed flows. Simulations with identical input data using representations of unaltered and modified catchments are then undertaken and the results of each compared. There are many runoff models that could be applied to this problem. The representation of small-scale RAF features would appear to require a fully-distributed, high resolution modelling approach. Such models are often highly-parameterised, with long run-times, making their use in uncertainty estimation frameworks challenging. To overcome such difficulties, in this study an implementation of the semi-distributed Dynamic TOPMODEL (Beven and Freer, 2001a) is employed. The model has been applied in many studies (see, for example, Liu et al., 2009; Page et al. 2007). In Chapter 3 a new implementation demonstrated robustness to spatial and temporal discretisation applied to a 3.6km² upland catchment. In Chapter 4 it was used to evaluate structures within the channel network of a small agricultural catchment in North Yorkshire, UK where an NFM scheme is proposed. This represented the in-channel barriers applied within a spatially-explicit network and hydraulic routing scheme, with the pattern of spatial runoff predicted by the hillslope component of Dynamic TOPMODEL.

The model extends TOPMODEL (Beven and Kirkby, 1979). The principles of the later version are detailed by, amongst others, Beven and Freer (2001a) and Metcalfe et al. (2015). The basic approach is the aggregation of "similar" landscape areas into Hydrological Response Units (HRUs) that are treated during the course of a simulation as having similar hydrological responses, based on common model parameters. The units may be of arbitrary size and not necessarily spatially contiguous, although they, along with their internal states, can be mapped back into space. This "discretisation" approach significantly reduces the complexity of the landscape model whilst retaining hydrological connectivity of the hillslope. The

improved subsurface routing algorithm introduced in Dynamic TOPMODEL allows a more flexible approach to aggregation of catchment areas. Of particular relevance in the current context is the ability to collect areas identified with RAF interventions into one or more HRUs. In realisations reflecting unaltered catchments these units behave identically to surrounding landscape areas. To simulate the effect of applying one or more RAFs the surface runoff routing through the corresponding units can be altered to reflect their reduced connectivity with the hillslope. Model parameters are shown in Table 6.1.

Table 6.1: Runoff model parameter and ranges applied in calibration and uncertainty analysis.

Parameter	Description	Units	Lower	Upper
v_{of}	Overland flow velocity	m/h	1	150
m	Exponential recession parameter	m	0.0011	0.033
srz_{max}	Max root zone storage	m	0.1	0.3
srz_0	Initial root zone storage	%	20	100
v_{chan}	Channel routing velocity	m/h	500	5000
$ln(T_0)$	Lateral saturated transmissivity	m²/h	3	12
sd_{max}	Maximum effective storage deficit	m	0.5	-
ex_{min}	Minimum surface storage	m	0	-
ex_{max}	Maximum surface storage	m	1	1

Once a HRU discretisation has been defined using relevant spatial overlays the model is run against rainfall and potential evapotranspiration data for a specified time period. For that period, it produces a time series of simulated discharges at the catchment outlet and time series of the internal states of each of the HRUs.

6.2.2. Overland flow routing in Dynamic TOPMODEL

Hunter et al. (2007) suggest that in some situations simplified, but physically-based, surface flow models can perform as well as a fully hydrodynamic formulations such

as the Shallow Water Equations. In TOPMODEL and the first version of Dynamic TOPMODEL (Beven and Freer, 2001a) a network width approach was taken to routing surface flow (see Beven, 2012). In the implementation described in Chapter 3 a semi-distributed, storage-based surface flow routing module was introduced. This uses a routing scheme similar to that applied to the subsurface. Saturation excess from upslope HRUs is routed to downslope units by a surface flow distribution matrix $\boldsymbol{W_{of}}$ derived from the surface topography:

$$\boldsymbol{W_{of}} = \begin{pmatrix} 1 & 0 & \cdots & 0 \\ r_1 & p_{11} & \cdots & p_{1n} \\ \vdots & \vdots & \ddots & \vdots \\ r_n & p_{n1} & \cdots & p_{nn} \end{pmatrix} \quad r_i + \sum_{j=1}^{n} p_{ij} = 1 \qquad \text{(Eqn.6.1)}$$

Each row gives the proportions of the corresponding unit's flow that is directed to other units. For example, p_{ij} is the proportion of unit *i*'s flow that is directed to unit *j* and p_{ii} is the proportion that remains within unit *i*. The vector $\boldsymbol{r}$ represents a lumped "river" unit such that r_j is the proportion of downslope flux entering the channel network from unit number *j*. With an extended matrix a multi-reach river unit can also be defined. The matrix approximates transfer of flux between the different landscape units by averaging the inter-cell slopes of the elevation raster between cells falling into each of the landscape categories.

An assumption of a linear storage-discharge relationship is now made, whereby the discharge overland per unit contour out of a unit is proportional to depth of flow *d*. This implies a uniform velocity profile, so that the specific discharge per unit contour length from each HRU is $q_{out} = v_{of}d$, with v_{of} its mean overland wave velocity. It can be shown (Metcalfe et al., 2015) that this leads to a coupled series of ordinary differential equations for the average surface storages $\boldsymbol{s}$ within the HRUs:

$$\frac{d\boldsymbol{s}}{dt} = \left(\boldsymbol{W}^T \left(\boldsymbol{A} \circ \boldsymbol{v_{of}} \circ \boldsymbol{s}\right)\right) \oslash \boldsymbol{A} - \boldsymbol{v_{of}} \circ \boldsymbol{s}$$

where $\boldsymbol{A}$ is the vector of areas for each of the units, and $\circ$ and $\oslash$ the element-wise multiplication and division operations respectively.

This system can be solved analytically by the so-called Eigenvalue method (Dummit, 2012). The storage distributed downslope is calculated to the end of the simulation time interval and any runoff routed to the channel is routed to the outlet using the network width approach. Surface excess storage redistributed to other units across the interval are added to the rainfall input for those units in the next time step. This approach allows for possible re-infiltration given a soil moisture deficit in downslope units. This is known as run-on. NFM measures such as tree shelter-belts that improve soil structure to enhance infiltration (e.g. Caroll et al., 2004) may have this effect in moderate events. Any excess over the saturated storage capacity of the profile is treated as the equivalent quantity of overland flow and routed in the same fashion. Run-on is also handled in models such as MAHLERAN (Model for Assessing Hillslope-Landscape Erosion, Runoff And Nutrients; Wainwright et al., 2008).

6.2.3. Approaches to modelling of RAFs

Physically-based models in general employ a gridded digital terrain model (DTM) to represent the surface. Features can be introduced into the landscape representation within the model by raising cells on their boundary to represent wooden walls or bunds. A fully-distributed hydrodynamic model, TUFLOW (Two-dimensional Unsteady FLOW; Syme, 2001), was applied using this approach across the 74km² Tarland Burn catchment in Aberdeenshire, Scotland (Ghmire et al., 2010). In the Eden, Hankin et al. (2017) simulated hillslope ponds by deepening the appropriate cells in a 2m DEM and applied designed rainfall events to the JFLOW model. Both approaches may be sufficient to represent ponds and impermeable bunds, but it will be difficult to account dynamically for infiltration, evaporation and losses through

permeable walls, and thus the areas will be unable to drain down during the course of a simulation. The method will have limitations when applied to multiple storm events where recovery of storage capacity during recession periods is likely have an effect.

Hydraulic models of individual structures could be achieved by applying analogies to engineered interventions whose characteristics are better understood. In Chapter 4 the effects of the wooden channel barriers were modelled by analogy with underflow sluices employed in in irrigation schemes. Chow (1959) describes analytical storage-discharge relationships for such structures that utilise empirically-determined parameters. RAFs constructed of spaced timber members could be modelled by the Kirschmer-Mosonyi formula for flow through trash screens (Mosonyi, 1966), such as used in the intakes to power plants and waste-water treatment works. Overflow of these structures running out of capacity during the course of a storm event could be modelled analytically as though across a weir, another well-studied structure. The approaches developed by Puttock et al. (2017) to model the hydraulic characteristics of beaver dams could be utilised.

Wilkinson et al. (2010b) used a lumped representation of RAF storage. In this model a series of offline ponds representing the additional storage are connected to a single river reach. Flood discharge is routed through these treated as linear stores. The approach was applied in the Belford Burn catchment and suggested that 20000m³ of additional storage could have sufficient attenuation to prevent flooding in the smallest storm that would have caused damage. The storage was assumed to always be fully-utilised, but Metcalfe at al. (2017) showed that the interactions of a RAFs and the complex routing of flood waves down a realistic channel network meant that the storage associated with a scheme could be substantially underutilised, even during

large events. Conversely, they can run out of capacity too soon, before or in the rising limb of these storms, to mitigate the flood peak sufficiently.

RAFs may be most effectively applied to reduce hillslope connectivity with the channel by placement across fast surface runoff pathways (Wilkinson et al., 2010a; Quinn et al., 2013). Such pathways can be identified by observation during storms or by examination of debris after events. Opportunities may also be determined through application of a hydrodynamic runoff model to identify accumulation areas. In the study case, the surface runoff for a designed storm of a given return period were modelled by using JFLOW applied across a 2m x 2m DTM. Areas with maximum surface storage exceeding a given depth were identified with sites for potential RAFs.

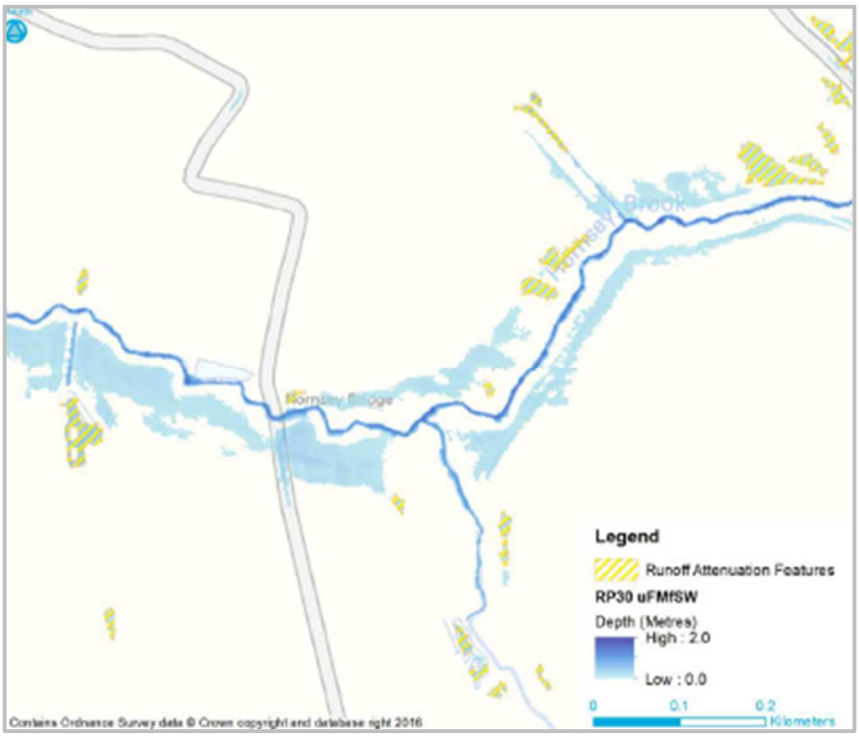

Figure 6.1: Hydrodynamic accumulation areas within Eden identified by JFLOW analysis for a designed storm of return period of 30 years (Hankin et al., 2017). Maximum water depths are indicated, and areas that exceed the threshold depth and other criteria (minimum area, slope angle and proximity to roads and buildings) are highlighted as potential sites for RAFs

Some areas identified with this technique within the Eden are shown in Figure 6.1.

6.2.4. Modelling RAFs with Dynamic TOPMODEL

Multiple-spatially distributed RAFs with similar characteristics can be lumped into individual response units. Characteristics could include height and permeability, position on the hillslope, upslope area, slope and proximity to the channel. Even if many such aspects are identified and result in multiple groupings, this approach will substantially reduce computational overheads against a fully-spatially distributed representation.

Drainage is an important aspect of a RAF's behaviour. If operational the ground behind the RAF is likely to be saturated and little storage will infiltrate to the subsurface. There may still be evapotranspiration losses, which will occur at the maximum potential rate from the open surface, but this is likely to be minimal, especially during and between winter events. Direct drainage from the RAF could be via a pipe which, ignoring friction, gives a dependence of discharge on the square of the hydrostatic head. Leaky wooden structures or permeable bunds may instead drain as though through a porous medium. In this case it be more realistic to relate output discharge linearly with the head (Beven, 2012). The structure could also be impermeable so that storage is lost downslope only when the features starts overflowing.

Overflow characteristics will also vary between features. In deepened hollows and ground scrapes any overflow in excess of the storage capacity will leave the feature in a similar direction and velocity as across the unmodified hillslope. In both leaky and impermeable structures, assuming they are designed to maximise interception by following the local contours, the directions are again likely to be similar. Overflow rates over the feature will, however, depend on its construction, but in general can be

represented by a form of non-contracted Weir equation (see Chow, 1959; Brater and King, 1976). If $q_{over}$is the specific overflow and h the water surface height above the weir crest, then

$$q_{over} = C_d h^{1.5} \qquad \text{(Eqn. 6.2)}$$

where C_d is a coefficient that reflects the energy loss across the overflowing edge of the structure and the associated hydraulic jump as the flow becomes critical.

For wide, smooth bunds a broad-crested weir might be the best representation, where critical flow occurs at some point across the edge. In this case C_d is a function of the weir breadth and the upstream head. Brater and King (1976) tabulate empirically determined values of C_d against weir breadth and head for broad-crested weirs. Screens or barriers could more realistically be modelled as sharp-crested weirs, where the critical section occurs in the free drop outside the structure. In this case the discharge coefficient can be calculated from the ratio of the crest height to the water depth h_c (Chow, 1959):

$$C_d = 3.27 + 0.4\frac{h}{h_c} \qquad \text{(Eqn. 6.3)}$$

If the barrier is constructed of rounded members such as natural timber the value of $C_d$calculated above increases proportionally with their radius (Jones, 1917). There are other functional forms when the weir discharge is submerged, outlined by Brater and King (1976).

The semi-distributed surface routing algorithm outlined in Section 6.2.2 is now applied to model groupings of RAFs. Units associated with a grouping of RAFs are modified so that a smaller proportion of the downslope flux is directed to units than for the unaltered landscape representation, and thus the feature fills when there is a net input of runoff. For features that are partly excavated or a bunded surface depression

there will be an initial priming storage that must be filled before water starts draining downhill over the surface. This requires as an additional HRU parameter ex_{min}. Any surface excess storage below the surrounding ground surface (i.e. $ex_s < ex_{min}$) stays in the same unit and the remainder overflows across the surrounding hillslope.

The proportion of water lost from HRUs corresponding to permeable RAFs is emulated by altering the corresponding row in the surface distribution matrix (Eqn.6.1) to reflect the "leakiness" of the walls. A factor $\Lambda \in [0,1]$ is defined as the proportion of flux draining downslope out of a RAF HRU unit. A modified routing matrix is developed where the elements of row *i* control the flux distribution out of an aggregated RAF identified with unit *i*. In the case of a leaky dam on a hillslope the sum of the elements excluding the diagonal is $\sigma_i = r_i + \sum_{j=1\cdots n, j\neq i}^{n} p_{,\boldsymbol{i,j}}$. Setting $p_{\boldsymbol{i,i}} = 1 - \Lambda$ and scaling the other elements of the *i*-th row by the factor Λ/σ_i the row again adds to 1, as required. For a channel screen or woody debris dam the drainage direction is likely to be towards the nearest channel. For unit *i* the river element $r_{\boldsymbol{i}}$ of $\boldsymbol{W_{over}}$ is set to Λ , the diagonal component $p_{\boldsymbol{i,i}}$ set to $1 - \Lambda$ and all the other $p_{,\boldsymbol{i,j}}$ set to zero.

Note that only overland flow, represented by saturated excess, is routed out of the RAF HRU by the modified distribution. matrix. Subsurface routing beneath the structure is unaltered. Each unit in effect behaves for the duration of a time step as a linear store with residence time $T_{res}(\Lambda, v_{of,i}) = \frac{1}{\Lambda v_{of,i}}$. For a roughly rectangular area storage could be considered as proportional to water depth. A parameter ex_{max} [L] can be introduced to control the maximum storage; if $ex > ex_{max}$ the structure starts to overflow. An additional overflow matrix $\boldsymbol{W_{over}}$ is now defined to direct excess water

out of the lumped features. For ground scrapes and bunded depressions this is identical with the unaltered surface distribution matrix $\boldsymbol{W_{surf}}$.

6.3. Uncertainty estimation framework

There is significant uncertainty in predictions of the spatial distribution and quantities of runoff generation (Beven, 2006, 2009, 2012). Attempts to assess the effectiveness of NFM will compare predictions for unaltered and modified catchments thus introduce even further uncertainty. In the case of the RAF interventions uncertainty will be introduced by, for example, feature location and their geometry and discharge characteristics. In addition, reduction in capacity through sedimentation or damage due to loading will mean that their performance may be non-stationary.

Uncertainty estimation and sensitivity analysis can provide a realistic assessment of the reliability of predictions of the impacts of NFM. These techniques will, however, require the generation of thousands or even millions of model realisations in which parameters are sampled from prior distributions of feasible values. With continued growth in computing power it is now feasible to run the fully-distributed JFLOW model over 750km² with a 2m resolution grid (175 million cells) in approximately real-time (Hankin et al., 2017). Metcalfe et al. (2017) were, through the use of parallel processing technology, able to produce around 2000 realisations of storm routing with various channel and floodplain configurations and roughness. The introduction of in-channel interventions, simulated with a hydraulic model, increased run-times significantly and they were able to run only a limited sensitivity analysis of different configurations and dimensions. Thus, while high-performance computing may be fast enough for assessment for a selection of features and hillslope properties, it may still be inadequate for uncertainty analysis across larger catchments and wide-scale NFM

schemes comprising the large number of features required to meet the storage requirements to significantly attenuate real flood events.

A traditional approach to runoff modelling assumes a single landscape realisation, but it has been observed in many studies that different parameterisations can lead to very similar results, or equifinality (Beven, 2006). The approach taken by the project is a form of the Generalised Likelihood Uncertainty Estimation methodology (GLUE: Binley and Beven 1992; Beven and Binley, 2014) employed in many studies (e.g. Beven and Freer, 2001b; Beven and Blazkova, 2004; Liu et al., 2009). GLUE accepts the possibility of many model realisations that can fit the observed behaviour. In the course of a calibration or other modelling exercise those realisations whose outputs meet an acceptability threshold with respect to some type of likelihood score calculated for each are retained; the score thenceforth being maintained alongside the corresponding realisation.

Typically, a large number of model parameters are sampled with a Monte Carlo approach from one or more prior distributions derived from, possibly subjective, knowledge of acceptable or likely ranges. These are then applied in turn to the system model and a simulation performed, resulting in multiple model realisations. Each is scored with a likelihood that takes as parameters relevant observables of the simulation, or performance metrics derived from it and observational data. Only those simulations achieving an acceptability threshold are retained yielding a "behavioural" parameter set. This gives a posterior distribution of model realisations, each associated with a likelihood, or weighting, from which distributions of predicted variables can be obtained.

A triangular weighting function is commonly applied to the weightings for individual observations, whereby the value is unity at the likeliest value of the acceptability

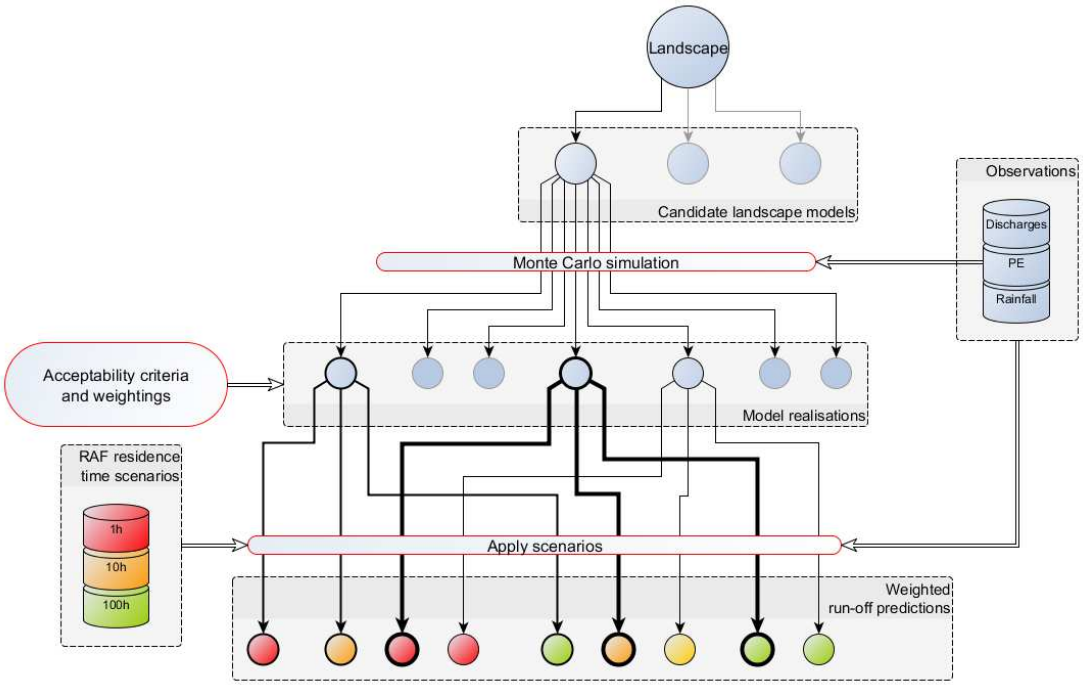

Figure 6.2: Suggested work flow diagram for Monte Carlo simulation of storm runoff, and selection and weighting of behavioural realisations and application of NFM scenarios for forward prediction of change. The weight of lines leading from acceptable simulations reflects the weighting likelihood score in the validity of that realisation.

interval, zero at either limit, and linearly interpolated between these points. A trapezoidal form (e.g. Blazkova and Beven, 2009) could also be applied, whereby the value is unity between two threshold values and linearly interpolated outside these to the acceptability criteria. The individual weights are combined, possibly with weighting applied to one or more measures, and normalised to produce a value between 0 and 1 (Beven and Freer, 2001b; Beven, 2006; Beven and Blazkova, 2009; Liu et al., 2009). All of the predicted values of the observables must lie within acceptable ranges or the realisation is rejected, even if the overall sum of weights is non-zero.

A suggested approach, applied in the case study described, for incorporating the uncertainty framework into evaluation of RAF interventions is shown in Figure 6.2.

Behavioural model realisations for the unaltered catchment model are obtained from a large number of randomly chosen model runs. Subsequently one or more modifications due to the applications of RAF interventions are applied to each of the base realisations. For each altered realisation the weighting score can be carried through from the baseline case, or if there is available information on the likelihoods of the effects of the interventions a score for the modified realisation can be calculated and combined with the weighting of the associated behavioural model.

6.4. Case study

6.4.1. Study catchment and calibration period

The Eden headwater catchments modelled in the study cover its area draining from the source near the border of Cumbria and North Yorkshire to the flow gauge, EA number 760101, at Great Musgrave Bridge (2.363234 W, 54.5126 N), a drainage area of 223km² (see Figure 6.3). The catchment is 55.4% acid, improved or rough grassland and 36.0% bog or scrub and heath. Bedrock geology is Permian and Triassic sandstones lain on Carboniferous limestones and there is some influence of groundwater pathways (Ockenden & Chappell, 2010). Tree cover is minimal, comprising just 2.5% of its area, though there has been significant recent tree planting that is not yet thought to have had any major effect on flood peaks. Overall annual rainfall is in the region of 1200mm, but there is a strong synoptic and orographic influence (EA, 2009). In early November 2015 a south-westerly airflow became established that brought warm moisture-laden air from subtropical regions. This was followed by a period of exceptional storm events that included Storms Abigail (15th-16th November), Barney (18th November) and Desmond (5th-6th December). The final extra-tropical cyclone caused significant damage and over 2000 homes were flooded at Carlisle, further downstream. A record 1680m³/s discharge was recorded at 9am on

December 6th at Sheepmount Weir (54.905332 N, 2.952091 W) in Carlisle. The town of Appleby (54.578719 N, 2.488839 W), was also badly affected by this event; a peak discharge of 372 m³ was recorded at 18:00 on the 5th of December at the UK Environment Agency gauge at Great Musgrave Bridge a few kilometres upstream.

The early autumn period of 2015 was unusually dry and soil water deficits were in October more than 10mm greater than the long-term average (Marsh et al., 2016). The

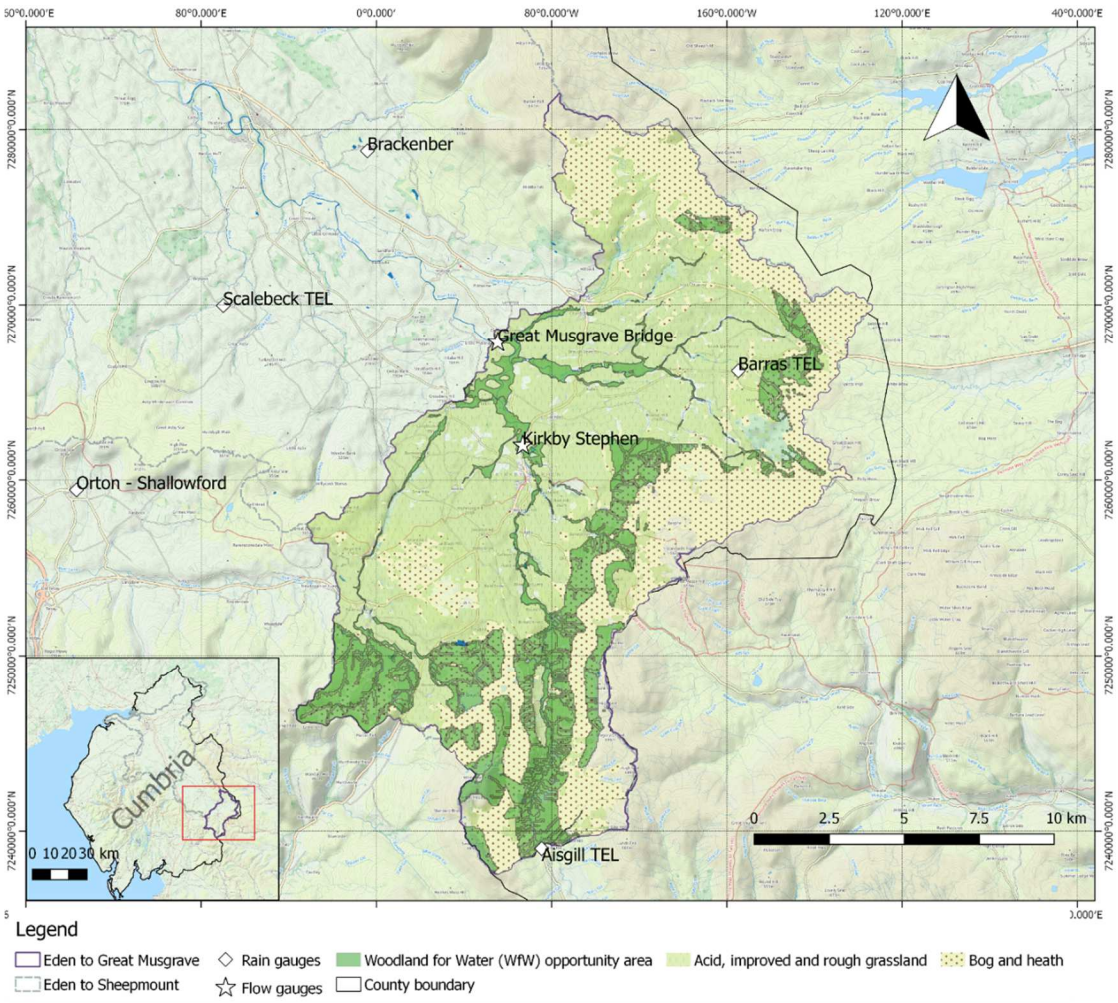

Figure 6.3. Study catchment, the Eden headwaters to Great Musgrave Bridge (223km²), showing context within Cumbria, UK, predominant land cover types and location of TBR rain gauges and gauging stations and predominant land cover. Woodlands for Water opportunity areas are shown. These were applied in another application of the NFM modelling framework developed for the project described, which is not discussed in detail here.

calibration period chosen begins at the end of this month when the soil moisture deficit was at its peak and ends in the recession period of Storm Desmond. Processed 15 minute time series of rated discharges were obtained for gauge 760101. There is one other flow gauge within the catchment, at Kirkby Stephen (see Figure 6.3). Tipping-bucket recorder (TBR) rainfall data at 15 minute intervals were provided by the EA and a set of these gauges lying within 10 km of the catchment were identified. Given the extreme rainfall, some gauges went off-line during the storms and were removed from the set, leaving four gauges with complete records over the calibration period from which a rainfall record was interpolated. This met the water balance to within 5% and applied to the entire catchment area.

Although significant events, Storms Abigail and Barney did not cause damaging flooding in this catchment. This suggests that a reduction of the 7.0 mm/h peak of Storm Desmond to that of Abigail, at 2.4 mm/h, the larger of these events, would be a very successful outcome of any NFM intervention. This corresponds to a reduction of around 4.6 mm/h or 65%. It should be borne in mind the potential for a large degree of uncertainty in the rating of these discharges, particularly at the extreme levels seen during Storm Desmond.

6.4.2. Identification and modelling of intervention areas

The catchment was divided into 8 response units according to the topographic wetness index (TWI, see Beven & Kirkby, 1979). JFLOW was run across the catchment using a design event of 30 year return period. Areas that accumulated significant water depths, such as natural depressions, flow pathways or small channels, were tagged as suitable candidates for enhanced storage. Their areas were then constrained in size to between 100 and 5000 m² and those within 2m of roads and buildings excluded. In principle, times to peak at the outlets of individual subcatchments estimated from the

modelled runoff designed event could be used to exclude faster responding areas from the introduction of features designed to slow their flood waves and thus mitigate the possibility of synchronisation. This was not undertaken in the Eden, however, but Hankin et al. (2016) applied the approach in the Kent headwater catchments to the SW. This yielded 4500 distinct sites of average area 506m², occupying 4.0% of the catchment, with a potential of just over 8 million m³ static storage.

The areas were tagged as being a unique HRU in the catchment discretisation, overriding any underlying classification determined from the TWI. This unit was treated as though a single aggregated feature bunded or dammed by a "leaky" barrier 1m in height with upslope sides open to receive surface runoff. Overflow was directed over the top of the barrier in the same direction as the original distributions given by the surface flow weighting matrix. The specific overflow per unit length along the top side of the feature was calculated as though for a broad-crested weir of width 50cm. Discharge coefficients are taken from the appropriate entries in the tables provided by Brater and King (1976). The unit took the same hydrological parameters as the surrounding regions. Three scenarios were considered, labelled RAF1, RAF10 and RAF100, corresponding to Λ factors equivalent to residence times of 1, 10 and 100 hours, respectively.

6.4.3. Monte Carlo analysis and identification of behavioural model realisations

An initial calibration exercise sampled 5000 parameters non-informative, uniform, prior distributions with ranges given in Table 6.1. The observables used to calculate likelihood weighting score were: A_c, the maximum saturated contributing area, or area proportion of the catchment that generates overland flow, the Nash-Sutcliffe statistic (NSE), and q_{max}, the maximum simulated discharge relative to the observed rated

value. The acceptability criteria for A_c were derived from considerations of physically-feasible values obtained from field observations, such as those in Chappell et al. (2006), and subjective, expert opinion of the likely values in an extreme event as such Storm Desmond. Remotely-sensed data such as that from thermal imaging (Luscombe et al., 2015) could be used to estimate A_c through actual events and thus provide estimates for likely ranges. The criteria observables are given in Table 6.2, alongside their limits of acceptability. The likelihood score for the NSE was the actual value calculated from the simulated discharges versus the observed, rated values. For the others, the likelihood score was triangular in the corresponding acceptability intervals, with value of unity at the midpoint of the range. The overall weighting score for a realisation is then calculated by taking the mean of the individual scores. The behavioural sets identified by applying the limits shown in Table 6.2 are then used as the basis for investigation of the effects of applying a number of NFM scenarios.

Table 6.2. Observables collected for each model realization and acceptability criteria applied

Metric	Description	Units	Criteria applied
NSE	Nash Sutcliffe statistic	-	>= 0.85
A_c	Maximum saturated contributing area	%	[10, 95]
q_{max}	Maximum specific discharge	mm/h	[5.2, 8.2]

6.5. Results

Of the 5000 realisations undertaken, 384 were identified with outputs that met the acceptability criteria given in Table 6.2. Figure 6.4 shows the discharges simulated by these behavioural realisations alongside the observed rated discharges at the EA gauge at Great Musgrave bridge.

The “dotty” plots in Figure 6.5 show the GLUE weightings for the three metrics used as the basis for selection of these acceptable cases. The maximum saturated area, A_c,

shown in the leftmost plot, has a discontinuous shape. This is because when a response unit reaches saturation it contributes its entire area at once. Within the behavioural realisations only a limited number of HRUs, along with the RAF unit, ever contribute saturated surface flow, leading to just seven distinct values for A_c. Points corresponding to likelihood weightings for realisations producing these distinct values of A_c are shown in the leftmost plot using a different colour for each. The same colours are applied to points corresponding to the same realisations in the other plots. The stratified appearance of the NSE plot is a by-product of its correlation with the contributing area; the correlation with the maximum predicted discharge is less clear. A value of A_c around 65% is associated with the best NSE fits, but is spread throughout the maximum discharges. The bias towards higher values suggests that realisations producing more fast overland flow better reflect the storm response in this period. This would be consistent with the extreme nature of the storms and, albeit limited, observational evidence (e.g. Marsh et al., 2016).

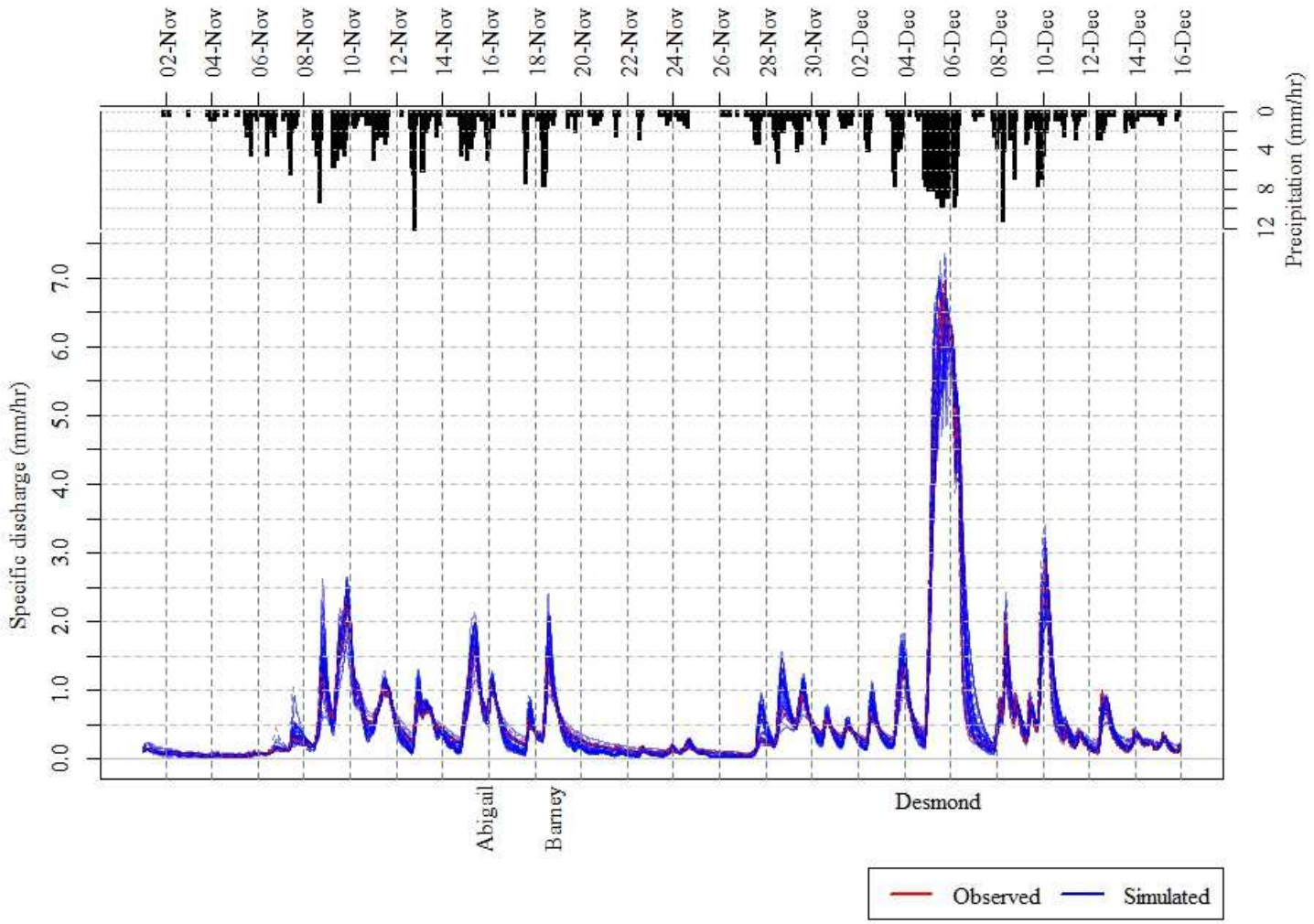

Figure 6.4. Simulated discharges at Great Musgrave Bridge across the calibration period described in the main text for behavioural realisations, shown alongside rated observed discharges. The periods of the three named storms are indicated.

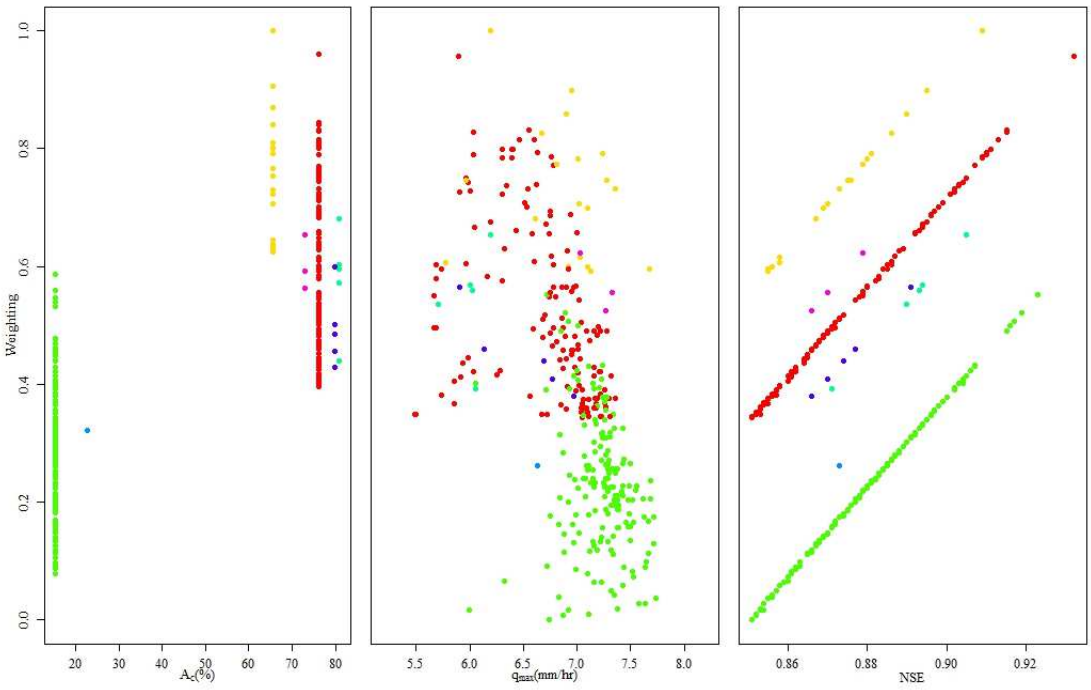

Figure 6.5. GLUE "dotty" plots showing overall weighting (likelihood) scores for each of the 348 behavioural runoff simulations identified against the three model outputs described in the text. The discontinuous appearance of the maximum saturated contributing area A_c is due to the relatively coarse discretisation applied such that once a HRU begins to produce any saturated overland flow, its entire area is added. Each unique A_c value takes a separate colour that is carried through to corresponding points in the other plots.

Parameters for each of the 384 accepted cases were applied to catchment models modified to reflect insertion of RAF networks with each of the residence times considered, and the simulations re-run. The statistics for each of the events and intervention levels are given in Table 6.3 and the impacts on the arrival time of the main peaks of each in Table 6.4. The Kolmogorov-Smirnov test included is a non-parametric approach to comparing empirical distribution, equal to the maximum vertical separation of the CDF of the discharges. This allows an evaluation of the relative effectiveness of each intervention. Reduction in peak Δq for a RAF case is defined as the difference between a base line case and intervention simulation based on this case.

Table 6.3. Statistics for each RAF interventions across the named storms in the simulation period: Δq_{max} = maximum relative reduction in peak (%); $\overline{\Delta q}$ = mean relative reduction in peak (%); K-S = Kolmogorov-Smirnov Statistic

	Abigail			**Barney**			**Desmond**		
	Δq_{max}	$\overline{\Delta q}$	**K-S**	Δq_{qmax}	$\overline{\Delta q}$	**K.S.**	Δq_{max}	$\overline{\Delta q}$	**K.S.**
RAF1	13.8	6.4	0.14	22.2	9.4	0.12	17.7	4.3	0.45
RAF10	49.6	30.2	0.77	66.4	26.8	0.43	25.4	14.5	0.82
RAF100	42.5	16.6	0.33	64	20.4	0.30	28.7	4.9	0.44

Figure 6.6 shows, as rainfall equivalent specific storages across the entire catchment using the 90% percentile weighted realisations, for the aggregated RAF unit throughout the whole simulation period. The crest height will exceed the maximum storage across the entire unit of at 1m as overflow across the top of the features, thus providing more storage than predicted by the hydrostatic analysis.

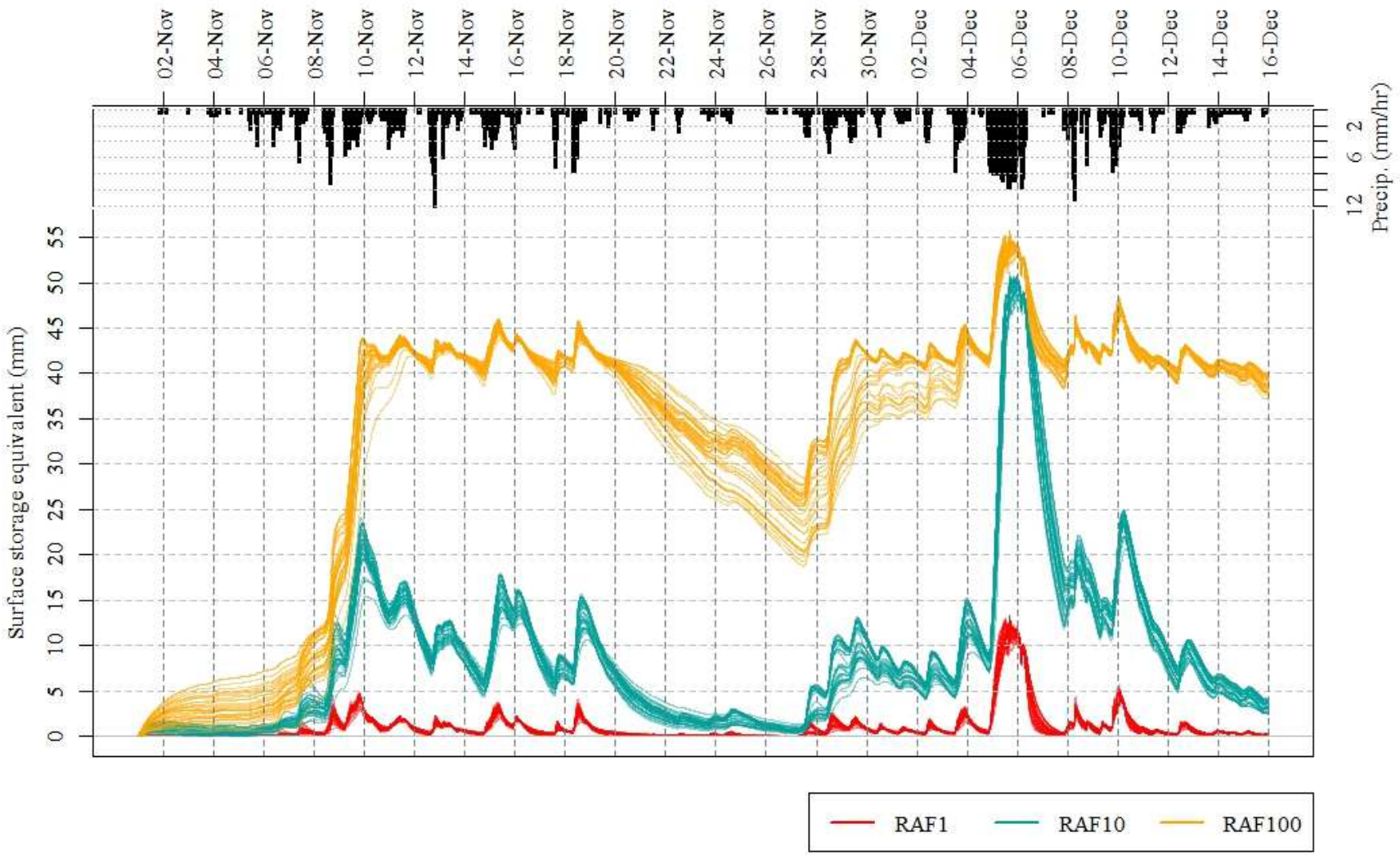

Figure 6.6. Surface excess storages, expressed as specific rainfall equivalent, across one of the lumped RAF units with maximum storage 1m through a single intervention cases and for the three mean residences times considered. The slight excess at the peaks of the storm reflects the weir crest

In the RAF1 case the areas drain quickly and appear to never fill completely. The available storage therefore appears not to be utilised effectively: the maximum utilised, at the peak of Storm Desmond, is 29% of the theoretical hydrostatic capacity, equivalent to 2,446,203m³ volume of storage retained across the catchment. The corresponding effect on the hydrograph is small, with a mean reduction in the peak of Storm Desmond of 4.3%; a few cases even show a small increase. For RAF10 the features appear under-utilised in the earlier storms, peaking at about 50% capacity, and recover almost all their capacity in the recession period after Storm Barney. Due to hydrodynamic storage utilisation exceeds 100% at the peak of Storm Desmond, with maximum filled storage volume across the catchment of just over 10 million m³.The impact of the additional storage is significant in the final storm and reduces the peak by an average of 14.4%, the greatest impact of any of the interventions. Combined with more conventional FRM measures this could have significantly mitigated the effects even of this extreme event.

In the RAF100 case the features fill completely during the course of Storm Abigail near the start of the period and the drain-down is too slow to allow complete recovery of capacity before the final event. They are overflowing during much of the event, with the excess following the fast pathways to the channel blocked by the RAFs The impact is therefore much reduced compared with the 10 hr case, with a mean reduction of 4.8% in the peak.

Ensemble hydrographs through each of the named storms are shown in the following figures. These present the discharges simulated for the unmodified catchment model using the parameters for each of the acceptable cases against those produced by applying the corresponding parameters to catchment models with the insertion of RAFs.

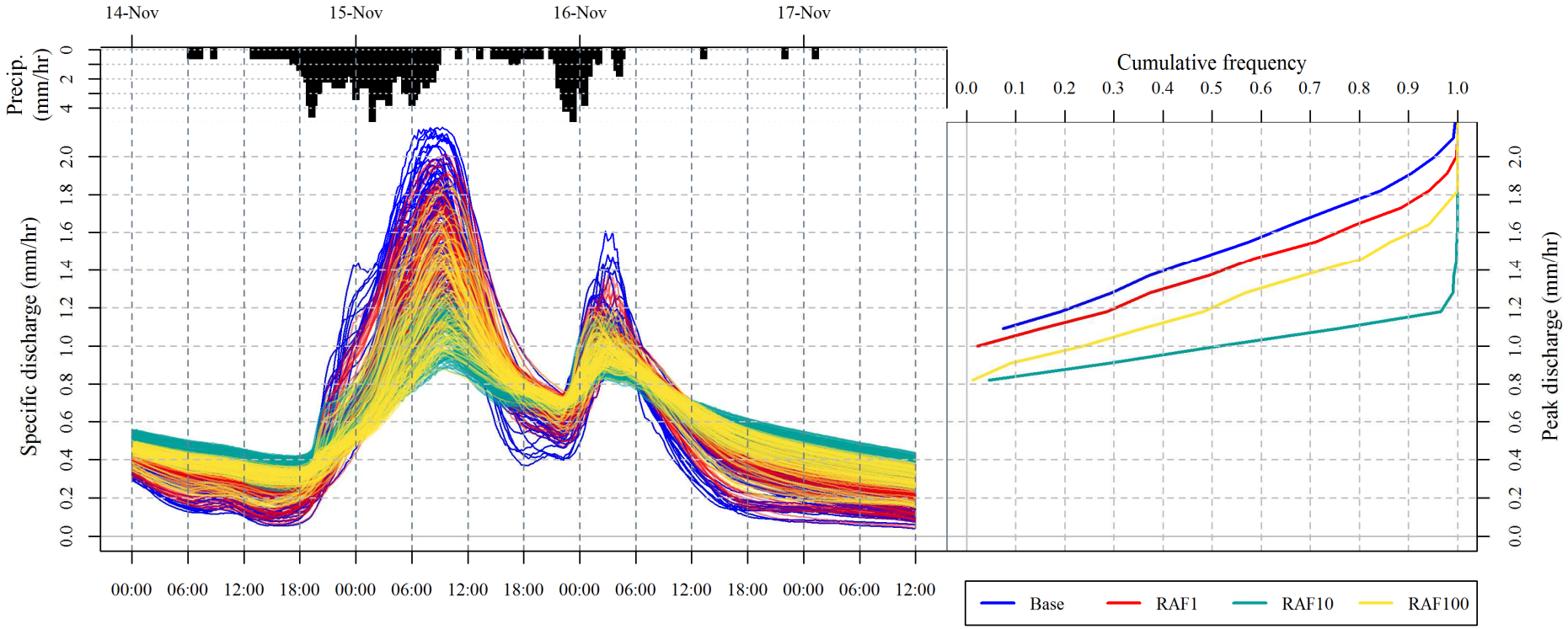

Figure 6.7. (L) 90 percentile weighted scored baseline and corresponding RAF intervention cases through Storm Abigail. (R) Likelihood-weighted cumulative frequency plot peak discharges for base and intervention cases. The K-S statistic for each is the maximum horizontal displacement between their lines and the leftmost, unaltered cases. Note that, in order to share the same vertical axis, the cumulative frequency plot is transposed relative to convention.

In the initial storm, Abigail (Figure 6.7), the first peak is attenuated as much by the RAF100 case as the RAF10 case, but in the second peak RAF10 again provides much greater reduction. The RAF1 case has the lowest impact on all of the peaks. The arrival of the main peak is retarded most by the RAF100 case, with a median delay of 30 minutes. The later peak appears to be brought forward marginally by the RAF100 cases, however. This may indicate that the RAF unit has run out of storage and is delivering water downslope by overflow. In all cases the recession curve is extended by the intervention, indicating that stored water is draining for some time after the storm peak.

In the second event, Barney (Figure 6.8), the RAF100 case appears to have most impact than any of the other cases across the initial peak but then becomes less effective than RAF10 through the main peak. There is less delay to the arrival of the main peak than for Abigail, with a median delay of only 15 minutes for the RAF10 and RAF100 cases. In the RAF10 case the median brings the peak forward by 15 minutes. This might indicate that their effect has been to slow down fast-responding catchments so that their flood waves contribute more to the rising limb of the overall storm hydrograph.

In the largest event, Desmond (Figure 6.9), the RAF10 case significantly outperforms the others, suggesting that it has recovered much more capacity. There is virtually no attenuation from the other cases and the peak is hardly delayed for RAF1 and RAF100**.** From Figure 6.6 it is clear that the RAF100 units fill quickly during Abigail and are full for the duration of Barney and Desmond, with only a week-long period in later November when they recover a little capacity through drainage during the recession period of Barney.

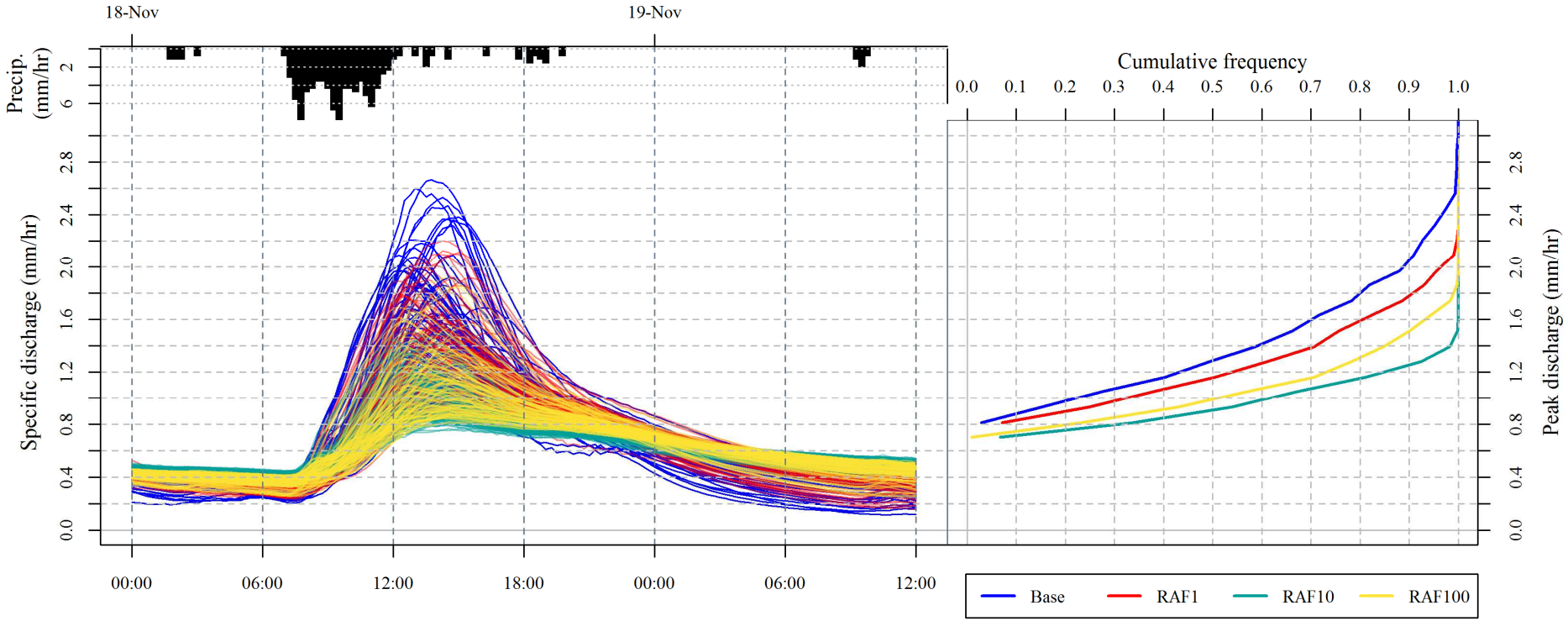

Figure 6.8. (L) Selection of base line and corresponding RAF intervention cases through Storm Barney. (R) Likelihood-weighted cumulative frequency plot of peak discharges for base and intervention cases.

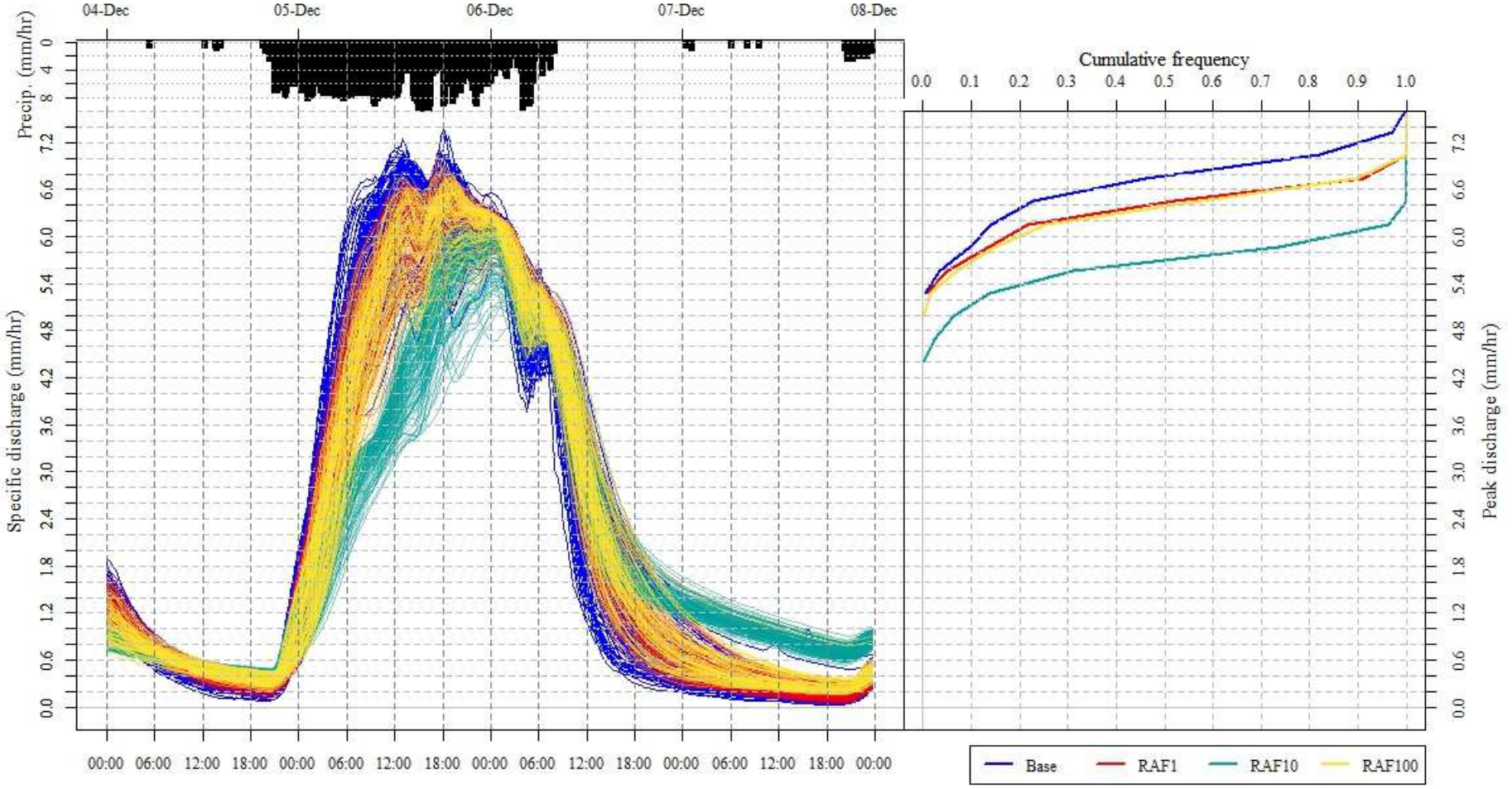

Figure 6.9. (L) Selection of base line and corresponding RAF intervention cases through Storm Desmond. (R) Likelihood-weighted cumulative frequency plot of peak discharges for base and intervention cases.

The RAF10 case has the greatest impact on the flood peak for all storms, with its advantage over the other cases increasing through the period. In Abigail the K-S distance of the RAF10 case is 150% that of the RAF100 case, whereas across Desmond this has increased to 350%.

6.6. Discussion

The surface routing algorithm is computationally very efficient, particularly as it can be solved analytically. The storage-based approach to RAF representation is straightforward and allows examination of relevant characteristics such as the drainage times and multiple model runs that apply different network configurations. More sophisticated physically-based modelling of surface flow will introduce computational overheads without accounting for large uncertainties in the input, and may not add greater insight into the catchment response.

The RAF10 case was significantly more effective across the largest event than the other two cases, as features had recovered capacity during the previous recession and drained sufficiently to have an impact on the flood peak in Storm Desmond. The mitigation was less across the earlier events but, given they did not cause significant flooding, this was not a consideration. This behaviour, whereby features that fill less quickly during intermediate events but also recover capacity that can mitigate later, more damaging, flood peaks, was simulated for in-channel NFM measures in Chapter 4.

NFM practitioners have previously designed schemes on the basis of the additional storage (hillslope and channel) that, when fully utilised, would retain sufficient runoff from a particular magnitude of event to reduce its peak to below the level where flooding would occur (see for example Nicholson et al., 2012). These results,

however, provide further evidence that the theoretical storage provided by an NFM scheme can be significantly underutilised, assuming it is configured so that it can recover capacity effectively between storms events. It has already been suggested that the effectiveness in reducing flood risk of a NFM intervention is not a simple function of the additional storage it provides, but also of its contribution to desynchronising a subcatchment's flood wave with those downstream (Thomas and Nisbet, 2007; Blanc et al., 2012).

A more sophisticated approach to implementing NFM is required. For instance, the locations on the hillslopes of interventions (such as RAFs) are likely to be a significant factor on a scheme's performance as they will influence flood wave timing. In this study the network width approach to routing channel flow was applied across the entire headwater catchment, and flood wave size and timings were not available for the individual subcatchments. It was thus unclear from the results what proportion of attenuation of storm hydrographs were due to desynchronisation of flood waves, as opposed to simple retention of surface runoff. A regression analysis similar to that undertaken by Pattinson et al. (2013), including as predictor variable the hillslope storage provided by the RAFs, could provide insight on the relative contributions of additional hillslope storage and flood wave desynchronisation on downstream flood mitigation. This can be done in a further analysis, but does raise the question of how to calibrate meaningfully flood wave velocities for the individual subcatchments.

The model gave good fits to the observed hydrographs, with many realisations exceeded efficiencies of 0.9 (although the uncertainties introduced through rating of discharges at extreme storm levels should be noted). The values of the maximum saturated area, A_c were highly discontinuous, however, as when the response units start to produce saturated excess flow they contribute their entire area to the metric. A

more fine-grained discretisation than the eight HRUs applied would produce a more continuous distribution, which might be advantageous in terms of better identification of saturated contributing areas, in particular how the positioning of RAFs in proposed schemes may influence runoff from these areas.

The features appeared to have an effect through the course of even the largest storm, albeit that the slowest-draining cases were full and overflowing for much of the simulation period. There is, however, a possibility that features will be unable to withstand hydraulic loading across such extreme events, or across a series of storms. Complete or partial failure could lead to debris being introduced to the flood waters and potential damage or blockage of downstream infrastructure which will increase risk of flood damage. Ideally, these scenarios should be incorporated in a risk reduction – cost matrix but there is, as yet, little information about the potential for failures that can be used to estimate residual risk., although initial findings suggest that failure sequences can behave non-linearly.

The RAFs were treated as a single unit in the catchment discretisation. A more considered approach to grouping features would be to categorise them by their type (e.g. bunded or screened ephemeral channels, enhanced hillslope depressions, or leaky dams), their geometries and their position on the hillslopes. The number of possibilities will increase rapidly according to the number of varieties and configurations defined, but these will be constrained by considerations of realistic design and implementation issues. In addition, the simplified representation used in this study allows for relatively rapid investigation of many different configurations. This approach can be incorporated into a sensitivity analysis to determine which characteristics are most important to the impact of RAFs on the storm response. A Monte Carlo approach selecting from multiple design event sets, for example

generated by the method of Keef et al. (2013), could help assess the robustness of the conclusions drawn from modelling and help to site features more strategically. It could also help identify situations where flood waves become synchronised by emplacement of features at different catchment scales.

6.7. Conclusions

This study has analysed the performance across a series of extreme events of a natural flood management scheme incorporating many "leaky" hillslope runoff attenuation features within the headwaters of a large catchment. The model incorporated a simplified overland routing module and achieved a high level of efficiency in simulating the observed discharges. The best base line simulations were applied to the catchment model with NFM features incorporated into the model. RAFs were simulated using a simple aggregated linear store model. It has been shown that their aggregated impact could have significantly attenuated the flood peak, by up to a maximum of almost 30%, even during the largest storm, but that their impact was contingent on the permeability of the RAF features that allowed them to recover capacity between events. The study demonstrates that uncertainty estimation can be applied to NFM in this context. A well-established uncertainty analysis framework was used, whereby multiple realisation of a hillslope runoff model applied to the events were enacted and scored against physically measurable characteristics and selected according to limits of acceptability of those observables. This allowed results to presented to project and catchment stakeholders alongside meaningful estimates of their uncertainty.

The RAF representation is efficient and allows investigation of many different configurations whilst retaining the important aspects of their behaviour and impacts, namely storage addition and residence times It contains many assumptions and

simplifications, however, and a key aim of further work will be to determine whether other significant characteristics are adequately simulated in this representation, and which will require refinement. For example, in actual applications there is likely to be a more complex storage-water depth relationship than the straightforward equivalence used here. Hydrodynamic analysis of simulated individual structures sited in realistic topographic representations may provide insights into the applicability of the simplification across a range of loading scenarios.

The RAF features considered in this study were lumped into a single HRU to maximise computational efficiency. A more sophisticated approach could utilise many more feature classifications derived from position on the hillslope, distance from access tracks, the channel and sources of construction material, type of location (e.g. within ephemeral channels, shallow hillslope accumulation areas or on the floodplain). More work will be needed to determine which of these characteristics will be most significant and how well classifications reflect actual implementations by NFM practitioners.

It may be that the most beneficial effects of RAF emplacement are likely to be seen on a smaller scale, in reaches immediately downstream of a feature or sets of features. It could be, even given the overall mitigation effect, that some asynchronous flood peaks in the unmodified catchment model became synchronised when the RAFs were introduced and thus reduced the overall effectiveness of the interventions. Much further work is required to better understand the synchronisation problem, particularly as catchment scale increases.

Obtaining observational evidence to support modelling predictions will be difficult in the field as, by their nature, the extreme events that load features are rare and gradual processes such as sediment deposition difficult to measure or simulate everywhere. An

innovative experimental approach is needed to address these questions. Detailed hydrometric data are required, collected by instruments such as stage and flow gauges upslope, downslope and within features. However only 6% of NFM schemes in the UK currently have any type of monitoring (JBA Trust, 2016). The effects of the RAFs on the overall flood hydrograph will be increasingly difficult to discern as the catchment size increases, including the potential for synchronicity effects. The methodology used in this paper, however, extended to incorporate better-supported representations of small scale impacts due to feature emplacement will provide a productive way to take forward research into natural flood management and its effectiveness.

Chapter 7. Conclusions

Through meeting its stated objectives this work has achieved its aim of developing a scalable and efficient computerised modelling framework for the design and assessment of distributed, soft-engineered approaches to flood-risk management.

The initial objective was to develop a scalable, robust, computationally efficient runoff model. Although fully-distributed models such as HydroGeoSphere (Therrien et al., 2010) and MIKE-SHE (Refsgaard & Storm, 1995) (see Chapter 2) operate at high-resolutions, they are highly-parameterised and computationally-demanding. This drastically limits their scalability. Lumped-conceptual models such as FEH (Institute of Hydrology, 1999) and ReFH (Kjeldsen et al., 2005) are readily-scalable but lack spatial and temporal resolution. The implementation of Dynamic TOPMODEL developed in Chapter 3, illustrates a semi-distributed hydrological runoff model which meets this objective by being both scalable and computationally efficient. The model is also open source.

The second objective was to develop a model which could simulate individual in-channel features and their combined effect on the storm flows within the channel network. Thomas and Nisbet (2012) modelled leaky debris dams, for example, but this study was limited to few features on a single reach. In contrast, the hydraulic channel routing model presented in Chapter 4 allowed the modelling of the effect of the storm runoff on any configuration of in-channel structures, from individual features to large arrays distributed across the channel network. When applied to a real storm event, information returned for individual proposed in-channel features allowed the strategic improvement of the overall scheme.

The third objective was to develop a scalable surface routing method that could represent the effects of measures to intercept overland storm runoff. Existing fully-distributed models, such as JFLOW (Lamb et al., 2009) and TUFLOW (Syme, 2001), can simulate surface flows at high resolution, but cannot easily or rapidly simulate the installation of a large number of features to intercept such runoff. A semi-distributed overland flow routing model was implemented in Dynamic TOPMODEL (Chapter 3). This approach allowed individual hillslope features to be aggregated as a single response unit. The filling and drainage characteristics of this could then be modified to reflect the presence of features and their permeability. The approach was relatively simple and could be solved analytically, thus improving its performance considerably.

The fourth objective of the work was to develop a framework for modelling the effects of widely distributed hillslope interventions at a catchment scale. There have been few attempts to model NFM in this way, with Wilkinson and Quinn (2010) adopting a simple static lumped storage approach. Dynamic TOPMODEL was extended and applied during a research project (Chapter 5). This evaluated the potential for a variety of NFM interventions in mixed-use, large catchments (up to 220km^2), by simulating the hillslope runoff and the effects of varying the hydrological parameters of the areas where interventions were applied. The scalability of the model allowed simulation of interventions from the size of individual hillslope features to the scale of large reforested areas.

The final objective of the project was to apply the model developed in objective 4 within an uncertainty estimation framework. Despite the lack of knowledge surrounding the actual impact of NFM interventions, uncertainty estimation has not yet been integrated into modelling studies. In contrast, the widely-applied GLUE uncertainty framework (Beven & Binley, 1992), was used in the final part of this

research (Chapters 5 and 6). The computational efficiency of the extended Dynamic TOPMODEL allowed the use of Monte Carlo simulations, with parameters sampled from likely ranges. The approach allowed outputs to be displayed alongside realistic estimations of their uncertainty.

The successful application of this new modelling framework, in real catchments, led to a number of significant outcomes relevant to the actual implementation of flood risk management schemes.

Previous studies, e.g. (Wilkinson & Quinn, 2010), have relied on static analysis of the storage requirements of a distributed scheme. The channel routing model developed for the Brompton catchment (Chapter 4), which allowed the simultaneous hydraulic modelling of individual features across an entire catchment, showed that the storage retained by a scheme is highly distributed across space and time. Both the Brompton and Cumbrian case studies (Chapters 4, 5 and 6) modelled the behaviour of schemes across a series of storms and demonstrated that effective storage would vary greatly across the sequence of events. Without allowing sufficient drain down time between storms, the ability of a scheme to mitigate later events would be severally impacted.

In static models, e.g. (Quinn et al., 2013), multiple interventions are simulated as a combined volume of storage which is subtracted from the flood peak.. Here, the ability to model individual features at spatially explicit locations revealed that the location of the features was significant in the overall effectiveness of the scheme. Of greatest interest, poorly considered placement of interventions could result in the synchronisation of sub-catchment flood waves. This, in turn, would result in a larger downstream flood wave.

The ability to examine the behaviour of features at specific spatial locations within the channel network also permitted an assessment of their relative effectiveness within the

scheme. For Brompton (Chapter 4), the storage provided by features increased exponentially the further downstream they were placed. This indicates that the model could play an important role in the strategic placement of features within a scheme, with associated cost benefits.

In summary, this project has succeeded in developing a much more strategic, quantifiable and cost-effective way of designing NFM schemes than has previously been possible.

7.1. Further work

As more NFM schemes come online, monitoring of their actual effects and improvement of the evidence base will become increasingly important. For any proposed intervention it is important to understand whether our models reflect real-world behaviour. In the case of leaky dams a monitoring setup could comprise flow and stage meters upstream, downstream, and on the structure. For larger scale interventions such as tree planting, stock reduction and peat restoration, it is far more difficult to establish monitoring procedures. In these cases, plot-scale empirical studies may provide evidence of hydrological impacts. A reliable means of extrapolating these to the catchment scale has yet to be developed and will form an important aspect of future work.

Ground-truthing by walkover survey etc., will allow spatial optimisation of features, both in and out of channel. Identification of overland flow pathway could, for example, be made through direct monitoring or via more qualitative evidence such as wrack marks.

The synchronisation issue could be investigated by an experimental modelling approach, coupled with data from intensive monitoring regimes across multiple subcatchments.

The network width approach to channel routing, adopted in Chapters 3, 5 and 6, applies a single wave speed throughout the channel network and demonstrates good fits to the observed discharges. It cannot predict the impacts of out-of-bank flow and the complex interactions between the floodplain and channel. An improved routing model will be required to predict the location, extent and quantity of overbank flow.. This will allow wider scale assessment of the impacts of NFM measures designed to provide additional roughness to the floodplain.

Infiltration excess overland flow is a potential source of fast runoff but was not considered in our models. Modifications will allow simulation of this process.

This work indicates that application of NFM alone is unlikely to prevent very large-scale flood events. However, the techniques employed may be applied in complementary ways. Hillslope runoff attenuation features could, for example, be used to disconnect overland pathways between sources of pollutants and water bodies.

Optimisation to allow execution in parallel or on arrays of GPUs would greatly improve the run times of these models. This will facilitate an experimental modelling approach whereby the behaviour of the system during millions of storm event sets can be simulated, and robust conclusions drawn.

7.2. Summary

The framework developed here has been applied successfully to evaluate nature-based flood mitigation schemes in a variety of contexts and against a range of events. The

approach has been applied from the scale of small upland catchments to large mixed-use basins and across medium to extreme storms.

Flooding will continue to cause damage, and no scheme or approach will entirely remove the risks it presents. The techniques developed in this work have, however, already contributed towards providing the means to develop integrated management plans that work with natural processes in order to increase flood resilience, both effectively and sustainably.

Further information

Source code and data and the following outputs arising from this work can be found through the links supplied, or by request from the author:

- With the author's help, Chaney et al. (2016) used the implementation of Dynamic TOPMODEL, described in Chapter 3, to supply soil moisture deficits to the HydroBlocks land-surface model within a 610 km² scale catchment in Oklahoma, US. The DOI is doi: 10.1002/hyp.10891
- The UK Environment Agency undertook a review of current approaches to flood modelling, "How to model and map catchment processes when flood risk modelling.". This included a case study detailing the modelling work presented in Chapter 4, which can be found at http://evidence.environment-agency.gov.uk/FCERM/Libraries/FCERM_Project_Documents/SC120015_case_study_2.sflb.ashx;
- The technical report for the Rivers Trust Life IP project, described in Chapter 5 and Chapter 6, is found at http://naturalcourse.co.uk/uploads/2017/04/2016s4667-Rivers-Trust-Life-IP-NFM-Opportunities-Technical-Report-v8.0.pdf;
- Findings from Chapter 4 were presented at an oral session at EGU in Vienna, April 2016: "Natural flood management in context: evaluating and enhancing the impact." This is located at http://presentations.copernicus.org/EGU2016-8831_presentation.ppt.

Appendix 1. Flux calculations in Dynamic TOPMODEL

Note: the Hadamard product, or element-wise, multiplication of vectors and matrices is written as $\boldsymbol{q_1} \circ \boldsymbol{q_2}$. This operation is commutative, distributive and associative. Element-wise division is denoted $\boldsymbol{q_1} \oslash \boldsymbol{q_2}$.

A.1.1. Root and unsaturated zone flux calculations

Actual evapotranspiration out of unsaturated areas, E_a [L]/[T], is calculated using a common formulation $E_a = E_p \frac{s_{rz}}{s_{rz,max}}$ where E_p is the potential evapotranspiration s_{rz} the root zone storage and $s_{rz,max}$ its maximum capacity. This significantly minimises parametric demands (Beven, 2012):

Drainage specific flux q_{uz} ([L]/[T]; mm/hr) into the water table from the unsaturated zone is calculated as:

$$q_{uz} = \frac{s_{uz}}{d.\, t_d} \qquad \text{(Eqn. A.1.1)}$$

where s_{uz} is the unsaturated storage for each group, d the specific storage deficits, and t_d ([T]/[L]) a time delay parameter reflecting the effective permeability of the soil across each unit.

A.1.2. Initialisation of subsurface state

Assuming an initial quasi-steady specific discharge of q_0 from the catchment, recharge to the water table by unsaturated gravity drainage must also equal q_0. Rain recharge will be reduced by any evapotranspiration but can be assumed sufficient to provide the required precipitation excess. Scaling up by the units' areas gives the total drainage flux within each as $\boldsymbol{Q_{uz}} = q_0\, \boldsymbol{A}$.

Equating inputs and outputs across all units:

$$\boldsymbol{Q_{uz} + W^T Q_b = Q_b} \quad \text{(Eqn. A.1.2)}$$

$$\boldsymbol{\Longrightarrow (I - W^T) Q_b = Q_{uz}} \quad \text{(Eqn. A.1.3)}$$

$$\boldsymbol{Q_b = (I - W^T)^{-1} Q_{uz}} \quad \text{(Eqn. A.1.4)}$$

where $\boldsymbol{I}$ is the identity matrix. The inverse to $(\boldsymbol{I - W^T})$, if one exists, and a solution for the initial base flows can, for example, be found with the `solve` method in R. This function makes use of the LAPACK compiled library (see Anderson et al., 1999) and is therefore extremely fast.

Denoting specific downslope discharge from a single unit as q_b, Beven (2012) shows that, using an exponential transmissivity profile, an estimate for the corresponding initial average saturated storage deficits is $\overline{D}_0 = -m.ln(\bar{q}/q_b)$, where m is the exponential recession parameter applied across that unit and $\bar{q} = e^{-\gamma}$, with γ the areal average across the unit of the soil topographic index (Beven, 1986a),. This is given by

$$\gamma = \frac{1}{A}\sum_{i}^{n} A_i ln\left(\frac{a}{T_0 tan(\beta)}\right)) \quad \text{(Eqn. A.1.5)}$$

with A_i the area of the grid cells comprising the unit, A its total area, a the upslope drainage area and T_0 the saturated transmissivity. The corresponding unsaturated zone drainage may be estimated by substituting $\overline{D}_0$ and q_0 and solving for q_{uz}.

A.1.3. Subsurface routing

In the subsurface, mass continuity with storage (expressed as storage deficit, D) as the conserved variable and x ([L]; m) in the downslope direction can be expressed as

$$\frac{\partial D}{\partial t} = \frac{\partial q}{\partial x} - q_{uz} \quad \text{(Eqn. A.1.6)}$$

where q_{uz} ([L]/[T]; m/hr) is specific recharge from the unsaturated zone due to gravity drainage and q the specific subsurface flux in the downslope direction. Li et al. (1975)

suggested that using q rather than D as the dependent variable would be more likely to result in convergence in a numeric scheme to solve for the time-varying quantities. Hence, incorporating the functional dependence of discharge on storage, the kinematic formulation for the downslope flux per unit contour is:

$$\frac{\partial q}{\partial t} = -c\frac{\partial q}{\partial x} + cq_{uz} \qquad \text{(Eqn. A.1.7)}$$

Here $c = \frac{dq}{dD}$ ([L]/[T]; m/hr) is the downslope speed of propagation of a change in subsurface storage and is referred to as the kinematic wave velocity or celerity. With the exponential transmissivity profile adopted by TOPMODEL it can be shown that c is directly proportional to q. Application of the Chain Rule shows that for each unit the downslope flux is related to the storage deficit by the differential equation:

$$\frac{dq}{dt} = \frac{dq}{dD}\frac{dD}{dt} = -\frac{q}{m}\frac{dD}{dt} \qquad \text{(Eqn. A.1.8)}$$

The vector of total downslope output fluxes $\boldsymbol{Q_b}$ from the response units are the specific fluxes multiplied by their plan areas i.e. $\boldsymbol{A} \circ \boldsymbol{q_b}$. Subsurface lateral inputs from upslope areas $\boldsymbol{Q_{in}}$ can be estimated from these flows redistributed by the flux distribution matrix $\boldsymbol{W}$:

$$\boldsymbol{Q_{in}} = \boldsymbol{W}^T\boldsymbol{Q_b} = \boldsymbol{W}^T(\boldsymbol{A} \circ \boldsymbol{q_b}) \qquad \text{(Eqn. A.1.9)}$$

Specific upslope inputs are therefore

$$\boldsymbol{q_{in}} = \boldsymbol{W^T}(\boldsymbol{A} \circ \boldsymbol{q_b}) \oslash \boldsymbol{A} \qquad \text{(Eqn. A.1.10)}$$

Writing the average specific storage deficit at time t across each response unit as the vector $\boldsymbol{D}$ yields the expression:

$$\frac{d\boldsymbol{D}}{dt} = \boldsymbol{q_b} - \boldsymbol{q_{in}} - \boldsymbol{q_{uz}} \qquad \text{(Eqn. A.1.11)}$$

where $\boldsymbol{q_{uz}}$ is the specific recharge from the unsaturated zone, assumed constant over the time step. Substitution gives:

$$\frac{d\boldsymbol{D}}{dt} = \boldsymbol{q_b} - \boldsymbol{W}^T\,(\boldsymbol{A} \circ \boldsymbol{q_b}) \oslash \boldsymbol{A} - \boldsymbol{q_{uz}} \qquad \text{(Eqn. A.1.12)}$$

Substitution for each element of $\boldsymbol{D}$ yields a system of differential equations for the downslope fluxes:

$$\frac{d\boldsymbol{q_b}}{dt} = -\boldsymbol{q_b} \oslash \boldsymbol{m} \circ (\boldsymbol{q_b} - \boldsymbol{W}^T\,(\boldsymbol{A} \circ \boldsymbol{q_b}) \oslash \boldsymbol{A} - \boldsymbol{q_{uz}}) \qquad \text{(Eqn. A.1.13)}$$

where $\boldsymbol{m}$ is a vector comprising the exponential coefficients for the response units.

Supplying the base flow at the previous step as the initial conditions, the system of non-linear ODEs given in (3.7) can be solved using a standard numerical approach to give an estimate for $\boldsymbol{q_b}$ at the end of each time step. The programme employs the `lsoda` algorithm (Livermore Solver for Ordinary Differential Equations, Petzold & Hindmarsh, 1983) accessed via the `deSolve` package (Seibert et al., 2010). It automatically selects the approach most suitable for the system supplied. For "non-stiff" systems it employs an explicit predictor-corrector solution, whereas for "stiff" systems an implicit backwards differentiation formula (BDF) is used. The algorithm is found in ODEPACK (Hindmarsh, 1983) and it, and its FORTRAN source, are available from NetLib http://www.netlib.org

A.1.4. Overland flow routing

If storage deficit predicted by the model falls below zero within any of the response units, excess storage and further input into that unit during the remainder of the time step is routed to a saturated excess store. After subsurface fluxes and storages have been updated, the surface excess of all HRUs is redistributed as overland flow into downslope units. Overland flow entering channel units (usually HRU#1) is routed to the outlet as for redistributed subsurface flow. Updated surface storage remaining on the land HRU is reallocated to the rainfall input of the corresponding units for the next time step, and the store emptied.

Any surface excess is assumed to be distributed evenly across the area of each unit. Given a vector of specific surface excess storages $\boldsymbol{s}$, and assuming a small storage depth so that non-linearity is minimised, surface flows downslope out of the units are approximately:

$$\boldsymbol{q_{surf}} = \boldsymbol{v} \circ \boldsymbol{s} \circ (\boldsymbol{q_b} - \boldsymbol{W^T}\,(\boldsymbol{A} \circ \boldsymbol{q_b}) \oslash \boldsymbol{A} - \boldsymbol{q_{uz}}) \qquad \text{(Eqn. A.1.14)}$$

The elements of $\boldsymbol{v}$ are the fixed overland flow velocities supplied for each HRU. These may vary according to surface roughness and slope and be determined, for example, by supplying a Manning *n* value and average gradient within each unit. Surface flow is now distributed downslope between units in the same proportions as for the subsurface. The vector of specific input flux from upslope units is therefore:

$$\boldsymbol{q_{in}} = \left(\boldsymbol{W}^T\,\left(\boldsymbol{A} \circ \boldsymbol{q_{surf}}\right)\right) \oslash \boldsymbol{A} \qquad \text{(Eqn. A.1.15)}$$

with $\boldsymbol{A}$ and $\boldsymbol{W}$ as previously defined. Combining the previous equations results in a system of linear ordinary differential equations for $\boldsymbol{s}$:

$$\frac{d\boldsymbol{s}}{dt} = \left(\boldsymbol{W}^T\,(\boldsymbol{A} \circ \boldsymbol{v} \circ \boldsymbol{s})\right) \oslash \boldsymbol{A} - \boldsymbol{v} \circ \boldsymbol{s} \qquad \text{(Eqn. A.1.16)}$$

A solution to this system at the end of each time interval can again be obtained with the `ode` method found in the `deSolve` package. It can also be shown that an analytical solution exists that can be solved by the Eigenvalue method (see Dummit, 2012).

A.1.5. Determination of maximum subsurface flow

Storm flow routed from upslope areas that exceeds a downslope unit's subsurface throughput capacity will return to the surface as base flow excess. The programme identifies this situation and the capacity at which base flow excess starts is calculated for each unit at the start of a programme run.

Beven (2012) gives the expression for the discharge Q_b from catchment of area *A*:

$$Q_b = Q_0 e^{-\overline{D}/m} \quad \text{(Eqn. A.1.17)}$$

Where $\overline{D}$ is the average storage deficit and $Q_0 = Ae^{-\gamma}$ with γ as defined in (3.2). Assuming limiting transmissivity is constant within the HRU:

$$\gamma = ln(T_0) - \lambda \quad \text{(Eqn. A.1.18)}$$

where $\lambda = \frac{1}{A}\sum_i^n A_i ln(\frac{a}{tan(\beta)})$

λ is a constant for the response unit. This may therefore be calculated in the pre-processing module and supplied as a run-time parameter. Setting $\overline{D} = 0$, the maximum specific base flow from a unit is seen to be:

$$q_{max} = e^{-\gamma} = \frac{T_0}{e^{\lambda}} \quad \text{(Eqn. A.1.19)}$$

Clearly not all elements within a HRU share the same topography but the above expression provides a constraint on its total downslope flow, and indicates when some areas will start to generate base flow excess overland flow. Larger values of limiting transmissivity indicate a higher potential subsurface flow. Flat or convergent topography or areas far downslope will saturate relatively more frequently, as is observed in the field.

Appendix 2. Hydraulic channel routing scheme

The depth-averaged one-dimensional St Venant equations for open-channel flow in a prismatic channel with an arbitrary profile, expressed in terms of flow area *A*, water level *h* and total discharge *Q* through the area, are (see Henderson, 1966; Cunge et al., 1980; Knight, 2006; Beven, 2012 and many others):

$$\frac{\partial A}{\partial t} + \frac{\partial Q}{\partial x} = r \qquad \text{(Eqn. A.2.1)}$$

$$\frac{\partial Q}{\partial t} + \frac{\partial}{\partial x}\left(\beta \frac{Q^2}{A}\right) + gA\left(\frac{\partial h}{\partial x} + s_f - s_0\right) = 0 \qquad \text{(Eqn. A.2.2)}$$

x is the distance measured in the downstream direction and *r* the lateral recharge per unit length of the channel. Recharge is the sum of specific subsurface base flow q_{bf} and any overland flow q_{of} and is supplied by the hydrological component described in the main text. The total channel input at each time step is distributed between the reaches according to a weighting matrix derived from the surface topography, similar to that used to route base flows between landscape units in Dynamic TOPMODEL. For reach *i* the recharge r_i is then applied uniformly along its length.

The channel bed slope, assumed constant over the reach is s_0, β is a momentum correction coefficient to account for variation of flow velocity across the flow area, which, in the absence of further information, can be taken as unity. Given these assumptions the mean channel velocity is taken as $V = Q/A$. Here s_f is the head loss due to friction against the bed per unit length of downstream flow.

For uniform flow the friction slope can be approximated using the Manning relationship:

$$s_f = \frac{V|V|n^2}{R^{4/3}} \qquad \text{(Eqn. A.2.3)}$$

with n the roughness and R the hydraulic radius calculated from the wetted perimeter and flow area. If gradually-varied and subcritical flow is assumed, the first two terms in Eqn, A.2.2, representing the temporal and advective acceleration, can be neglected, leading to a diffusive wave approximation for open channel flow:

$$\frac{\partial h}{\partial x} + s_f - s_0 = 0 \qquad \text{(Eqn. A.2.4)}$$

Substituting and rearranging gives an expression for the mean flow velocity. Multiplication by the flow area then leads to an analytical expression for the discharge:

$$Q = \frac{AR^{2/3}}{n}\sqrt{s_0 - \frac{\partial h}{\partial x}} \qquad \text{(Eqn. A.2.5)}$$

Given a channel network comprised of M reaches, a numerical scheme is now constructed as follows in order to solve for channel flows at discrete time steps across a simulation.

In order to reduce the problem from a system of partial differential equations in two independent variables x and t to a coupled system of ordinary differential equations (ODEs) the spatial dimension x is discretised. This is known as the Method of Lines (MOL, see Hamdi et al., 2007). Reach i is subdivided into N_i segments, each of length Δx_i. If the flow out of segment j is Q_j, its end point at downstream position $x_j = j\Delta x_i$, then mass continuity is approximated in this segment by

$$\left.\frac{dA}{dt}\right|_{x=x_j} \approx r_i - \frac{\left(Q_j - Q_{j-1}\right)}{\Delta x_i}, j = 1, N_i \qquad \text{(Eqn. A.2.6)}$$

Water levels h_j are calculated at the boundary of all segments using the chosen channel geometry and the flow area at the current time step. For a rectangular channel of width w the water level is simply A/w but any profile may be specified, including

ones where a shallow floodplain is defined. This allows the water surface gradient $\frac{\partial h}{\partial x} - s_0$ to be estimated for the segment. A "downwind" scheme is used so that the effects of afflux behind constrictions and backwater effects at confluences can be propagated upstream, hence:

$$\left.\frac{\partial h}{\partial x}\right|_{x=x_j} \approx \frac{\left(h_{j+1} - h_j\right)}{\Delta x_i} \qquad \text{(Eqn. A.2.7)}$$

The channel is divided into overbank and in-channel components that may take distinct geometries and roughness values. If the flow remains in channel the appropriate values for the channel may be simply substituted to obtain the overall discharges. Where water goes overbank the discharges in and out of channel are calculated separately and added to give the overall flow through the subreach. The overbank area is deemed to be that lying above the floodplain; the area above the channel but above the bankfull depth *D* is allocated to the in-channel flow. In a typical trapezoidal channel this results in the overbank area making a broad-based triangle on each bank with the in-channel component a hexagon. The values for *R* and *A* are calculated in each of the areas and they and the appropriate Manning *n* and the water surface gradient are substituted into and summed.

The input, Q_0, into the first segment must be determined by the upstream inputs, if any, and likewise for the downstream water level. This is accomplished as follows.

Reaches are defined strictly between the entry points of tributaries. The channel network is formalised as a directed graph whose edges correspond to the channel reaches and the vertices to springs, confluences and the catchment outlet. A flow direction, or adjacency, matrix ***F*** is constructed from the graph, describing how flow is routed downstream out of the reaches. Its elements F_{ij} are equal to 1 if reach *j* flows into reach *i*, zero otherwise.

If flows out of all reaches is held in the vector $\boldsymbol{Q_{out}}$ and the upstream inputs (zero for source reaches with no upstream input) by $\boldsymbol{Q_0}$ then mass and momentum conservation is enforced by setting $\boldsymbol{Q_0 = FQ_{out}}$.

In channels with arbitrary profiles mass conservation implies that flow areas, rather than water levels, are additive. That is, if reaches *i* and *j* with final flow areas A_i and A_j converge to form reach *k* then, assuming no other inputs, the flow area at the first segment of reach k is $A_k = A_i + A_j$. For source reaches A_0 will be zero. Assuming quasi-steady flow for the duration of the time step, if $\boldsymbol{A'_0}$ is the vector of flow areas at the start of reaches that have an upstream input, given by the vector $\boldsymbol{A_{out}}$, and $\boldsymbol{F'}$ the adjacency matrix for just those reaches then the upstream flow areas can be estimated as $\boldsymbol{A'_0 = F'^{-1}A_{out}}$.

The corresponding water level will be calculated according to the relationship for the channel profile applied. This allows the water surface gradient calculated to be determined at the end of each reach. At the outlet as there is no downstream reach supplied the water surface gradient is carried through from the previous segment.

The resulting system of $\sum_{i=1}^{M} N_i$ ODEs is now solved to the end of the time step. A variable time step is used internally within the algorithm; convergence is not predicated on the external time step employed. Details of the runoff dynamics could be lost at longer time intervals and a step of 15 minutes is typically used. The Livermore Solver for Ordinary Differential Equations (`lsode`, Petzold, 1993) is utilised to solve the system. It is open-source compiled FORTRAN optimised for both stiff and non-stiff systems. It automatically employs an implicit backwards Euler scheme in periods of non-linearity and a forward (explicit) approach when flows are more stable.

Segment lengths must be chosen that are short enough to determine the flux gradient reasonably accurately but long enough to prevent it being over-estimated and giving rise to numerical instabilities in front of a flood wave. Samuels (1989) suggests a minimum segment length given by the expression $\Delta x_{min} = \frac{0.15D}{s_0}$; 50m has been used in the analysis presented in the main text.

A.2.1. Representation of in-channel features

Given an appropriate stage-discharge relationship for a particular type of runoff attenuation, such as those presented below, the above scheme may be modified to take into account the effect of adding features with the channels.

Features may be sited within at the end of any subreach, index *f*, say, within the network. The value for the output discharge, $Q_f$is replaced by the appropriate value calculated from the stage-discharge relationship for the feature. If the feature vertical extent is below the bankfull level then overbank flow is assumed to bypass the feature and is calculated as before. An additional overflow component is added to the in-channel flow through the feature, calculated as a function of the water level above its top. This is typically a weir-type equation (ISO, 1980):

$$Q_{over} = \frac{2}{3} C_{\mathrm{w}} w_b \sqrt{2g} (h - h_{max})^{3/2} \qquad \text{(Eqn. A.2.8)}$$

where w_b is the dam's width h_{max} along its top side, its maximum height above the channel bed, and C_{w} a weir coefficient, which must be empirically determined. A typical value is 0.68 for a sharp, non-contracted rectangular weir but will differ for other geometries.When the water overtops the feature, additional flow is calculated by its overflow function applied across the top width.

Approximate storage-discharge relationships for typical runoff attenuation features are presented in Appendix 3. These include bunds, large woody debris (LWD), underflow ditch barriers or screens and overflow storage basins.

Appendix 3. Hydraulic characteristics of runoff attenuation features

As previously described, in order to incorporate runoff attenuation features in the routing scheme it is required to specify a stage-discharge relationship appropriate to that structure. For most the downstream water will have some impact on the discharge through the feature. In the routing scheme described in the previous section this is approximated by the level at the start of the time step.

A.3.1. Bunds

A simple feature to add storage is a small earth dam (also known as a bund) placed across the channel or in an overland flow pathway. In the case of a bund placed in a channel with maximum height h_{max} above its bed, with the outlet treated as one or more smooth pipes close to the base each with diameter $d << h_{max}$ the discharge may simply be calculated by consideration of conservation of energy.

The Torricelli equation gives the discharge velocity, $v = \sqrt{2g\Delta h}$ where Δh is the head difference. This is calculated by the difference between upstream and downstream water levels, v the outlet cross sectional average velocity and g the gravitational constant. For smooth outlet pipe(s) of total cross-sectional area a_p the outlet discharge is thus $Q = a_p\sqrt{2g\Delta h}$. For realistic pipes a coefficient in the range 0.5 to 1 could be applied to account for friction loss.

The above assumes that the water immediately behind the feature is effectively stationary. In practice the approach velocity will affect upstream level, as the velocity head will be translated into potential energy. Equating the upstream and downstream heads:

$$h_2 = \frac{v_1^2}{2g} + h_1 \qquad \text{(Eqn. A.3.1)}$$

where v_1 is the approach velocity, h_1 the water level upstream of the dammed, stationary subreach, and h_2 the water level immediately behind the feature. A typical approach velocity of around 1m/s would therefore result in an additional water depth of around 5cm.

For a dam placed across a rectangular channel of width *w* filled to a level *h* the specific storage ([L]³/[L]) immediately upstream is simply *hw*. A more realistic profile would be a symmetrical inverted trapezoidal prism. The channel forms its shortest width *w*, also taken as the width of the base of the dam. The banks to the top of the dam are assumed approximately straight with slope s_b. The specific storage per reach length given a water level *h* at the upstream edge of a dam feature placed within this profile can be shown to be $s = h\left(\frac{h}{s_b} + w\right)$.This allows the dammed water level h for a given specific storage *s* to be calculated as

$$h = \frac{s_b}{2}\left(-w + \sqrt{w^2 + \frac{4s}{s_b}}\right) \qquad \text{(Eqn. A.3.2)}$$

A functional relationship between storage and discharge can now be established.

When the dam is overtopped the weir equation (ISO, 1980) can be used to predict the overflow discharge:

$$Q_{over} = \frac{2}{3} C_{\mathrm{w}} w_b \sqrt{2g} (h - h_{max})^{3/2} \qquad \text{(Eqn. A.3.3)}$$

where w_b is the dam's width, h_{max} along its top side, its maximum height above the channel bed, and C_{w} a weir coefficient, which must be empirically determined. A typical value is 0.68 for a sharp, non-contracted rectangular weir but will differ for other geometries. When the water overtops the feature, flow calculated by this

function is added to the discharge through the outlet pipe(s) to obtain the total discharge through the feature.

In practice an earth or wooden bund would be losing water both through infiltration and seepage through its walls. In this case it may be more realistically modelled as a woody debris dam with tightly-spaced members (see Section A.3.3).

A.3.2. Ditch barriers

Barriers or screens, typically wooden, can be placed across the channel a small distance above the normal water level. These allow unobstructed drainage at for levels below the top of the barrier opening flows but increasingly impede discharge as the water level rises above this. They are hydraulically similar to underflow sluices (gates) such as those employed in irrigation networks or canals, but in a natural flood management scheme are unlikely to be manually operated.

Consider a horizontal barrier whose top is at a height h_{max} above the channel bed with a clearance of the underside of the barrier from the channel bed of a and an upstream water level at a particular time of h_0. As can be seen from the diagram there is a section of supercritical flow immediately downstream of the barrier. After a short distance and hydraulic jump the flow returns to subcriticality and the water level recovers. The level of the critical flow section is h_1 and the subcritical downstream, or tailwater, level is h_2.

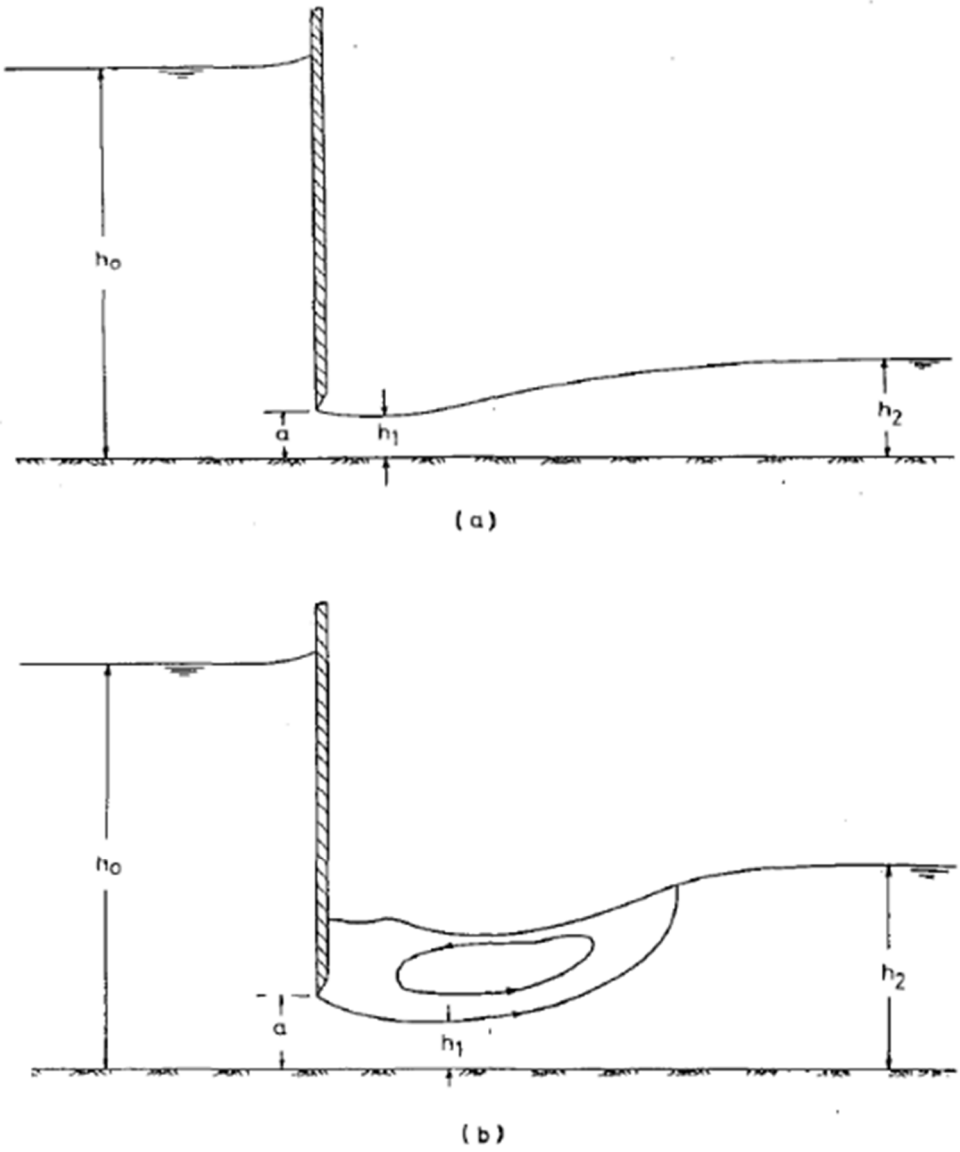

Figure A.3.1. Definition sketch for underflow barrier (Swamee, 1992)

The modes of operation of the feature are (Swamee, 1992):

1. $h_0 < a$: no impediment to flow due to barrier;
2. $h_0 \geq a$: barrier in operation with free discharge;
3. $h_1 \geq a$: barrier in operation with submerged discharge;
4. $h_0 \geq h_{max}$: overflow discharge in addition to modes 2 or 3.

The standard depth-discharge relationship for the operational underflow sluice is (Chow, 1959):

$$Q = C_d w_b a\sqrt{2ga} \qquad \text{(Eqn. A.3.4)}$$

where w_b is the width of the barrier at its base. This can be seen as analogous with the Torrecelli Equation but with the addition of a energy gain/loss factor C_d, termed the Coefficient of Discharge. C_d incorporates upstream velocity head, friction and energy loss through the hydraulic jump. The development of C_d with h_0 and h_2 must be empirically determined.

For the first mode the open-channel routing approach described in the main paper is applied. For the operational barrier with free discharge (mode 2) Swamee (1992) identifies an approximate functional relationship between C_d and h_0 through experimental results due to Henry (1950):

$$C_{d,free}(h_0) = 0.611\left(\frac{h_0 - a}{h_0 + 15a}\right)^{0.072} \qquad \text{(Eqn. A.3.5)}$$

He also derives a condition to determine the existence of free discharge

$$h_0 \geq h_{thresh}(h_2) = 0.81.h_2\left(\frac{h_2}{a}\right)^{0.72} \qquad \text{(Eqn. A.3.6)}$$

He then suggests for submerged discharge (mode 3) the following relationship:

$$C_{d,sub}(h_0, h_2) = \frac{C_{d,free}(h_0)\Delta h^{0.7}}{(0.32.(h_{thresh} - h_0)^{0.7} + \Delta h^{0.7})} \qquad \text{(Eqn. A.3.7)}$$

where $\Delta h = h_0 - h_2$. Overflow when the feature is overtopped is calculated as for a bund.

The incorporation of this type of feature into the channel network for flood mitigation purposes is tested in the main paper. When a feature was incorporated in the routing scheme it was found necessary to define a short transitional region for water levels

just above the barrier. This is to prevent a discontinuity between discharges in modes 1 and 2 or 3 which prevents the scheme from converging. In the transitional zone the discharge is linearly interpolated between its value in mode 1 immediately below the barrier at in mode 2 at the top of the region. This region could be thought of corresponding to the regime where the barrier is just impinging the flow, with orifice flow starting to become apparent.

A.3.3. Large woody Debris (LWD) or "leaky" dams

A barrier comprised of tree trunks, large branches, timber lengths or fallen trees placed across the channel adds a significant resistive component to flow. Unlike the impermeable barriers described in the previous section, where water behind the barrier is treated as being effectively stationary, the velocity through the barrier will be non-negligible and the resistance will be proportional to this velocity. This approximation will become inaccurate with increasing approach velocity and the velocity head attains a similar magnitude to the hydrostatic head. The head loss across the barrier can be estimated by the density and shape of the timber pieces. This structure could be seen as analogous to a trash screen such as those employed to trap debris upstream of structures such as culverts or before the intakes to water treatment works and power plants.

Kirschmer's equation (Kirschmer, 1926) may be used to estimate the proportion of upstream velocity head lost through the structure. Equating total head upstream and downstream of the barrier allows a head loss coefficient, *c*, to be calculated ,such that

$$c = \beta \left(\frac{s}{b}\right)^{4/3} sin(\delta) \qquad \text{(Eqn. A.3.8)}$$

where b is the distance between the bars, s their thickness, δ the angle of inclination to the horizontal and β a coefficient reflecting the flow resistance due to the shape of the

bars making up the dam. Setting δ to reflect a fairly steep angle, e.g. π/3, and using the value β=1.79 given for round bars and openings between one quarter and three quarters the size of the timber gives an approximate range $3< c < 10$.

Equating total head upstream and downstream of the barrier allows the discharge given an upstream velocity head and downstream head to be calculated, giving the required stage-discharge relationship:

$$Q = Av_{down} = A\sqrt{g\Delta h + (1-c)v_{up}^2} \qquad \text{(Eqn. A.3.9)}$$

A.3.4. Brush and rubble weirs

A matrix of brush or loose rubble placed in the channel also provides a resistance to flow that reduces its velocity and potentially adds some upstream storage at high flows. It could be modelled as a reach of very high Manning roughness or as a finely-spaced trash screen.

Alternatively, discharge through the weir could be treated as a steady state with a power law relationship between velocity *v* and water surface slope through the dam:

$$v = fL\left(\frac{dh}{dx}\right)^n \qquad \text{(Eqn. A.3.10)}$$

where *x* is the distance from the upstream side, *h* is the local water level, *f* ($[T]^{-1}$) a frictional resistance factor per unit width of the dam material, assumed constant, and *L* the width through the dam. For smooth laminar flow *n*=1 and for completely turbulent flow *n*=2. At normal levels flow is likely to be partially turbulent so $1 < n < 2$.

Substituting the discharge per unit channel width *q*($[L]^3/[L]$) = *vh*. Eqn. A.3.10 and rearranging to separate variables:

$$\frac{q}{fL} = h\left(\frac{dh}{dx}\right)^n \qquad \text{(Eqn. A.3.11)}$$

$$\left(\frac{q}{fL}\right)^{1/n} dx = \left(h^{1/n}\right) dh \qquad \text{(Eqn. A.3.12)}$$

where h1 and h2 are defined as before. Integration through the dam gives

$$\left(\frac{q}{fL}\right)^{1/n} \int_0^L dx = \int_{h_{up}}^{h_{down}} \left(h^{1/n}\right) dh = \frac{1}{m}(h_2^m - h_1^m) \qquad \text{(Eqn. A.3.13)}$$

with $m = \frac{1}{n} + 1 = \frac{n+1}{n}$. Thus $Q = fL\left(\frac{h_3}{mL}\right)^n$ where $h_3 = (h_1^m - h_2^m)$.

The suitability of such features in mid and lower reaches of a catchment may be called into question. Here they may be subject to significant hydraulic loads during a storm event with the potential for failure and the resulting debris causing damage to structures further downstream.

A.3.5. Culverts and bridges

A culvert is a tunnel to convey a stream through an embankment or underground, for example under a road or railway. Culverts are hydraulically complex due to their distinct flow modes (Chow, 1959; Ackers et al., 2015). Bridges are similar to culverts except that their openings are larger and the longitudinal dimension is typically much smaller relative to the size of the opening. A structure is generally regarded as a bridge if the opening width is > 2m or the ratio of its width with respect to downstream flow versus the height of the openings is < 5 (Ackers et al., 2015).

Culverts may be utilised as “ready-made” online RAFs by placing a screen or gate on one end to restrict its throughput capacity and so retain storm runoff.

One way of modelling such a feature is as an impermeable dam drained by a smooth semi-circular pipe. When the culvert is partially full the cross sectional flow area *A* is calculated as

$$A = r^2 acos(1 - h'/r) - (r - h')\sqrt{2rh' - h'} \qquad \text{(Eqn. A.3.14)}$$

where *r* is the culvert diameter and *h'* the clearance of the water level below the soffit. Discharge can then be estimated either using a linear routing algorithm assuming a fixed celerity discharging through the area, or, if more detailed information of the culvert geometry were known, the Manning equation could be applied to give a mean velocity across the profile. When the culvert is full the pipe-flow derivation given in (A.3.1) may be employed, albeit that in some modes both entrances may be submerged but the barrel itself not completely filled (Chow, 1959).

In the main paper this approach is applied to the tunnel under a railway line. The effect of applying 0.5m and 1m diameter opening is simulated, and the backwater effects cause an extensive area of marginal land and arable pasture to be inundated. In an urban area this may cause problematic flooding and the approach is not recommended in such environments.

A.3.6. Overflow storage basins

Flood flow may be diverted into a storage area close to the channel, either actively by opening a sluice gate or passively by lowering the bank to allow localised overflow into the basin. Likewise, egress from the basin may be controlled by a manually-operated gate or by a channel in the basin side whose base is at the height of the desired level. Reinforcement to prevent scouring in both cases will be important (Wilkinson et al., 2010b; Quinn et al., 2013; SEPA, 2016).

In an NFMS an unsupervised approach is more likely to be considered. This could be modelled by inserting additional reaches within the DRN: one for the section next to the inlet, one for the basin itself, and one in the main channel at the outlet. Excess flow from the first reach, calculated for example by a Weir equation, would be entirely routed into the "basin" reach.

References

Abbott, M. B., Bathurst, J. C., Cunge, J. A., O'connell, P. E., & Rasmussen, J. (1986). An introduction to the European Hydrological System—Systeme Hydrologique Europeen,"SHE", 2: Structure of a physically-based, distributed modelling system. Journal of hydrology, 87(1-2), 61-77.

Ackers, J., Rickard, C. & Gill, D. (eds) (2015). Fluvial Design Guide. Environment Agency, Bristol, UK

Acreman, M., & Holden, J. (2013). How wetlands affect floods. Wetlands, 33(5), 773-786.

Åkesson, A., Worman, A., & Bottacin-Busolin, A. (2015). Hydraulic response in flooded stream networks, Water Resour. Res., 51, 213–240, doi:10.1002/2014WR016279

Anderson. E. and ten others (1999). *LAPACK Users' Guide*. Third Edition. SIAM. Available on-line at http://www.netlib.org/lapack/lug/lapack_lug.html.

Andison, E., Burgess, P., Elliott, M. (2017). Case study 15. Devon Beaver Project and River Otter Beaver Trial. In Environment Agency (2017). Working with natural processes to reduce flood risk. Science report SC150005/S. Bristol: Environment Agency.

Andrews, F. T., Croke, B. F. W., & Jakeman, A. J. (2011). An open software environment for hydrological model assessment and development. Environmental Modelling & Software, 26, 1171-1185. doi:10.1016/j.envsoft.2011.04.006.

Archer, N.A.L., Bonell, M., Coles, N., MacDonald, A.M., Auton, C.A. & Stevenson, R. (2013). Soil characteristics and land cover relationships on soil hydraulic conductivity at a hillslope scale: a view towards local flood management. J. Hydrol. 497: 208–222.

Archer, N.A.L., Bonell, M., Coles, N., MacDonald, A.M., Stevenson, R. & Hallett, P. (2012). The relationship of forest and improved grassland to soil water storage and its implication on Natural Flood Management in the Scottish Borders. In: BHS 11th National Symposium, Hydrology for a Changing World, Dundee, Scotland, 9–11 July (2012). doi: 10.7558/bhs.(2012).ns04.

Barber, N. J., & Quinn, P. F. (2012). Mitigating diffuse water pollution from agriculture using soft-engineered runoff attenuation features. Area, 44(4), 454-462.

Barling, R.D., Moore, I.D. & Grayson, R.B. (1994). A quasi-dynamic wetness index for characterizing the spatial distribution of zones of surface saturation and soil water content. Water Resources Research 30(4): 1029–(1044).

Bashford, K. E., Beven, K. J. & Young, P C, 2002, Observational data and scale dependent parameterisations: explorations using a virtual hydrological reality, Hydrol. Process.,16(2), 293-312.

Baudoin, J. M., Burgun, V., Chanseau, M., Larinier, M., Ovidio, M., Sremski, W. & Voegtle, B. (2014). Assessing the passage of obstacles by fish. Concepts, design and application. France: Onema.

Beedell, J., Morris, J., Hess, T.M. (2011). Mobilising the Contribution of Rural Land Management to Flood Risk Management in Scotland. Report to Scottish Government CR/2010/14.

Bell, V. A., & Moore, R. J. (1998). A grid-based distributed flood forecasting model for use with weather radar data: Part 1. Formulation. Hydrology and Earth System Sciences Discussions, 2(2/3), 265-281.

Bell, V. A., Kay, A. L., Jones, R. G., & Moore, R. J. (2007). Development of a high resolution grid-based river flow model for use with regional climate model output. *Hydrology and Earth System Sciences*, *11*(1), 532-549.

Beven, K. (1979). A sensitivity analysis of the Penman-Monteith actual evapotranspiration estimates. Journal of Hydrology, 44(3-4), 169-190.

Beven, K. (1981). Kinematic subsurface stormflow. Water Resour. Res., 17(5), 1419-1424

Beven, K. (1986). Runoff production and flood frequency in catchments of order *n*: an alternative approach. In V.K. Gupta, I. Rodriguez-Iturbe, E.F. Wood (Eds.), Scale Problems in Hydrology, D. Reidel, Dordrecht, pp. 107–131

Beven, K. (1989). Changing ideas in hydrology—the case of physically-based models. Journal of hydrology, 105(1-2), 157-172.

Beven, K. (1993). Prophecy, reality and uncertainty in distributed hydrological modelling. Adv. Water Resour., 16(1), 41-51.

Beven, K. (1997). TOPMODEL: a critique. Hydrological processes, 11(9) (1069)-(1085).

Beven, K. (2000), On the future of distributed modelling in hydrology. Hydrol. Process., 14: 3183–3184. doi: 10.1002/1099-1085(200011/12)14:16/17<3183::AID-HYP404>3.0.CO;2-K

Beven, K. (2002). Towards a coherent philosophy for modelling the environment. Proceedings of the Royal Society of London. Series A: 458(2026), 2465-2484.

Beven, K. (2006). A manifesto for the equifinality thesis. Journal of hydrology, 320(1), 18-36.

Beven, K. (2009). Environmental Modelling: An Uncertain Future? Routledge, ISBN10:0-415-45759-9

Beven, K. (2010). Preferential flows and travel time distributions : Defining adequate hypothesis tests for hydrological process models, Hydrol. Processes, 24(12), 1537–1547.

Beven, K. (2012). Rainfall-Runoff Modelling: The Primer (2nd Edition), Wiley-Blackwell: Chichester, UK ISBN: 978-0-

Beven, K., Cloke, H., Pappenberger, F, Lamb, R and Hunter, N. (2015). Hyperresolution information and hyperresolution ignorance in modelling the hydrology of the land surface. Science China Earth Sciences, 58 (1): 25-35.

Beven, K. & Binley, A. (1992). The future of distributed models: model calibration and uncertainty prediction. Hydrological Processes, 6 (3), 279-298.

Beven, K. & Binley, A. (2014). GLUE: 20 years on. Hydrological Processes, 28(24), 5897-5918.

Beven, K., Cloke, H.L. (2012). Comment on “Hyperresolution global land surface modeling: Meeting a grand challenge for monitoring Earth's terrestrial water” by Eric, F. Wood et al. Water Resources Research 48: W01801.

Beven, K., Cloke, H., Pappenberger, F., Lamb, R., Hunter, N. (2015). Hyperresolution information and hyperresolution ignorance in modelling the hydrology of the land surface. Science China Earth Sciences 58(1): 25–35.

Beven, K. & Freer, J. (2001a). A Dynamic TOPMODEL. Hydrological Processes, 15(10) 1993-2011.

Beven, K. & Freer, J., (2001b). Equifinality, data assimilation, and uncertainty estimation in mechanistic modelling of complex environmental systems using the GLUE methodology. Journal of Hydrology, 249(1), 11-29.

Beven, K. & Germann, P. (1982). Macropores and water flow in soils. Water Resources research, 18(5), 1311-1325.

Beven, K., & Germann, P. (2013). Macropores and water flow in soils revisited. Water Resources Research, 49(6), 3071-3092.

Beven, K. and Kirkby, M. (1979). A physically based variable contributing area model of basin hydrology. Hydrol. Sci. Bull 24(1): 43-69.

Beven, K., Lamb, R., Quinn, P., Romanowicz, R., and Freer, J. (1995). Topmodel. In V. P. Singh (Ed.) *Computer Models* of *Watershed Hydrology*, Water Resource Publications, CO, 627-668.

Beven, K. J., & Smith, P. J. (2014), Concepts of Information Content and Likelihood in Parameter Calibration for Hydrological Simulation Models, ASCE J. Hydrol. Eng., DOI: 10.1061/(ASCE)HE.1943-5584.0000991.

Beven, K.. Smith, P., Westerberg, I, & Freer, J. (2012), Comment on ‘‘Pursuing the method of multiple working hypotheses for hydrological modeling’’ by M. P. Clark et al., Water Resour. Res., 48, W11801, doi:10.1029/2012WR012282.

Beven, K., & Wood, E. F. (1983). Catchment geomorphology and the dynamics of runoff contributing areas. Journal of Hydrology, 65(1–3), 139-158. doi: http://dx.doi.org/10.1016/0022-1694(83)90214-7

Bilotta, G. S., Brazier, R. E., & Haygarth, P. M. (2007). The impacts of grazing animals on the quality of soils, vegetation, and surface waters in intensively managed grasslands. Advances in agronomy, 94, 237-280.

Bivand, R. (2014). spgrass6: Interface between GRASS 6 and R. R package version 0.8-6. http://CRAN.R-project.org/package=spgrass6

Bivand, R. Keitt, T. & Rowlingson, B. (2014). rgdal: Bindings for the Geospatial Data Abstraction Library. R package version 0.8-16. http://CRAN.R-project.org/package=rgdal

Bivand, R. & Rundel, C. (2014). rgeos: Interface to Geometry Engine - Open Source (GEOS). R package version 0.3-4. http://CRAN.R-project.org/package=rgeos

Black, T.A. & Kelliher, F.M. (1989). Process controlling understory evapotranspiration. Phil. Trans. R. Soc. Lond. B 324: 207–231.

Blanc, J., Wright. G. & Arthur, S. (2012), Natural Flood Management knowledge system: Part 2 – The effect of NFM features on the desynchronising of flood peaks at a catchment scale. CREW report.

Blazkova, S., & Beven, K. (2004). Flood frequency estimation by continuous simulation of subcatchment rainfalls and discharges with the aim of improving dam safety assessment in a large basin in the Czech Republic. Journal of Hydrology, 292(1), 153-172.

Blazkova, S. & Beven, K. (2009). A limits of acceptability approach to model evaluation and uncertainty estimation in flood frequency estimation by continuous simulation : Skalka catchment, Czech Republic. Water Resources Research. 45, W00B16

Boorman, D.B., Hollis, J.M. & Lilly, A. (1995). Hydrology of Soil Types: a hydrologically-based classification of the soils of the United Kingdom. IH Report No. 126. Institute of Hydrology, Wallingford.

Blöschl, G. (1996). Scale and scaling in hydrology. Techn. Univ., Inst. f. Hydraulik, Gewässerkunde u. Wasserwirtschaft.

Bosch, J. M., & Hewlett, J. D. (1982). A review of catchment experiments to determine the effect of vegetation changes on water yield and evapotranspiration. Journal of hydrology, 55(1-4), 3-23.

Bradbrook, K. (2006). JFLOW: a multiscale two-dimensional dynamic flood model. Water and Environment Journal, 20(2), 79-86.

Brater, E. F., & King, H. W. (1976). Handbook of hydraulics for the solution of hydraulic engineering problems, 6th ed. McGraw-Hill. New York.

Broadmeadow, S., Thomas, H., Nisbet, T. (2014). Opportunity Mapping for woodland creation to reduce diffuse pollution and flood risk for England and Wales. Forest Research.

Brown, A.E., Zhang, L., McMahon, T.A., Western, A.W., & Vertessy, R.A. (2005). A review of paired catchment studies for determining changes in water yield resulting from alterations in vegetation. J. Hydrol. 310: 28-61.

Brunner, G. W. (2002). HEC-RAS river analysis system: User's manual. US Army Corps of Engineers, Institute for Water Resources, Hydrologic Engineering Center.

Brunner, P., & Simmons, C. T. (2012). HydroGeoSphere: a fully integrated, physically based hydrological model. *Groundwater*, *50*(2), 170-176.

Buytaert ,W. & Beven, K. (2009). Regionalization as a learning process, Water Resources Research, 45, ISSN: 0043-1397

Buytaert, W., Reusser, D., Krause, S., & Renaud, J.-P. (2008). Why can't we do better than Topmodel? Hydrological Processes, 22, 4175-4179.

Buytaert, W. (2011). `topmodel`: Implementation of the hydrological model TOPMODEL in R. R package version 0.7.2-2. http://CRAN.R-project.org/package=topmodel

Buytaert, W., Reusser, D., Krause, S., & Renaud, J.-P. (2008). Why can't we do better than Topmodel? Hydrological Processes, 22, 4175-4179.

Calder, I. R. (2003) Assessing the water use of short vegetation and forests: Development of the Hydrological Land Use Change model. Water Resources Research, 39 (1319)-1328.

Calder, I. R. & Aylward, B. (2006). Forest and floods: Moving to an evidence-based approach to watershed and integrated flood management. Water International, 31(1), 87-99.

Calder, I. R., Harding, R. J. and Rosier, P. T. W. (1983). An objective assessment of soil-moisture deficit models. Journal of Hydrology, 60(1-4), 329-355.

Calder, I.R., Reid, I., Nisbet, T.R., Green, J.C. (2003). Impact of lowland forests in England on water resources: application of the Hydrological Land Use Change (HYLUC) model. Water Resources Research 39: 1319

Calver, A., & Wood, W. L. (1995). The Institute for Hydrology distributed model. In Singh, V.P. (Ed.) *Computer models of watershed hydrology* (pp. 595-626). Water Resources Publications

Carroll, Z.L., Bird, S.B., Emmett, B.A., Reynolds, B. & Sinclair, F.L. (2004). Can tree shelterbelts on agricultural land reduce flood risk?. Soil use and Management, 20(3), pp.357-359.

Chandler, K.R. & Chappell, N.A. (2008). Influence of individual oak (Quercus robur) trees on saturated hydraulic conductivity. Forest Ecology and Management 256: 1222-1229.

Chappell, N.A. & Lancaster, J.W. (2007). Comparison of methodological uncertainty within permeability measurements. Hydrological Processes 21: 2504-2514.

Chappell, N.A., Jones, T.D., Tych, W. & Krishnaswamy, J. (2017). Role of rainstorm intensity underestimated by data-derived flood models: emerging global evidence from subsurface-dominated watersheds. Environmental Modelling and Software 87: in press. DOI: 10.1016/j.envsoft.(2016).10.009

Chappell, N.A., McKenna, P., Bidin, K., Douglas, I. & Walsh, R.P.D. (1999). Parsimonious modelling of water and suspended-sediment flux from nested-catchments affected by selective tropical forestry. Phil. Trans. Roy. Soc. Lond. B 354: 1831-1846.

Chappell, N.A. & Ternan, J.L. (1992). Flow-path dimensionality and hydrological modelling. Hydrological Processes 6: 327-345.

Chappell, N.A. & Ternan, J.L. (1997). Ring permeametry: design, operation and error analysis. Earth Surface Processes and Landforms 22: 1197-1205.

Chappell, N.A., Tych, W., Chotai, A., Bidin, K. Sinun, W. & Thang, H.C. (2006). BARUMODEL: Combined Data Based Mechanistic models of runoff response in a managed rainforest catchment. Forest Ecology and Management 224: 58-80.

Chaney, N. W., Metcalfe, P., & Wood, E. F. (2016). HydroBlocks: a field-scale resolving land surface model for application over continental extents. *Hydrological Processes*, *30*(20), 3543-3559.

Chow V T. (1959). Open Channel Hydraulics, International Edition, McGraw-Hill, 680 p.

Chow, V.T., Maidment, D.R., Mays, L.W. (1988), Applied Hydrology. McGraw-Hill. ISBN 0-07-010810-2

Clark, M. P. & Kavetski, D. (2010), Ancient numerical daemons of conceptual hydrological modeling: 1. Fidelity and efficiency of time stepping schemes, Water Resour. Res.,46, W10510, doi:10.1029/2009WR008894.

Clark, M.P., Kavetski, D. & Fenicia, F. (2011). Pursuing the method of multiple working hypotheses for hydrological modeling. Water Resour. Res. 47 (9).

Cook, H.L. (1946). The infiltration approach to the calculation of surface runoff. Trans. Am. Geophys. Union 27: 726–743.

Courant, R., Friedrichs, K., & Lewy, H. (1967). On the partial difference equations of mathematical physics. *IBM journal of Research and Development*,*11*(2), 215-234.

Crawford, N. H. & Linsley, R. K. (1966). Digital simulation in hydrology: Stanford Watershed Model IV. Stanford Univ. Dept. of Civil Engineering. 39: p.210.

Cunge, J. A., Holly, F. M., & Verwey, A. (1980). Practical aspects of computational river hydraulics. Pitman, London.

Dadson, S. J., Hall, J. W., Murgatroyd, A., Acreman, M., Bates, P., Beven, K., Heathwaite, L., Holden, J., Holman I.P., Lane, S.N., O'Connell, E., Penning-Rowsell, E., Reynard, N., Sear, D., Thorne, C., & Wilby, R. (2017). A restatement of the natural science evidence concerning catchment-based "natural" flood management in the United Kingdom. UKProc. R. Soc. A 473: 20160706. http://dx.doi.org/10.1098/rspa.(2016).0706

Davies, J. & Beven, K. (2012). Comparison of a multiple interacting pathways model with a classical kinematic wave subsurface flow solution, Hydrol. Sci. J., 57(2), 203–216.

Davies, J., Beven, K., Nyberg, L., & Rodhe, A. (2011). A discrete particle representation of hillslope hydrology: hypothesis testing in reproducing a tracer experiment at Gårdsjön, Sweden. Hydrological Processes, 25(23), 3602-3612.

Davies, J., Beven, K., Rodhe, A., Nyberg, L., & Bishop, K. (2013). Integrated modeling of flow and residence times at the catchment scale with multiple interacting pathways. Water resources research, 49(8), 4738-4750.

Deasy, C., Quinton, J.N., Silgram, M., Stoate, C., Jackson, R., Stevens, C.J. &Bailey, A.P. (2010). Mitigation Options for Phosphorus and Sediment (MOPS): reducing pollution in runoff from arable fields. The Environmentalist 108: 12-17.

Dixon, S. J., Sear, D. A., Odoni, N. A., Sykes, T. & Lane, S. N. (2016). The effects of river restoration on catchment scale flood risk and flood hydrology. Earth Surface Processes and Landforms, 41(7), 997-(1008).

Dowle, M., Short, T., Lianoglou, S., Srinivasan, A. with contributions from R Saporta and E Antonyan (2014). `data.table`: Extension of data.frame. R package version 1.9.4. http://CRAN.R-project.org/package=data.table

Dummit, E (2012). Differential Equations (part 3): Systems of First-Order Differential Equations. Downloaded 16/01/2015 from http://www.math.wisc.edu/~dummit/docs/diffeq_3_systems_of_linear_diffeq.pdf

Dunne, T. & Black, R.D. (1970). Partial area contributions to storm runoff in a small New England watershed. Water Resour. Res. 6: 1296–1311.

Environment Agency (2008). River Eden, Cumbria, Catchment Flood Management Plan. Environment Agency, Bristol, UK.

Environment Agency (2009). Using airborne remote sesnsing for flood risk management with the Environment Agency. Downloaded 12/12/2015 from http://www.ggy.bris.ac.uk/hydrology/bhsmeeting/AlastairDuncan.pdf

Environment Agency (2010). The costs of the summer 2007 floods in England. Report SC070039/R. Environment Agency, Bristol, UK.

Environment Agency (2012). Greater working with natural processes in flood and coastal erosion risk management – a response to Pitt Review Recommendation 27. Environment Agency led working group, Bristol, UK.

Environment Agency (2013), What is the updated Flood Map for Surface Water? (https://www.gov.uk/government/uploads/system/uploads/attachment_data/file/297432/LIT_8988_0bf634.pdf)

Environment Agency (2017). Working with natural processes to reduce flood risk. Science report SC150005/S. Bristol: Environment Agency.

Environment Agency (2016). The costs and impacts of the winter 2013 to 2014 floods. Report SC140025/R1. Environment Agency, Bristol, UK.

European Environment Agency (2011). Disasters in Europe: more frequent and causing more damage. EEA, Copenhagen K, Denmark

Ewen, T. (1995). Contaminant transport component of the catchment modelling system SHETRAN. In Trudgill, S. T. (ed.) Solute modelling in catchment system (pp. 417-441). Wiley, Chichester, UK.. ISBN: 978-0-471-95717-1

Famiglietti, J.S. & Wood, E.F. (1995). Effects of spatial variability and scale on areally averaged evapotranspiration. Water Resources Research 31(3): 699–712.

FAO-UNESCO (1990). Soil map of the world. Revised legend. Soils Bulletin 66. F.A.O., Rome.

Finch, J.W. (2000). Modelling the soil moisture deficits developed under grass and deciduous woodland: the implications for water resources. Journal of the Chartered Institution of Water and Environmental Management 14: 371–376.

Freer, J., Beven, K.J. & Peters, N.E. (2003), Multivariate seasonal period model rejection within the generalised likelihood uncertainty estimation procedure, in *Calibration of Watershed Models*, edited by Q. Duan, H. Gupta, S. Sorooshian, A. N. Rousseau and R. Turcotte, pp. 69-88, AGU, Water Science and Application Series, Washington.

Freer, J., McDonnell, J., Beven, K.J., Brammer, D., Burns, D., Hooper, R.P., Kendal, C. (1997). Topographic controls on subsurface storm flow at the hillslope scale for two hydrologically distinct small catchments. Hydrol. Process.

Freer, J., McMillan, H., McDonnell, J. J., & Beven, K. J. (2004). Constraining dynamic TOPMODEL responses for imprecise water table information using fuzzy rule based performance measures. Journal of Hydrology, 291(3), 254-277.

Freeze, R. & Harlan, R. (1969). "Blueprint for a physically-based, digitally-simulated hydrologic response model." *Journal of Hydrology 9*(3): 237-258.

Furrer, R., Sain, S. (2010). `spam`: A Sparse Matrix R Package with Emphasis on MCMC Methods for Gaussian Markov Random Fields. Journal of Statistical Software, 36(10), 1-25. URL http://www.jstatsoft.org/v36/i10/.

Ghimire, S. (2013). Application of a 2D hydrodynamic model for assessing flood risk from extreme storm events. Climate, 1 (3), 148-162. Available from: https://www.mdpi.com/2225-1154/1/3/148/pdf

Ghimire, S., Wilkinson, M. & Donaldson-Selby, G. (2014). Application of 1D and 2D numerical models for assessing and visualizing effectiveness of natural flood management (NFM) measures. Paper presented at 11th International Conference on Hydroinformatics, New York City, U.S.A.

Gilman, K., & Newson, M. D. (1980). Soil pipes and pipeflow. A hydrological study in upland Wales. Geobooks: Norwich.

Graham, D. N., & Butts, M. B. (2005). Flexible, integrated watershed modelling with MIKE SHE. Watershed models, 849336090, 245-272.

Guha-Sapir, D., Below, R., Hoyois, Ph. (2014). EM-DAT: The CRED/OFDA International Disaster Database – www.emdat.be – Université Catholique de Louvain – Brussels – Belgium.

Gupta, V.H., Kling, H., Yilmaz, K.K. & Martinez, G.F. (2009). Decomposition of the mean squared error and NSE performance criteria: implications for improving hydrological modelling. Journal of Hydrology 377(1-2): 80–91.

Hall, J. W., Le Masurier, J. W., Baker-Langman, E. A., Davis, J. P., & Taylor, C. A. (2004). A decision-support methodology for performance-based asset management. Civil Engineering and Environmental Systems, 21(1), 51-75.

Hailemariam, F. M., Brandimarte, L., & Dottori, F. (2014). Investigating the influence of minor hydraulic structures on modeling flood events in lowland areas. *Hydrological Processes*, 28(4) (1742)-1755.

Hall, J.W., Dawson, R.J., Sayers, P., Rosu, C., Chatterton, J., Deakin, R. (2003). A methodology for national-scale flood risk assessment. Proceedings of the Institution of Civil Engineers - Water & Maritime Engineering 2003, 156(3), 235-247.

Hamdi, S., Schiesser, W., Griffiths, G. (2007). Method of lines. Scholarpedia, 2(7):2859., revision #124335

Hankin, B., Burgess-Gamble, L., Bentley, S., Rose, S. (2016). How to model and map catchment processes when flood risk management planning. Science report SC120015/R1. Environment Agency, Bristol

Hankin, B., Chappell, N., Page, T., Kipling, K., Whitling, M., Burgess-Gamble, L., (2017). Mapping the potential for Working with Natural Processes – user guide Science report SC150005. Environment Agency, Bristol.

Hankin, B., Craigen I., Chappell, N., Metcalfe, P., Page, T. (2016). The Rivers Trust Life-IP Natural Course Project: Strategic Investigation of Natural Flood Management in Cumbria.Technical Report. Available at http://naturalcourse.co.uk/uploads/2017/04/2016s4667-Rivers-Trust-Life-IP-NFM-Opportunities-Technical-Report-v8.0.pdf. Rivers Trust, Callington, Cornwall, UK.

Hankin, B., Lamb, R., Craigen, I., Page, T., Chappell, N., Metcalfe, P. (2017). A whole catchment approach to improve flood resilience in the Eden: https://consult.defra.gov.uk/water-and-flood-risk-management/flood-risk-management-modelling-competition/results/jba_defra_winning_entry_full_report.pdf.

Hankin, B., Metcalfe, P., Johnson, D., Chappell, N., Page, T., Craigen, I., Lamb, R., Beven, K. (2017). Strategies for Testing the Impact of Natural Flood Risk Management Measures. In Hromadka, T. & Rao, P. (eds). Flood Risk Management. InTech, Czech Republic. ISBN 978-953-51-5526-3.

Hannaford, J., and T. J. Marsh (2007), High flow and flood trends in a network of undisturbed catchments in the UK, Int. J. Climatol., 28(10), 1325–1338

Hargreaves, G. H., & Samani, Z. A. (1982). Estimating potential evapotranspiration. *Journal of the Irrigation and Drainage Division*, *108*(3), 225-230.

Heathwaite, A. L., Quinn, P. F., & Hewett, C. J. M. (2005). Modelling and managing critical source areas of diffuse pollution from agricultural land using flow connectivity simulation. *Journal of Hydrology*, *304*(1), 446-461.

Heber Green, W., & Ampt, G. (1911). Studies on Soil Phyics. *The Journal of Agricultural Science, 4*(1), 1-24.

Henderson, F. M. (1966). Open channel flow. MacMillan, New York.

Henry, H. R. (1950). Discussion of Diffusion of submerged jets, Transaction. In ASCE (Vol. 115, pp. 687-694).

Herbst, M., Rosier, P.T.W., McNeil, D.D., Harding, R.J., Gowing, D.J. (2008). Seasonal variability of interception evaporation from the canopy of a mixed deciduous forest. Agric. For. Meteorol. 148: (1655)–1667.

Hester, N., Rose, S. & Worrall P.(2016). Holnicote demonstration project – Somerset. In Hankin, B., Burgess-Gamble, L., Bentley, S., Rose, S. (Eds.). How to model and map catchment processes when flood risk management planning. Science report SC120015/R1, Environment Agency, Bristol, UK.

Hijmans, R (2014). `raster`: Geographic data analysis and modeling. R package version 2.2-31. http://CRAN.R-project.org/package=raster

Hill, C. (2015). Flood Modeller Pro.

Hindmarsh, A. C. (1983) `ODEPACK`, A Systematized Collection of ODE Solvers. In Stepleman, R.W. et al.(Eds) *Scientific Computing*, North-Holland, Amsterdam. pp.55–64.

Hirabayashi, Y., Mahendran, R., Koirala, S., Konoshima, L., Yamazaki, D., Watanabe, S., Kim, H. & Kanae, S. (2013). Global flood risk under climate change. Nature Climate Change, 3(9), 816-821.

Holden, J., Burt, T.P., Evans, M.G. & Horton, M. (2006). Impact of land drainage on peatland hydrology. J. Environ. Qual. 35: 1764 – 1778.

Holden, J., Kirkby, M.J., Lane, S.N., Milledge, D.G., Brookes, C.J., Holden, V., & McDonald, A.T. (2008). Overland flow velocity and roughness properties in peatlands. Water Resources Research 44: DOI: 10.1029/2007wr006052

Holden, J., Wallage, Z. E., Lane, S. N., & McDonald, A. T. (2011). Water table dynamics in undisturbed, drained and restored blanket peat. Journal of Hydrology, 402(1), 103-114.

Horton, R.E. (1933). The role of infiltration in the hydrologic cycle. Transactions, American Geophysical Union 14: 446–460.

Hunter, N.M., Bates, P.D., Horritt, M.S. and Wilson, M.D. (2007). Simple spatially-distributed models for predicting flood inundation: a review. Geomorphology, 90(3), pp.208-225.

Iacob, O., Rowan, J. S., Brown, I. & Ellis, C. (2014). Evaluating wider benefits of natural flood management strategies: an ecosystem-based adaptation perspective. Hydrology Research, 45(6), 774-787.

Institute of Hydrology (2009). Flood Estimation Handbook, Institute of Hydrology, Wallingford, UK.

IPCC (2014). Climate Change 2014: Synthesis Report. Contribution of Working Groups I, II and III to the Fifth Assessment Report of the Intergovernmental Panel on Climate Change [Core Writing Team, R.K. Pachauri and L.A. Meyer (eds.)]. IPCC, Geneva, Switzerland, 151 pp.

ISO (1980).International Organization of Standards.ISO 1438/1-1980(E).Water flow measurement in open channels using weirs and venturi flumes - Part 1: Thin plate weirs.(1980).Available from Global Engineering Documents at http://global.ihs.comF

Jackson, B. M., Wheater, H. S., McIntyre, N. R., Chell, J., Francis, O. J., Frogbrook & Solloway, I. (2008). The impact of upland land management on flooding: insights from a multiscale experimental and modelling programme. Journal of Flood Risk Management, 1(2), 71-80.

Jakeman, A. J., & Hornberger, G. M. (1993). How much complexity is warranted in a rainfall-runoff model?. Water resources research, 29(8), 2637-2650.

Jakeman, A. J., & Letcher, R. A. (2001). Integrated assessment and information systems for catchment management. In *Proceedings of the International Congress on Modelling and Simulation* (Vol. 1, pp. 31-42).

Jakeman, A. J. & Hornberger, G. M. (1993). How much complexity is warranted in a rainfall-runoff model?, Water Resour. Res., *29*(8), 2637–2649, DOI:10.1029/93WR00877.

Janes, V. J., Grabowski, R. C., Mant, J., Allen, D., Morse, J. L. & Haynes, H. (2016). The Impacts of Natural Flood Management Approaches on In-Channel Sediment Quality. River Research and Applications.

Jarvis, R.A., Bendelow, V.C., Bradley, R.I., Carroll, D.M., Furness, R.R., Kilgour, I.N.L. & King, S.J. (1984). Soils and their Use in Northern England. Soil Survey of England and Wales Bulletin No 10, Harpenden.

JBA Trust (2016). Working with Natural Processes: A catalogue of nature-based flood risk management projects in the UK http://naturalprocesses.jbahosting.com/

Jencso, K. G., McGlynn, B. L., Gooseff, M. N., Wondzell, S. M., Bencala, K. E. & Marshall, L. A. (2009). Hydrologic connectivity between landscapes and streams: Transferring reach-and plot-scale understanding to the catchment scale. Water Resour. Res., 45(4): W04428, DOI: 10.1029/2008WR007225

Jones, J. (2010). Soil piping and catchment response. Hydrological processes, 24(12), 1548-1566.

Jones, O. (1917). The Effect on Orifice and Weir Flow of Slight Roundings of the Upstream Edge. The Cornell Civil Engineer, 26 (2)

Jones, T.D., Chappell, N.A. & Tych, W. (2014). First dynamic model of dissolved organic carbon derived directly from high frequency observations through contiguous storms. Environmental Science and Technology 48: 13289-13297.

Keef, C., Tawn, J.A. & Lamb, R. (2013). Estimating the probability of widespread flood events. Environmetrics, vol 24, no. 1, pp. 13-21., 10.1002/env.2190

Keitt, T. H., Bivand, R., Pebesma, E. & Rowlingson, B. (2011). `rgdal`: bindings for the Geospatial Data Abstraction Library. R package version 0.7-1, URL http://CRAN. R-project. org/package= rgdal.

Kirby, C., Newson, M. & Gilman, K. (1991). Plynlimon research: The first two decades. IH Report No.109. Wallingford, Institute of Hydrology.

Kirkby, M. (1976). Hydrograph modelling strategies. In: Peel, R., Chisholm, M., Haggett, P. (Eds.), Processes in Physical and Human Geography. Academic Press, London, pp. 69-90.

Kirkby, M. J. (1997). TOPMODEL: A personal view. Hydrological processes, 11(9), 1087-1097.

Kirschmer, O. (1926). Untersuchungen über den Gefällsverlust an Rechen, vol. 1. Mitteilungen des hydraulischen Instituts der TH München, Munich, Germany.

Kjeldsen, T. R., Stewart, E. J., Packman, J. C., Folwell, S. & Bayliss, A. C. (2005). Revitalisation of the FSR/FEH Rainfall-Runoff Method. Defra R&D Technical Report FD1913/T.R.

Knight, D. (2005). River flood hydraulics: validation issues in one-dimensional flood routing models. In Knight, D., & Shamseldin, A. (Eds.). *River basin modelling for flood risk mitigation*. CRC Press.

Kral, F.; Fry, M.; Dixon, H. (2015). Integrated Hydrological Units of the United Kingdom: Groups. NERC Environmental Information Data Centre. https://doi.org/10.5285/f1cd5e33-2633-4304-bbc2-b8d34711d902

Kundzewicz, Z. W., Pińskwar, I., & Brakenridge, G. R. (2013). Large floods in Europe, 1985–2009. Hydrological Sciences Journal, 58(1), 1-7.

Lamb, R. & Beven, K. (1997). Using interactive recession curve analysis to specify a general catchment storage model. Hydrology and Earth System Sciences Discussions, 1(1), 101-113.

Lamb, R., Crossley, A. & Waller, S. (2009). A fast 2D floodplain inundation model. Proceedings of the Institution of Civil Engineers: Water Management, Volume 162.

Lamb, R., Keef, C., Tawn, J., Laeger, S., Meadowcroft, I., Surendran, S., Dunning, P. & Batstone, C. (2010). A new method to assess the risk of local and widespread flooding on rivers and coasts, Journal of Flood Risk Management. 3, 4, p. 323-336 14 p, DOI: 10.1111/j.1753-318X.(2010).0(1081).x

Lane, S. N. (2017). Natural flood management. Wiley Interdisciplinary Reviews: Water, 4(3).

Lane, S. N., Brookes, C. J., Kirkby, M. J., & Holden, J. (2004). A network-index-based version of TOPMODEL for use with high-resolution digital topographic data. Hydrological Processes, 18(1), 191-201.

Lane, S. N., Odoni, N., Landström, C., Whatmore, S. J., Ward, N., & Bradley, S. (2011). Doing flood risk science differently: an experiment in radical scientific method. Transactions of the Institute of British Geographers, 36(1), 15-36.

Lane, S., & Milledge, D. (2013). Impacts of upland open drains upon runoff generation: a numerical assessment of catchment-scale impacts. Hydrological Processes 27(12): 1701-1726.

Lane, S., Reaney, S. & Heathwaite, A. (2009). Representation of landscape hydrological connectivity using a topographically driven surface flow index. Water Resources Research, 45(8).

Lavers, T. & Charlesworth, S. (2016). Natural Flood Risk Management and its Role in Working with Natural Processes. In Charlesworth, S. and Booth, C. (eds.). Sustainable Surface Water Management: A Handbook for SU.D.S., p156-172. John Wiley and Sons.

Lehner, B., Verdin, K., & Jarvis, A. (2008). New global hydrography derived from spaceborne elevation data. Eos, Transactions American Geophysical Union, 89(10), 93-94.

Li, R.M., Simons, D.B., Stevens, M.A., 1975. Nonlinear kinematic wave approximation for water routing. Water Resour. Res. 11 (2), 245-252.

Liu, Y, Freer, J., Beven, K.J. & Matgen, P (2009), Towards a limits of acceptability approach to the calibration of hydrological models: extending observation error, J. Hydrol., 367:93-103, doi:10.1016/j.jhydrol.2009.01.016.

Linsley, R. K. (1943). A simple procedure for the day-to-day forecasting of runoff from snow-melt. Eos, Transactions American Geophysical Union, 24(3), 62-67.

Maidment, D.R. (1993). Handbook of hydrology. McGraw-Hill: New York, U.S.A.

Marc, V., & Robinson, M. (2007). The long-term water balance (1972–2004) of upland forestry and grassland at Plynlimon, mid-Wales. Hydrology and Earth System Sciences, 11(1), 44-60.

Marsh, T.J., Kirby, C., Muchan, K., Barker, L., Henderson, E. & Hannaford, J. (2016). The winter floods of 2015/2016 in the UK - a review. Centre for Ecology & Hydrology, Wallingford, UK

Marshall, M. R., Ballard, C. E., Frogbrook, Z. L., Solloway, I., McIntyre, N., Reynolds, B., & Wheater, H. S. (2014). The impact of rural land management changes on soil hydraulic properties and runoff processes: results from experimental plots in upland UK. Hydrological Processes, 28(4), 2617-2629.

McDonnell, J. J., Freer, J., Hooper, R., Kendall, C., Burns, D., Beven, K., & Peters, J. (1996). New method developed for studying flow on hillslopes. EOS, Transactions American Geophysical Union, 77(47), 465-472.

McDonnell, J J. & Beven, K J (2014), Debates—The future of hydrological sciences: A (common) path forward? A call to action aimed at understanding velocities, celerities, and residence time distributions of the headwater hydrograph, Water Resour. Res., 50, doi:10.1002/2013WR015141.

McDonnell, J. J., Sivapalan, M., Vaché, K., Dunn, S., Grant, G., Haggerty, R., ... & Weiler, M. (2007). Moving beyond heterogeneity and process complexity: A new vision for watershed hydrology. Water Resour. Res., 43, W07301, doi:10.1029/2006WR005467.

McGuire, K. J., & McDonnell, J. J. (2006), A review and evaluation of catchment transit time modeling, J. Hydrol., 330, 543–563, doi:10.1026/j.hydrol.2006.04.020.

McGuire, K. J., & McDonnell, J. J. (2010). Hydrological connectivity of hillslopes and streams: Characteristic time scales and nonlinearities. Water Resources Research, 46(10): W10543 DOI: 10.1029/2010WR009341

McLean, L., Beevers, L., Pender, G., Haynes, H., & Wilkinson, M. (2013). Variables for Measuring Multiple Benefits and Ecosystem Services. Infrastructure and Environment Scotland 1 st Postgraduate Conference.

McNeil, D. D. (1997). Direct measurement of evaporation from grassland at Plynlimon. Hydrology and Earth System Sciences Discussions, 1(3), 447-452

Medeiros, S.C., Hagen, S.C., & Weishampel, J.F. (2012), Comparison of floodplain surface roughness parameters derived from land cover data and field measurements. Journal of Hydrology 452–453 (2012) 139–149

Mehrotra, R., Li, J., Westra, S., Sharma, A. (2015). A programming tool to generate multi-site daily rainfall using a two-stage semi parametric model. Environ. Model. Softw. 63, 230e239.

Met Office, (2006): UK Hourly Rainfall Data, Part of the Met Office Integrated Data Archive System (MIDAS). NCAS British Atmospheric Data Centre

Metcalfe P. (2016). Case study 2. Brompton runoff attenuation modelling. In Hankin, B., Burgess-Gamble, L., Bentley, S., Rose, S. (Eds.). How to model and map catchment processes when flood risk management planning. Science report SC120015/R1, Environment Agency, Bristol, UK.. Available at http://evidence.environment-agency.gov.uk/FCERM/Libraries/FCERM_Project_Documents/SC120015_case_study_2.sflb.ashx.

Metcalfe, P., Beven, K. & Freer, J. (2015). Dynamic TOPMODEL: a new implementation in R and its sensitivity to time and space steps. Environmental Modelling and Software, 72, 155-172.

Metcalfe, P., Beven, K. & Freer, J. (2016). `dynatopmodel`: Implementation of the Dynamic TOPMODEL Hydrological Model. R package version 1.1.

Metcalfe, P., Beven, K., Hankin, B. And Lamb, R. (2016). Natural Flood Management in context: evaluating and enhancing the impact. EGU General Assembly Conference Abstracts 2016, abstract 8831.

Metcalfe, P., Beven, K., Hankin, B. & Lamb, R. (2017). A modelling framework for evaluation of the hydrological impacts of nature-based approaches to flood risk management, with application to in-channel interventions across a 29km² scale catchment in the United Kingdom. Hydrological Processes. DOI 10.1002/hyp.11140

Monteith, J. L. (1965). Evaporation and environment. In *Symp. Soc. Exp. Biol*(Vol. 19, No. 205-23, p. 4).

Moore, R. J. (2007). The PDM rainfall-runoff model. Hydrology and Earth System Sciences Discussions, 11(1), 483-499.

Moore, R. J., & Clarke, R. T. (1981). A distribution function approach to rainfall runoff modeling. Water Resources Research, 17(5), 1367-1382.

Moors for the Future Partnership (2005). Peak District Moorland Gully Blocking in Deep Peat. Moors for the Future Research Note No 2

Morton, D., Rowland, C., Wood, C., Meek, L., Marston, C., Smith, G., Wadsworth, R. & Simpson, I. (2011). Final Report for LCM2007-the new UK land cover map. Countryside Survey Technical Report No 11/07.

Mosonyi, E. (1966). Wassrekraftwerke, Band, I., Niederdruckanlagen. Düsseldorf.

Murilloa, J., Pallarés, M. R., & Andrés-Urrutia, A. (2008). A Mathematical Model for Numerical Simulation of Shallow Water Flow: Description and Practical Application of GUAD| 2D.

Nash, J.E. & Sutcliffe, J.V. (1970). River flow forecasting through conceptual models part I - A discussion of principles. Journal of hydrology, 10(3), pp.282-290.

National Trust (2015). From source to sea: natural flood management – the Holnicote experience. Final Report to Defra.

Neal, C., Reynolds, B., Kirchner, J.W., Rowland, P., Norris, D., Sleep, D., Lawlor, A., Woods, C., Thacker, S., Guyatt, H. & Vincent, C. (2013). High-frequency precipitation and stream water quality time series from Plynlimon, Wales: an openly accessible data resource spanning the periodic table. Hydrological Processes, 27(17), 2531-2539.

Newson, A. J. (1976a). Some aspects of the rainfall of Plynlimon, mid-Wales. Report No. 30. Wallingford: Institute of Hydrology.

Newson, M. D. (1976b). The physiography, deposits and vegetation of the Plynlimon catchments.(A synthesis of published work and initial findings).Report No. 34. Wallingford: Institute of Hydrology.

Newson, M. D., & Gilman, K. (Eds.). (1991). Plynlimon research: the first two decades (p. 188). Wallingford: Institute of Hydrology.

Nicholson, A. R., Wilkinson, M. E., O'Donnell, G. M., & Quinn, P. F. (2012). Runoff attenuation features: a sustainable flood mitigation strategy in the Belford catchment, UK Area, 44(4), 463-469.

Nicholson, A.R. (2013) Quantifying and simulating the impact of flood mitigation features in a small rural catchment. PhD thesis, Newcastle University, UK

Nisbet, T.R., Marrington, S.. Thomas, H., Broadmeadow, S. & Valatin, G. (2011). Slowing the flow at Pickering. Final Report to Defra, 28pp.

Nisbet, T. & Page, T. (2016). Case study 16. Pontbren catchment land use change study. In Hankin, B., Burgess-Gamble, L., Bentley, S., Rose, S. (Eds.). How to model and map catchment processes when flood risk management planning. Science report SC120015/R1, Environment Agency, Bristol, UK.. Available at http://evidence.environment-agency.gov.uk/FCERM/Libraries/FCERM_Project_Documents/SC120015_case_study_16.sflb.ashx.

Nisbet, T., Silgram, M., Shah, N., Morrow, K. & Broadmeadow, S. (2011). Woodland for water: woodland measures for meeting WFD objectives. Forest Research Monograph, 4, Forest Research, Surrey, 156 pp.

Nisbet, T.R. & Thomas, H. (2008). Restoring floodplain woodland for flood alleviation. Final report for the Department of environment, food and rural affairs (Defra), Project SLD2316. Defra, London.

Ockenden, M.C. & Chappell, N.A. (2011). Identification of the dominant runoff pathways from the data-based mechanistic modelling of nested catchments in temperate, UK Journal of Hydrology 402: 71-79.

O'Connell, P. E., Ewen, J., O'Donnell, G., & Quinn, P. , 2007. Is there a link between agricultural land-use management and flooding?. *Hydrology and Earth System Sciences*, *11*(1), 96-107.

Odoni, N.A. & Lane, S.N. (2010). Assessment of the impact of upstream land management measures on flood flows in Pickering using OVERFLOW. Contract report to Forest Research for the Slowing the Flow at Pickering Project. Durham University, Durham.

Packman, J.C. Quinn, P.F., Hollis, J., O'Connell, P.E. (2004). Review of impacts of rural land use and management on flood generation Short-term improvement to the FEH rainfall-runoff model: Technical background. R&D Project Record FD2114/PR3. (2004)

Page, T., Beven, K. J., Freer, J., & Neal, C. (2007). Modelling the chloride signal at Plynlimon, Wales, using a modified dynamic TOPMODEL incorporating conservative chemical mixing (with uncertainty). Hydrological Processes, 21(3), 292-307.

Palmer, R. C., & Smith, R. P. (2013). Soil structural degradation in SW England and its impact on surface-water runoff generation. Soil Use and Management, 29(4), 567-575.

Pattison, I., Lane, S.N., Hardy, R.J., Reaney, S.M. (2014). The role of tributary relative timing and sequencing in controlling large floods. Water Resources Research 50(7): 5444-5458.

Penning-Rowsell, E., Johnson, C., Tunstall, S., Tapsell, S., Morris, J., Chatterton, J., & Green, C. (2005). The benefits of flood and coastal risk management: a manual of assessment techniques Middlesex University Press.

PERC UK Flooding after Storm Desmond. (2015). http://www.jbatrust.org/wp-content/uploads/2016/08/flooding-after-storm-desmond-PUBLISHED-24-August-(2016).pdf

Peters, N. E., J. Freer, and K. Beven (2003), Modelling hydrologic responses in a small forested catchment (Panola Mountain, Georgia, USA): a comparison of the original and a new Dynamic TOPMODEL, Hydrological Processes, 17(2), 345-362.

Petzold, L. (1983) Automatic Selection of Methods for Solving Stiff and Nonstiff Systems of Ordinary Differential Equations. *Siam J. Sci. Stat. Comput.* 4, 136–148.

Philip, J. R. (1957). The theory of infiltration: 1. The infiltration equation and its solution. Soil science, 83(5), 345-358.

Pitt, M. (2008), The Pitt Review. Learning lessons from the 2007 floods. . London: Cabinet Office.

Priestley, C. H. B., & Taylor, R. J. (1972). On the assessment of surface heat flux and evaporation using large-scale parameters. *Monthly weather review*, *100*(2), 81-92.

PROFILE DTM [DXF geospatial data], Scale 1:10000, Tiles: sn89sw,sn89se,sn88sw,sn88nw,sn88ne,sn88se,sn78ne,sn78se,sn79se, Updated: November 2009, Ordnance Survey (GB), Using: EDINA Digimap Ordnance Survey Service, <http://edina.ac.uk/digimap>, Downloaded: Thu Jul 04 17:24:10 GMT 2013

Puttock, A., Graham, H. A., Cunliffe, A. M., Elliott, M., & Brazier, R. E. (2017). Eurasian beaver activity increases water storage, attenuates flow and mitigates diffuse pollution from intensively-managed grasslands. Science of the Total Environment, 576, 430-443.

Quinn, P., Beven, K., Chevallier, P., & Planchon, O. (1991). The prediction of hillslope flow paths for distributed hydrological modelling using digital terrain models. Hydrological processes, 5(1), 59-79.

Quinn, P., O'Donnell, G., Nicholson, A., Wilkinson, M., Owen, G., Jonczyk, J., Barber, N., Hardwick, M., Davies, G. (2013). Potential use of Runoff Attenuation Features in small rural catchments for flood mitigation. England: Newcastle University, Environment Agency, Royal Haskoning, D.H.V.

Ramsbottom, D., Sayers, P., & Panzeri, M. (2012). Climate change risk assessment for the floods and coastal erosion sector. Defra Project Code GA0204. Report to Defra, London, UK

R Core Team (2013). R: A language and environment for statistical computing. R Foundation for Statistical Computing, Vienna, Austria. ISBN 3-900051-07-0, URL http://www.R-project.org/.

Reaney, S. M., Bracken, L. J., & Kirkby, M. J. (2007). Use of the connectivity of runoff model (CRUM) to investigate the influence of storm characteristics on runoff generation and connectivity in semi-arid areas. *Hydrological Processes*,*21*(7), 894-906.

Refsgaard, J.C. & Storm B., (1995). MIKE SHE. In Singh, V. (Ed.). *Computer Models of Watershed Hydrology* (pp. 809-846). Water Resources Publications, Colorado.

Reynolds, E.R.C. & Henderson, C.S. (1967). Rainfall Interception by beech, larch and Norway Spruce. Forestry 40: 165-184.

Richards, L. A. (1931). Capillary conduction of liquids in porous media, Physics, 1, 318–333, .

RICS (2016). RICS/RAU Rural Land Market Survey. Available online at http://www.rics.org/uk/knowledge/market-analysis/ricsrau-rural-land-market-survey-h2-2013/

Rinaldo, A., Beven, K. J., Bertuzzo, E., Nicotina, L., Davies, J., Fiori, A. & Botter, G. (2011). Catchment travel time distributions and water flow in soils. Water resources research, 47(7).

Roberts, J.M. & Rosier, P.T.W. (1994). Comparative estimates of transpiration of ash and beech forests at a chalk site in southern Britain. J. Hydrol. 162: 229-245.

Roberts, W.M., Gonzalez-Jimenez, J.L., Doody, D.G., Jordan, P. and Daly, K. (2017) Assessing the risk of phosphorus transfer to high ecological status rivers: Integration of nutrient management with soil geochemical and hydrological conditions. Science of The Total Environment, 589. 25 – 35

Rutter, A. J., Kershaw, K. A., Robins, P. C., & Morton, A. J. (1972). A predictive model of rainfall interception in forests, 1. Derivation of the model from observations in a plantation of Corsican pine. *Agricultural Meteorology*, *9*, 367-384.

Ryan, J. A., & Ulrich, J. M. (2008). `xts`: Extensible Time Series. R package version 0.0-5, URL http://CRAN. R-project. org/package= xts.

Rychnovská, M. (1976). Transpiration in wet meadows and some other types of grassland. Folia Geobotanica & Phytotaxonomica 11: 427-432.

Samuels, P.G. (1989). Backwater lengths in rivers. Proceedings -- Institution of Civil Engineers, Part 2, Research and Theory, 87, 571-582.

Saulnier, G. M., Beven, K., & Obled, C. (1997). Including spatially variable effective soil depths in TOPMODEL. Journal of hydrology, 202(1), 158-172.

Scottish Environment Protection Agency (SEPA) (2012). Natural Flood Management Position Statement: the role of SEPA in natural flood management. Available online at:http://www.sepa.org.uk/flooding.aspx.

Scottish Environment Protection Agency (2016). The Natural Flood Management Handbook. Available at: http://www.sepa.org.uk/media/163560/sepa-natural-flood-management-handbook1.pdf

Shaw, E. M., Beven, K. J., Chappell, N. A., & Lamb, R. (2011). *Hydrology in practice*. CRC Press.

Singh, V. P. (1995). *Computer models of watershed hydrology*. Water Resources Publications.

Sivapalan, M., Beven, K., Wood, E.F. (1987). On hydrologic similarity 2. A Scaled model of storm runoff production. Water Resources Research 23(12): 2266–2278.

Skublics, D., & Rutschmann, P. (2015). Progress in natural flood retention at the Bavarian Danube. Natural Hazards, 75, 51.

Soetaert, K., Petzoldt, T & Woodrow Setzer, R. (2010). Solving Differential Equations in R: Package `deSolve` Journal of Statistical Software, 33(9), 1--25. URL http://www.jstatsoft.org/v33/i09/.

Soil Survey of England and Wales, (1983). Soils of England and Wales, Sheet 1: Northern England.

Stewart, L., Vesuviano, G., Morris, D. & Prosdocimi, I. (2014). The new FEH rainfall depth-duration-frequency model: results, comparisons and implications.Environment Agency, Bristol, UK.

Swamee, P. K. (1992). Sluice-gate discharge equations. Journal of Irrigation and Drainage Engineering, 118(1), 56-60.

Syme W.J. (2001). TUFLOW – Two & one-dimensional Unsteady FLOW Software for Rivers, Estuaries and Coastal Waters, IEAust Water Panel Workshop on 2D Models, Sydney, NSW, 2001.

Tarboton, DG, 1997, A new method for the determination of flow directions and upslope areas in grid digital elevation models, Water Resources Research, 33(2): 309-319 DOI: 10.1029/96WR03137

Therrien, R., McLaren, R. G., Sudicky, E. A., & Panday, S. M. (2010). HydroGeoSphere: A three-dimensional numerical model describing fully-integrated subsurface and surface flow and solute transport. Groundwater Simulations Group, University of Waterloo, Waterloo, ON.

Thomas, H. & Nisbet, T. (2007). An assessment of the impact of floodplain woodland on flood flows. Water and Environment Journal 21(2): 114-126.

Thomas, H. & Nisbet, T. (2012). Modelling the hydraulic impact of reintroducing large woody debris into watercourses. Journal of Flood Risk Management, 5(2), 164-174.

Thomas, I.A., Jordan, P., Mellander, P.E., Fenton, O., Shine, O., Ó hUallacháin, D., Creamer, R., McDonald, N.T., Dunlop, P. & Murphy, P.N.C. (2016). Improving the identification of hydrologically sensitive areas using LiDAR DEMs for the delineation and mitigation of critical source areas of diffuse pollution. *Science of the Total Environment*, *556*, pp.276-290.

Thurow, T.L., Blackburn, W.H. & Taylor, C.A. (1987). Rainfall interception losses by midgrass, shortgrass, and live oak mottes. Journal of Range Management 40: 455–460.

Turner, S. W. D. & Galelli, S. (2016) Water supply sensitivity to climate change: An R package for implementing reservoir storage analysis in global and regional impact studies, Environmental Modelling & Software. Volume 76, 13-19.

Verón, S.R., Paruelo, J.M. & Oesterheld, M. (2011). Grazing-induced losses of biodiversity affect the transpiration of an arid ecosystem. Oecologia 165: 501-510

Vieira, J. D. (1983). Conditions governing the use of approximations for the Saint-Venant equations for shallow surface water flow. Journal of Hydrology, 60(1-4), 43-58.

Villanueva, I., Pender, G., Lin, B., Mason, D.C., Falconer, R.A., Neelz, S., Crossley, A.J., Bates, P.D., Liang, D., Hunter, N.M. and Wright, N.G., (2008). Benchmarking 2D Hydraulic Models for Urban Flooding. In Proc. ICE–Water Management (Vol. 161, pp. 13-30).

Vincke, C., Granier, A. Breda, N. & Devillez, F. (2005). Evapotranspiration of a declining Quercus robur (L.) stand from 1999 to 2001. I.I. Daily actual evapotranspiration and soil water reserve. Ann. For. Sci. 62: 615-623.

Wainwright, J., Parsons, A. J., Müller, E. N., Brazier, R. E., Powell, D. M., & Fenti, B. (2008). A transport□distance approach to scaling erosion rates: 1. Background and model development. Earth Surface Processes and Landforms, 33(5), 813-826.

Werritty, A. (2006). Sustainable flood management: oxymoron or new paradigm?. Area, 38(1), 16-23.

Westra, S., Fowler, H. J., Evans, J. P., Alexander, L. V., Berg, P., Johnson, F., Kendon E.J., Lenderink, G. & Roberts, N. M. (2014). Future changes to the intensity and frequency of short-duration extreme rainfall. Reviews of Geophysics, 52(3), 522-555.

Wharton, G., & Gilvear, D. J. (2007). River restoration in the UK: Meeting the dual needs of the European Union Water Framework Directive and flood defence?. International Journal of River Basin Management, 5(2), 143-154.

Wheater, H., & Evans, E. (2009). Land use, water management and future flood risk. Land Use Policy, 26, S251-S264

Wheater, H., Reynolds, B., McIntyre, N., Marshall, M., Jackson, B., Frogbrook, Z. & Chell, J. (2008). Impacts of upland land management on flood risk: Multi-scale modelling methodology and results from the Pontbren Experiment.

Whitehead, P. G., Wilson, E. J., & Butterfield, D. (1998). A semi-distributed Integrated Nitrogen model for multiple source assessment in Catchments (INCA): Part I—model structure and process equations. Science of the Total Environment, 210, 547-558.

Wigmosta, M. S., & Lettenmaier, D. P. (1999). A comparison of simplified methods for routing topographically driven subsurface flow. *Water Resources Research*, *35*(1), 255-264.

Wilkinson, M. E., & Quinn, P. F. (2010). Belford catchment proactive flood solutions: a toolkit for managing runoff in the rural landscape. Climate, Water and Soil: Science, Policy and Practice, 103.

Wilkinson, M.E., Quinn, P.F., Welton, P. (2010). Runoff management during the September 2008 floods in the Belford catchment, Northumberland. *Journal of Flood Risk Management*, 3(4): 285-295.

Wilkinson, M. & Jackson-Blake, L. (2016). Case study 1. Tarland Burn runoff attenuation modelling. In Hankin, B., Burgess-Gamble, L., Bentley, S., Rose, S. (Eds.). How to model and map catchment processes when flood risk management planning. Science report SC120015/R1, Environment Agency, Bristol, UK.

Williams, J. R., Nicks, A. D., & Arnold, J. G. (1985). Simulator for water resources in rural basins. Journal of Hydraulic Engineering, 111(6), 970-986.

Younger, P. M., Freer, J. E., & Beven, K. J. (2009). Detecting the effects of spatial variability of rainfall on hydrological modelling within an uncertainty analysis framework. Hydrological Processes, 23(14), 1988-2003.

Yamazaki, D., Kanae, S., Kim, H., & Oki, T. (2011). A physically based description of floodplain inundation dynamics in a global river routing model. Water Resources Research, 47(4).

Younger, P. M., Gadian, A. M., Wang, C. G., Freer, J. E., & Beven, K. J. (2008). The usability of 250 m resolution data from the UK Meteorological Office Unified Model as input data for a hydrological model. Meteorological Applications, 15(2), 207-217.

Zeileis, A., & Grothendieck, G. (2005). zoo: S3 infrastructure for regular and irregular time series. Journal of Statistical Software, 14(6), 1-27. URL http://www.jstatsoft.org/v14/i06/

Zinke, P. J. (1967). Forest interception studies in the United States (pp. 137-161). Forest Hydrology. Oxford, UK: Pergamon Press.